

Lagrangian fillings for Legendrian links of finite or affine Dynkin type

Byung Hee An, Youngjin Bae, and Eunjeong Lee

Abstract. We prove that there are at least as many exact embedded Lagrangian fillings as seeds for Legendrian links of finite type ADE or affine type \widetilde{DE} . We also provide as many Lagrangian fillings with rotational symmetry as seeds of type B, G_2 , \widetilde{G}_2 , \widetilde{B} , or \widetilde{C}_2 , and with conjugation symmetry as seeds of type F_4 , C, $E_6^{(2)}$, \widetilde{F}_4 , or $A_5^{(2)}$. These families are the first known Legendrian links with (infinitely many) exact Lagrangian fillings (with symmetry) that exhaust all seeds in the corresponding cluster structures beyond type AD. Furthermore, we show that the N -graph realization of (twice of) Coxeter mutation of type \widetilde{DE} corresponds to a Legendrian loop of the corresponding Legendrian links. Especially, the loop of type \widetilde{D} coincides with the one considered by Casals and Ng.

1. Introduction

1.1. Background

Legendrian knots are central objects in the study of 3-dimensional contact manifolds. Classification of Legendrian knots is important in its own right and also plays a prominent role in classifying 4-dimensional Weinstein manifolds.

Classical Legendrian knot invariants are Thurston–Bennequin number and rotation number [31] which distinguish the pair of Legendrian knots with the same knot type. There are non-classical invariants, including the Legendrian contact algebra via the method of Floer theory [17, 20], and the space of constructible sheaves using microlocal analysis [32, 44]. These non-classical invariants distinguish the Chekanov pair, a pair of Legendrian knots of type $m5_2$ having the same classical invariants.

Recently, the study of exact Lagrangian fillings for Legendrian links has been extremely plentiful. In the context of Legendrian contact algebra, an exact Lagrangian filling gives an augmentation through the functorial viewpoint [19]. There are several levels of equivalence between augmentations and the constructible sheaves for Legendrian links from counting to categorical equivalence [38]. Using the idea of

Mathematics Subject Classification 2020: 53D10 (primary); 57R17, 13F60 (secondary).

Keywords: Legendrian link, Lagrangian filling, cluster algebra.

augmentations and constructible sheaves, people construct infinitely many fillings for certain Legendrian links [12, 15, 29]. Here is the summarized list of methods of constructing Lagrangian fillings for Legendrian links:

- (1) Decomposable Lagrangian fillings via pinching sequences and Legendrian loops [13, 19, 37].
- (2) Alternating Legendrians and their conjugate Lagrangian fillings [43].
- (3) Legendrian weaves via N -graphs and Legendrian mutations [15, 45].
- (4) Donaldson–Thomas transformation on augmentation varieties [29, 30, 42].

Cluster algebras, introduced by Fomin and Zelevinsky [25], play a crucial role in the above constructions and applications. More precisely, the space of augmentations and the moduli of constructible sheaves of microlocal rank one adapted to Legendrian links admit structures of cluster pattern and Y -pattern, respectively [30, 42, 43]. Note that a Y -seed of cluster algebra consists of a quiver whose vertices are decorated with variables, called *coefficients*. An involutory operation at each vertex, called *mutation*, generates all seeds of the Y -pattern. The main point is to identify the mutation in the Y -pattern and an operation in the space of Lagrangian fillings. This geometric operation is deeply related to the Lagrangian surgery [40] and the wall-crossing phenomenon [3].

Indeed, a Legendrian torus link of type $(2, n)$ admits as many exact Lagrangian fillings as Catalan number up to exact Lagrangian isotopy [39, 43, 45]. Interestingly enough, the Catalan number is the number of seeds in a cluster pattern of Dynkin type A_{n-1} . There are also Legendrian links corresponding to finite Dynkin type DE and affine Dynkin type \widetilde{DE} [29]. A conjecture by Casals [11, Conjecture 5.1] says that the number of distinct exact embedded Lagrangian fillings (up to exact Lagrangian isotopy) for Legendrian links of type ADE is exactly the same as the number of seeds of the corresponding cluster algebras.

Furthermore, it is also conjectured by Casals [11, Conjecture 5.4] that, for Legendrian links of type A_{2n-1} , D_{n+1} , E_6 and D_4 , Lagrangian fillings having certain $\mathbb{Z}/2\mathbb{Z}$ or $\mathbb{Z}/3\mathbb{Z}$ -symmetry form the cluster patterns of type B_n , C_n , F_4 , and G_2 , which are Dynkin diagrams obtained by *folding* as explained in [27].

1.2. The results

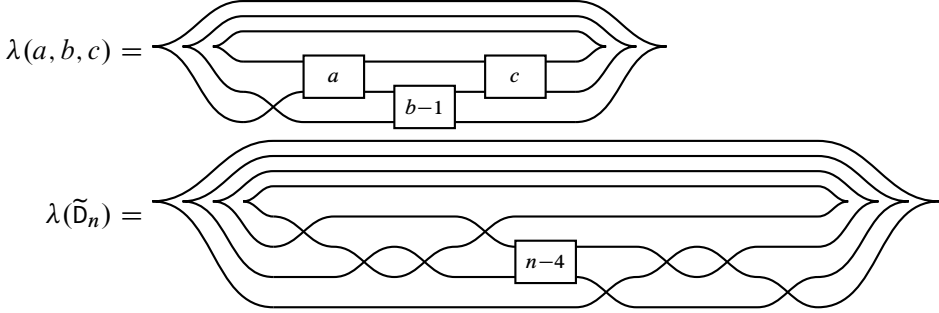
1.2.1. Lagrangian fillings for Legendrians of type ADE or \widetilde{DE} . Our main result is that there are at least as many Lagrangian fillings for Legendrian links of finite type as seeds in the corresponding cluster structures. We deal with N -graphs introduced by Casals and Zaslow [15] to construct the Lagrangian fillings. An N -graph \mathcal{G} on \mathbb{D}^2 gives a Legendrian surface $\Lambda(\mathcal{G})$ in $J^1\mathbb{D}^2$ while the boundary $\partial\mathcal{G}$ on \mathbb{S}^1 induces

a Legendrian link $\lambda(\partial\mathcal{G})$. Then, projection of $\Lambda(\mathcal{G})$ along the Reeb direction becomes a Lagrangian filling of $\lambda(\partial\mathcal{G})$.

As mentioned above, we interpret an N -graph as a Y -seed in the corresponding Y -pattern. A one-cycle in the Legendrian surface $\Lambda(\mathcal{G})$ corresponds to a vertex of the quiver, and a signed intersection between one-cycles gives an arrow between corresponding vertices. From constructible sheaves adapted to $\Lambda(\mathcal{G})$, one can assign a monodromy to each one-cycle which becomes the coefficient at each vertex.

There is an operation so called a *Legendrian mutation* μ_γ on an N -graph \mathcal{G} along one-cycle $[\gamma] \in H_1(\Lambda(\mathcal{G}))$ which is the counterpart of the mutation on the Y -pattern; see Proposition 3.43. The delicate and challenging part is that we do not know whether Legendrian mutations are always possible or not. Simply put, this is because the mutation in cluster side is algebraic, whereas the Legendrian mutation is rather geometric.

The main idea of our construction is to consider N -graphs $\mathcal{G}(a, b, c)$ and $\mathcal{G}(\tilde{D}_n)$ bounding Legendrian links $\lambda(a, b, c)$ and $\lambda(\tilde{D}_n)$, respectively,



Note that the above Legendrians $\lambda(a, b, c)$ and $\lambda(\tilde{D}_n)$ can be obtained by (-1) -closure of the following braids, respectively,

$$\begin{aligned}\beta(a, b, c) &= \sigma_2 \sigma_1^{a+1} \sigma_2 \sigma_1^{b+1} \sigma_2 \sigma_1^{c+1}, \\ \beta(\tilde{D}_n) &= (\sigma_2 \sigma_1^3 \sigma_2 \sigma_1^3 \sigma_2 \sigma_1^k \sigma_3) \cdot (\sigma_2 \sigma_1^3 \sigma_2 \sigma_1^3 \sigma_2 \sigma_1^\ell \sigma_3),\end{aligned}$$

where $k = \lfloor \frac{n-3}{2} \rfloor$ and $\ell = \lfloor \frac{n-4}{2} \rfloor$; see Section 4. Those braids provide boundary data of the following N -graphs which represent exact Lagrangian fillings of corresponding Legendrian links.

Here, the orange - and green -shaded edges indicate a tuple of one-cycles \mathcal{B} in the corresponding Legendrian surface. See Section 3.3 for the details.

The Legendrians $\lambda(a, b, c)$, $\lambda(\tilde{D}_n)$ are the rainbow closure of *positive braids*. By the work of Shen–Weng [42], it is direct to check that the corresponding cluster structure of Legendrian $\lambda(Z)$ is indeed of type Z for $Z \in \{A, D, E, \tilde{D}, \tilde{E}\}$. More precisely, the coordinate ring of the moduli space $\mathcal{M}_1(\lambda(Z))$ of microlocal rank one sheaves in $\text{Sh}_{\lambda(Z)}^\bullet(\mathbb{R}^2)$ admits the aforementioned Y -pattern structure.

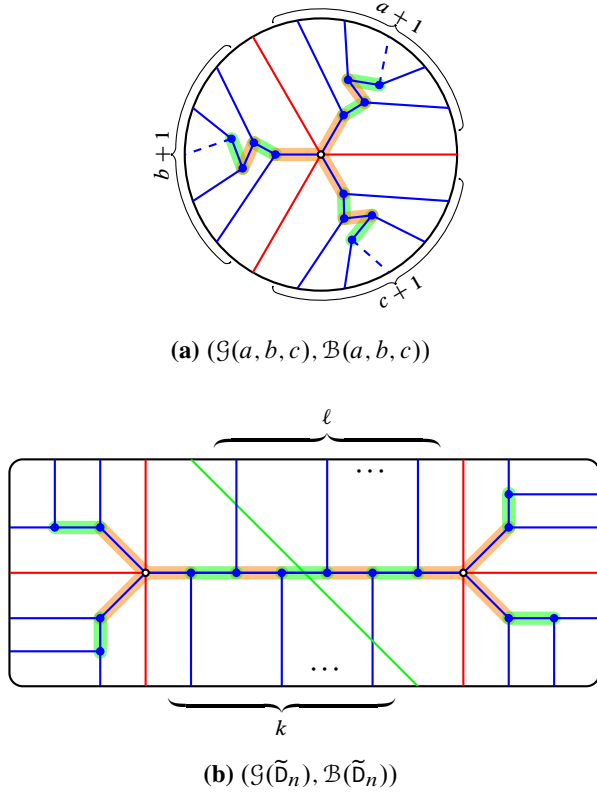


Figure 1. Pairs of N -graphs and tuples of cycles.

The (candidate) Legendrians of type \tilde{A} are not the rainbow closure of positive braids, in general. Indeed, Casals–Ng [13] considered a Legendrian link of type $\tilde{A}_{1,1}$ which is not the rainbow closure of a positive braid. So, we cannot directly apply the subsequent argument to Legendrians of type \tilde{A} .

To prove the realizability of each Y -seed in the corresponding Y -pattern, we use an induction argument on the rank of the type Z . More precisely, for each Y -pattern, we consider the *exchange graph*, whose vertices are the Y -seeds and whose edges connect the vertices related by a single mutation. It has been known that the exchange graph of a Y -pattern is determined by the Dynkin type Z of the Y -pattern when Z is finite or affine (cf. Theorem 2.28 and Proposition 2.29). Because of this, we denote by $\text{Ex}(\Phi(Z))$ the exchange graph of a Y -pattern of type Z . Here, $\Phi(Z)$ is the root system of type Z . Note that when Z is of finite type, the exchange graph $\text{Ex}(\Phi(Z))$ becomes the one-skeleton of a polytope, called the (*generalized*) *associahedron* (see Figures 2 and 12).

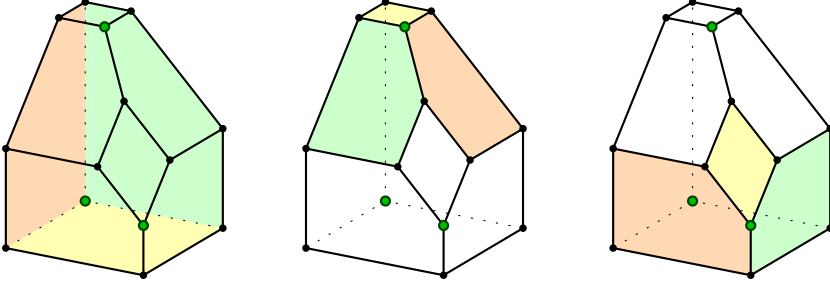


Figure 2. The type A_3 associahedron.

A (fixed) sequence of mutations corresponding to a chosen Coxeter element provides an action on the exchange graph. We call this specific sequence of mutations a *Coxeter mutation* $\mu_{\mathcal{Q}}$. The orbit of the initial seed is called *bipartite belt*. The green dots in Figure 2 present the elements of the bipartite belt. We notice that the facets meeting at the initial seed correspond to the exchange graphs $\text{Ex}(\Phi(Z \setminus \{i\}))$. In Figure 2, there are two pentagons and one square intersecting a green dot. Indeed, a pentagon is the type A_2 generalized associahedron; a square is the type $A_1 \times A_1$ generalized associahedron. Moreover, by applying the Coxeter mutation on these facets iteratively, one can obtain all facets in the associahedron. Even though we do not have a polytope model for the exchange graph of affine type, similar properties hold; that is, one can reach any Y -seed in the exchange graph from the initial seed by taking Coxeter mutations and then applying a certain sequence of mutations omitting at least one vertex.

The following good properties of the above pairs $(\mathcal{G}(a, b, c), \mathcal{B}(a, b, c))$ and $(\mathcal{G}(\tilde{D}_n), \mathcal{B}(\tilde{D}_n))$ play a crucial role in interpreting the Coxeter mutation $\mu_{\mathcal{Q}}$ in terms of N -graphs.

- (1) The geometric and algebraic intersection numbers between chosen one-cycles coincide.
- (2) The corresponding quivers $\mathcal{Q}(a, b, c), \mathcal{Q}(\tilde{D}_n)$ are bipartite; see Section 3.5 for the details.

The property (2) naturally splits \mathcal{B} into two subsets \mathcal{B}_+ and \mathcal{B}_- . In Figure 1, they consist of orange- and green-shaded edges, respectively. Then, the property (1) enables us to perform the *Legendrian Coxeter mutation*, which is the N -graph realization of the Coxeter mutation defined by the sequence of Legendrian mutations:

$$\mu_{\mathcal{G}} = \prod_{\gamma \in \mathcal{B}_+} \mu_{\gamma} \cdot \prod_{\gamma \in \mathcal{B}_-} \mu_{\gamma}.$$

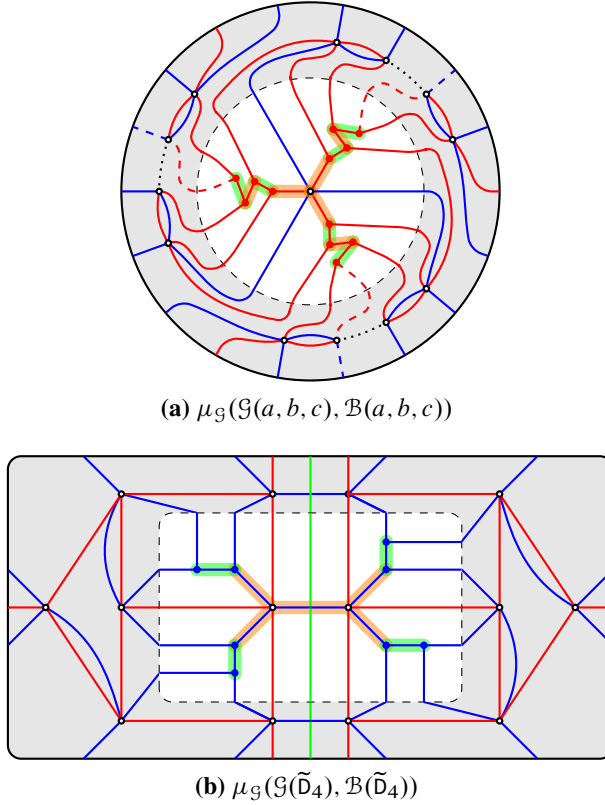


Figure 3. After applying Legendrian Coxeter mutation on the initial pair.

Then, the resulting N -graphs $\mu_{\mathcal{G}}(\mathcal{G}(a, b, c), \mathcal{B}(a, b, c))$ and $\mu_{\mathcal{G}}(\mathcal{G}(\tilde{D}_n), \mathcal{B}(\tilde{D}_n))$ become the N -graphs shown in Figure 3 up to a sequence of Move (II) in Figure 18.

Removing the gray-shaded annulus region, two N -graphs $(\mathcal{G}(\tilde{D}_n), \mathcal{B}(\tilde{D}_n))$ and $\mu_{\mathcal{G}}(\mathcal{G}(\tilde{D}_n), \mathcal{B}(\tilde{D}_n))$ are identical, and the only difference between $(\mathcal{G}(a, b, c), \mathcal{B}(a, b, c))$ and $\mu_{\mathcal{G}}(\mathcal{G}(a, b, c), \mathcal{B}(a, b, c))$ is the reverse of the color. Note that the intersection pattern among one-cycles and the Legendrian mutability are preserved under the action of the Legendrian Coxeter mutation $\mu_{\mathcal{G}}$. By the induction argument on the rank of root system, we conclude that there is no (geometric) obstruction to realize each seed via the N -graph.

Note that the N -graphs $\mathcal{G}(a, b, c)$ and $\mathcal{G}(\tilde{D}_n)$ include Lagrangian fillings of Legendrian links of type $Z \in \{A, D, E, \tilde{D}, \tilde{E}\}$; see Table 8. In particular, $\mathcal{G}(a, b, c)$ is of type ADE or $\tilde{D}\tilde{E}$ if and only if $\frac{1}{a} + \frac{1}{b} + \frac{1}{c} > 1$ or $\frac{1}{a} + \frac{1}{b} + \frac{1}{c} = 1$, respectively.

This guarantees that there are at least as many Lagrangian fillings as seeds for $\lambda(Z)$ for $Z \in \{A, D, E, \tilde{D}, \tilde{E}\}$.

Theorem 1.1 (Theorem 4.32). *Let λ be a Legendrian knot or link of type ADE or type \widetilde{DE} . Then, it admits at least as many distinct exact embedded Lagrangian fillings up to exact Lagrangian isotopy (rel boundary) as the number of seeds in the seed pattern of the same type. See Table 4 for the number of seeds of finite type.*

There are several ways of constructing exact embedded Lagrangian fillings as mentioned above. Especially, in D_4 case, there are 34 distinct Lagrangian fillings constructed by the method of the alternating Legendrians [5, 43], while the above N -graphs give 50 distinct Lagrangian fillings which is the number of seeds of the corresponding cluster pattern. Most recently, for Legendrian links of type D_n , Hughes [33] makes use of 3-graphs together with 1-cycles to show that every sequence of quiver mutations can be realized by Legendrian weave mutations. Compared with our strategy using structural results of the cluster pattern, he studies 3-graph moves arising from quivers of type D_n in a more direct and concrete way. As a corollary, he also obtained at least as many Lagrangian fillings as seeds in the cluster algebra of type D_n .

There are many results showing the existence of (infinitely many) distinct Lagrangian fillings for Legendrian links; see [12, 13, 15, 19, 29, 39, 43, 45]. To the best of authors' knowledge, Theorem 1.1 is the first results of (infinitely many) Lagrangian fillings of Legendrian links which exhaust all seeds in the corresponding cluster pattern beyond type AD.

The gray-shaded annular N -graphs in the above figure can be seen as exact Lagrangian cobordisms. In particular, the annular N -graph $\mathcal{C}(\widetilde{D}_4)$ for $\mu_{\mathcal{G}}(\mathcal{G}(\widetilde{D}_4), \mathcal{B}(\widetilde{D}_4))$ corresponds to the cobordism from the Legendrian $\lambda(\widetilde{D}_4)$ to itself which defines a Legendrian loop $\vartheta(\widetilde{D}_4)$. See Figure 4 for the case of D_n for general $n \geq 4$. Note that this coincides with the Legendrian loop described in [13, Figure 2] up to Reidemeister moves. For type \widetilde{E} , the twice of Legendrian Coxeter mutation on the pair $(\mathcal{G}(a, b, c), \mathcal{B}(a, b, c))$ gives the Legendrian loop $\vartheta(a, b, c)$ of $\lambda(a, b, c)$, as shown in Figure 45. The Legendrian loop $\vartheta(a, b, c)$ can be interpreted as the move of the half-twist Δ_3 along the three-strand braid band, whereas the Legendrian loop $\vartheta(\widetilde{D}_n)$ is essentially the move of the half-twist Δ_2 along the two-strand braid band, as depicted in Figure 46.

Theorem 1.2 (Theorem 4.31). *The Legendrian Coxeter mutation $\mu_{\mathcal{G}}$ on $(\mathcal{G}(\widetilde{D}), \mathcal{B}(\widetilde{D}))$ and twice of Legendrian mutation $\mu_{\mathcal{G}}^2$ on $(\mathcal{G}(\widetilde{E}), \mathcal{B}(\widetilde{E}))$ induce Legendrian loops $\vartheta(\widetilde{D})$ and $\vartheta(\widetilde{E})$ in Figures 45 and 46, respectively. In particular, the order of the Legendrian loops is infinite as elements of the fundamental group of the space of Legendrians isotopic to $\lambda(\widetilde{D})$ and $\lambda(\widetilde{E})$, respectively.*

Note that the above idea of Coxeter mutation also works for $(\mathcal{G}(a, b, c), \mathcal{B}(a, b, c))$ with $\frac{1}{a} + \frac{1}{b} + \frac{1}{c} < 1$. Indeed, the operation $\mu_{\mathcal{Q}}$ is of infinite order, and so is $\mu_{\mathcal{G}}$; hence,

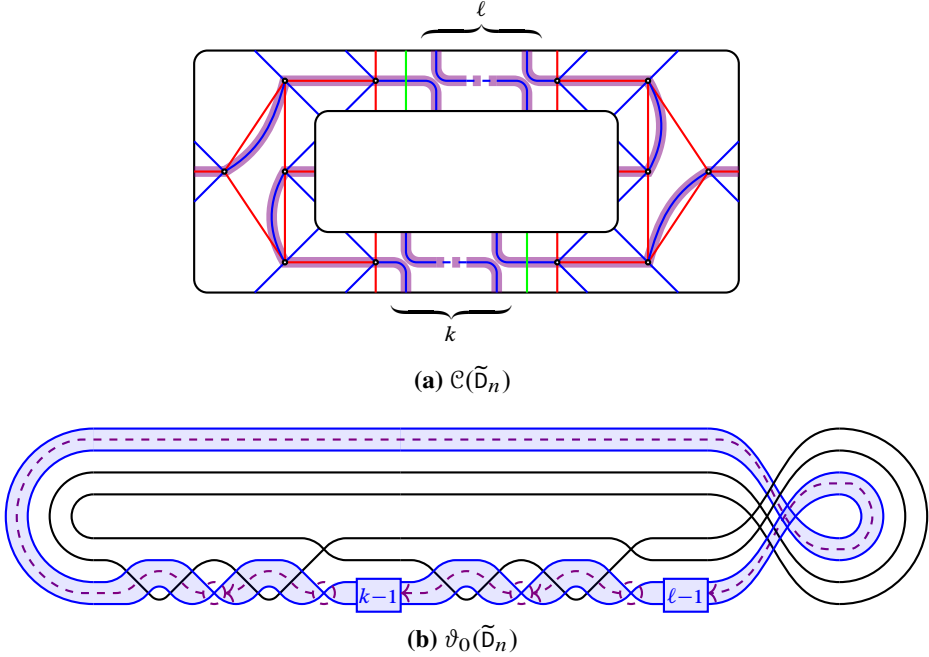


Figure 4. Legendrian Coxeter padding $\mathcal{C}(\tilde{D}_n)$ and the corresponding Legendrian loop $\vartheta_0(\tilde{D}_n)$.

Legendrian weaves

$$\Lambda(\mu_{\mathcal{G}}^r(\mathcal{G}(a, b, c), \mathcal{B}(a, b, c)))$$

produce infinitely many distinct Lagrangian fillings. The quiver $\mathcal{Q}(a, b, c)$ is also bipartite, and one can perform the Legendrian Coxeter mutation $\mu_{\mathcal{G}}$ on the N -graph $\mathcal{G}(a, b, c)$ by stacking the gray-shaded annulus as before. Therefore, there is no obstruction to realize seeds obtained by mutations $\mu_{\mathcal{G}}^r$ via the N -graphs. Since the order of the Legendrian Coxeter mutation is infinite (see Lemma 2.36), we obtain infinitely many N -graphs and hence infinitely many exact embedded Lagrangian fillings for the Legendrian link $\lambda(a, b, c)$ with $\frac{1}{a} + \frac{1}{b} + \frac{1}{c} < 1$.

Theorem 1.3 (Theorem 4.24). *For each $a, b, c \geq 1$, the Legendrian knot or link $\lambda(a, b, c)$ has infinitely many distinct Lagrangian fillings if*

$$\frac{1}{a} + \frac{1}{b} + \frac{1}{c} < 1.$$

Gao–Shen–Weng [29] already proved the existence of infinitely many Lagrangian fillings for much general type of positive braid Legendrian links. Their main idea is to use the aperiodicity of *Donaldson–Thomas transformation* (DT) on cluster varieties.

An interesting observation is that the corresponding action of DT on the bipartite quivers in the Y -pattern coincides with the Coxeter mutation. See [29, Theorem 2.6] and its proof. Accordingly, Theorem 1.3 can be interpreted as an N -graph analogue of the aperiodicity of DT.

1.2.2. Lagrangian fillings for Legendrians of type BCFG or standard affine type with symmetry. Now, we move to cluster structure of type BCFG and standard affine types with certain symmetry. They are obtained by the folding procedure from type ADE or $\widetilde{\text{DE}}$; see Table 10.

In order to interpret those symmetries into Legendrians links and surfaces, we need to introduce corresponding actions on symplectic- and contact manifolds. Considering two actions on $\mathbb{S}^3 \times \mathbb{R}_u$, the rotation R_{θ_0} and conjugation η are as follows:

$$\begin{aligned} R_{\theta_0}(z_1, z_2, u) &= (z_1 \cos \theta_0 - z_2 \sin \theta_0, z_1 \sin \theta_0 + z_2 \cos \theta_0, u), \\ \eta(z_1, z_2, u) &= (\bar{z}_1, \bar{z}_2, u). \end{aligned}$$

Here, \mathbb{S}^3 is the unit sphere in \mathbb{C}^2 with coordinates $z_1 = r_1 e^{i\theta_1}$, $z_2 = r_2 e^{i\theta_2}$ with $r_1^2 + r_2^2 = 1$. Note that η is an anti-symplectic involution which naturally gives $\mathbb{Z}/2\mathbb{Z}$ -action on the symplectic manifold. Under certain coordinate changes, the restrictions of R_{θ_0} and η on $J^1\mathbb{S}^1$ become

$$\begin{aligned} R_{\theta_0}|_{J^1\mathbb{S}^1}(\theta, p_\theta, z) &= (\theta + \theta_0, p_\theta, z), \\ \eta|_{J^1\mathbb{S}^1}(\theta, p_\theta, z) &= (\theta, -p_\theta, -z). \end{aligned}$$

In turn, the rotation R_{θ_0} acts on the N -graph $\mathcal{G}(Z)$ by rotating the disk \mathbb{D}^2 , and η acts by flipping the z -coordinate.

Any Y -pattern of non-simply-laced finite or affine type can be obtained by folding a Y -pattern of type ADE or $\widetilde{\text{ADE}}$. In other words, those Y -patterns of non-simply-laced type can be seen as sub-patterns of ADE- or $\widetilde{\text{ADE}}$ -types consisting of Y -seeds with certain symmetries of finite group G action. We call such Y -seeds or N -graphs G -admissible, and the mutation in the folded cluster structure is a sequence of mutations respecting the G -orbits. We say that a Y -seed (or an N -graph) is *globally foldable* if it is G -admissible and its arbitrary mutations along G -orbits are again G -admissible.

Figure 5 illustrates the N -graphs with rotational symmetry and the corresponding Y -patterns of folding. Indeed, they are $\mathcal{G}(1, n, n)$, $\mathcal{G}(2, 2, 2)$, $\mathcal{G}(3, 3, 3)$, $\mathcal{G}(\widetilde{\text{D}}_{2n})$, $\mathcal{G}(\widetilde{\text{D}}_4)$ which admit $\mathbb{Z}/2\mathbb{Z}$ -, $\mathbb{Z}/3\mathbb{Z}$ -, $\mathbb{Z}/3\mathbb{Z}$ -, $\mathbb{Z}/2\mathbb{Z}$ -, $\mathbb{Z}/2\mathbb{Z}$ -action, respectively.

In order to present conjugation invariant N -graphs, we need to adopt a degenerate version of N -graphs which allows overlapping edges and cycles as in Figure 6. They are equivalent to $\mathcal{G}(\widetilde{\text{D}}_{n+1})$, $\mathcal{G}(\widetilde{\text{D}}_4)$, $\mathcal{G}(2, 3, 3)$, $\mathcal{G}(3, 3, 3)$, and $\mathcal{G}(2, 4, 4)$ up to ∂ -Legendrian isotopy, see Definition 3.20, respectively.

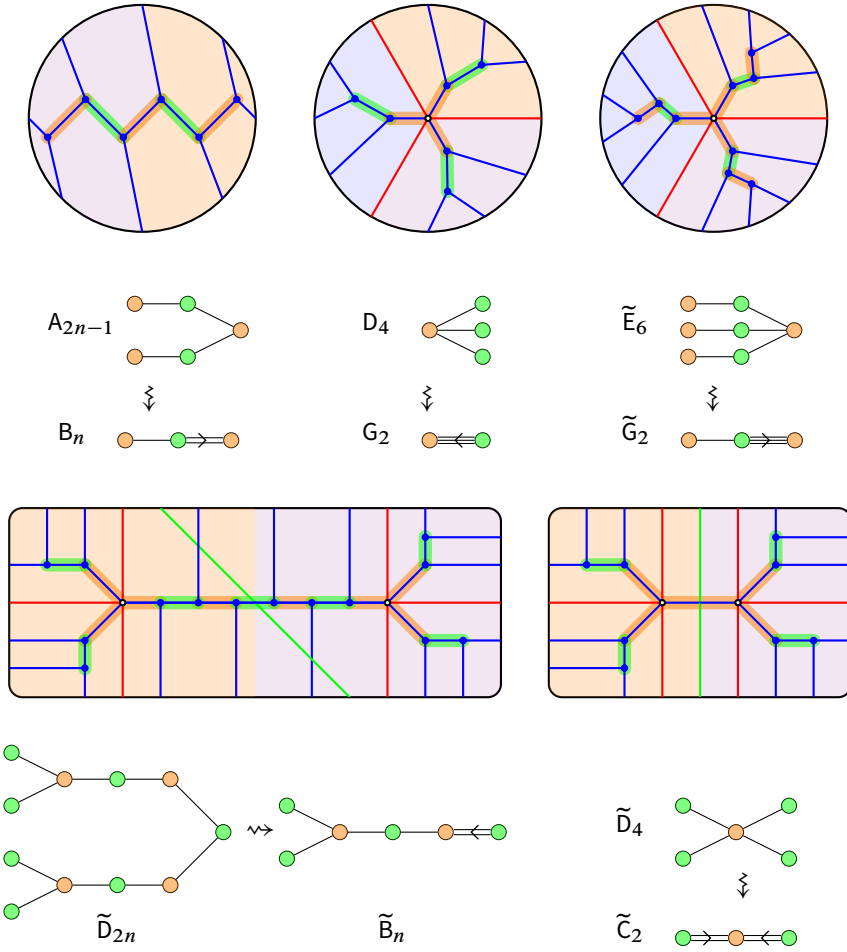


Figure 5. Examples of N -graphs with rotational symmetry.

Theorem 1.4 (Theorem 5.8). *The following hold.*

- (1) *The Legendrian $\lambda(A_{2n-1})$ has at least $\binom{2n}{n}$ distinct Lagrangian fillings up to exact Lagrangian isotopy (rel boundary) which are invariant under the π -rotation and admit the Y -pattern of type B_n .*
- (2) *The Legendrian $\lambda(D_4)$ has at least 8 distinct Lagrangian fillings up to exact Lagrangian isotopy (rel boundary) which are invariant under the $2\pi/3$ -rotation and admit the Y -pattern of type G_2 .*

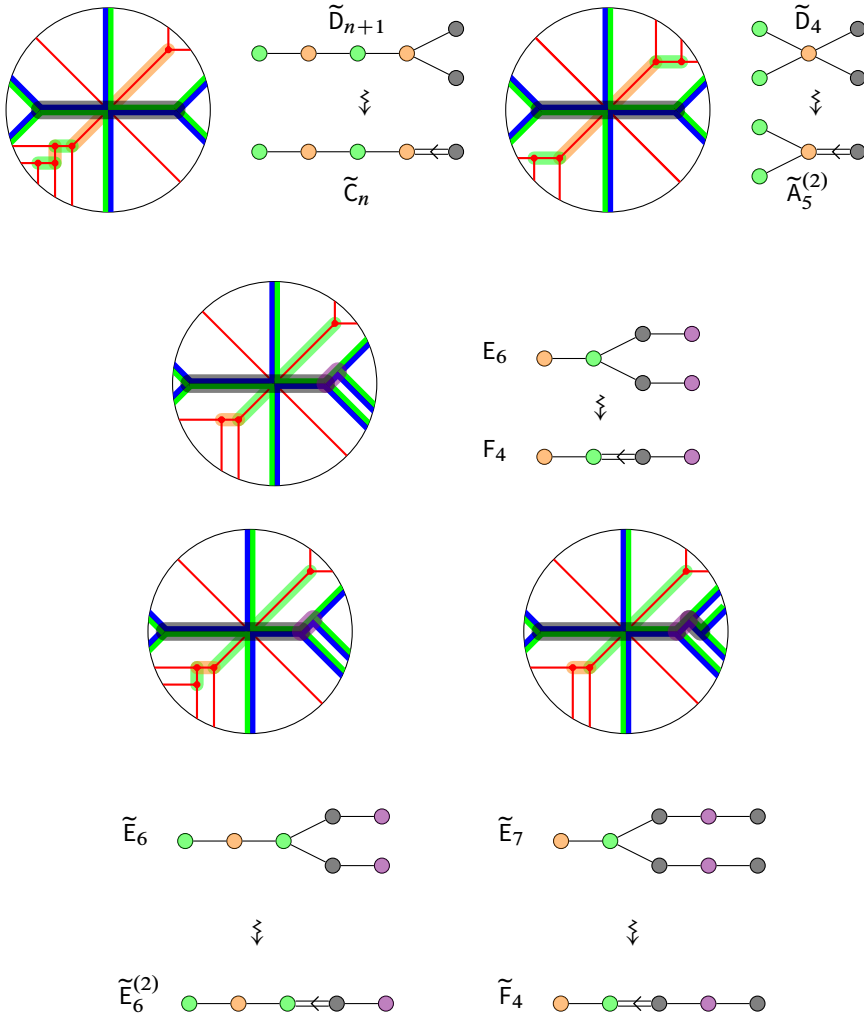


Figure 6. Examples of N -graphs with conjugation symmetry.

- (3) The Legendrian $\lambda(\tilde{E}_6)$ has infinitely many distinct Lagrangian fillings up to exact Lagrangian isotopy (rel boundary) which are invariant under the $2\pi/3$ -rotation and admit the Y -pattern of type \tilde{G}_2 .
- (4) The Legendrian $\lambda(\tilde{D}_{2n})$ with $n \geq 3$ has infinitely many distinct Lagrangian fillings up to exact Lagrangian isotopy (rel boundary) which are invariant under the π -rotation and admit the Y -pattern of type \tilde{B}_n .

- (5) *The Legendrian $\lambda(\tilde{\mathbb{D}}_4)$ has infinitely many distinct Lagrangian fillings up to exact Lagrangian isotopy (rel boundary) which are invariant under the π -rotation and admit the Y -pattern of type $\tilde{\mathcal{C}}_2$.*
- (6) *The Legendrian $\tilde{\lambda}(\mathbb{E}_6)$ has at least 105 distinct Lagrangian fillings up to exact Lagrangian isotopy (rel boundary) which are invariant under the antisymplectic involution and admit the Y -pattern of type \mathbb{F}_4 .*
- (7) *The Legendrian $\tilde{\lambda}(\mathbb{D}_{n+1})$ has at least $\binom{2n}{n}$ Lagrangian fillings up to exact Lagrangian isotopy (rel boundary) which are invariant under the antisymplectic involution and admit the Y -pattern of type \mathbb{C}_n .*
- (8) *The Legendrian $\tilde{\lambda}(\tilde{\mathbb{E}}_6)$ has infinitely many distinct Lagrangian fillings up to exact Lagrangian isotopy (rel boundary) which are invariant under the anti-symplectic involution and admit the Y -pattern of type $\mathbb{E}_6^{(2)}$.*
- (9) *The Legendrian $\tilde{\lambda}(\tilde{\mathbb{E}}_7)$ has infinitely many distinct Lagrangian fillings up to exact Lagrangian isotopy (rel boundary) which are invariant under the anti-symplectic involution and admit the Y -pattern of type $\tilde{\mathbb{F}}_4$.*
- (10) *The Legendrian $\tilde{\lambda}(\tilde{\mathbb{D}}_4)$ has infinitely many distinct Lagrangian fillings up to exact Lagrangian isotopy (rel boundary) which are invariant under the antisymplectic involution and admit the Y -pattern of type $\mathbb{A}_5^{(2)}$.*

The study of Lagrangian fillings with symmetry, again to the best of authors' knowledge, is started from [11]. We clarify the actions on the symplectic and contact manifold, together with the induced actions on Lagrangian fillings and Legendrian links. The items (1), (2), (6), (7) in Theorem 1.4 answer that the half of the conjecture [11, Conjecture 5.4], i.e., the surjectivity from fillings to seeds, is true, and furthermore, we extend our results to certain non-simply-laced affine types.

1.3. Organization of the paper

The rest of the paper is divided into six sections including appendices. We review, in Section 2, some basics on finite and affine cluster algebra. Especially, we focus on structural results about the combinatorics of exchange graphs using Coxeter mutations.

In Section 3, we recall how N -graphs and their moves encode Legendrian surfaces and the Legendrian isotopies. We also introduce degenerate N -graphs which will be used to construct Lagrangian fillings having conjugation symmetry. After that we review the assignment of Y -seeds in the cluster structure from N -graphs together with certain flag moduli. We also discuss the Legendrian mutation on (degenerate) N -graphs.

In Section 4, we investigate Legendrian links and N -graphs of type ADE or \widetilde{DE} . We discuss N -graph realization of the Coxeter mutation and prove Theorem 1.2 on the relationship between Coxeter mutations and Legendrian loops. By combining the structural results in the seed pattern of cluster algebra and N -graph realization of the Coxeter mutation, we construct as many Lagrangian fillings as seeds for Legendrian links of type ADE or \widetilde{DE} , hence proving Theorem 1.1.

In Section 5, we discuss rotation and conjugation actions on N -graphs and invariant N -graphs. We also prove Theorem 1.4.

In Appendix A, we argue that G -invariance of type ADE implies G -admissibility. Finally, in Appendix B, we collect several equivalences between different presentation of N -graphs.

If some readers are familiar with the notion of cluster algebra and N -graph, then one may skip Sections 2 and 3, respectively, and start from Section 4.

2. Cluster algebras

Cluster algebras, introduced by Fomin and Zelevinsky [25], are commutative algebras with specific generators, called *cluster variables*, defined recursively. In this section, we recall basic notions in the theory of cluster algebras. For more details, we refer the reader to [25, 26, 28].

Throughout this section, we fix $m, n \in \mathbb{Z}_{>0}$ such that $n \leq m$, and we let \mathbb{F} be the rational function field with m independent variables over \mathbb{C} .

2.1. Basics on cluster algebras

2.1.1. Cluster algebras. We first recall the definition of seeds and Y -seeds from [25, 26, 28].

Definition 2.1 (Cf. [25, 26, 28]). A seed and Y -seed are defined as follows.

- (1) A *seed* $(\mathbf{x}, \widetilde{\mathcal{B}})$ is a pair of
- a tuple $\mathbf{x} = (x_1, \dots, x_m)$ of algebraically independent generators of \mathbb{F} , that is, $\mathbb{F} = \mathbb{C}(x_1, \dots, x_m)$;
 - an $m \times n$ integer matrix $\widetilde{\mathcal{B}} = (b_{i,j})_{i,j}$ such that the *principal part* $\mathcal{B} := (b_{i,j})_{1 \leq i, j \leq n}$ is skew-symmetrizable; that is, there exist positive integers d_1, \dots, d_n such that

$$\text{diag}(d_1, \dots, d_n) \cdot \mathcal{B}$$

is a skew-symmetric matrix.

We refer to \mathbf{x} as the *cluster* of a seed $(\mathbf{x}, \tilde{\mathcal{B}})$, to elements x_1, \dots, x_m as *cluster variables*, and to $\tilde{\mathcal{B}}$ as the *exchange matrix*. Moreover, we call x_1, \dots, x_n *unfrozen* (or, *mutable*) variables and x_{n+1}, \dots, x_m *frozen* variables.

- (2) A *Y-seed* $(\mathbf{y}, \mathcal{B})$ is a pair of an n -tuple $\mathbf{y} = (y_1, \dots, y_n)$ of elements in \mathbb{F} and an $n \times n$ skew-symmetrizable matrix \mathcal{B} . We call \mathbf{y} the *coefficient tuple* of a *Y-seed* $(\mathbf{y}, \mathcal{B})$ and call y_1, \dots, y_n *coefficients*.

We say that two seeds $(\mathbf{x}, \tilde{\mathcal{B}})$ and $(\mathbf{x}', \tilde{\mathcal{B}}')$ are *equivalent*, denoted by $(\mathbf{x}, \tilde{\mathcal{B}}) \sim (\mathbf{x}', \tilde{\mathcal{B}}')$, if there exists a permutation σ on $[m]$ fixing $n+1, \dots, m$ such that

$$x'_i = x_{\sigma(i)} \quad \text{and} \quad b'_{i,j} = b_{\sigma(i),\sigma(j)} \quad \text{for } 1 \leq i \leq m, 1 \leq j \leq n,$$

where $\mathbf{x} = (x_1, \dots, x_m)$, $\mathbf{x}' = (x'_1, \dots, x'_m)$, $\tilde{\mathcal{B}} = (b_{i,j})$, and $\tilde{\mathcal{B}}' = (b'_{i,j})$. Similarly, two *Y-seeds* $(\mathbf{y}, \mathcal{B})$ and $(\mathbf{y}', \mathcal{B}')$ are *equivalent* and denoted by $(\mathbf{y}, \mathcal{B}) \sim (\mathbf{y}', \mathcal{B}')$ if there exists a permutation σ on $[n]$ such that

$$y'_i = y_{\sigma(i)} \quad \text{and} \quad b'_{i,j} = b_{\sigma(i),\sigma(j)} \quad \text{for } 1 \leq i, j \leq n.$$

To define cluster algebras, we introduce mutations on exchange matrices, and quivers, and seeds as follows.

- (1) (Mutation on exchange matrices). For an exchange matrix $\tilde{\mathcal{B}}$ and $1 \leq k \leq n$, the mutation $\mu_k(\tilde{\mathcal{B}}) = (b'_{i,j})$ is defined as follows:

$$b'_{i,j} = \begin{cases} -b_{i,j} & \text{if } i = k \text{ or } j = k, \\ b_{i,j} + \frac{|b_{i,k}|b_{k,j} + b_{i,k}|b_{k,j}|}{2} & \text{otherwise.} \end{cases}$$

We say that $\tilde{\mathcal{B}}' = (b'_{i,j})$ is the *mutation of $\tilde{\mathcal{B}}$ at k* .

- (2) (Mutation on quivers) We call a finite directed multigraph \mathcal{Q} a *quiver* if it does not have oriented cycles of length at most 2. The adjacency matrix $\tilde{\mathcal{B}}(\mathcal{Q})$ of a quiver is always skew-symmetric. Moreover, $\mu_k(\tilde{\mathcal{B}}(\mathcal{Q}))$ is again the adjacency matrix of a quiver \mathcal{Q}' . We define $\mu_k(\mathcal{Q})$ to be the quiver satisfying

$$\tilde{\mathcal{B}}(\mu_k(\mathcal{Q})) = \mu_k(\tilde{\mathcal{B}}(\mathcal{Q})),$$

and say that $\mu_k(\mathcal{Q})$ is the *mutation of \mathcal{Q} at k* .

- (3) (Mutation on seeds). For a seed $(\mathbf{x}, \tilde{\mathcal{B}})$ and an integer $1 \leq k \leq n$, the *mutation* $\mu_k(\mathbf{x}, \tilde{\mathcal{B}}) = (\mathbf{x}', \mu_k(\tilde{\mathcal{B}}))$ is defined as follows:

$$x'_i = \begin{cases} x_i & \text{if } i \neq k, \\ x_k^{-1} \left(\prod_{b_{j,k} > 0} x_j^{b_{j,k}} + \prod_{b_{j,k} < 0} x_j^{-b_{j,k}} \right) & \text{otherwise.} \end{cases}$$

- (4) (Mutation on Y -seeds). The Y -seed mutation (or, cluster \mathcal{X} -mutation, \mathcal{X} -cluster mutation) on a Y -seed $(\mathbf{y}, \mathcal{B})$ at $k \in [n]$ is a Y -seed $(\mathbf{y}' = (y'_1, \dots, y'_n), \mathcal{B}' = \mu_k(\mathcal{B}))$, where for each $1 \leq i \leq n$,

$$y'_i = \begin{cases} y_i y_k^{\max\{b_{i,k}, 0\}} (1 + y_k)^{-b_{i,k}} & \text{if } i \neq k, \\ y_k^{-1} & \text{otherwise.} \end{cases}$$

Example 2.2. Let $n = m = 2$. Suppose that an initial seed is given by

$$(\mathbf{x}_{t_0}, \tilde{\mathcal{B}}_{t_0}) = \left((x_1, x_2), \begin{pmatrix} 0 & 1 \\ -3 & 0 \end{pmatrix} \right).$$

Considering mutations $\mu_1(\mathbf{x}_{t_0}, \tilde{\mathcal{B}}_{t_0})$ and $\mu_2\mu_1(\mathbf{x}_{t_0}, \tilde{\mathcal{B}}_{t_0})$, we obtain the following:

$$\begin{aligned} \mu_1(\mathbf{x}_{t_0}, \tilde{\mathcal{B}}_{t_0}) &= \left(\left(\frac{1+x_2^3}{x_1}, x_2 \right), \begin{pmatrix} 0 & -1 \\ 3 & 0 \end{pmatrix} \right), \\ \mu_2\mu_1(\mathbf{x}_{t_0}, \tilde{\mathcal{B}}_{t_0}) &= \left(\left(\frac{1+x_2^3}{x_1}, \frac{1+x_1+x_2^3}{x_1x_2} \right), \begin{pmatrix} 0 & 1 \\ -3 & 0 \end{pmatrix} \right). \end{aligned}$$

Remark 2.3. Let k be a vertex in a quiver \mathcal{Q} on $[m]$. The mutation $\mu_k(\mathcal{Q})$ can also be described via a sequence of three steps.

- (1) For each directed two-arrow path $i \rightarrow k \rightarrow j$, add a new arrow $i \rightarrow j$.
- (2) Reverse the direction of all arrows incident to the vertex k .
- (3) Repeatedly remove directed 2-cycles until being unable to do so.

Remark 2.4. Let $\tilde{\mathcal{B}} = (b_{i,j})$ be an exchange matrix of size $m \times n$. For $k, \ell \in [n]$, if $b_{k,\ell} = b_{\ell,k} = 0$, then the mutations at k and ℓ commute with each other: $\mu_\ell(\mu_k(\tilde{\mathcal{B}})) = \mu_k(\mu_\ell(\tilde{\mathcal{B}}))$. Similarly, for a quiver \mathcal{Q} on $[m]$, if there does not exist an arrow connecting mutable vertices k and ℓ , then we have $\mu_\ell(\mu_k(\mathcal{Q})) = \mu_k(\mu_\ell(\mathcal{Q}))$.

We say a quiver \mathcal{Q}' is *mutation equivalent* to another quiver \mathcal{Q} if there exists a sequence of mutations $\mu_{j_1}, \dots, \mu_{j_\ell}$ which connects \mathcal{Q}' and \mathcal{Q} , that is,

$$\mathcal{Q}' = (\mu_{j_\ell} \cdots \mu_{j_1})(\mathcal{Q}).$$

Similarly, we say an exchange matrix $\tilde{\mathcal{B}}'$ is *mutation equivalent* to another matrix $\tilde{\mathcal{B}}$ if $\tilde{\mathcal{B}}'$ is obtained by applying a sequence of mutations to $\tilde{\mathcal{B}}$.

An immediate check shows that $\mu_k(\mathbf{x}, \tilde{\mathcal{B}})$ is again a seed, $\mu_k(\mathbf{y}, \mathcal{B})$ is a Y -seed, and a mutation is an involution; that is, its square is the identity. Also, note that the mutation on seeds does not change frozen variables x_{n+1}, \dots, x_m . Let \mathbb{T}_n denote the n -regular tree whose edges are labeled by $1, \dots, n$. Except for $n = 1$, there are

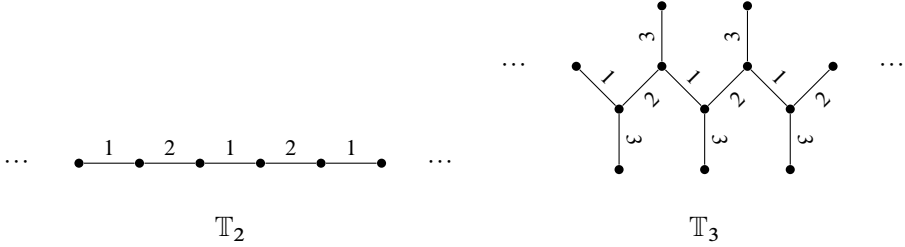


Figure 7. The n -regular trees for $n = 2$ and $n = 3$.

infinitely many vertices on the tree \mathbb{T}_n . For example, we present regular trees \mathbb{T}_2 and \mathbb{T}_3 in Figure 7. A *cluster pattern* (or *seed pattern*) is an assignment

$$\mathbb{T}_n \rightarrow \{\text{seeds in } \mathbb{F}\}, \quad t \mapsto (\mathbf{x}_t, \tilde{\mathcal{B}}_t)$$

such that if $t \xrightarrow{k} t'$ in \mathbb{T}_n , then

$$\mu_k(\mathbf{x}_t, \tilde{\mathcal{B}}_t) = (\mathbf{x}_{t'}, \tilde{\mathcal{B}}_{t'}).$$

Let $\{(\mathbf{x}_t, \tilde{\mathcal{B}}_t)\}_{t \in \mathbb{T}_n}$ be a cluster pattern with $\mathbf{x}_t = (x_{1;t}, \dots, x_{m;t})$. Since the mutation does not change frozen variables, we may let

$$x_{n+1} = x_{n+1;t}, \dots, x_m = x_{m;t}.$$

Similarly, we define a *cluster Y -pattern* (or a *Y -pattern*) $\{(\mathbf{y}_t, \mathcal{B}_t)\}_{t \in \mathbb{T}_n}$ by an assignment from \mathbb{T}_n to the set of Y -seeds regarding the mutation relations.

Definition 2.5 (Cf. [26]). Let $\{(\mathbf{x}_t, \tilde{\mathcal{B}}_t)\}_{t \in \mathbb{T}_n}$ be a cluster pattern with

$$\mathbf{x}_t = (x_{1;t}, \dots, x_{m;t}).$$

The *cluster algebra* $\mathcal{A}(\{(\mathbf{x}_t, \tilde{\mathcal{B}}_t)\}_{t \in \mathbb{T}_n})$ is defined to be the $\mathbb{C}[x_{n+1}, \dots, x_m]$ -subalgebra of \mathbb{F} generated by all the cluster variables $\bigcup_{t \in \mathbb{T}_n} \{x_{1;t}, \dots, x_{n;t}\}$.

If we fix a vertex $t_0 \in \mathbb{T}_n$, then a cluster pattern $\{(\mathbf{x}_t, \tilde{\mathcal{B}}_t)\}_{t \in \mathbb{T}_n}$ is constructed from the seed $(\mathbf{x}_{t_0}, \tilde{\mathcal{B}}_{t_0})$. In this case, we call $(\mathbf{x}_{t_0}, \tilde{\mathcal{B}}_{t_0})$ an *initial seed*. Because of this reason, we simply denote by $\mathcal{A}(\mathbf{x}_{t_0}, \tilde{\mathcal{B}}_{t_0})$ the cluster algebra given by the cluster pattern constructed from the initial seed $(\mathbf{x}_{t_0}, \tilde{\mathcal{B}}_{t_0})$.

Example 2.6. Let $n = m = 2$. Suppose that an initial seed is given by

$$(\mathbf{x}_{t_0}, \tilde{\mathcal{B}}_{t_0}) = \left((x_1, x_2), \begin{pmatrix} 0 & 1 \\ -1 & 0 \end{pmatrix} \right).$$

We present the cluster pattern obtained by the initial seed $(\mathbf{x}_{t_0}, \tilde{\mathcal{B}}_{t_0})$.

$$\begin{array}{ccc}
\left((x_2, x_1), \begin{pmatrix} 0 & -1 \\ 1 & 0 \end{pmatrix} \right) & \sim & (\mathbf{x}_{t_0}, \tilde{\mathcal{B}}_{t_0}) = \left((x_1, x_2), \begin{pmatrix} 0 & 1 \\ -1 & 0 \end{pmatrix} \right) \\
\uparrow \mu_1 & & \downarrow \mu_1 \\
\left(\left(\frac{1+x_1}{x_2}, x_1 \right), \begin{pmatrix} 0 & 1 \\ -1 & 0 \end{pmatrix} \right) & & \left(\left(\frac{1+x_2}{x_1}, x_2 \right), \begin{pmatrix} 0 & -1 \\ 1 & 0 \end{pmatrix} \right) \\
\uparrow \mu_2 & & \downarrow \mu_2 \\
\left(\left(\frac{1+x_1}{x_2}, \frac{1+x_1+x_2}{x_1 x_2} \right), \begin{pmatrix} 0 & -1 \\ 1 & 0 \end{pmatrix} \right) & \xleftrightarrow{\mu_1} & \left(\left(\frac{1+x_2}{x_1}, \frac{1+x_1+x_2}{x_1 x_2} \right), \begin{pmatrix} 0 & 1 \\ -1 & 0 \end{pmatrix} \right)
\end{array}$$

Accordingly, we have

$$\mathcal{A}(\Sigma_{t_0}) = \mathcal{A}(\{\Sigma_t\}_{t \in \mathbb{T}_n}) = \mathbb{C} \left[x_1, x_2, \frac{1+x_2}{x_1}, \frac{1+x_1+x_2}{x_1 x_2}, \frac{1+x_1}{x_2} \right].$$

We notice that there are only five seeds in this case. Indeed, it is a cluster pattern of type A_2 (see Example 2.16).

Remark 2.7. One can associate a Y -pattern to a given cluster pattern in the following way. Let $\{(\mathbf{x}_t, \tilde{\mathcal{B}}_t)\}_{t \in \mathbb{T}_n}$ be a cluster pattern with $\mathbf{x}_t = (x_{1;t}, \dots, x_{m;t})$. For $t \in \mathbb{T}_n$ and $i \in [n]$, define $\hat{\mathbf{y}}_t = (\hat{y}_{1;t}, \dots, \hat{y}_{n;t})$ to be

$$\hat{y}_{i;t} = \prod_{j \in [m]} x_{j;t}^{b_{i,j}^{(t)}}.$$

Here, $\tilde{\mathcal{B}}_t = (b_{i,j}^{(t)})$ and \mathcal{B}_t is the principal part of $\tilde{\mathcal{B}}_t$. Then, the assignment $t \mapsto (\hat{\mathbf{y}}_t, \mathcal{B})$ provides a Y -pattern and commutes with the mutation maps. Indeed, denoting by p^* the assignment $(\hat{\mathbf{y}}_t, \mathcal{B}) \mapsto (\mathbf{x}_t, \tilde{\mathcal{B}}_t)$, we obtain $\mu_k(p^*(\hat{\mathbf{y}}_t, \mathcal{B})) = p^*(\mu_k(\hat{\mathbf{y}}_t, \mathcal{B}))$.

2.1.2. Seed tori and cluster varieties. For each seed $\mathbf{x}_t = (x_{1;t}, \dots, x_{m;t})$, define a torus

$$T_{\mathcal{A};t} := \text{Spec } \mathbb{C}[x_{1;t}^{\pm 1}, \dots, x_{n;t}^{\pm 1}],$$

called a *seed tori*. Similarly, we define a Y -seed torus $T_{\mathcal{X};t} := \text{Spec } \mathbb{C}[y_{1;t}^{\pm 1}, \dots, y_{n;t}^{\pm 1}]$.

For every edge $t \xrightarrow{k} t'$ in \mathbb{T}_n , the associated seed tori are related by the mutation maps

$$T_{\mathcal{A};t} \xleftarrow{\mu_k} T_{\mathcal{A};t'} \quad T_{\mathcal{X};t} \xleftarrow{\mu_k} T_{\mathcal{X};t'}.$$

The \mathcal{A} -cluster variety \mathcal{A} (also called a cluster \mathcal{A} -variety or a cluster K_2 variety) is $\text{Spec}(\mathcal{A}(\{(\mathbf{x}_t, \tilde{\mathcal{B}}_t)\}_{t \in \mathbb{T}_n}))$. The \mathcal{X} -cluster variety \mathcal{X} (also called a cluster \mathcal{X} -variety or a cluster Poisson variety) is given by gluing the seed tori $T_{\mathcal{X};t}$. We call $T_{\mathcal{A};t}$ (respectively, $T_{\mathcal{X};t}$) a *cluster chart* when we consider it as an *embedded* torus in \mathcal{A} (respectively, in \mathcal{X}).

Remark 2.8. Let p^* be the assignment given in Remark 2.7. Then, p^* provides a map between two seed tori given by seeds \mathbf{x}_t and $\hat{\mathbf{y}}_t$:

$$p: \text{Spec } \mathbb{C}[x_{1;t}^{\pm 1}, \dots, x_{n;t}^{\pm 1}] \rightarrow \text{Spec } \mathbb{C}[\hat{y}_{1;t}^{\pm 1}, \dots, \hat{y}_{n;t}^{\pm 1}].$$

Indeed, we have a map $p: \mathcal{A} \rightarrow \mathcal{X}$, which is called the *ensemble map*.

Note that the mutation preserves the ranks of the exchange matrices. Indeed, it preserves the determinants of the principal parts of the exchange matrices up to sign as proved in [4, Lemma 3.2]. Accordingly, under the situation in Remark 2.7, if the exchange matrix $\tilde{\mathcal{B}}_t$ has full rank, then the variables $\hat{y}_{1;t}, \dots, \hat{y}_{n;t}$ are algebraically independent. Furthermore, if the exchange matrix $\tilde{\mathcal{B}}_t$ is square having determinant ± 1 , then p^* provides an isomorphism between the coordinate rings $\mathbb{C}[x_{1;t}^{\pm 1}, \dots, x_{n;t}^{\pm 1}]$ and $\mathbb{C}[\hat{y}_{1;t}^{\pm 1}, \dots, \hat{y}_{n;t}^{\pm 1}]$ of seed tori.

We summarize useful results for later use.

Proposition 2.9 ([30, Theorem A.12]). *Let \mathcal{Q} be a quiver of full rank, and let \mathcal{A} be the corresponding cluster \mathcal{A} -variety defined over \mathbb{C} . The cluster charts of distinct cluster seeds of \mathcal{A} do not coincide. Indeed, there is a bijective correspondence between the set of cluster charts and that of cluster seeds.*

The full rank condition in the above proposition does not necessarily hold in general. However, if one could find an appropriate *extension* of a given quiver by adding some vertices and edges, one could distinguish seed tori. We note that, for $n \leq m$, one can naturally embed the n -regular tree \mathbb{T}_n to the m -regular tree \mathbb{T}_m .

Corollary 2.10. *Let \mathcal{Q} be a quiver on $[m]$ of full rank whose exchange matrix is square having determinant ± 1 , and let $\{(\mathbf{y}_t, \mathcal{B}_t)\}_{t \in \mathbb{T}_m}$ be the corresponding Y -pattern. Let $\{T_{\mathcal{X};t}\}_{t \in \mathbb{T}_m}$ be the set of Y -cluster charts corresponding to \mathcal{Q} . For $n < m$, there is a bijective correspondence between the subset $\{T_{\mathcal{X};t}\}_{t \in \mathbb{T}_n}$ of Y -cluster charts and the subset $\{(\mathbf{y}_t, \mathcal{B}_t)\}_{t \in \mathbb{T}_n}$ of Y -cluster seeds.*

Proof. Since \mathcal{Q} is a quiver of full rank, by Proposition 2.9, there is a bijective correspondence between the set of seed tori $\{T_{\mathcal{A};t}\}_{t \in \mathbb{T}_m}$ and the set of cluster seeds $\{(\mathbf{x}_t, \tilde{\mathcal{B}}_t)\}_{t \in \mathbb{T}_m}$. On the other hand, since the exchange matrix of \mathcal{Q} is square having determinant ± 1 , the ensemble map provides an isomorphism between a seed torus $T_{\mathcal{A};t}$ and a Y -seed torus $T_{\mathcal{X};t}$. Accordingly, there is a bijective correspondence

between the set of Y -cluster charts $\{T_{\mathcal{X};t}\}_{t \in \mathbb{T}_m}$ and cluster charts $\{T_{\mathcal{A};t}\}_{t \in \mathbb{T}_m}$.

$$\begin{array}{ccccc}
 \{(\mathbf{y}_t, \mathcal{B}_t)\}_{t \in \mathbb{T}_n} & \hookrightarrow & \{(\mathbf{y}_t, \mathcal{B}_t)\}_{t \in \mathbb{T}_m} & \xleftrightarrow{\text{bijective}} & \{(\mathbf{x}_t, \tilde{\mathcal{B}}_t)\}_{t \in \mathbb{T}_m} \\
 \downarrow & & \updownarrow \text{bijective} & & \updownarrow \text{bijective} \\
 \{T_{\mathcal{X};t}\}_{t \in \mathbb{T}_n} & \hookrightarrow & \{T_{\mathcal{X};t}\}_{t \in \mathbb{T}_m} & \xleftrightarrow{\text{bijective}} & \{T_{\mathcal{A};t}\}_{t \in \mathbb{T}_m}
 \end{array}$$

Therefore, the correspondence between the set of Y -cluster charts $\{T_{\mathcal{X};t}\}_{t \in \mathbb{T}_m}$ and that of Y -cluster seeds $\{(\mathbf{y}_t, \mathcal{B}_t)\}_{t \in \mathbb{T}_m}$ is bijective. \blacksquare

2.2. Cluster algebras of Dynkin type

The number of cluster variables in Example 2.6 is finite even though the number of vertices in the graph \mathbb{T}_2 is infinite. We call such cluster algebras *of finite type*. More precisely, we recall the following definition.

Definition 2.11 ([26]). A cluster algebra is said to be *of finite type* if it has finitely many cluster variables.

It has been realized that classifying finite-type cluster algebras is related to studying exchange matrices. The *Cartan counterpart* $C(\mathcal{B}) = (c_{i,j})$ of the principal part \mathcal{B} of an exchange matrix $\tilde{\mathcal{B}}$ is defined by

$$c_{i,j} = \begin{cases} 2 & \text{if } i = j, \\ -|b_{i,j}| & \text{otherwise.} \end{cases}$$

Since \mathcal{B} is skew-symmetrizable, its Cartan counterpart $C(\mathcal{B})$ is symmetrizable.

We say that a quiver \mathcal{Q} is *acyclic* if it does not have directed cycles. Similarly, for a skew-symmetrizable matrix $\mathcal{B} = (b_{i,j})$, we say that it is *acyclic* if there are no sequences j_1, j_2, \dots, j_ℓ with $\ell \geq 3$ such that

$$b_{j_1, j_2}, b_{j_2, j_3}, \dots, b_{j_{\ell-1}, j_\ell}, b_{j_\ell, j_1} > 0.$$

We say a seed $\Sigma = (\mathbf{x}, \tilde{\mathcal{B}})$ is *acyclic* if so is its principal part \mathcal{B} .

Definition 2.12. For a finite or affine Dynkin type Z , we define a quiver \mathcal{Q} , a matrix $\tilde{\mathcal{B}}$, a cluster pattern $\{(\mathbf{x}_t, \tilde{\mathcal{B}}_t)\}_{t \in \mathbb{T}_n}$, a Y -pattern $\{(\mathbf{y}_t, \mathcal{B}_t)\}_{t \in \mathbb{T}_n}$, or a cluster algebra $\mathcal{A}(\mathbf{x}_{t_0}, \tilde{\mathcal{B}}_{t_0})$ of type Z as follows.

- (1) A quiver is *of type* Z if it is mutation equivalent to an *acyclic* quiver whose underlying graph is isomorphic to the Dynkin diagram of type Z .
- (2) A skew-symmetrizable matrix \mathcal{B} is *of type* Z if it is mutation equivalent to an acyclic skew-symmetrizable matrix whose Cartan counterpart $C(\mathcal{B})$ is isomorphic to the Cartan matrix of type Z .

- (3) A cluster pattern $\{(\mathbf{x}_t, \tilde{\mathcal{B}}_t)\}_{t \in \mathbb{T}_n}$ or a Y -pattern $\{(\mathbf{y}_t, \mathcal{B}_t)\}_{t \in \mathbb{T}_n}$ is of type Z if, for some $t \in \mathbb{T}_n$, the Cartan counterpart $C(\mathcal{B}_t)$ is of type Z .
- (4) A cluster algebra $\mathcal{A}(\mathbf{x}_{t_0}, \tilde{\mathcal{B}}_{t_0})$ is of type Z if its cluster pattern is of type Z .

Here, we say that two matrices C_1 and C_2 are *isomorphic* if they are conjugate to each other via a permutation matrix, that is, $C_2 = P^{-1}C_1P$ for some permutation matrix P . One may wonder whether there exist exchange matrices in the same seed pattern having different Dynkin types. However, it is proved in [9, Corollary 4] that if two acyclic skew-symmetrizable matrices are mutation equivalent, then there exists a sequence of mutations from one to another such that intermediate skew-symmetrizable matrices are all acyclic. Indeed, if two acyclic skew-symmetrizable matrices are mutation equivalent, then their Cartan counterparts are isomorphic.

Proposition 2.13 (Cf. [9, Corollary 4]). *Let \mathcal{B} and \mathcal{B}' be acyclic skew-symmetrizable matrices. Then, the following are equivalent:*

- (1) *the Cartan matrices $C(\mathcal{B})$ and $C(\mathcal{B}')$ are isomorphic;*
- (2) *\mathcal{B} and \mathcal{B}' are mutation equivalent.*

Accordingly, a quiver, a matrix, a cluster pattern, or a cluster algebra of type Z are well defined. The following theorem presents a classification of cluster algebras of finite type.

Theorem 2.14 ([26]). *Let $\{(\mathbf{x}_t, \tilde{\mathcal{B}}_t)\}_{t \in \mathbb{T}_n}$ be a cluster pattern with an initial seed $(\mathbf{x}_{t_0}, \tilde{\mathcal{B}}_{t_0})$. Let $\mathcal{A}(\mathbf{x}_{t_0}, \tilde{\mathcal{B}}_{t_0})$ be the corresponding cluster algebra. Then, the cluster algebra $\mathcal{A}(\mathbf{x}_{t_0}, \tilde{\mathcal{B}}_{t_0})$ is of finite type if and only if $\mathcal{A}(\mathbf{x}_{t_0}, \tilde{\mathcal{B}}_{t_0})$ is of finite Dynkin type.*

We provide a list of all of the irreducible finite-type root systems and their Dynkin diagram in Table 1 (cf. [34]). In Tables 2 and 3, we present lists of standard affine root systems and twisted affine root systems, respectively. They are the same as presented in [36, Tables Aff 1, Aff 2, and Aff 3, Chapter 4], and we denote by $\tilde{Z} = Z^{(1)}$. We notice that the number of vertices of the standard affine Dynkin diagram of type \tilde{Z}_{n-1} is n while we do not specify the vertex numbering.

We note that all Dynkin diagrams of finite or affine type but \tilde{A}_{n-1} do not have (undirected) cycles. Accordingly, we may omit the acyclicity condition in Definition 2.12 except \tilde{A}_{n-1} -type. On the other hand, if a quiver is a directed n -cycle, then the corresponding Cartan counterpart is of type \tilde{A}_{n-1} while it is mutation equivalent to a quiver of type D_n (see [46, Type IV]).

The mutation equivalence classes of acyclic quivers of type \tilde{A}_{n-1} are described in [22, Lemma 6.8]. Let \mathcal{Q} and \mathcal{Q}' be two n -cycles for $n \geq 3$. Suppose that, in \mathcal{Q} , there are p edges of one direction and $q = n - p$ edges of the opposite direction. Also, in \mathcal{Q}' , there are p' edges of one direction and $q' = n - p'$ edges of the opposite direction.

Φ	Dynkin diagram
$A_n (n \geq 1)$	
$B_n (n \geq 2)$	
$C_n (n \geq 3)$	
$D_n (n \geq 4)$	
E_6	
E_7	
E_8	
F_4	
G_2	

Table 1. Dynkin diagrams of finite type.

Then, two quivers \mathcal{Q} and \mathcal{Q}' are mutation equivalent if and only if the unordered pairs $\{p, q\}$ and $\{p', q'\}$ coincide. We say that a quiver \mathcal{Q} is of type $\tilde{A}_{p,q}$ if it has p edges of one direction and q edges of the opposite direction. We depict some examples for quivers of type $\tilde{A}_{p,q}$ in Figure 8.

For a Dynkin type Z , we say that Z is *simply-laced* if its Dynkin diagram has only single edges; otherwise, Z is *non-simply-laced*. Recall that the Cartan matrix associated to a Dynkin diagram Z can be read directly from the diagram Z as follows:

$c_{i,j} = -1$	$c_{i,j} = -2$	$c_{i,j} = -3$	$c_{i,j} = -4$	$c_{i,j} = -2$
$c_{j,i} = -1$	$c_{j,i} = -1$	$c_{j,i} = -1$	$c_{j,i} = -1$	$c_{j,i} = -2$

For example, the Cartan matrix $(c_{i,j})$ of the diagram of type G_2 is

$$\begin{pmatrix} 2 & -1 \\ -3 & 2 \end{pmatrix}. \tag{2.1}$$

Φ	Dynkin diagram
\tilde{A}_1	
$\tilde{A}_{n-1} (n \geq 3)$	
$\tilde{B}_{n-1} (n \geq 4)$	
$\tilde{C}_{n-1} (n \geq 3)$	
$\tilde{D}_{n-1} (n \geq 5)$	
\tilde{E}_6	
\tilde{E}_7	
\tilde{E}_8	
\tilde{F}_4	
\tilde{G}_2	

Table 2. Dynkin diagrams of standard affine root systems.

Therefore, for each non-simply-laced Dynkin diagram Z , any exchange matrix \mathcal{B} of type Z is *not* skew-symmetric but skew-symmetrizable. Hence, it never comes from any quiver.

Assumption 2.15. Throughout this paper, we assume that, for any cluster algebra, the principal part \mathcal{B}_{t_0} of the initial exchange matrix is acyclic of *finite or affine Dynkin* type unless mentioned otherwise.

Φ	Dynkin diagram
$A_2^{(2)}$	
$A_{2(n-1)}^{(2)} (n \geq 3)$	
$A_{2(n-1)-1}^{(2)} (n \geq 4)$	
$D_n^{(2)} (n \geq 3)$	
$E_6^{(2)}$	
$D_4^{(3)}$	

Table 3. Dynkin diagrams of twisted affine root systems.

In Table 4, we provide enumeration on the number of cluster variables and clusters in each cluster algebra of finite (irreducible) type (cf. [24, Figure 5.17]).

Example 2.16. Continuing Example 2.6, the Cartan counterpart of the principal part \mathcal{B}_{t_0} is given by

$$C(\mathcal{B}_{t_0}) = \begin{pmatrix} 2 & -1 \\ -1 & 2 \end{pmatrix},$$

which is the Cartan matrix of type A_2 . Accordingly, by Theorem 2.14, the cluster algebra $\mathcal{A}(\mathbf{x}_{t_0}, \tilde{\mathcal{B}}_{t_0})$ is of finite type. Indeed, there are only five seeds in the seed pattern.

2.3. Folding

Under certain conditions, one can *fold* cluster patterns to produce new ones. This procedure is used to study cluster algebras of non-simply-laced type from those of simply-laced type (see Figure 9 and Table 5). In this section, we recall *folding* of cluster algebras from [24]. We also refer the reader to [18].

Let \mathcal{Q} be a quiver on $[m]$. Let G be a finite group acting on the set $[m]$. The notation $i \sim i'$ will mean that i and i' lie in the same G -orbit. To study folding of cluster algebras, we prepare some terminologies.

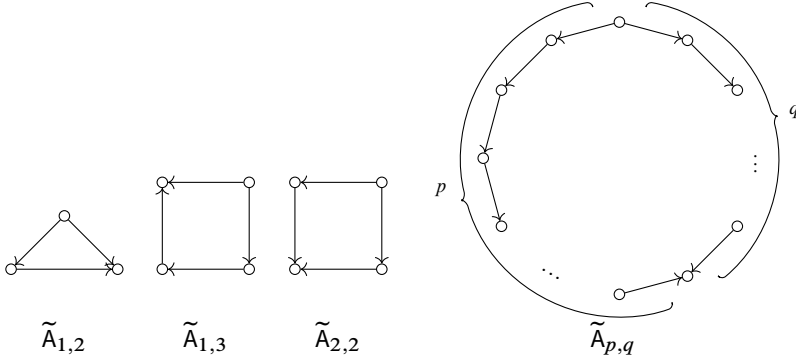


Figure 8. Quivers of type $\tilde{A}_{p,q}$.

Φ	A_n	B_n	C_n	D_n
#seeds	$\frac{1}{n+2} \binom{2n+2}{n+1}$	$\binom{2n}{n}$	$\binom{2n}{n}$	$\frac{3n-2}{n} \binom{2n-2}{n-1}$
#clvar	$\frac{n(n+3)}{2}$	$n(n+1)$	$n(n+1)$	n^2

Φ	E_6	E_7	E_8	F_4	G_2
#seeds	833	4160	25080	105	8
#clvar	42	70	128	28	8

Table 4. Enumeration of seeds and cluster variables.

Z	A_{2n-1}	D_{n+1}	E_6	D_4	$\tilde{A}_{2,2}$	$\tilde{A}_{n,n}$	\tilde{D}_4	
G	$\mathbb{Z}/2\mathbb{Z}$	$\mathbb{Z}/2\mathbb{Z}$	$\mathbb{Z}/2\mathbb{Z}$	$\mathbb{Z}/3\mathbb{Z}$	$\mathbb{Z}/2\mathbb{Z}$	$\mathbb{Z}/2\mathbb{Z}$	$(\mathbb{Z}/2\mathbb{Z})^2$	$\mathbb{Z}/3\mathbb{Z}$
Z^G	B_n	C_n	F_4	G_2	\tilde{A}_1	$D_{n+1}^{(2)}$	$A_2^{(2)}$	$D_4^{(3)}$
Z		\tilde{D}_n		\tilde{D}_{2n}		\tilde{E}_6	\tilde{E}_7	
G	$\mathbb{Z}/2\mathbb{Z}$	$\mathbb{Z}/2\mathbb{Z}$	$\mathbb{Z}/2\mathbb{Z}$	$(\mathbb{Z}/2\mathbb{Z})^2$	$\mathbb{Z}/3\mathbb{Z}$	$\mathbb{Z}/2\mathbb{Z}$	$\mathbb{Z}/2\mathbb{Z}$	
Z^G	\tilde{C}_{n-2}	$A_{2(n-1)-1}^{(2)}$	\tilde{B}_n	$A_{2n-2}^{(2)}$	\tilde{G}_2	$E_6^{(2)}$	\tilde{F}_4	

Table 5. Foldings appearing in finite and affine Dynkin diagrams.

We denote by $\tilde{\mathcal{B}} = \tilde{\mathcal{B}}(\mathcal{Q})$ the submatrix $(b_{i,j})_{1 \leq i \leq m, 1 \leq j \leq n}$ of the adjacency matrix $(b_{i,j})_{1 \leq i, j \leq m}$ of the quiver \mathcal{Q} . Also, we denote by $\mathcal{B} = \mathcal{B}(\mathcal{Q})$ the principal part of $\tilde{\mathcal{B}}(\mathcal{Q})$. For each $g \in G$, let $\mathcal{Q}' = g \cdot \mathcal{Q}$ be the quiver such that

$$\tilde{\mathcal{B}}(\mathcal{Q}') = (b'_{i,j})$$

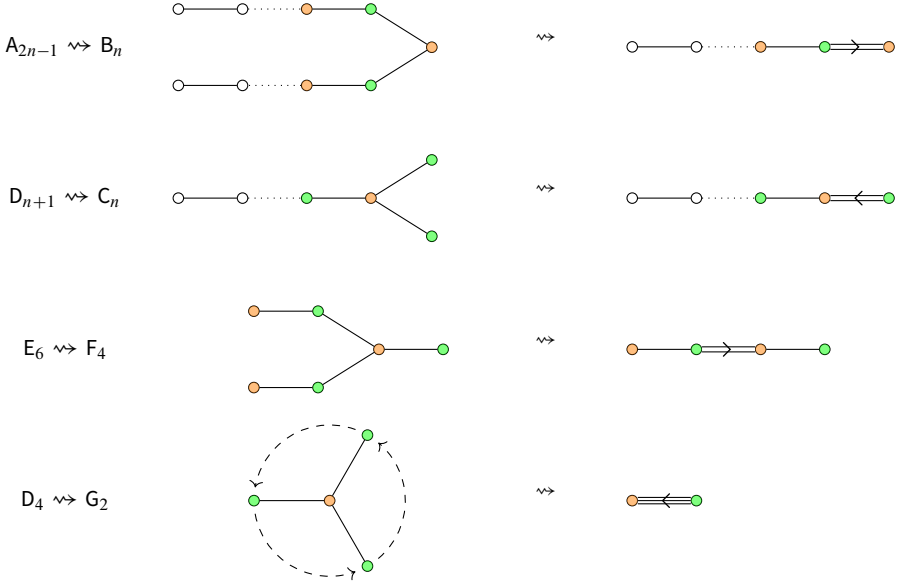


Figure 9. Foldings in Dynkin diagrams of finite type (for seed patterns).

is given by

$$b'_{i,j} = b_{g(i),b(j)}.$$

Definition 2.17 (Cf. [24, Section 4.4] and [18, Section 3]). Let \mathcal{Q} be a quiver on $[m]$ and G a finite group acting on the set $[m]$.

- (1) A quiver \mathcal{Q} is G -invariant if $g \cdot \mathcal{Q} = \mathcal{Q}$ for any $g \in G$.
- (2) A G -invariant quiver \mathcal{Q} is G -admissible if
 - (a) for any $i \sim i'$, index i is mutable if and only if so is i' ;
 - (b) for mutable indices $i \sim i'$, we have $b_{i,i'} = 0$;
 - (c) for any $i \sim i'$ and any mutable j , we have $b_{i,j}b_{i',j} \geq 0$.
- (3) For a G -admissible quiver \mathcal{Q} , we call a G -orbit *mutable* (respectively, *frozen*) if it consists of mutable (respectively, frozen) vertices.

For a G -admissible quiver \mathcal{Q} , we define the matrix

$$\tilde{\mathcal{B}}^G = \tilde{\mathcal{B}}(\mathcal{Q})^G = (b_{I,J}^G)$$

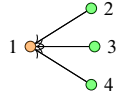
whose rows (respectively, columns) are labeled by the G -orbits (respectively, mutable G -orbits) by

$$b_{I,J}^G = \sum_{i \in I} b_{i,j},$$

where j is an arbitrary index in J . We then say $\tilde{\mathcal{B}}^G$ is obtained from $\tilde{\mathcal{B}}$ (or from the quiver \mathcal{Q}) by *folding* with respect to the given G -action.

Remark 2.18. We note that the G -admissibility and the folding can also be defined for exchange matrices.

Example 2.19. Let \mathcal{Q} be a quiver of type D_4 given as follows.



$$\rightsquigarrow \tilde{\mathcal{B}}(\mathcal{Q}) = \begin{pmatrix} 0 & -1 & -1 & -1 \\ 1 & 0 & 0 & 0 \\ 1 & 0 & 0 & 0 \\ 1 & 0 & 0 & 0 \end{pmatrix}$$

The finite group $G = \mathbb{Z}/3\mathbb{Z}$ acts on $[4]$ by sending $2 \mapsto 3 \mapsto 4 \mapsto 2$ and $1 \mapsto 1$. Here, we decorate vertices of the quiver \mathcal{Q} with **green** and **orange** colors for presenting sources and sinks, respectively. One may check that the quiver \mathcal{Q} is G -admissible. By setting $I_1 = \{1\}$ and $I_2 = \{2, 3, 4\}$, we obtain

$$b_{I_1, I_2}^G = \sum_{i \in I_1} b_{i, 2} = b_{1, 2} = -1,$$

$$b_{I_2, I_1}^G = \sum_{i \in I_2} b_{i, 1} = b_{2, 1} + b_{3, 1} + b_{4, 1} = 3.$$

Accordingly, we obtain the matrix $\tilde{\mathcal{B}}^G = \begin{pmatrix} 0 & -1 \\ 3 & 0 \end{pmatrix}$ whose Cartan counterpart is the Cartan matrix of type G_2 (cf. (2.1)).

For a G -admissible quiver \mathcal{Q} and a mutable G -orbit I , we consider a composition of mutations given by

$$\mu_I = \prod_{i \in I} \mu_i$$

which is well defined because of the definition of admissible quivers (cf. Remark 2.4). Moreover, $\mu_I(\mathcal{Q})$ is G -invariant by [18, Lemma 5.12]. If $\mu_I(\mathcal{Q})$ is G -admissible, then we have

$$(\mu_I(\tilde{\mathcal{B}}))^G = \mu_I(\tilde{\mathcal{B}}^G).$$

We notice that the quiver $\mu_I(\mathcal{Q})$ is *not* G -admissible in general. Therefore, we present the following definition.

Definition 2.20. Let G be a group acting on the vertex set of a quiver \mathcal{Q} . We say that \mathcal{Q} is *globally foldable* with respect to G if \mathcal{Q} is G -admissible, and moreover for any sequence of mutable G -orbits I_1, \dots, I_ℓ , the quiver $(\mu_{I_\ell} \cdots \mu_{I_1})(\mathcal{Q})$ is G -admissible.

For a globally foldable quiver, we can fold all the seeds in the corresponding seed pattern. Let \mathbb{F}^G be the field of rational functions in $\#([m]/G)$ independent variables. Let $\psi: \mathbb{F} \rightarrow \mathbb{F}^G$ be a surjective homomorphism. A seed $(\mathbf{x}, \tilde{\mathcal{B}})$ or a Y -seed $(\mathbf{y}, \mathcal{B})$ is called (G, ψ) -invariant or *admissible* if

- \mathcal{Q} is a G -invariant or admissible quiver, respectively;
- we have

$$\psi(x_i) = \psi(x_{i'}) \quad \text{or} \quad \psi(y_i) = \psi(y_{i'}) \quad \text{for any } i \sim i'. \quad (2.2)$$

In this situation, we define new “folded” seed $(\mathbf{x}, \tilde{\mathcal{B}})^G = (\mathbf{x}^G, \tilde{\mathcal{B}}^G)$ and Y -seed $(\mathbf{y}, \mathcal{B})^G = (\mathbf{y}^G, \mathcal{B}^G)$ in \mathbb{F}^G whose exchange matrix is given as before and cluster variables $\mathbf{x}^G = (x_I)$ and $\mathbf{y}^G = (y_I)$ are indexed by the G -orbits and given by $x_I = \psi(x_i)$ and $y_I = \psi(y_i)$ for a G -orbit I and $i \in I$.

We notice that, for a (G, ψ) -admissible seed $(\mathbf{x}, \tilde{\mathcal{B}})$ or a (G, ψ) -admissible Y -seed $(\mathbf{y}, \mathcal{B})$, the folding process is equivariant under the orbit-wise mutation; that is, for any mutable G -orbit I , we have

$$(\mu_I(\mathbf{x}, \tilde{\mathcal{B}}))^G = \mu_I((\mathbf{x}, \tilde{\mathcal{B}})^G) \quad \text{and} \quad (\mu_I(\mathbf{y}, \mathcal{B}))^G = \mu_I((\mathbf{y}, \mathcal{B})^G).$$

Proposition 2.21 (Cf. [24, Corollary 4.4.11]). *Let \mathcal{Q} be a quiver which is globally foldable with respect to a group G acting on the set of its vertices. Let $(\mathbf{x}, \tilde{\mathcal{B}})$ and $(\mathbf{y}, \mathcal{B})$ be a seed and a Y -seed in the field \mathbb{F} of rational functions freely generated by $\mathbf{x} = (x_1, \dots, x_m)$. Then, we have the following.*

- (1) *Let $\psi: \mathbb{F} \rightarrow \mathbb{F}^G$ be the homomorphism satisfying (2.2). Then, for any mutable G -orbits I_1, \dots, I_ℓ , the seed $(\mu_{I_\ell} \cdots \mu_{I_1})(\mathbf{x}, \tilde{\mathcal{B}})$ is (G, ψ) -admissible, and moreover, the folded seeds $((\mu_{I_\ell} \cdots \mu_{I_1})(\mathbf{x}, \tilde{\mathcal{B}}))^G$ form a seed pattern in \mathbb{F}^G with the initial seed $(\mathbf{x}, \tilde{\mathcal{B}})^G = (\mathbf{x}^G, \tilde{\mathcal{B}}^G)$.*
- (2) *Let $\psi: \mathbb{F} \rightarrow \mathbb{F}^G$ be the homomorphism satisfying (2.2). Then, for any mutable G -orbits I_1, \dots, I_ℓ , the Y -seed $(\mu_{I_\ell} \cdots \mu_{I_1})(\mathbf{y}, \mathcal{B})$ is (G, ψ) -admissible, and moreover, the folded Y -seeds $((\mu_{I_\ell} \cdots \mu_{I_1})(\mathbf{y}, \mathcal{B}))^G$ form a Y -pattern in \mathbb{F}^G with the initial seed $(\mathbf{y}, \mathcal{B})^G = (\mathbf{y}^G, \mathcal{B}^G)$.*

Example 2.22. The quiver in Example 2.19 is globally foldable, and moreover, the corresponding seed pattern is of type G_2 . In fact, seed patterns of type BCFG are obtained by folding quivers of type ADE; seed patterns of type $\tilde{\text{BCFG}}$ are obtained by folding quivers of type $\tilde{\text{DE}}$ (cf. [21]). In Figures 9 and 10, we present the corresponding quivers of type ADE and type $\tilde{\text{E}}$. We decorate vertices of quivers with **green** and **orange** colors for presenting source and sink, respectively. As one may see, we put arrows on the Dynkin diagram alternatingly. The alternating colorings on quivers of type ADE provide those on quivers of type BCFG, as displayed in the right column

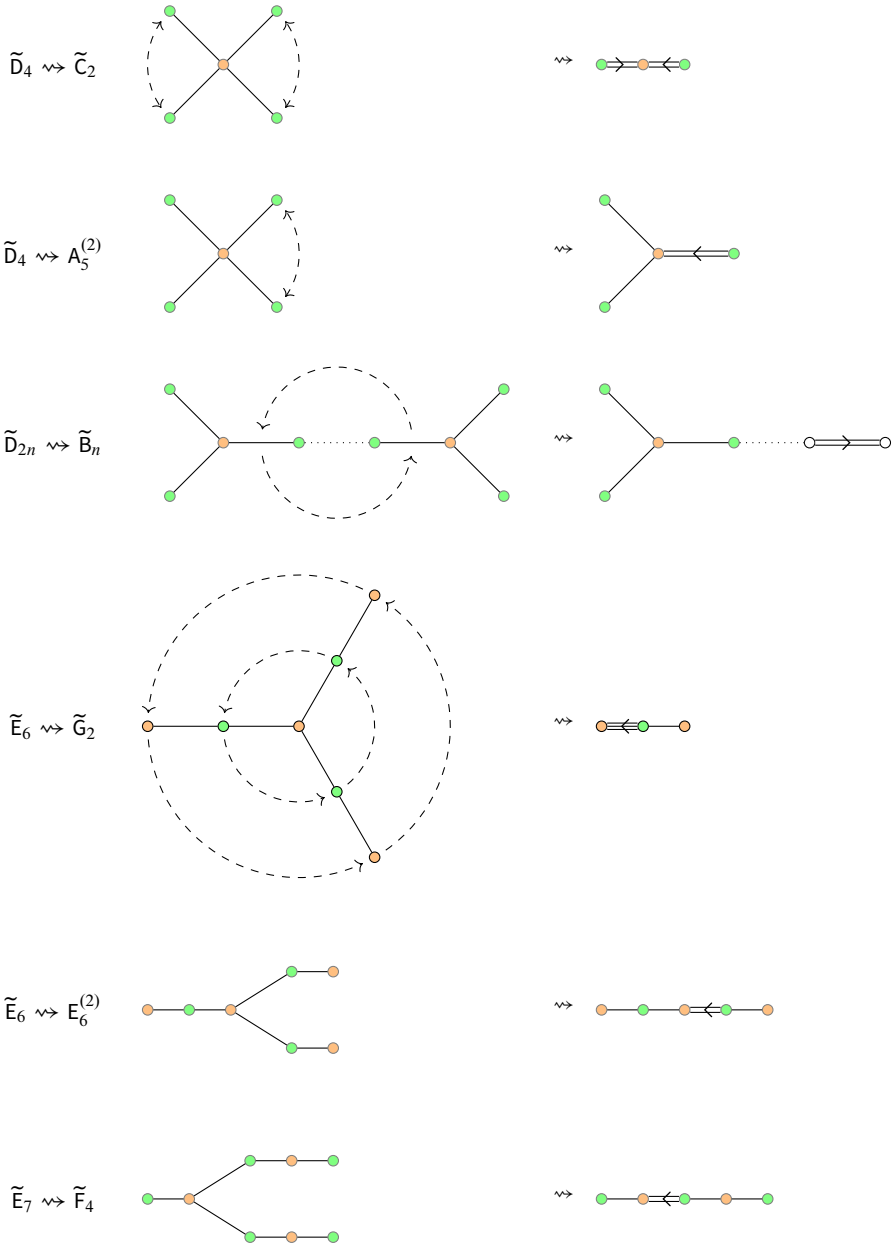


Figure 10. Foldings in Dynkin diagrams of affine type (for seed patterns).

of Figure 9. Foldings between simply-laced and non-simply-laced finite and affine Dynkin diagrams are given in Table 5.

For any quiver of type ADE, one can prove that the G -invariance is equivalent to the G -admissible as follows.

Theorem 2.23. *Let \mathcal{Q} be a quiver of type ADE, which is invariant under the G -action given by Figure 9. Then, the quiver \mathcal{Q} is G -admissible.*

We notice that the quiver considering in Theorem 2.23 can have any orientations so long as they are G -invariant. The proof of Theorem 2.23 is given in Appendix A. As a direct corollary of Theorem 2.23, we have the following.

Corollary 2.24. *Let \mathcal{Q} be a quiver of type ADE, which is invariant under the G -action given by Figure 9. Then, the quiver \mathcal{Q} is globally foldable.*

Proof. Let I be a mutable G -orbit. The quiver $\mu_I(\mathcal{Q})$ is again G -invariant (see [18, Lemma 5.12]), so it is G -admissible according to Theorem 2.23. Therefore, \mathcal{Q} is globally foldable. ■

As we saw in Definition 2.17, if a seed $\Sigma = (\mathbf{x}, \mathcal{Q})$ is (G, ψ) -admissible, then Σ is (G, ψ) -invariant. The converse holds when we consider the foldings presented in Table 5, and moreover, they form the folded cluster pattern.

Theorem 2.25 ([1]). *Let (Z, G, Z^G) be a triple given by a column of Table 5. Let $\Sigma_{t_0} = (\mathbf{x}_{t_0}, \mathcal{Q}_{t_0})$ be a seed in the field \mathbb{F} . Suppose that \mathcal{Q}_{t_0} is of type Z and G -admissible. Let $\psi: \mathbb{F} \rightarrow \mathbb{F}^G$ be the homomorphism satisfying (2.2). Then, for any seed $\Sigma = (\mathbf{x}, \mathcal{Q})$ in the cluster pattern, if the quiver \mathcal{Q} is G -invariant, then it is G -admissible. Indeed, \mathcal{Q} is globally foldable. Moreover, any (G, ψ) -invariant seed $\Sigma = (\mathbf{x}, \mathcal{Q})$ can be reached with a sequence of orbit mutations from the initial seed. Indeed, the set of such seeds forms the cluster pattern of the ‘folded’ cluster algebra $\mathcal{A}(\Sigma_{t_0}^G)$ of type Z^G .*

2.4. Combinatorics of exchange graphs

The *exchange graph* of a cluster pattern or a Y -pattern is the n -regular (finite or infinite) connected graph whose vertices are the seeds of the cluster pattern and whose edges connect the seeds related by a single mutation. In this section, we recall the combinatorics of exchange graphs which will be used later. For more details, we refer the reader to [26–28].

Definition 2.26 (Exchange graphs). Exchange graphs for seed patterns or Y -patterns are defined as follows.

- (1) The *exchange graph* $\text{Ex}(\{(\mathbf{x}_t, \tilde{\mathcal{B}}_t)\}_{t \in \mathbb{T}_n})$ of the cluster pattern $\{(\mathbf{x}_t, \tilde{\mathcal{B}}_t)\}_{t \in \mathbb{T}_n}$ is a quotient of the tree \mathbb{T}_n modulo the equivalence relation on vertices defined by setting $t \sim t'$ if and only if $(\mathbf{x}_t, \tilde{\mathcal{B}}_t) \sim (\mathbf{x}_{t'}, \tilde{\mathcal{B}}_{t'})$.

- (2) The *exchange graph* $\text{Ex}(\{(y_t, \mathcal{B}_t)\}_{t \in \mathbb{T}_n})$ of the Y -pattern $\{(y_t, \mathcal{B}_t)\}_{t \in \mathbb{T}_n}$ is a quotient of the tree \mathbb{T}_n modulo the equivalence relation on vertices defined by setting $t \sim t'$ if and only if $(y_t, \mathcal{B}_t) \sim (y_{t'}, \mathcal{B}_{t'})$.

For example, the exchange graph in Example 2.6 is a cycle graph with 5 vertices. As we already have seen in Theorem 2.14, cluster algebras of finite type are classified by Cartan matrices of finite type. Moreover, for a cluster algebra of finite or affine type, the exchange graph depends only on the exchange matrix (see Theorem 2.28). To explain this observation, we need some terminologies.

For $\Sigma_{t_0} = (\mathbf{x}_{t_0}, \tilde{\mathcal{B}}_{t_0})$, the cluster algebra $\mathcal{A}(\Sigma_{t_0})$ is said to have *principal coefficients* if the exchange matrix $\tilde{\mathcal{B}}_{t_0}$ is a $(2n \times n)$ -matrix of the form $\begin{pmatrix} \mathcal{B}_{t_0} \\ \mathcal{I}_n \end{pmatrix}$, and have *trivial coefficients* if $\tilde{\mathcal{B}}_{t_0} = \mathcal{B}_{t_0}$. Here, \mathcal{I}_n is the identity matrix of size $n \times n$. We recall the following result on the combinatorics of exchange graphs.

Theorem 2.27 ([28, Theorem 4.6]). *The exchange graph of an arbitrary cluster pattern $\{(\mathbf{x}_t, \tilde{\mathcal{B}}_t)\}_{t \in \mathbb{T}_n}$ is covered by¹ that of the cluster pattern $\{(\mathbf{x}_t, \tilde{\mathcal{B}}'_t)\}_{t \in \mathbb{T}_n}$ having principal coefficients such that the principal parts of $\tilde{\mathcal{B}}_t$ and $\tilde{\mathcal{B}}'_t$ are the same.*

Moreover, the exchange graph of the cluster pattern $\{(\mathbf{x}_t, \tilde{\mathcal{B}}_t)\}_{t \in \mathbb{T}_n}$ having trivial coefficients is covered by the exchange graph of the cluster pattern whose initial exchange matrix has the principal part $\tilde{\mathcal{B}}_{t_0}$. For a fixed principal part of the exchange matrix, the cluster pattern having principal coefficients has the largest exchange graph while that having trivial coefficients has the smallest one (see [28, Section 4]).

However, it is unknown whether the largest exchange graph is strictly larger than the smallest one or not. Indeed, it is conjectured in [28, Conjecture 4.3] that the exchange graph of a cluster pattern is determined by the initial principal part \mathcal{B}_{t_0} only. The conjecture is confirmed for finite cases [26] or exchange matrices coming from quivers [16]. We furthermore extend this result to cluster algebras whose initial exchange matrices are of affine type.

Theorem 2.28 (Cf. [26, Theorem 1.13] and [16, Theorem 4.6]). *Let $\Sigma_{t_0} = (\mathbf{x}_{t_0}, \tilde{\mathcal{B}}_{t_0})$ be an initial seed. If the principal part \mathcal{B}_{t_0} of $\tilde{\mathcal{B}}_{t_0}$ is of finite or affine type, then the exchange graph of the cluster pattern $\{(\mathbf{x}_t, \tilde{\mathcal{B}}_t)\}_{t \in \mathbb{T}_n}$ only depends on \mathcal{B}_{t_0} .*

Proof. We first notice that the statement holds if the principal part \mathcal{B}_{t_0} is of finite type [26, Theorem 1.13] or exchange matrices are obtained from quivers [16, Theorem 4.6]. It is enough to consider the case when the principal part is of *non-simply-laced*

¹We say that a graph \tilde{G} is a *covering graph* of another graph G , or say G is *covered* by \tilde{G} , if there is a covering map f from the vertex set $V(\tilde{G})$ of \tilde{G} to the vertex set $V(G)$ of G . Here, a *covering map* f is a surjection such that the neighborhood of a vertex v in \tilde{G} is mapped bijectively onto the neighborhood of the vertex $f(v)$ in G .

affine type. Let (Z, G, Z^G) be a column in Table 5. Let $\mathcal{Q}(Z)$ be the quiver of type Z , and let $\mathcal{B}(Z) = \mathcal{B}(\mathcal{Q}(Z))$ be the adjacency matrix of $\mathcal{Q}(Z)$, which is a square matrix of size n . Let $\tilde{\mathcal{B}}(Z) = \begin{pmatrix} \mathcal{B}(Z) \\ I_n \end{pmatrix}$ be the $(2n \times n)$ matrix having principal coefficients whose principal part is $\mathcal{B}(Z)$. On the other hand, we consider a quiver $\bar{\mathcal{Q}}(Z)$ by adding $n^G := \#([n]/G)$ frozen vertices and n arrows. Here, each frozen vertex is indexed by a G -orbit, and we draw an arrow from the frozen vertex to each mutable vertex in the corresponding G -orbit. For algebraic independent elements $\mathbf{x} = (x_1, \dots, x_n)$, $\bar{\mathbf{x}} = (x_1, \dots, x_n, x_{n+1}, \dots, x_{n+n^G})$, and $\tilde{\mathbf{x}} = (x_1, \dots, x_n, x_{n+1}, \dots, x_{2n})$ in \mathbb{F} , we obtain seeds

$$\tilde{\Sigma}_{t_0} = (\tilde{\mathbf{x}}, \tilde{\mathcal{B}}(Z)), \quad \bar{\Sigma}_{t_0} = (\bar{\mathbf{x}}, \mathcal{B}(\bar{\mathcal{Q}}(Z))), \quad \text{and} \quad \Sigma_{t_0} = (\mathbf{x}, \mathcal{B}(Z)).$$

Since the exchange matrices come from quivers, the exchange graphs given by seeds $\tilde{\Sigma}_{t_0}, \bar{\Sigma}_{t_0}, \Sigma_{t_0}$ are isomorphic:

$$\text{Ex}(\{\tilde{\Sigma}_t\}_{t \in \mathbb{T}_n}) \cong \text{Ex}(\{\bar{\Sigma}_t\}_{t \in \mathbb{T}_n}) \cong \text{Ex}(\{\Sigma_t\}_{t \in \mathbb{T}_n}).$$

Indeed, we have

$$\{\tilde{\Sigma}_t\}_{t \in \mathbb{T}_n} / \sim = \{\bar{\Sigma}_t\}_{t \in \mathbb{T}_n} / \sim = \{\Sigma_t\}_{t \in \mathbb{T}_n} / \sim. \quad (2.3)$$

Extending the action of G on \mathcal{Q} of type Z to $\bar{\mathcal{Q}}(Z)$ such that G acts trivially on frozen vertices, the quiver $\bar{\mathcal{Q}}(Z)$ becomes a globally foldable quiver with respect to G (see [24, Lemma 5.5.3]). Moreover, via $\psi: \mathbb{F} \rightarrow \mathbb{F}^G$, the folded seed $\bar{\Sigma}_{t_0}^G = (\bar{\mathbf{x}}, \bar{\mathcal{Q}}(Z))^G$ produces the principal coefficient cluster algebra of type Z^G . This produces the following diagram.

$$\begin{array}{ccccc} \{\tilde{\Sigma}_t\}_{t \in \mathbb{T}_n} / \sim & \xlongequal{\quad} & \{\bar{\Sigma}_t\}_{t \in \mathbb{T}_n} / \sim & \xlongequal{\quad} & \{\Sigma_t\}_{t \in \mathbb{T}_n} / \sim \\ & & \uparrow & & \uparrow \\ & & \{(G, \psi)\text{-admissible seeds } \bar{\Sigma}_t\} / \sim & \xrightarrow{\quad} & \{(G, \psi)\text{-admissible seeds } \Sigma_t\} / \sim \\ & & \parallel & & \parallel \\ & & \{\bar{\Sigma}_t^G\}_{t \in \mathbb{T}_n} / \sim & \xrightarrow{\quad} & \{\Sigma_t^G\}_{t \in \mathbb{T}_n} / \sim \end{array}$$

The equalities on the top row are obtained by (2.3). The surjectivity in the bottom row is induced by the maximality of the exchange graph of a cluster algebra having principal coefficients in Theorem 2.27. Moreover, the equalities connecting the second and third rows are given by Theorem 2.25. This proves that there is a bijective correspondence between the set of vertices of $\text{Ex}(\{\bar{\Sigma}_t^G\}_{t \in \mathbb{T}_n})$ and that of $\text{Ex}(\{\Sigma_t^G\}_{t \in \mathbb{T}_n})$. On the other hand, the graph $\text{Ex}(\{\Sigma_t^G\}_{t \in \mathbb{T}_n})$ is covered by $\text{Ex}(\{\bar{\Sigma}_t^G\}_{t \in \mathbb{T}_n})$ by Theorem 2.27. Accordingly, two graphs are the same, and this proves the theorem. \blacksquare

We recall from [10] the relation between the cluster pattern and Y -pattern having the *same* initial exchange matrix.

Proposition 2.29 ([10, Theorem 2.5]). *Let $(\mathbf{y}_{t_0}, \mathcal{B}_{t_0})$ be an initial Y -seed, and let $\{(\mathbf{y}_t, \mathcal{B}_t)\}_{t \in \mathbb{T}_n}$ be the Y -pattern. Let $(\mathbf{x}_{t_0}, \tilde{\mathcal{B}}_{t_0})$ be a cluster seed such that the principal part of the exchange matrix $\tilde{\mathcal{B}}_{t_0}$ is \mathcal{B}_{t_0} , and let $\{(\mathbf{x}_t, \tilde{\mathcal{B}}_t)\}_{t \in \mathbb{T}_n}$ be the cluster pattern. Suppose that the initial variables $y_{1;t_0}, \dots, y_{n;t_0}$ are algebraically independent. Then, we have*

$$\text{Ex}(\{(\mathbf{x}_t, \tilde{\mathcal{B}}_t)\}_{t \in \mathbb{T}_n}) = \text{Ex}(\{(\mathbf{y}_t, \mathcal{B}_t)\}_{t \in \mathbb{T}_n}).$$

Because of Assumption 2.15, Theorem 2.28, and Proposition 2.29, when the initial variables $y_{1;t_0}, \dots, y_{n;t_0}$ are algebraically independent, all the following exchange graphs are the same:

$$\text{Ex}(\{(\tilde{\mathbf{x}}_t, \tilde{\mathcal{B}}_t)\}_{t \in \mathbb{T}_n}) = \text{Ex}(\{(\mathbf{x}_t, \mathcal{B}_t)\}_{t \in \mathbb{T}_n}) = \text{Ex}(\{(\mathbf{y}_t, \mathcal{B}_t)\}_{t \in \mathbb{T}_n}).$$

We simply denote the above exchange graphs with the associated root system Φ by

$$\text{Ex}(\Phi) = \text{Ex}(\{(\tilde{\mathbf{x}}_t, \tilde{\mathcal{B}}_t)\}_{t \in \mathbb{T}_n}) = \text{Ex}(\{(\mathbf{x}_t, \mathcal{B}_t)\}_{t \in \mathbb{T}_n}) = \text{Ex}(\{(\mathbf{y}_t, \mathcal{B}_t)\}_{t \in \mathbb{T}_n}). \quad (2.4)$$

Since the exchange graph of a cluster pattern and that of a Y -pattern having the same type are the same, we will mainly treat exchange graphs of cluster patterns of finite or affine type from now on.

Let Φ be the root system defined by the Cartan counterpart of \mathcal{B} . It is proved in [26, 41] that there is a bijective correspondence between a subset $\Phi_{\geq -1} \subset \Phi$, called *almost positive roots*, and the set of cluster variables:

$$\Phi_{\geq -1} \xleftrightarrow{1:1} \{\text{cluster variables in } \mathcal{A} \text{ of type } Z\} \quad (2.5)$$

More precisely, one may associate the set $-\Pi$ of negative simple roots with the set of cluster variables $x_{1;t_0}, \dots, x_{n;t_0}$ in the initial seed $(\mathbf{x}_{t_0}, \tilde{\mathcal{B}}_{t_0})$; a positive root $\sum_{i=1}^n d_i \alpha_i$ is associated to a (non-initial) cluster variable of the form

$$\frac{f(\mathbf{x}_{t_0})}{x_{1;t_0}^{d_1} \cdots x_{n;t_0}^{d_n}}, \quad f(\mathbf{x}_{t_0}) \in \mathbb{C}[x_{1;t_0}, \dots, x_{m;t_0}].$$

Accordingly, each vertex of the exchange graph $\text{Ex}(\Phi)$ corresponds to an n -subset of $\Phi_{\geq -1}$. We notice that when Φ is of finite type, the set $\Phi_{\geq -1}$ is given by

$$\Phi_{\geq -1} := \Phi^+ \cup -\Pi.$$

Here, Φ^+ is the set of positive roots and $\Pi = \{\alpha_1, \dots, \alpha_n\}$ is the set of simple roots.

To study the combinatorics of exchange graphs, we prepare some terminologies. Let Φ be a rank n root system. For every subset $J \subset [n]$, let $\Phi(J)$ denote the root subsystem of Φ spanned by the set of simple roots $\{\alpha_i \mid i \in J\}$. Indeed, the Dynkin

Φ	A_n	B_n	C_n	D_n	E_6	E_7	E_8	F_4	G_2
h	$n + 1$	$2n$	$2n$	$2n - 2$	12	18	30	12	6

Table 6. Coxeter numbers.

diagram of $\Phi(J)$ is the full subdiagram on the vertices in J . Note that $\Phi(J)$ may not be irreducible even if Φ is.

A *Coxeter element* is a product of the simple reflections. The order h of a Coxeter element in W is called the *Coxeter number* of Φ . We present the known formula of Coxeter numbers h in Table 6 (see [6, Appendix]).

The Dynkin diagrams of finite or affine root systems do not have cycles except of type \tilde{A}_{n-1} for $n \geq 3$. We consider *bipartite coloring* on Dynkin diagrams except of type \tilde{A} ; that is, we have a function

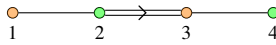
$$\varepsilon: [n] \rightarrow \{+, -\},$$

called a *coloring*, such that any two vertices i and j connected by an edge have different colors. Since we are considering tree-shaped diagrams, they admit bipartite colorings. We notice that a bipartite coloring on a Dynkin diagram decides a *bipartite skew-symmetrizable matrix* $\mathcal{B} = (b_{i,j})$ of the same type by setting

$$b_{i,j} > 0 \Leftrightarrow \varepsilon(i) = + \text{ and } \varepsilon(j) = -. \quad (2.6)$$

Here, a skew-symmetrizable matrix is called *bipartite* if there exists a coloring ε satisfying (2.6). Moreover, for a simply-laced Dynkin diagram, a bipartite coloring defines a *bipartite quiver*; that is, each vertex of the quiver is either source or sink. More precisely, we let i be a source if $\varepsilon(i) = +$; otherwise, a sink.

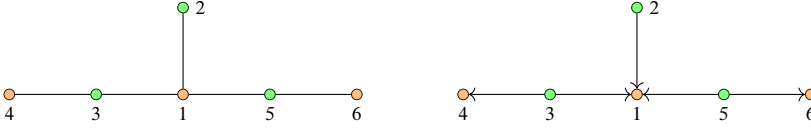
Example 2.30. Consider the coloring on the Dynkin diagram of F_4 .



Here, **green** nodes have color $+$; **orange** nodes have color $-$. This coloring gives a skew-symmetrizable matrix \mathcal{B} whose Cartan counterpart $C(\mathcal{B})$ is of type F_4 .

$$\mathcal{B} = \begin{pmatrix} 0 & -1 & 0 & 0 \\ 1 & 0 & 2 & 0 \\ 0 & -1 & 0 & -1 \\ 0 & 0 & 1 & 0 \end{pmatrix}, \quad C(\mathcal{B}) = \begin{pmatrix} 2 & -1 & 0 & 0 \\ -1 & 2 & -2 & 0 \\ 0 & -1 & 2 & -1 \\ 0 & 0 & -1 & 2 \end{pmatrix}.$$

The coloring on the Dynkin diagram of E_6 as shown on the left provides the bipartite quiver like the one on the right.



Let I_+ and I_- be two parts of the set of vertices of the Dynkin diagram given by a bipartite coloring; they are determined uniquely up to renaming. Consider the composition $\mu_{\mathcal{Q}} = \mu_+ \mu_-$ of a sequence of mutations where

$$\mu_{\varepsilon} = \prod_{i \in I_{\varepsilon}} \mu_i \quad \text{for } \varepsilon \in \{+, -\},$$

which is well defined (cf. Remark 2.4). We call $\mu_{\mathcal{Q}}$ a *Coxeter mutation*. Because of the definition, for a bipartite skew-symmetrizable matrix \mathcal{B} or a bipartite quiver \mathcal{Q} , we obtain

$$\mu_{\mathcal{Q}}(\mathcal{B}) = \mathcal{B}, \quad \mu_{\mathcal{Q}}(\mathcal{Q}) = \mathcal{Q}.$$

The initial seed $\Sigma_{t_0} = \Sigma_0 = (\mathbf{x}_0, \tilde{\mathcal{B}}_0)$ is included in the *bipartite belt* consisting of the seeds $\Sigma_r = (\mathbf{x}_r, \tilde{\mathcal{B}}_0)$ for $r \in \mathbb{Z}$ defined by

$$\Sigma_r = (\mathbf{x}_r, \tilde{\mathcal{B}}_0) = \begin{cases} \mu_{\mathcal{Q}}^r(\Sigma_0) & \text{if } r > 0, \\ (\mu_- \mu_+)^{-r}(\Sigma_0) & \text{if } r < 0. \end{cases}$$

We write

$$\mathbf{x}_r = (x_{1;r}, \dots, x_{n;r}) \quad \text{for } r \in \mathbb{Z}.$$

It is known from [27, 41] that both μ_+ and μ_- act on the set $\Phi_{\geq -1}$ of almost positive roots and on the set $V(\text{Ex}(\Phi))$ of vertices via the bijective correspondence (2.5). We summarize the properties of the action of Coxeter mutation as follows.

Proposition 2.31 (Cf. [27, Propositions 2.5, 3.5, and 3.6] for finite type; [41, Propositions 5.4 and 5.14] for affine type). *Let Φ be a finite or affine root system of type Z . Let $\{(\mathbf{x}_t, \tilde{\mathcal{B}}_t)\}_{t \in \mathbb{T}}$ be a cluster pattern of type Z and $\text{Ex}(\Phi)$ its exchange graph. Then, the following holds.*

- (1) *For $\ell \in [n]$ and $r \in \mathbb{Z}$, we denote by $\text{Ex}(\Phi, x_{\ell;r})$ the induced subgraph of $\text{Ex}(\Phi)$ consisting of seeds having the cluster variable $x_{\ell;r}$. Then, we have*

$$\text{Ex}(\Phi, x_{\ell;r}) \cong \text{Ex}(\Phi([n] \setminus \{\ell\})).$$

- (2) *Both μ_+ and μ_- act on the exchange graph $\text{Ex}(\Phi)$.*

(3) For any seed $(\mathbf{x}, \tilde{\mathcal{B}}) \in \text{Ex}(\Phi)$, there exists $r \in \mathbb{Z}$ such that

$$|\{x_{1;r}, \dots, x_{n;r}\} \cap \{x_1, \dots, x_n\}| \geq 2.$$

Furthermore, if Φ is of finite type having even Coxeter number $h = 2e$, then $r \in \{0, 1, \dots, e\}$.

As a direct consequence of Proposition 2.31, we have the following lemma which will be used later.

Lemma 2.32. *Let $(\mathbf{y}_{t_0}, \mathcal{B}_{t_0})$ be a Y -seed such that the Cartan counterpart $C(\mathcal{B}_{t_0})$ is of finite or affine type. For a Y -seed $(\mathbf{y}, \mathcal{B})$ in the seed pattern, there exist $r \in \mathbb{Z}$, $\ell \in [n]$, and $j_1, \dots, j_L \in [n] \setminus \{\ell\}$ such that a sequence $\mu_{j_1}, \dots, \mu_{j_L}$ of mutations connects $\mu_{\mathcal{Q}}^r(\mathbf{y}_{t_0}, \mathcal{B}_{t_0})$ and $(\mathbf{y}, \mathcal{B})$, that is,*

$$(\mathbf{y}, \mathcal{B}) = (\mu_{j_L} \cdots \mu_{j_1})(\mu_{\mathcal{Q}}^r(\mathbf{y}_{t_0}, \mathcal{B}_{t_0})).$$

Furthermore, if Φ is of finite type and has even Coxeter number $h = 2e$, then $r \in \{0, 1, \dots, e\}$.

Proof. Since the exchange graph $\text{Ex}(\{(\mathbf{y}_t, \mathcal{B}_t)\}_{t \in \mathbb{T}_n})$ is the graph $\text{Ex}(\Phi)$ by Proposition 2.29, it is enough to prove the claim in terms of seeds. Let $(\mathbf{x}, \tilde{\mathcal{B}}) \in \text{Ex}(\Phi)$ be a seed. By Proposition 2.31 (3), there exist $\ell \in [n]$ and $r \in \mathbb{Z}$ such that $x_{\ell;r} \in \{x_1, \dots, x_n\}$. Accordingly, both seeds $\mu_{\mathcal{Q}}^r(\mathbf{x}_{t_0}, \tilde{\mathcal{B}}_{t_0})$ and $(\mathbf{x}, \tilde{\mathcal{B}})$ are contained in the induced subgraph $\text{Ex}(\Phi, x_{\ell;r})$. Since the subgraph $\text{Ex}(\Phi, x_{\ell;r})$ itself is the exchange graph of the root subsystem $\Phi([n] \setminus \{\ell\})$ by Proposition 2.29 (1), it is connected. Therefore, two seeds $\mu_{\mathcal{Q}}^r(\mathbf{x}_{t_0}, \tilde{\mathcal{B}}_{t_0})$ and $(\mathbf{x}, \tilde{\mathcal{B}})$ are connected without applying mutations at the vertex ℓ ; that is, there exists a sequence $j_1, \dots, j_L \in [n] \setminus \{\ell\}$ such that $(\mathbf{x}, \tilde{\mathcal{B}}) = (\mu_{j_L} \cdots \mu_{j_1})(\mu_{\mathcal{Q}}^r(\mathbf{x}_{t_0}, \tilde{\mathcal{B}}_{t_0}))$, as desired. Furthermore, if Φ is of finite type and has even Coxeter number $h = 2e$, then $r \in \{0, 1, \dots, e\}$ because of Proposition 2.31 (3). ■

For a finite root system Φ , the exchange graph $\text{Ex}(\Phi)$ becomes the one-skeleton of an n -dimensional polytope $P(\Phi)$, called the *generalized associahedron*. Moreover, there is a bijective correspondence between the set $\mathcal{F}(P(\Phi))$ of codimension-one faces, called *facets*, of $P(\Phi)$ and the set of almost positive roots $\Phi_{\geq -1}$. We denote by F_{β} the facet of the polytope $P(\Phi)$ corresponding to a root $\beta \in \Phi_{\geq -1}$. We demonstrate Proposition 2.31 for root systems of type A_3 and D_4 .

Example 2.33. Consider the root system Φ of type A_3 . In this case, the Coxeter number is 4, which is even (cf. Table 6). In Table 7, we present how $\mu_{\mathcal{Q}}$ acts on the set of almost positive roots. Here, we use the convention that $I_+ = \{1, 3\}$ and $I_- = \{2\}$. The generalized associahedron of type A_3 is presented in Figure 11. We label each

r	$\mu_{\mathbb{Q}}^r(-\alpha_1)$	$\mu_{\mathbb{Q}}^r(-\alpha_2)$	$\mu_{\mathbb{Q}}^r(-\alpha_3)$
0	$-\alpha_1$	$-\alpha_2$	$-\alpha_3$
1	$\alpha_1 + \alpha_2$	α_2	$\alpha_2 + \alpha_3$
2	α_3	$\alpha_1 + \alpha_2 + \alpha_3$	α_1

Table 7. Computation $\mu_{\mathbb{Q}}^r(-\alpha_i)$ for type A_3 .

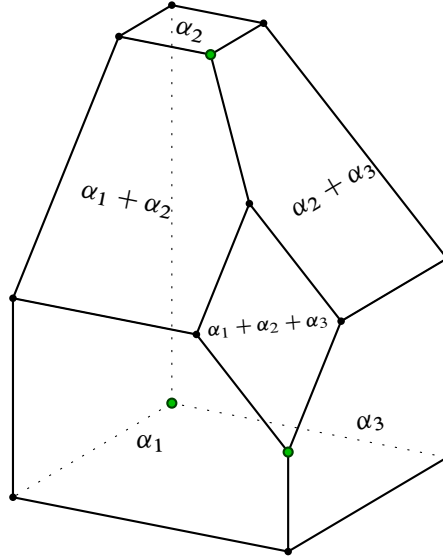


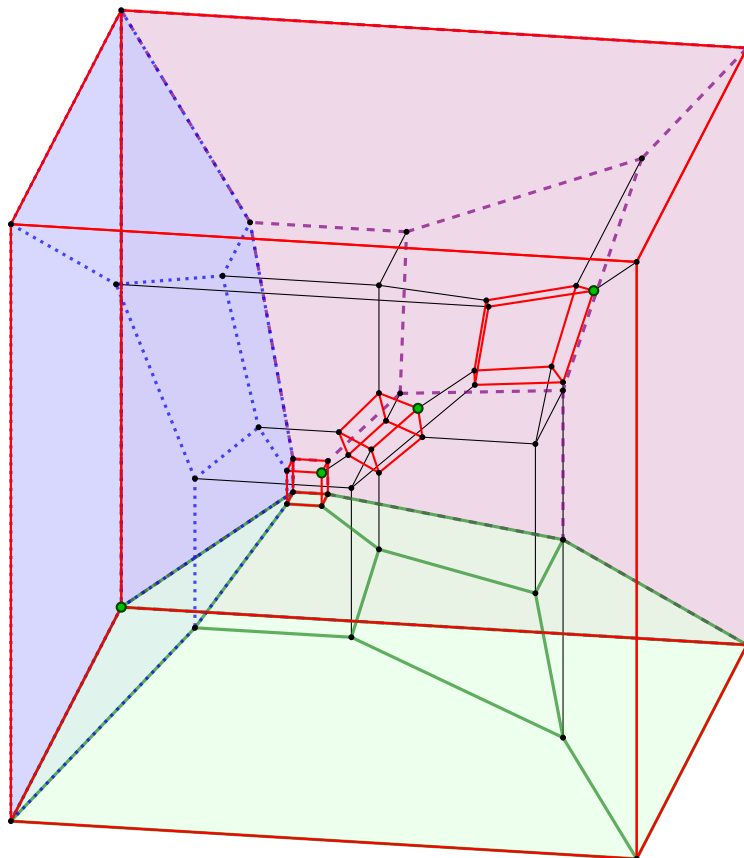
Figure 11. The type A_3 generalized associahedron.

codimension-one face the corresponding almost positive root. The back-side facets are associated with the set of negative simple roots. As one may see that the face posets of $\mu_{\mathbb{Q}}^r(F_{-\alpha_i})$ are the same as those of the generalized associahedron $P(\Phi([n] \setminus \{i\}))$. Indeed, the facets $\mu_{\mathbb{Q}}^r(F_{-\alpha_1})$ and $\mu_{\mathbb{Q}}^r(F_{-\alpha_3})$ are pentagons, and the facets $\mu_{\mathbb{Q}}^r(F_{-\alpha_2})$ are squares. For

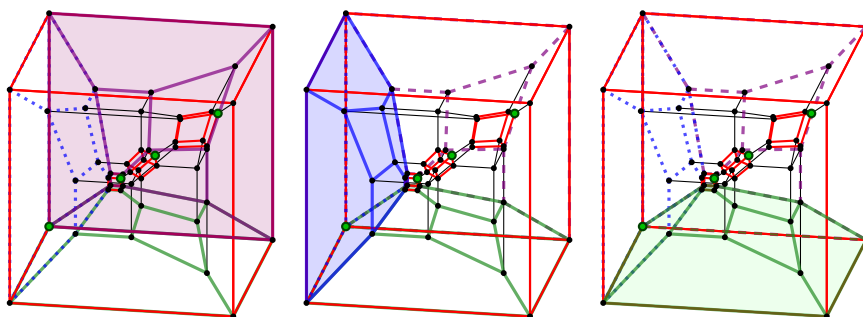
$$(\mathbf{x}, \tilde{\mathcal{B}}) = F_{-\alpha_1} \cap F_{-\alpha_2} \cap F_{-\alpha_3},$$

we decorate the vertices $\{\mu_{\mathbb{Q}}^r(\mathbf{x}, \tilde{\mathcal{B}}) \mid r = 0, 1, 2\}$ with green. As one can see, the orbits of $F_{-\alpha_1}, F_{-\alpha_2}, F_{-\alpha_3}$ exhaust all vertices as claimed in Proposition 2.31 (3).

Example 2.34. We consider the generalized associahedron of type D_4 and present four facets corresponding to the negative simple roots in Figure 12. The facet corresponding to $-\alpha_2$ is combinatorially equivalent to $P(\Phi(\{1\})) \times P(\Phi(\{3\})) \times P(\Phi(\{4\}))$, which is a 3-cube presented in the boundary. The intersection of these four facets is a



(a) The generalized associahedron of type D_4



(b) $F_{-\alpha_1}$

(c) $F_{-\alpha_3}$

(d) $F_{-\alpha_4}$

Figure 12. The generalized associahedron of type D_4 and facets corresponding to some negative simple roots $-\alpha_1$, $-\alpha_3$, and $-\alpha_4$.

vertex sits in the bottom colored in green. The Coxeter mutation $\mu_{\mathcal{Q}}$ acts on the face poset of the permutohedron, and four green vertices are in the same orbit.

Remark 2.35. As seen in Example 2.22, bipartite coloring on quivers of type ADE induces that on quivers of type BCFG. Accordingly, if a seed pattern of simply-laced type Z gives a seed pattern of type Z^G via the folding procedure, then the Coxeter mutation of type Z^G is the same as that of type Z . More precisely, for a globally foldable Y -seed $(\mathbf{y}, \mathcal{B})$ with respect to G of type Z and its Coxeter mutation $\mu_{\mathcal{Q}}^Z$, we have

$$\mu_{\mathcal{Q}}^{Z^G}((\mathbf{y}, \mathcal{B})^G) = (\mu_{\mathcal{Q}}^Z(\mathbf{y}, \mathcal{B}))^G.$$

Here, $\mu_{\mathcal{Q}}^{Z^G}$ is the Coxeter mutation on the seed pattern determined by $(\mathbf{y}, \mathcal{B})^G$.

Moreover, Coxeter numbers of Z and Z^G are the same. Indeed,

$$\begin{aligned} h(A_{2n-1}) &= h(B_n) = 2n, \\ h(D_{n+1}) &= h(C_n) = 2n, \\ h(E_6) &= h(F_4) = 12, \\ h(D_4) &= h(G_2) = 6. \end{aligned}$$

In the remaining part of this section, we recall [28] which considers the combinatorics on mutations. Let \mathcal{Q} be a bipartite quiver and I_+ and I_- the bipartite decomposition of the vertex set of \mathcal{Q} . Consider the composition $\mu_{\mathcal{Q}} = \mu_+ \mu_-$ of a sequence of mutations where

$$\mu_{\varepsilon} = \prod_{i \in I_{\varepsilon}} \mu_i \quad \text{for } \varepsilon \in \{+, -\}.$$

We call $\mu_{\mathcal{Q}}$ a *Coxeter mutation* as before. We enclose this section by recalling the result [28, Theorem 8.8] on the order of Coxeter mutation on the cluster pattern. Recall from Proposition 2.29 that for an exchange matrix $\tilde{\mathcal{B}}_{t_0}$, if \mathcal{B}_{t_0} is skew-symmetric, then the exchange graph of a seed pattern $\{(\mathbf{x}_t, \tilde{\mathcal{B}}_t)\}_{t \in \mathbb{T}_n}$ and that of a Y -pattern $\{(\mathbf{y}_t, \mathcal{B}_t)\}_{t \in \mathbb{T}_n}$ having algebraically independent variables $y_{1;t_0}, \dots, y_{n;t_0}$ are the same. Accordingly, we obtain the following from [28, Theorem 8.8].

Lemma 2.36 (Cf. [28, Theorem 8.8]). *Let $(\mathbf{y}_{t_0}, \mathcal{B}_{t_0})$ be an initial Y -seed. Suppose that $\mathcal{B}_{t_0} = \mathcal{B}(\mathcal{Q})$ for a bipartite quiver \mathcal{Q} and $y_{1;t_0}, \dots, y_{n;t_0}$ are algebraically independent. Then, the set $\{\mu_{\mathcal{Q}}^r(\mathbf{y}_{t_0}, \mathcal{B}_{t_0})\}_{r \in \mathbb{Z}_{\geq 0}}$ of Y -seeds is finite if and only if \mathcal{B}_{t_0} is of finite type.*

Moreover, for such a quiver \mathcal{Q} , the order the $\mu_{\mathcal{Q}}$ -action is given by $(h+2)/2$ if h is even, or $h+2$ otherwise, where h is the corresponding Coxeter number.

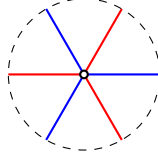


Figure 13. A hexagonal point.

3. Legendrians and N -graphs

We recall from [15] the notion of N -graphs and their combinatorial moves which encode the Legendrian isotopy data of corresponding Legendrian surfaces. As an application, we review how N -graphs can be used to find and to distinguish Lagrangian fillings for Legendrian links.

3.1. N -graphs and Legendrian weaves

Definition 3.1 ([15, Definition 2.2]). An N -graph \mathcal{G} on a smooth surface S is an $(N - 1)$ -tuple of graphs $(\mathcal{G}_1, \dots, \mathcal{G}_{N-1})$ satisfying the following conditions.

- (1) Each graph \mathcal{G}_i is embedded, trivalent, possibly empty, and non-necessarily connected.
- (2) Any consecutive pair of graphs $(\mathcal{G}_i, \mathcal{G}_{i+1})$, $1 \leq i \leq N - 2$, intersects only at hexagonal points depicted as in Figure 13.
- (3) Any pair of graphs $(\mathcal{G}_i, \mathcal{G}_j)$ with $1 \leq i, j \leq N - 1$ and $|i - j| > 1$ intersects transversely at edges.

Let $\pi_F : J^1S \cong T^*S \times \mathbb{R} \rightarrow S \times \mathbb{R}$ be the front projection, and we call the image $\pi_F(\Lambda)$ of a Legendrian $\Lambda \subset J^1S$ a *wavefront*. Since J^1S is equipped with the contact form $dz - p_x dx - p_y dy$, the coordinates (p_x, p_y) of the Legendrian Λ are recovered from (x, y) -slope of the tangent plane $T_{(x,y,z)}\pi_F(\Lambda)$:

$$p_x = \partial_x z(x, y), \quad p_y = \partial_y z(x, y).$$

For any N -graph \mathcal{G} on a surface S , we associate a Legendrian surface $\Lambda(\mathcal{G}) \subset J^1S$. Basically, we construct the Legendrian surface by weaving the wavefronts in $S \times \mathbb{R}$ constructed from a local chart of S .

Let $\mathcal{G} \subset S$ be an N -graph. A finite cover $\{U_i\}_{i \in I}$ of S is called \mathcal{G} -compatible if

- (1) each U_i is diffeomorphic to the open disk $\mathring{\mathbb{D}}^2$,
- (2) $U_i \cap \mathcal{G}$ is connected, and
- (3) $U_i \cap \mathcal{G}$ contains at most one vertex.

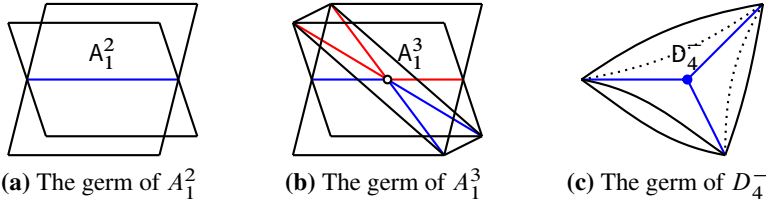


Figure 14. Three types of wavefronts of Legendrian singularities.

For each U_i , we associate a wavefront

$$\Gamma(U_i) \subset U_i \times \mathbb{R} \subset S \times \mathbb{R}.$$

Note that there are only five types of non-degenerate local charts for any N -graph \mathcal{G} as follows.

Type 1 A chart without any graph component whose corresponding wavefront becomes

$$\bigcup_{i=1, \dots, N} \mathring{\mathbb{D}}^2 \times \{i\} \subset \mathring{\mathbb{D}}^2 \times \mathbb{R}.$$

Type 2 A chart with single edge. The corresponding wavefront is the union of the A_1^2 -germ along the two sheets $\mathring{\mathbb{D}}^2 \times \{i\}$ and $\mathring{\mathbb{D}}^2 \times \{i+1\}$ and trivial disks $\mathbb{D}^2 \times \{j\}$, $j \in \{1, \dots, N\} \setminus \{i, i+1\}$. The local model of A_1^2 comes from the origin of the singular surface

$$\Gamma(A_1^2) = \{(x, y, z) \in \mathbb{R}^3 \mid x^2 - z^2 = 0\}.$$

See Figure 14a and the first picture of Figure 15.

Type 3 A chart with two transversely intersecting edges. The wavefront consists of two A_1^2 -germs of $\mathring{\mathbb{D}}^2 \times \{i, i+1\}$ and $\mathring{\mathbb{D}}^2 \times \{j, j+1\}$ with $|i-j| > 1$ and trivial disks $\mathbb{D}^2 \times \{k\}$, $k \in \{1, \dots, N\} \setminus \{i, i+1, j, j+1\}$. See the second picture of Figure 15.

Type 4 A chart with a monochromatic trivalent vertex whose wavefront is the union of the D_4^- -germ, see [2, Section 2.4] and trivial disks $\mathbb{D}^2 \times \{j\}$, $j \in \{1, \dots, N\} \setminus \{i, i+1\}$. The local model for Legendrian singularity of type D_4^- is given by the image at the origin of

$$\delta_4^- : \mathbb{R}^2 \rightarrow \mathbb{R}^3 : (x, y) \mapsto \left(x^2 - y^2, 2xy, \frac{2}{3}(x^3 - 3xy^2) \right).$$

See Figure 14c and the third picture of Figure 15.

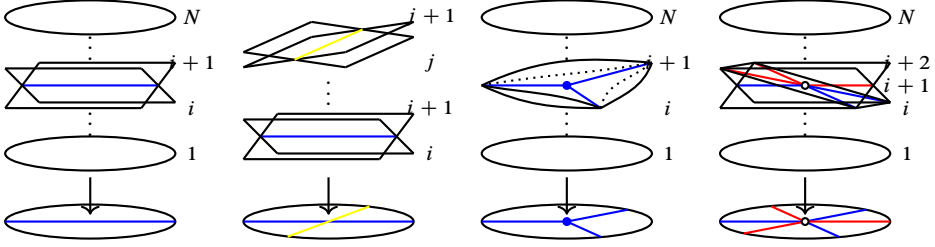


Figure 15. Local charts for N -graphs of types 2, 3, 4, and 5.

Type 5 A chart with a bichromatic hexagonal point. The induced wavefront is the union of the A_1^3 -germ along the three sheets $\mathbb{D}^2 \times \{*\}$, $*$ = $i, i + 1, i + 2$, and the trivial disks $\mathbb{D}^2 \times \{j\}$, $j \in \{1, \dots, N\} \setminus \{i, i + 1, i + 2\}$. The local model of A_1^3 is given by the origin of the singular surface

$$\{(x, y, z) \in \mathbb{R}^3 \mid (x^2 - z^2)(y - z) = 0\}.$$

See Figure 14b and the last picture of Figure 15.

Definition 3.2 ([15, Definition 2.7]). Let \mathcal{G} be an N -graph on a surface S . The *Legendrian weave* $\Lambda(\mathcal{G}) \subset J^1 S$ is an embedded Legendrian surface whose wavefront

$$\Gamma(\mathcal{G}) \subset S \times \mathbb{R}$$

is constructed by weaving the wavefronts $\{\Gamma(U_i)\}_{i \in I}$ from a \mathcal{G} -compatible cover $\{U_i\}_{i \in I}$ with respect to the gluing data given by \mathcal{G} .

Remark 3.3. When an N -graph \mathcal{G} is fixed, the space of possible Legendrian weaves $\Lambda(\mathcal{G})$ is contractible via Legendrian isotopy. So, $\Lambda(\mathcal{G})$ is well defined up to Legendrian isotopy.

We also list certain degenerate local models of N -graph as follows.

Type D1 A chart with double edges whose wavefront consists of two A_1^2 -germs of $\mathbb{D}^2 \times \{i, i + 1\}$ and $\mathbb{D}^2 \times \{j, j + 1\}$ for $|i - j| > 1$, and trivial disks $\mathbb{D}^2 \times \{k\}$, $k \in \{1, \dots, N\} \setminus \{i, i + 1, j, j + 1\}$. See the left-hand side of Figure 16a.

Type D2 A chart with double trivalent vertices whose wavefront consists of two D_4^- -germs at the level of $i, i + 1$, and $j, j + 1$ with $|i - j| > 1$. The other levels are trivial disks. See the right-hand side of Figure 16a.

Type D3 A chart with trichromatic graph of $(\mathcal{G}_{i-1}, \mathcal{G}_i, \mathcal{G}_{i+1})$ satisfies the following:

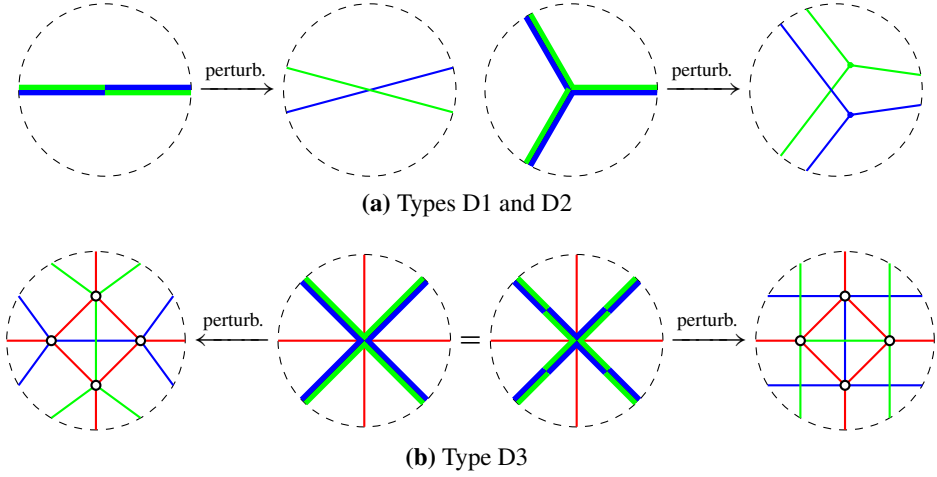
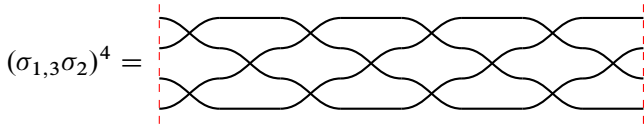


Figure 16. Local models for degenerate N -graphs and their perturbations.

- each has a unique vertex of four valent,
- \mathcal{G}_{i-1} and \mathcal{G}_{i+1} are identical, and
- \mathcal{G}_i and \mathcal{G}_{i+1} are intersecting at the vertex of eight valent in an alternating way; see the middle one in Figure 16b.

For $i = 2$, the wavefront corresponding to a chart of **Type D3** inside $\mathbb{D}^2 \times \mathbb{R}$ consists of four disks ($\mathbb{D}_1, \dots, \mathbb{D}_4$), which is the cone $C(\lambda) = \lambda \times [0, 1]/\lambda \times \{0\}$ of the following Legendrian front λ in $S^1 \times \mathbb{R}$:



where $\sigma_{1,3}$ is a 4-braid isotopic to $\sigma_1\sigma_3$ (or equivalently, $\sigma_3\sigma_1$) such that two crossings σ_1 and σ_3 occur simultaneously.

Remark 3.4. The cone point neighborhood of the wavefront for the degenerate N -graph of **Type D3** is diffeomorphic to the union of four planes, $\{z = x\}$, $\{z = -x\}$, $\{z = y\}$, and $\{z = -y\}$ in \mathbb{R}^3 ; see Figure 17.

We obtain (regular) N -graphs from degenerate N -graphs via (generic) perturbation of the wavefront as depicted in Figure 16.

The idea of N -graph is useful in the study of Legendrian surface because the Legendrian isotopy of the Legendrian weave $\Lambda(\mathcal{G})$ can be encoded in combinatorial moves of N -graphs.

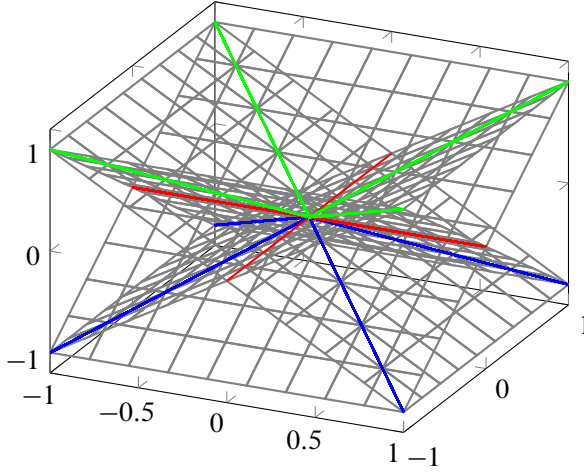


Figure 17. A wavefront for the degenerate N -graph.

Theorem 3.5 ([15, Theorem 1.1]). *Let \mathcal{G} be a non-degenerate local N -graph. The combinatorial moves (I) \sim (VI') in Figure 18 are Legendrian isotopies for $\Lambda(\mathcal{G})$.*

We denote the equivalence class of an N -graph \mathcal{G} up to the moves (I) \sim (VI') in Figure 18 by $[\mathcal{G}]$. Let us also list the combinatorial moves (DI) and (DII) for Legendrian isotopies involving degenerate N -graphs as depicted in Figure 18.

Corollary 3.6. *Let \mathcal{G} be a local degenerate N -graph. The combinatorial moves (DI) and (DII) in Figure 18 are Legendrian isotopies for $\Lambda(\mathcal{G})$.*

Proof. It is direct to check that the moves (DI) and (DII) for degenerate N -graphs can be obtained by composing the perturbations in Figure 16 and moves in Figure 18. See Appendix B.1. ■

Definition 3.7. An N -graph \mathcal{G} on S is called *free* if the induced Legendrian weave $\Lambda(\mathcal{G}) \subset J^1S$ can be woven without interior Reeb chord.

Example 3.8 ([15, Example 7.3]). Let $\mathcal{G} \subset \mathbb{D}^2$ be a 2-graph such that $\mathbb{D}^2 \setminus \mathcal{G}$ is simply connected relative to the boundary $\partial\mathbb{D}^2 \cap (\mathbb{D}^2 \setminus \mathcal{G})$. Then, \mathcal{G} is free if and only if \mathcal{G} has no faces contained in $\mathring{\mathbb{D}}^2$. Note that each of such faces admits at least one Reeb chord; see Figure 19.

In particular, we have the following lemma whose proof is omitted.

Lemma 3.9. *Let $\mathcal{G} = (\mathcal{G}_1, \dots, \mathcal{G}_{N-1})$ be an N -graph on \mathbb{D}^2 . Suppose that each \mathcal{G}_i is a tree or empty. Then, \mathcal{G} is free.*

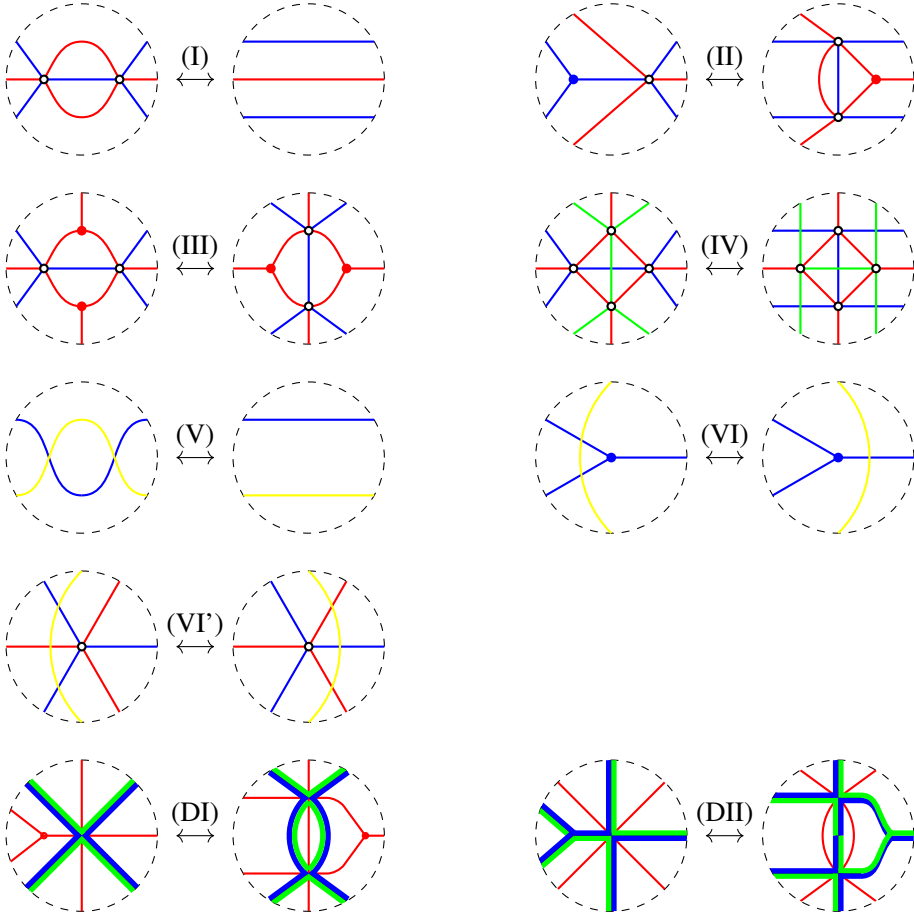


Figure 18. Combinatorial moves for Legendrian isotopies of surface $\Lambda(\mathcal{G})$. Here, the pairs (blue, red) and (red, green) are consecutive. Other pairs are not.

Let us consider the Lagrangian projection $\pi_L : J^1S \cong T^*S \times \mathbb{R} \rightarrow T^*S$. Then, the image

$$L(\mathcal{G}) := \pi_L(\Lambda(\mathcal{G}))$$

of the Legendrian weave gives us an exact, possibly immersed Lagrangian surface in T^*S . The following lemma is a direct consequence of Theorem 3.5 and Definition 3.7.

Lemma 3.10. *Let \mathcal{G} and \mathcal{G}' be two N -graphs on S . Then, the following statements hold.*

- (1) *If \mathcal{G} is free, then the Lagrangian surface $L(\mathcal{G}) = \pi_L(\Lambda(\mathcal{G}))$ is exact and embedded.*

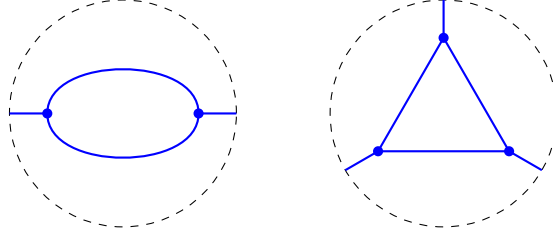


Figure 19. N -graphs with Reeb chords.

(2) If $[\mathcal{G}] = [\mathcal{G}']$, then two Lagrangian surfaces

$$L(\mathcal{G}) = \pi_L(\Lambda(\mathcal{G})) \quad \text{and} \quad L(\mathcal{G}') = \pi_L(\Lambda(\mathcal{G}'))$$

in T^*S are exact Lagrangian isotopic relative to boundary.

3.2. N -graphs on \mathbb{D}^2 and \mathbb{A}

In this section, we consider Legendrian links in \mathbb{R}^3 or \mathbb{S}^3 and Lagrangian fillings in \mathbb{R}^4 and how to describe them in terms of N -graphs.

3.2.1. Geometric setup. Let us fix basic notions from 3- and 5-dimensional contact geometry. Let (θ, p_θ, z) be the coordinates of $J^1\mathbb{S}^1$ with the contact form $\alpha_{J^1\mathbb{S}^1} = dz - p_\theta d\theta$. The Legendrian unknot λ_{unknot} in $J^1\mathbb{S}^1$ is given by

$$\lambda_{\text{unknot}} = \{(\theta, 0, 0) \mid \theta \in \mathbb{S}^1\} \subset J^1\mathbb{S}^1.$$

The symplectization of $J^1\mathbb{S}^1$ is

$$(J^1\mathbb{S}^1 \times \mathbb{R}_s, d(e^s(dz - p_\theta d\theta))),$$

and its contactization becomes

$$(J^1\mathbb{S}^1 \times \mathbb{R}_s \times \mathbb{R}_t, dt + e^s(dz - p_\theta d\theta))$$

which is contactomorphic to $(J^1(\mathbb{S}^1 \times \mathbb{R}_{r>0}), dw - p_\vartheta d\vartheta - p_r dr)$ under the strict contactomorphism ϕ given by

$$(\theta, p_\theta, z, s, t) \mapsto (\vartheta, r, p_\vartheta, p_r, w) = (\theta, e^s, e^s p_\theta, z, t + e^s z).$$

For each symplectization level $s = s_0$, the map ϕ induces a contact embedding

$$J^1\mathbb{S}^1 \hookrightarrow J^1(\mathbb{S} \times \mathbb{R}_{r>0})$$

especially into $J^1(\mathbb{S}^1 \times \mathbb{R}_{r>0}) \cap \{r = e^{s_0}\}$.

Furthermore, there is a strict contactomorphism

$$\psi: (J^1(\mathbb{S}^1 \times \mathbb{R}_{r>0}), dw - p_\vartheta d\vartheta - p_r dr) \rightarrow (J^1(\mathbb{R}^2 \setminus \{\mathbf{0}\}), dw - y_1 dx_1 - y_2 dx_2)$$

defined by

$$(x_1, x_2, y_1, y_2, w) = \left(r \cos \vartheta, r \sin \vartheta, p_r \cos \vartheta - \frac{\sin \vartheta}{r} p_\vartheta, p_r \sin \vartheta + \frac{\cos \vartheta}{r} p_\vartheta, w \right).$$

By compactifying the origin $\mathbf{0} \in \mathbb{R}^2$, we have the following diagram:

$$\begin{array}{ccc} J^1\mathbb{S}^1 \times \mathbb{R}_s \times \mathbb{R}_t & \xrightarrow[\cong]{\phi} & J^1(\mathbb{S}^1 \times \mathbb{R}_{r>0}) & \xrightarrow[\cong]{\psi} & J^1(\mathbb{R}^2 \setminus \{\mathbf{0}\}) & \hookrightarrow & J^1\mathbb{R}^2 = T^*\mathbb{R}^2 \times \mathbb{R}_w \\ \downarrow \pi_t & & & & & & \downarrow \pi_L \\ J^1\mathbb{S}^1 \times \mathbb{R}_s & \xleftarrow{\hspace{10em} \Phi \hspace{10em}} & & & & & T^*\mathbb{R}^2 \end{array}$$

Here, the symplectic embedding $\Phi: J^1\mathbb{S}^1 \times \mathbb{R}_s \hookrightarrow T^*\mathbb{R}^2$ is defined by

$$\begin{aligned} & (\theta, p_\theta, z, s) \\ & \mapsto (x_1, x_2, y_1, y_2) = (e^s \cos \theta, e^s \sin \theta, z \cos \theta - p_\theta \sin \theta, z \sin \theta + p_\theta \cos \theta). \end{aligned}$$

On the other hand, we have another symplectomorphism

$$\begin{aligned} \varphi: (\mathbb{S}^3 \times \mathbb{R}_u, d(e^u \alpha_{\mathbb{S}^3})) & \rightarrow (T^*\mathbb{R}^2 \setminus \{(\mathbf{0}, \mathbf{0})\}, dx_1 \wedge dy_1 + dx_2 \wedge dy_2), \\ (z_1, z_2, u) & \mapsto e^{u/2}(r_1 \cos \theta_1, r_2 \cos \theta_2, r_1 \sin \theta_1, r_2 \sin \theta_2), \end{aligned}$$

where \mathbb{S}^3 is the unit sphere in \mathbb{C}_{z_1, z_2}^2 , $z_1 = r_1 e^{i\theta_1}$, $z_2 = r_2 e^{i\theta_2}$, and with the contact form

$$\alpha_{\mathbb{S}^3} = \frac{1}{2} r_1^2 d\theta_1 + \frac{1}{2} r_2^2 d\theta_2, \quad r_1^2 + r_2^2 = 1.$$

So far, we have the following diagram of symplectic embeddings:

$$\begin{array}{ccc} J^1\mathbb{S}^1 \times \mathbb{R}_s & \xrightarrow{\hspace{10em} \Phi \hspace{10em}} & T^*\mathbb{R}^2 \setminus \{(\mathbf{0}, \mathbf{0})\} \\ & \searrow \Psi & \nearrow \cong \\ & & \mathbb{S}^3 \times \mathbb{R}_u \end{array}$$

where the map $\Psi(\theta, p_\theta, z, s) = (z_1, z_2, u)$ is defined by

$$\begin{aligned} z_1 &= \frac{e^s \cos \theta + i(z \cos \theta - p_\theta \sin \theta)}{\sqrt{e^{2s} + z^2 + p_\theta^2}}, \\ z_2 &= \frac{e^s \sin \theta + i(z \sin \theta + p_\theta \cos \theta)}{\sqrt{e^{2s} + z^2 + p_\theta^2}}, \\ e^u &= e^{2s} + z^2 + p_\theta^2. \end{aligned}$$

Let us define $\iota: J^1\mathbb{S}^1 \rightarrow \mathbb{S}^3$ as the composition of the inclusions $J^1\mathbb{S}^1 \cong J^1\mathbb{S}^1 \times \{s=0\} \rightarrow J^1\mathbb{S}^1 \times \mathbb{R}_s$, $\Psi: J^1\mathbb{S}^1 \times \mathbb{R}_s \rightarrow \mathbb{S}^3 \times \mathbb{R}^u$ and the projection $\mathbb{S}^3 \times \mathbb{R}_u \rightarrow \mathbb{S}^3$ so that

$$\iota(\theta, p_\theta, z) := \left(\frac{\cos \theta + i(z \cos \theta - p_\theta \sin \theta)}{\sqrt{1 + z^2 + p_\theta^2}}, \frac{\sin \theta + i(z \sin \theta + p_\theta \cos \theta)}{\sqrt{1 + z^2 + p_\theta^2}} \right).$$

Then, the image of the Legendrian unknot $\lambda_{\text{unknot}} \subset J^1\mathbb{S}^1$ becomes

$$\{(z_1, z_2) \mid z_1 = \cos \theta, z_2 = \sin \theta, \theta \in \mathbb{S}^1\} \subset \mathbb{S}^3 \subset \mathbb{C}^2.$$

Recall the stereographic projection of \mathbb{S}^3 with respect to $(0, -i) \in \mathbb{C}^2$, and see the corresponding image of λ_{unknot} :

$$\begin{aligned} (\mathbb{S}^3 \setminus \{(0, -i)\}, \alpha_{\mathbb{S}^3}) &\rightarrow (\mathbb{R}^3, dz' + x'dy' - y'dx') \cong \mathbb{C} \times \mathbb{R}, \\ (z_1, z_2) &\mapsto \left(\frac{iz_1}{i + z_2}, \frac{-\text{Re}(z_2)}{|i + z_2|^2} \right), \\ (\cos \theta, \sin \theta) &\mapsto \left(\frac{\cos \theta}{1 + \sin^2 \theta}, \frac{\cos \theta \sin \theta}{1 + \sin^2 \theta}, \frac{-\sin \theta}{1 + \sin^2 \theta} \right). \end{aligned}$$

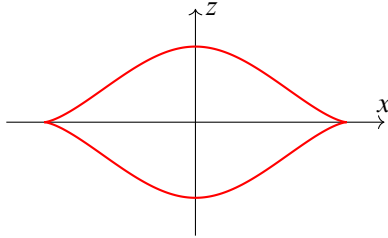
Under the strict contactomorphism

$$\begin{aligned} (\mathbb{R}^3, dz' + x'dy' - y'dx') &\rightarrow (J^1\mathbb{R}, dz - ydx), \\ (x', y', z') &\mapsto (x, y, z) = (x', 2y', z' + x'y'), \end{aligned}$$

the image of λ_{unknot} becomes

$$\left(\frac{\cos \theta}{1 + \sin^2 \theta}, \frac{2 \cos \theta \sin \theta}{1 + \sin^2 \theta}, \frac{-2 \sin^3 \theta}{(1 + \sin^2 \theta)^2} \right)$$

whose front projection looks like as follows:



Let $\lambda \subset J^1\mathbb{S}^1$ be a Legendrian link. Then, the image $\iota(\lambda)$ can be isotoped into a neighborhood of the Legendrian unknot in \mathbb{R}^3 . We consider a Legendrian surface $\widehat{\Lambda} \subset J^1(\mathbb{S}^1 \times \mathbb{R}_{r>0})$ having cylindrical ends so that, for some $S_1 > S_2$,

$$\widehat{\Lambda} \cap J^1(\mathbb{S}^1 \times \mathbb{R}_{r \geq e^{S_1}}) \cong \lambda_1 \times \mathbb{R}_{s \geq S_1}, \quad \widehat{\Lambda} \cap J^1(\mathbb{S}^1 \times \mathbb{R}_{r \leq e^{S_2}}) \cong \lambda_2 \times \mathbb{R}_{s \leq S_2}.$$

Then, the projection $L_{\widehat{\Lambda}} = \pi_L(\psi(\widehat{\Lambda}))$ of the surface $\widehat{\Lambda}$ inside $\mathbb{S}^3 \times \mathbb{R}_u$ becomes an exact Lagrangian cobordism from $\iota(\lambda_1)$ to $\iota(\lambda_2)$.

Similarly, let $\widehat{\Lambda} \subset J^1\mathbb{R}^2$ be a Legendrian surface having a cylindrical end. That is, for some $S \in \mathbb{R}$,

$$\widehat{\Lambda} \cap J^1\mathbb{R}_{r \geq e^S}^2 \cong \lambda \times \mathbb{R}_{s \geq S}.$$

Then, the projection $L_{\widehat{\Lambda}} = \pi_L(\widehat{\Lambda})$ in $T^*\mathbb{R}^2 \cong (\mathbb{C}^2, \omega_{\text{st}})$ becomes an exact Lagrangian filling of $\iota(\lambda)$. Note that the Lagrangian $\pi_L(\widehat{\Lambda})$ is embedded if and only if the Legendrian surface $\widehat{\Lambda}$ has no Reeb chords.

Lemma 3.11. *Let $\widehat{\Lambda}$ and $\widehat{\Lambda}'$ be two Legendrian surfaces in $J^1\mathbb{R}^2$ without Reeb chords having the identical cylindrical ends*

$$\widehat{\Lambda} \cap J^1\mathbb{R}_{r \geq e^S}^2 \cong \lambda \times \mathbb{R}_{s \geq S} \cong \widehat{\Lambda}' \cap J^1\mathbb{R}_{r \geq e^S}^2$$

for some $S \in \mathbb{R}$. If the exact embedded Lagrangian fillings $L_{\widehat{\Lambda}} = \pi_L(\widehat{\Lambda})$ and $L_{\widehat{\Lambda}'} = \pi_L(\widehat{\Lambda}')$ of $\iota(\lambda)$ are exact Lagrangian isotopic, then $\widehat{\Lambda}, \widehat{\Lambda}'$ are Legendrian isotopic.

On the other hand, any compact Legendrian surface $\Lambda \subset J^1\mathbb{D}^2$ can be extended to $\widehat{\Lambda} \subset J^1\mathbb{R}^2$ by attaching the cylindrical end $\partial\Lambda \times [1, \infty)$ in a smooth way. For two compact Legendrian surfaces $\Lambda, \Lambda' \subset J^1\mathbb{D}^2$, $\widehat{\Lambda}$ and $\widehat{\Lambda}'$ are Legendrian isotopic if and only if Λ and Λ' are Legendrian isotopic relative to boundary.

Corollary 3.12. *Let $\lambda \subset J^1\mathbb{S}^1$ be a Legendrian link and $\Lambda, \Lambda' \subset J^1\mathbb{D}^2$ two Legendrian surfaces without Reeb chords whose boundaries are λ . Then, two exact embedded Lagrangian fillings $\pi_L(\Lambda)$ and $\pi_L(\Lambda')$ are exact Lagrangian isotopic relative to boundary if and only if Λ and Λ' are Legendrian isotopic relative to boundary without making Reeb chords during the isotopy.*

Remark 3.13. We are interested in exact Lagrangian fillings of Legendrian links up to *exact Lagrangian isotopy* relative to boundary, an isotopy through exact Lagrangian fillings which fixes the Legendrian boundary. This is equivalent to exact Lagrangian fillings up to *Hamiltonian isotopy*, which is an isotopy through Hamiltonian diffeomorphism fixing the boundary. The similar holds for Lagrangian cobordisms.

We end this section by investigating certain actions on the symplectic manifold $\mathbb{S}^3 \times \mathbb{R}_u$ and induced actions on $J^1\mathbb{S}^1$. Especially, we are interested in actions on $\mathbb{S}^3 \times \mathbb{R}_u$ preserving the \mathbb{R}_u -coordinate, the symplectization coordinate. So, actions on \mathbb{S}^3 determine the actions on the symplectic manifold $\mathbb{S}^3 \times \mathbb{R}_u$.

Recall that \mathbb{S}^3 is the unit sphere in \mathbb{C}^2 , i.e., coordinates $z_1 = r_1 e^{i\theta_1}$, $z_2 = r_2 e^{i\theta_2}$ with $r_1^2 + r_2^2 = 1$.

Rotation. A symplectomorphism $R_{\theta_0}: \mathbb{S}^3 \times \mathbb{R}_u \rightarrow \mathbb{S}^3 \times \mathbb{R}_u$, called *rotation*, is defined by

$$R_{\theta_0}(z_1, z_2, u) = (z_1 \cos \theta_0 - z_2 \sin \theta_0, z_1 \sin \theta_0 + z_2 \cos \theta_0, u).$$

Note that the restriction $R_{\theta_0}|_{\mathbb{S}^3}$ fixes the contact form $\alpha_{\mathbb{S}^3}$. Under the symplectic embedding $\Psi: J^1\mathbb{S}^1 \times \mathbb{R}_s \hookrightarrow \mathbb{S}^3 \times \mathbb{R}_u$, we have the following induced symplectomorphism:

$$J^1\mathbb{S}^1 \times \mathbb{R}_s \rightarrow J^1\mathbb{S}^1 \times \mathbb{R}_s, \quad (\theta, p_\theta, z, s) \mapsto (\theta + \theta_0, p_\theta, z, s).$$

By restricting R_{θ_0} on $J^1\mathbb{S}^1$, we obtain

$$J^1\mathbb{S}^1 \rightarrow J^1\mathbb{S}^1, \quad (\theta, p_\theta, z) \mapsto (\theta + \theta_0, p_\theta, z).$$

We are especially interested in $\theta_0 = \pi, 2\pi/3$. They produce $\mathbb{Z}/2\mathbb{Z}$ - and $\mathbb{Z}/3\mathbb{Z}$ -action on the symplectic manifold $\mathbb{S}^3 \times \mathbb{R}_u$ and Lagrangian fillings of satellite links of the Legendrian unknot, respectively. See Figure 20a.

Conjugation. An anti-symplectic involution $\tau: \mathbb{S}^3 \times \mathbb{R}_u \rightarrow \mathbb{S}^3 \times \mathbb{R}_u$, which we call *conjugation*, is defined by

$$(z_1, z_2, u) \mapsto (\bar{z}_1, \bar{z}_2, u).$$

It is direct to check that τ reverses the sign of symplectic form $\frac{i}{2}(dz_1 \wedge d\bar{z}_1 + dz_2 \wedge d\bar{z}_2)$, and its restriction on \mathbb{S}^3 also reverses the sign of $\alpha_{\mathbb{S}^3}$. Again, by the symplectic embedding Ψ , the conjugation induces an action on $J^1\mathbb{S}^1 \times \mathbb{R}_s$

$$(\theta, p_\theta, z, s) \mapsto (\theta, -p_\theta, -z, s)$$

whose restriction on $J^1\mathbb{S}^1$ becomes

$$(\theta, p_\theta, z) \mapsto (\theta, -p_\theta, -z).$$

This anti-symplectic involution naturally produces $\mathbb{Z}/2\mathbb{Z}$ -action on the symplectic manifold and Lagrangian fillings as in the actions from the rotations. See Figure 20b.

Lemma 3.14. *Let R_{θ_0} and η be rotation and conjugation defined on $\mathbb{S}^3 \times \mathbb{R}$ as above, respectively. Then, the induced maps on the front projection $\pi_F: J^1\mathbb{S}^1 \rightarrow \mathbb{S}^1 \times \mathbb{R}$ become as follows:*

$$\begin{aligned} R_{\theta_0}|_{\mathbb{S}^1 \times \mathbb{R}} &: (\theta, z) \mapsto (\theta + \theta_0, z), \\ \eta|_{\mathbb{S}^1 \times \mathbb{R}} &: (\theta, z) \mapsto (\theta, -z). \end{aligned}$$

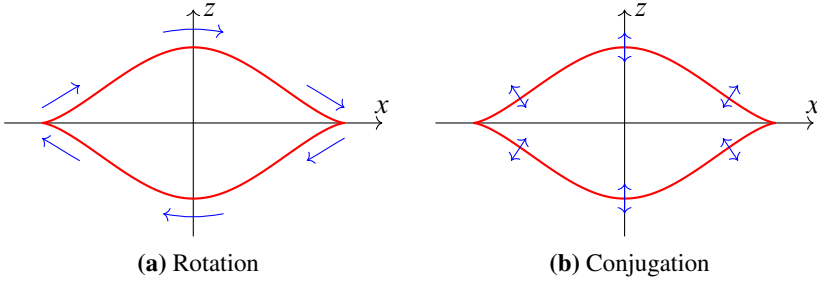


Figure 20. Rotation and conjugation near the Legendrian unknot.

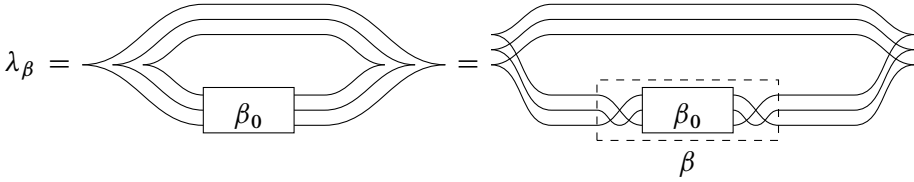


Figure 21. Rainbow and (-1) -closures of positive braids β_0 and β .

3.2.2. Positive N -braids. A *positive N -braid* is a braid of N -strands represented by a finite word of positive generators $\sigma_1, \dots, \sigma_{N-1}$. One may regard a positive N -braid β as a Legendrian in $J^1\mathbb{R}^1$ (with cylindrical ends) whose front projection is the same as the usual braid diagram of β .

Let us start with two ways of obtaining a Legendrian link from a positive braid. The *rainbow closure* is to close up a positive braid via nested copies of the Legendrian unknot. The other way is called the *(-1) -closure*, and it closes up a positive braid by considering parallel copies of the Legendrian unknot with respect to the Reeb direction. Notice that the rainbow closure of β_0 is the same as the (-1) -closure of $\beta = \Delta_N \beta_0 \Delta_N$ as seen in Figure 21. We will use the *closure* to indicate the (-1) -closure unless mentioned otherwise.

For the closure λ_β of an N -braid β , the front projection $\pi_F(\lambda_\beta) \subset \mathbb{S}^1 \times \mathbb{R}$ of λ_β consists of N -strands with double points corresponding to the braid word β . Hence, the Legendrian λ_β gives us an $(N - 1)$ -tuple $(\lambda_1, \lambda_2, \dots, \lambda_{N-1})$ of subsets of points in \mathbb{S}^1 , each of which corresponds to the generator σ_i in the braid word β .

Conversely, let $(\lambda_1, \dots, \lambda_{N-1})$ be an $(N - 1)$ -tuple of disjoint² finite subsets of \mathbb{S}^1 . Then, from this data $(\lambda_1, \dots, \lambda_{N-1})$, one can build the Legendrian link λ , which

²This condition can be weakened as follows: $\lambda_i \cap \lambda_{i+1} = \emptyset$ for each $1 \leq i < N$.

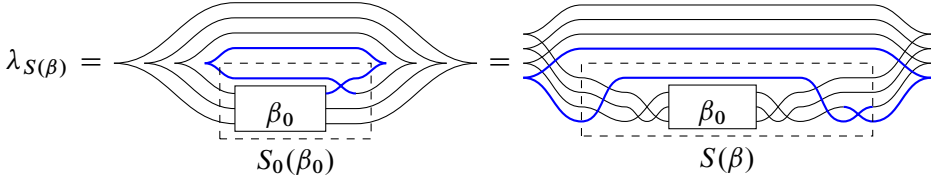


Figure 22. A stabilization $\lambda_{S(\beta)}$ of a Legendrian link λ_β .

is the branched N -fold covering space of \mathbb{S}^1 such that the i -th and $(i + 1)$ -st covers are branched along the set λ_i .

For a positive N -braid β_0 , a *stabilization* $\tilde{\beta}$ is a positive $(N + 1)$ -braid which satisfies the following:

- (1) the rainbow closures of β_0 and $\tilde{\beta}_0$ are Legendrian isotopic in \mathbb{S}^3 , and
- (2) the braid β_0 can be recovered by forgetting a strand from $\tilde{\beta}_0$.

The most typical example of a stabilization is as follows: for a positive N -braid β_0 , we introduce a notation $S_0(\beta_0)$ for a specific type of *stabilization* which is a positive $(N + 1)$ -braid defined by $S_0(\beta_0) = \beta_0\sigma_N$, where β_0 in $S_0(\beta_0)$ is regarded as an $(N + 1)$ -braid by adding a trivial $(N + 1)$ -st strand. For $\beta = \Delta_N\beta_0\Delta_N$, we introduce another notation $S(\beta) = (\sigma_1 \cdots \sigma_N)\beta(\sigma_N \cdots \sigma_1)\sigma_1$. Then, we have the following:

$$S(\beta) = \Delta_{N+1}S_0(\beta_0)\Delta_{N+1} \doteq \beta(\sigma_N \cdots \sigma_2\sigma_1^3\sigma_2 \cdots \sigma_N),$$

where \doteq means the same up to cyclic permutation of braid words. See Figure 22.

The Legendrian $\lambda_{S(\beta)}$ does depend on the braid word β_0 . For example, for each pair of positive N -braids $\beta_0^{(1)}$ and $\beta_0^{(2)}$ with $\beta_0 = \beta_0^{(1)}\beta_0^{(2)}$, let $\beta'_0 = \beta_0^{(2)}\beta_0^{(1)}$ and $\beta' = \Delta_N\beta'_0\Delta_N$. Then, two Legendrian links λ_β and $\lambda_{\beta'}$ are Legendrian isotopic but $\lambda_{S(\beta)}$ and $\lambda_{S(\beta')}$ are *not* Legendrian isotopic in general. Therefore, a stabilization of a Legendrian link λ which is a closure of a positive braid may not be uniquely determined.

Example 3.15. Let $\beta_0(a, b, c) = \sigma_2\sigma_1^a\sigma_2^{b-1}\sigma_1^c$ and $\beta_0(A_n) = \sigma_1^{n+1}$; then, we deduce

$$\beta(a, b, c) \doteq \sigma_2\sigma_1^{a+1}\sigma_2\sigma_1^{b+1}\sigma_2\sigma_1^{c+1} \quad \text{and} \quad \beta(A_n) = \sigma_1^{n+3};$$

see Section 4.1.1 for details. For each $b, c \geq 1$ with $b + c - 1 = n$, since $\beta(A_n) = \sigma_1^{n+3} = \sigma_1^c\sigma_1^{b+2}$, we have

$$S(\beta(A_n)) = (\sigma_1\sigma_2)\sigma_1\sigma_1^{c-1}\sigma_1^{b+1}\sigma_1(\sigma_2\sigma_1)\sigma_1 = \beta(1, b, c).$$

Therefore, $\beta(1, b, c)$ is a stabilization of $\beta(n)$ for each $b + c - 1 = n$.

Example 3.16. Let $\beta_{\text{degen},0}(p, q, r) = \sigma_{1,3} \sigma_2^p \sigma_{1,3}^{q-1} \sigma_2^r$, where $\sigma_{1,3}$ is a 4-braid isotopic to $\sigma_1 \sigma_3$ (or equivalently, $\sigma_3 \sigma_1$) such that two crossings σ_1 and σ_3 occur simultaneously. Now, consider

$$\beta_{\text{degen}}(p, q, r) = \Delta_4 \tilde{\beta}_0(p, q, r) \Delta_4 \doteq \sigma_2^{p+1} \sigma_{1,3} \sigma_2^q \sigma_{1,3}^{r+1} \sigma_{1,3} \sigma_2^2.$$

See Lemma 4.8.

Let

$$\begin{aligned} \beta'_0(a, b, b) &= \sigma_2^{b-1} \sigma_1 \sigma_2^a \sigma_1^{b-1} \sigma_2 \doteq \beta_0(a, b, b) \quad \text{and} \\ \beta'(a, b, b) &= \Delta_3 \beta'_0(a, b, b) \Delta_3. \end{aligned}$$

Then, $\beta(a, b, b) \doteq \beta'(a, b, b)$, and so, $\lambda_{\beta(a,b,b)} = \lambda_{\beta'(a,b,b)}$. Moreover,

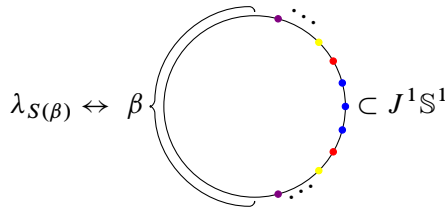
$$\begin{aligned} S(\beta'(a, b, b)) &\doteq \Delta_4 \sigma_1 \sigma_2^a \sigma_1^{b-1} \sigma_2 \sigma_3 \sigma_2^{b-1} \Delta_4 \\ &\doteq \Delta_4 \sigma_{1,3} \sigma_2^a \sigma_{1,3}^{b-1} \sigma_2 \Delta_4 = \beta_{\text{degen}}(a, b, 1), \end{aligned}$$

and so, we conclude that the Legendrian $\lambda_{\beta_{\text{degen}}(a,b,1)}$ is a stabilization of $\lambda_{\beta(a,b,b)}$.

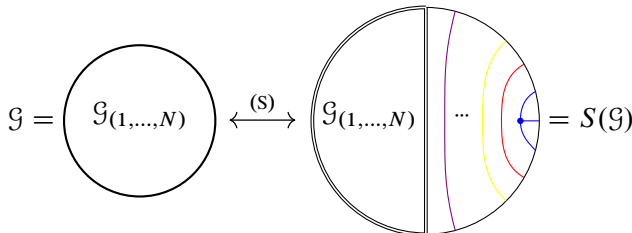
Recall the conjugate action on \mathbb{C}^2 , which turns links upside down so that in terms of braid words, it interchanges σ_i and σ_{N-i} for each N -braid. Hence, for 4-braids, it preserves $\sigma_{1,3}$. Therefore, $\beta_{\text{degen}}(p, q, r)$ is invariant under conjugation, and so is $\lambda_{\beta_{\text{degen}}(p,q,r)}$.

Corollary 3.17. *The Legendrian $\lambda_{\beta_{\text{degen}}(p,q,r)}$ is invariant under conjugation.*

On the other hand, a stabilization $\lambda_{S(\beta)}$ of λ_β will be represented by N -colored dots in S^1 while λ_β uses only $(N - 1)$ colors. That is,



Then, one can transfer an N -graph \mathcal{G} for λ_β into an $(N + 1)$ -graph $S(\mathcal{G})$ for $\lambda_{S(\beta)}$ as follows:



3.2.3. N -graphs on \mathbb{D}^2 and \mathbb{A} . Let $\mathcal{G} = (\mathcal{G}_1, \dots, \mathcal{G}_{N-1})$ be an N -graph on \mathbb{D}^2 . The boundary $\partial\mathcal{G}$ of \mathcal{G} is a Legendrian link defined by an N -graph on $\mathbb{S}^1 = \partial\mathbb{D}^2$ as

$$\partial\mathcal{G} = (\partial\mathcal{G}_1, \dots, \partial\mathcal{G}_{N-1}), \quad \partial\mathcal{G}_i := \mathcal{G}_i \cap \mathbb{S}^1 \subset \mathbb{S}^1.$$

We say that \mathcal{G} is of type λ or λ admits an N -graph \mathcal{G} if $\partial\mathcal{G} = \lambda$.

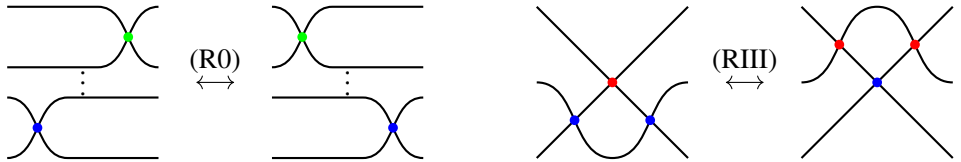
Let \mathbb{A} be the oriented annulus with two boundary components $\partial_+\mathbb{A}$ and $\partial_-\mathbb{A}$. For an N -graph \mathcal{G} on \mathbb{A} , let $\partial_\pm\mathcal{G} := \mathcal{G} \cap \partial_\pm\mathbb{A}$ be Legendrian links at two boundaries $\partial_\pm\mathbb{A}$, respectively. We say that \mathcal{G} is of type (λ_+, λ_-) if $\partial_\pm\mathcal{G} = \lambda_\pm$, respectively.

A typical example of annular N -graphs comes from Lagrangian cobordism between Legendrian links, which are closures of positive braids. In particular, for two closures λ_1 and λ_2 of positive braids β_1 and β_2 , any sequence of Legendrian braid moves from λ_2 to λ_1 will give us a special annular N -graph $\mathcal{G}_{\lambda_2\lambda_1}$.³ Hence, for an N -graphs \mathcal{G} with $\partial\mathcal{G} = \lambda_1$, we have the N -graph $\mathcal{G}_{\lambda_2\lambda_1}\mathcal{G}$ with boundary

$$\partial(\mathcal{G}_{\lambda_2\lambda_1}\mathcal{G}) = \lambda_2.$$

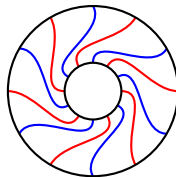
Remark 3.18. We are dealing with both Legendrian links λ and surfaces Λ . In order to avoid the confusion, we use the terminologies “ ∂ -Legendrian isotopy” and “Legendrian isotopy” for isotopies between Legendrian links and surfaces, respectively.

Since a closure of a Legendrian positive braid in $J^1\mathbb{S}^1$ should not have any cusp, possible ∂ -Legendrian isotopies are either plane isotopies (R0) or the third Reidemeister move (RIII) as follows:



Therefore, any annular N -graph corresponding to a sequence of Reidemeister moves between Legendrian links is a concatenation of elementary annular N -graphs, which are $\mathcal{G}_{(R0)}$ and $\mathcal{G}_{(RIII)}$ on the annulus \mathbb{A} as depicted in Figure 23. We call an annular N -graph tame if it is a concatenation of elementary annular N -graphs.

Example 3.19. A rotational annular N -graph, which has no vertices and rotates a certain angle as depicted below, is tame.



³One may call the N -graph $\mathcal{G}_{\lambda_2\lambda_1}$ a strict concordance since it is a union of cylinders.

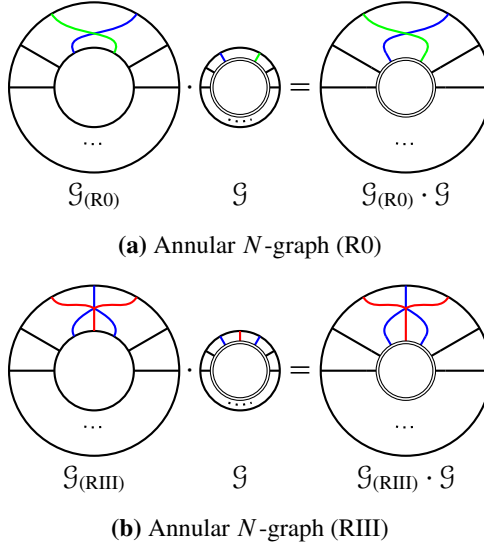


Figure 23. ∂ -Legendrian isotopy and elementary annulus N -graphs.

It is known that the rotational annular N -graph acts on the set of N -graphs for the Legendrian torus link $\lambda(n, m)$ of maximal Thurston–Bennequin number. This type of annular N -graphs plays a crucial role in producing a sequence of distinct exact Lagrangian fillings of positive braid Legendrian links; see [12, 29, 37].

Definition 3.20. We say that two N -graphs \mathcal{G} and \mathcal{G}' with $\partial\mathcal{G} = \lambda_1$ and $\partial\mathcal{G}' = \lambda_2$ are ∂ -Legendrian isotopic if there exists a tame annular N -graph $\mathcal{G}_{\lambda_2\lambda_1}$ such that $[\mathcal{G}'] = [\mathcal{G}_{\lambda_2\lambda_1}\mathcal{G}]$.

3.2.4. Annular N -graphs and Legendrian loops. Let $\beta, \beta_+, \beta_- \subset J^1\mathbb{R}^1$ be Legendrian positive N -braids. We denote by $\mathcal{N}\text{graphs}(\beta)$ and $\mathcal{N}\text{graphs}(\beta_+, \beta_-)$ the sets of equivalence classes of (degenerate) N -graphs on \mathbb{D}^2 and \mathbb{A} satisfying boundary conditions given by the closure λ_β or a pair of closures $(\lambda_{\beta_+}, \lambda_{\beta_-})$ up to local (degenerate) moves in Figure 18 relative to the boundary:

$$\begin{aligned} \mathcal{N}\text{graphs}(\beta) &:= \{[\mathcal{G}] \mid \mathcal{G} \text{ is an } N\text{-graph on } \mathbb{D}^2 \text{ of type } \lambda_\beta\}, \\ \mathcal{N}\text{graphs}(\beta_+, \beta_-) &:= \{[\mathcal{G}] \mid \mathcal{G} \text{ is an } N\text{-graph on } \mathbb{A} \text{ of type } (\lambda_{\beta_+}, \lambda_{\beta_-})\}. \end{aligned}$$

Here, we are assuming that we are aware of where each braid word starts.

By a direct consequence of Theorem 3.5 and Corollary 3.6, if $[\mathcal{G}] = [\mathcal{G}']$ as in the elements of $\mathcal{N}\text{graphs}(\beta_+, \beta_-)$, then $\Lambda(\mathcal{G})$ and $\Lambda(\mathcal{G}')$ are Legendrian isotopic relative to the boundary $(\lambda_{\beta_+}, \lambda_{\beta_-})$.

Then, it is direct to check that these sets are invariant under the cyclic rotation of the braid words up to bijection. More precisely, for N -braids $\beta^{(1)}$, $\beta^{(2)}$ and $\beta_{\pm}^{(1)}$, $\beta_{\pm}^{(2)}$, closures of $\beta^{(1)}\beta^{(2)}$ and $\beta^{(2)}\beta^{(1)}$ are identical in $J^1\mathbb{S}^1$ and there are one-to-one correspondences between sets of N -graphs:

$$\begin{aligned} \mathcal{N}\text{graphs}(\beta^{(1)}\beta^{(2)}) &\cong \mathcal{N}\text{graphs}(\beta^{(2)}\beta^{(1)}), \\ \mathcal{N}\text{graphs}(\beta_+, \beta_-^{(1)}\beta_-^{(2)}) &\cong \mathcal{N}\text{graphs}(\beta_+, \beta_-^{(2)}\beta_-^{(1)}), \\ \mathcal{N}\text{graphs}(\beta_+^{(1)}\beta_+^{(2)}, \beta_-) &\cong \mathcal{N}\text{graphs}(\beta_+^{(2)}\beta_+^{(1)}, \beta_-). \end{aligned}$$

Indeed, there are infinitely many bijections in each case which are induced by rotating a boundary (counter)clockwise by appropriate angle, and so, indexed canonically by the set \mathbb{Z} . We omit the details.

Suppose that $\mathcal{G}_1 \in \mathcal{N}\text{graphs}(\beta_2, \beta_1)$ and $\mathcal{G}_2 \in \mathcal{N}\text{graphs}(\beta_3, \beta_2)$. Then, two N -graphs can be merged or piled in a natural way to obtain the annular N -graph, denoted by

$$\mathcal{G}_2\mathcal{G}_1 \in \mathcal{N}\text{graphs}(\beta_3, \beta_1).$$

On the other hand, for $\mathcal{G} \in \mathcal{N}\text{graphs}(\beta)$ and $\mathcal{G}_1 \in \mathcal{N}\text{graphs}(\beta', \beta)$, the concatenation $\mathcal{G}_1\mathcal{G} \in \mathcal{N}\text{graphs}(\beta')$ is well defined by gluing along the boundary λ_β . Hence, we have two natural maps

$$\begin{aligned} \mathcal{N}\text{graphs}(\beta_3, \beta_2) \times \mathcal{N}\text{graphs}(\beta_2, \beta_1) &\rightarrow \mathcal{N}\text{graphs}(\beta_3, \beta_1), \\ \mathcal{N}\text{graphs}(\beta', \beta) \times \mathcal{N}\text{graphs}(\beta) &\rightarrow \mathcal{N}\text{graphs}(\beta'). \end{aligned}$$

In particular, for each ∂ -Legendrian isotopy from $\lambda' = \lambda_{\beta'}$ and $\lambda = \lambda_\beta$, we have a tame annular N -graph $\mathcal{G}_{\lambda'\lambda} \in \mathcal{N}\text{graphs}(\beta', \beta)$, where λ and λ' are closures of β and β' , respectively. Moreover, we also have a tame annular N -graph $\mathcal{G}_{\lambda'\lambda}^{-1}$ obtained by flipping the annulus inside out corresponding to the inverse isotopy from λ to λ' . Hence, we have two maps inverse to each other:

$$\mathcal{N}\text{graphs}(\beta) \rightarrow \mathcal{N}\text{graphs}(\beta') \quad \text{and} \quad \mathcal{N}\text{graphs}(\beta') \rightarrow \mathcal{N}\text{graphs}(\beta),$$

defined by

$$\mathcal{G} \mapsto \mathcal{G}_{\lambda'\lambda} \cdot \mathcal{G}, \quad \text{and} \quad \mathcal{G}' \mapsto \mathcal{G}_{\lambda'\lambda}^{-1} \cdot \mathcal{G}',$$

respectively.

Let $\mathcal{N}\text{graphs}_0(\beta, \beta)$ be the subset of tame annular N -graphs of type (β, β) .

Lemma 3.21. *Let β be a Legendrian positive N -graph. The set $\mathcal{N}\text{graphs}_0(\beta, \beta)$ becomes a group under the concatenation which acts on the set $\mathcal{N}\text{graphs}(\beta)$.*

Proof. It is easy to see that the set $\mathcal{N}\text{graphs}_0(\beta, \beta)$ is closed under the concatenation, which is associative. The trivial ∂ -Legendrian isotopy gives us the identity annular N -graph.

Finally, for each $\mathcal{G} \in \mathcal{N}\text{graphs}_0(\beta, \beta)$, the N -graph \mathcal{G}^{-1} plays the role of the inverse of \mathcal{G} due to the Move (I) and (V) of N -graphs described in Figure 18. Hence, $\mathcal{N}\text{graphs}_0(\beta, \beta)$ becomes a group acting on the set $\mathcal{N}\text{graphs}(\beta)$ by concatenation, and so, we are done. ■

Definition 3.22 (Legendrian loop). Let $\lambda \subset (\mathbb{R}^3, \xi_{\text{st}})$ be a Legendrian link, and let $\mathcal{L}(\lambda)$ be the space of Legendrian links isotopic to λ . A *Legendrian loop* ϑ is a continuous map

$$\vartheta: (\mathbb{S}^1, \text{pt}) \rightarrow (\mathcal{L}(\lambda), \lambda)$$

and said to be *tame* if the Legendrian $\vartheta(\theta)$ is a closure of a positive braid for each $\theta \in \mathbb{S}^1$.

Remark 3.23. One can regard each Legendrian loop ϑ for λ as an element of the fundamental group $\pi_1(\mathcal{L}(\lambda), \lambda)$.

Let λ be the closure of a positive braid β . Then, each tame Legendrian loop for λ corresponds to a ∂ -Legendrian isotopy from λ to λ and can be regarded as an element \mathcal{G}_ϑ in $\mathcal{N}\text{graphs}_0(\beta, \beta)$. Conversely, any element \mathcal{G} in $\mathcal{N}\text{graphs}_0(\beta, \beta)$ defines a tame Legendrian loop $\vartheta_{\mathcal{G}}$ obviously.

In summary, we have the following lemma.

Lemma 3.24. *Let β be a Legendrian positive N -braid. Then, there is one-to-one correspondence between $\mathcal{N}\text{graphs}_0(\beta, \beta)$ and the subset of homotopy classes of tame Legendrian loops for $\lambda = \lambda_\beta$. In particular, each tame Legendrian loop acts on $\mathcal{N}\text{graphs}(\beta)$.*

3.3. One-cycles in Legendrian weaves

Let us recall from [15] how to construct a seed from an N -graph \mathcal{G} . Each one-cycle in $\Lambda(\mathcal{G})$ corresponds to a vertex of the quiver, and a monodromy along that cycle gives a coordinate function at that vertex. The quiver is obtained from the intersection data among one-cycles. Moreover, there is an operation in N -graph, called *Legendrian mutation*, which is a counterpart of the mutation in the cluster structure. The Legendrian mutation is crucial in constructing and distinguishing N -graphs. In turn, these will give as many Lagrangian fillings of a given Legendrian links as seeds in the associated cluster pattern to the link which will be discussed in Section 4.

Let $\mathcal{G} \subset \mathbb{D}^2$ be a free N -graph, and let $\Lambda(\mathcal{G})$ be the induced Legendrian weave. We express one-cycles of $\Lambda(\mathcal{G})$ in terms of subgraphs of \mathcal{G} .

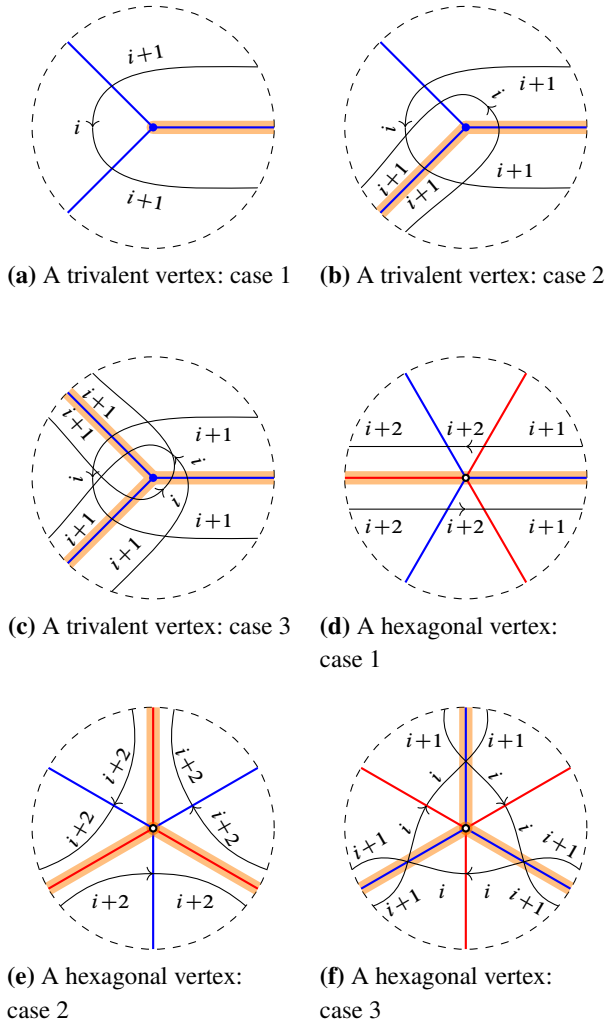


Figure 24. Local configurations on cycles and corresponding arcs of $\mathcal{G} \subset \mathbb{D}^2$.

Definition 3.25. A subgraph T of a non-degenerate N -graph \mathcal{G} is said to be *admissible* if, at each vertex, it looks locally one of pictures depicted in Figure 24. For a degenerate N -graph \mathcal{G} , a subgraph T is *admissible* if so is its perturbation as a subgraph of the perturbation of \mathcal{G} . See Figure 25.

For an admissible subgraph $T \subset \mathcal{G}$, let $\ell(T) \subset \mathbb{D}^2$ be an oriented, immersed, labeled loop given by gluing paths whose local pictures look as depicted in Figure 24.

The loop $\ell(T)$ defines a unique lift $\tilde{\ell}(T) \subset \Gamma(\mathcal{G})$ via $\pi_{\mathbb{D}^2} : \Gamma(\mathcal{G}) \rightarrow \mathbb{D}^2$ so that each s_j -labelled arc in $\ell(T)$ is contained in the s_j -th sheet of $\Gamma(\mathcal{G})$. Moreover, the

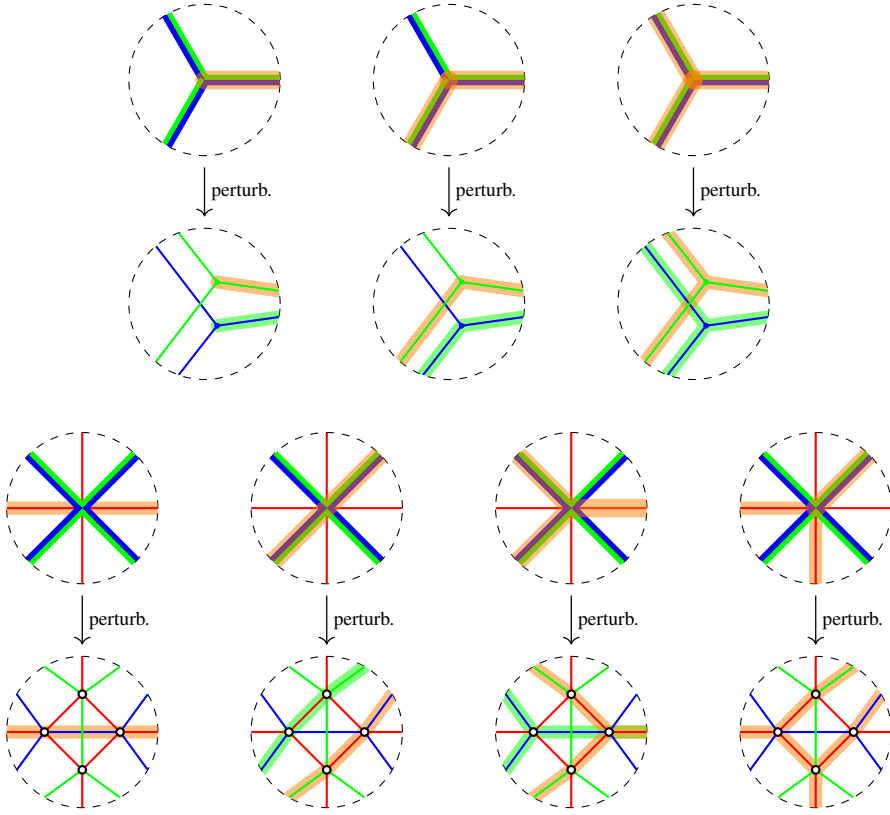


Figure 25. Local configurations on degenerate cycles and its perturbation.

immersed loop $\tilde{\ell}(\mathbb{T})$ lifts uniquely to an embedded loop $\gamma(\mathbb{T})$ in $\Lambda(\mathcal{G})$ via the front projection $\pi_F : \Lambda(\mathcal{G}) \rightarrow \Gamma(\mathcal{G})$.

Definition 3.26 (T-cycle). For an admissible subgraph $\mathbb{T} \subset \mathcal{G}$, if $\mathbb{T} \cap \partial\mathbb{D}^2 = \emptyset$, we call the cycle $[\gamma(\mathbb{T})] \in H_1(\Lambda(\mathcal{G}); \mathbb{Z})$ a *T-cycle*. When $\mathbb{T} \cap \partial\mathbb{D}^2 \neq \emptyset$, we then call the relative cycle $[\gamma(\mathbb{T})] \in H_1(\Lambda(\mathcal{G}), \lambda(\partial\mathcal{G}); \mathbb{Z})$ a *relative T-cycle*.

Example 3.27 ((Long) l-cycles). For an edge e of \mathcal{G} connecting two trivalent vertices, let $l(e)$ be the subgraph of \mathcal{G} consisting of a single edge e . Then, the cycle $[\gamma(l(e))]$ depicted in Figure 26a is called an *l-cycle*. Similarly, for an edge e of \mathcal{G} connecting a point on the boundary $\partial\mathbb{D}^2$ and a trivalent vertex, we call the induced relative cycle $[\gamma(l(e))]$ in $H_1(\Lambda(\mathcal{G}), \lambda(\partial\mathcal{G}))$ a *relative l-cycle*.

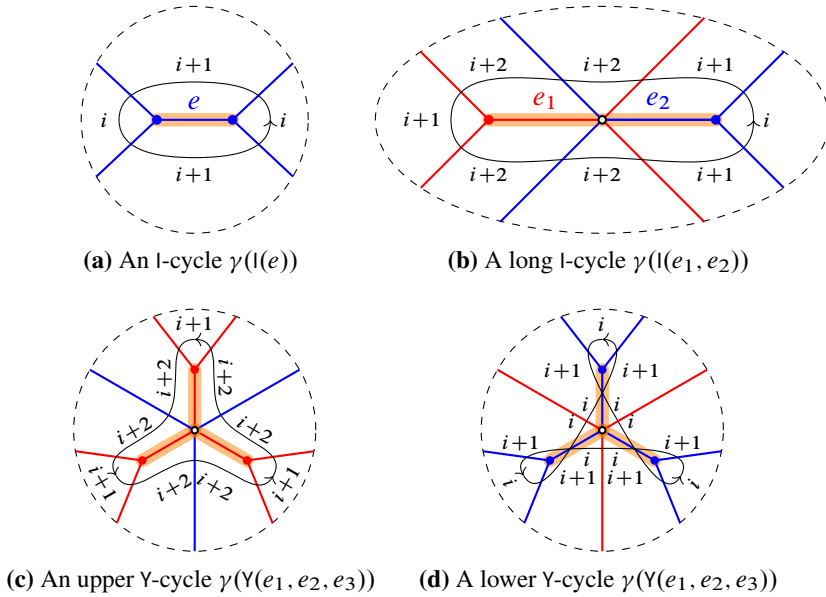


Figure 26. (Long) l- and Y-cycles.

In general, a linear chain of edges (e_1, e_2, \dots, e_n) satisfying the following:

- e_i connects a trivalent vertex and a hexagonal point for $i = 1, n$;
- e_i and e_{i+1} meet at a hexagonal point in the opposite way, see Figure 26b, for $i = 2, \dots, n - 1$

forms an admissible subgraph $l(e_1, \dots, e_n)$, and the cycle $[\gamma(l(e_1, \dots, e_n))]$ is called a *long l-cycle*. See Figure 26b.

Example 3.28 (Y-cycles). Let e_1, e_2, e_3 be monochromatic edges joining a hexagonal point h and trivalent vertices v_i for $i = 1, 2, 3$. Then, the subgraph $Y(e_1, e_2, e_3)$ consisting of three edges e_1, e_2 , and e_3 is an admissible subgraph of \mathcal{G} and it defines a cycle $[\gamma(Y(e_1, e_2, e_3))]$ called an *upper* or *lower* Y-cycle according to the relative position of sheets that edges represent. See Figures 26c and 26d.

One of the benefits of cycles from admissible subgraphs is that one can keep track of how cycles are changed under the N -graph moves described in Figure 18, especially under Move (I) and Move (II). Note that Move (III) can be decomposed into a sequence of Move (I) and Move (II). Some of such changes are given in Figure 27.

Remark 3.29. It is important to note that not every cycle can be represented by a subgraph. For example, the cycle on the left of the following picture cannot be expressed

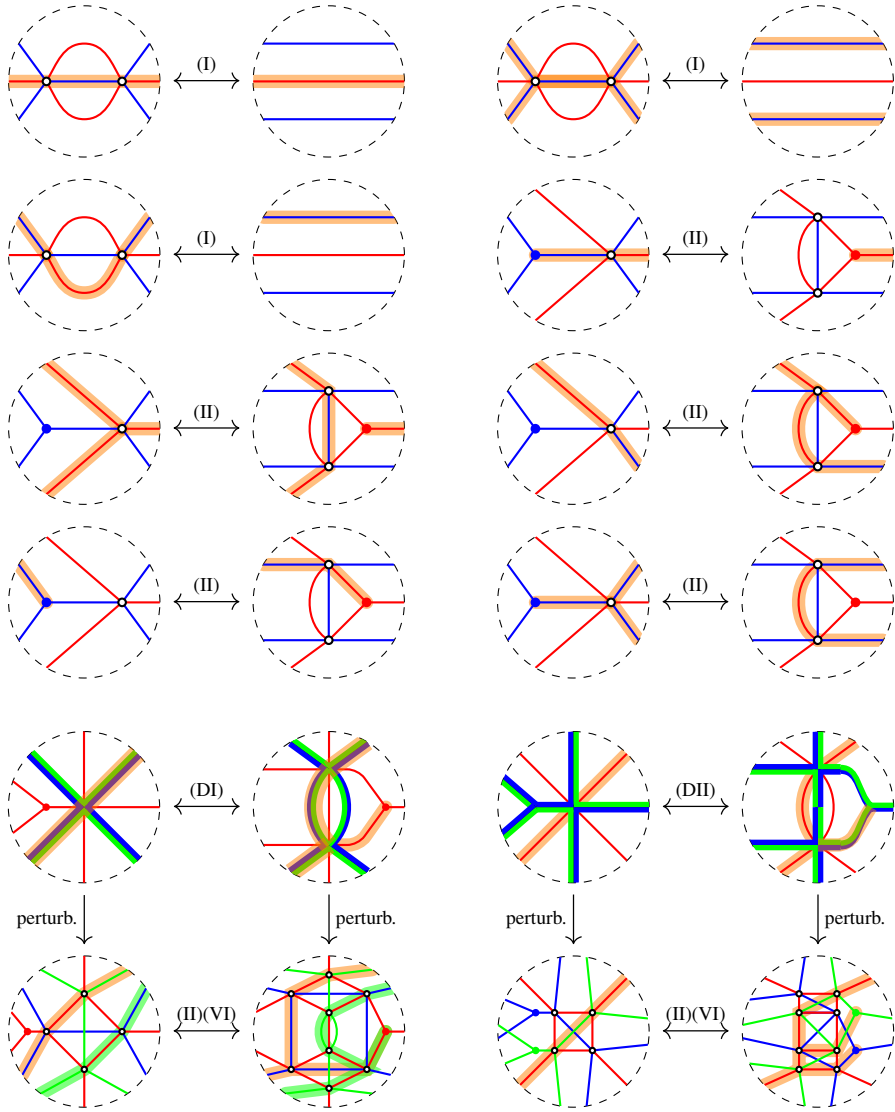
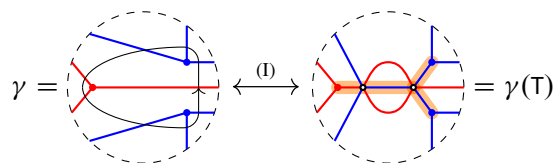
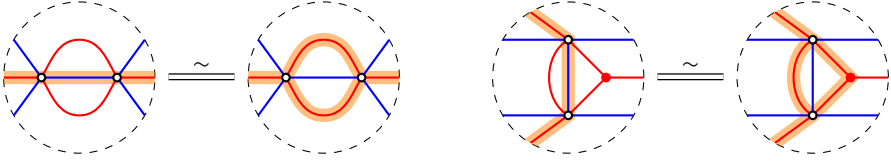


Figure 27. Cycles under Moves (I), (II), (DI), and (DII).

by a subtree but it can be after Move (I).



On the other hand, there might be a one-cycle having two different subgraph presentations as follows:

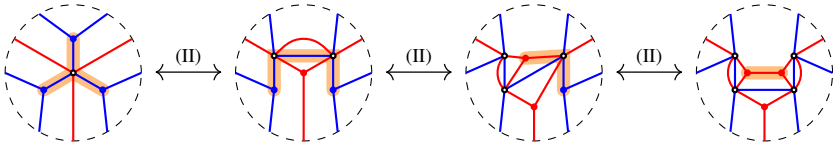


Therefore, there is a bit subtle issue for picking up nice cycles in a consistent way.

Definition 3.30. Let $\mathcal{G} \subset \mathbb{D}^2$ be an N -graph, and let $\Lambda(\mathcal{G})$ be an induced Legendrian surface in $J^1\mathbb{D}^2$. A (relative) cycle $[\gamma]$ in $H_1(\Lambda(\mathcal{G}))$ or $H_1(\Lambda(\mathcal{G}), \lambda(\partial\mathcal{G}))$ is *good* if $[\gamma]$ can be transformed to an (relative) I-cycle in $H_1(\Lambda(\mathcal{G}'))$ or $H_1(\Lambda(\mathcal{G}'), \lambda(\partial\mathcal{G}'))$ for some $[\mathcal{G}'] = [\mathcal{G}]$, respectively.

Example 3.31. The following cycles are good.

- (1) All (long) I- and Y-cycles.



- (2) The cycle $\gamma(T)$ for an admissible tree T without local configurations depicted in Figures 24b and 24c.

Definition 3.32. Let $(\mathcal{G}, \tilde{\mathcal{B}})$ and $(\mathcal{G}', \tilde{\mathcal{B}}')$ be pairs of an N -graph and a set of good (relative) cycles. We say that $(\mathcal{G}, \tilde{\mathcal{B}})$ and $(\mathcal{G}', \tilde{\mathcal{B}}')$ are *equivalent* if $[\mathcal{G}] = [\mathcal{G}']$ and the induced isomorphism

$$H_1(\Lambda(\mathcal{G}), \lambda(\partial\mathcal{G})) \cong H_1(\Lambda(\mathcal{G}'), \lambda(\partial\mathcal{G}'))$$

identifies $\tilde{\mathcal{B}}$ with $\tilde{\mathcal{B}}'$. We denote the equivalent class of $(\mathcal{G}, \tilde{\mathcal{B}})$ by $[\mathcal{G}, \tilde{\mathcal{B}}]$.

3.4. Flag moduli spaces

We recall from [15, 44] central algebraic invariants $\mathcal{M}(\lambda)$ and $\mathcal{M}(\mathcal{G})$ of the Legendrians λ and $\Lambda(\mathcal{G})$, respectively. The main idea is to consider moduli spaces of constructible sheaves adapted to the Legendrians.

3.4.1. Flag moduli spaces for Legendrian links. Let $\lambda = \lambda_\beta$ be a Legendrian in $J^1\mathbb{S}^1$; then, β gives us an $(N - 1)$ -tuple of points $X = (X_1, \dots, X_{N-1})$ in \mathbb{S}^1 . Notice that we are not assuming that all X_i 's are disjoint.

Remark 3.33. By abuse of notation, we regard β as a braid word on \mathbb{S}^1 , where two generators can occur simultaneously, such as $\sigma_{1,3}$. In this case, X_1 and X_3 are not disjoint.

The position of the points in X_i corresponds to the position of σ_i in β for $i = 1, \dots, N-1$. Let $\{f_k\}_{k \in K}$ be the set of closures of connected components of $\mathbb{S}^1 \setminus X$.

In order to introduce a legible model for the constructible sheaves adapted to λ_β , let us consider a full flag, i.e., a nested sequence of subspaces in \mathbb{C}^N :

$$\mathcal{F}^\bullet \in \{(\mathcal{F}^i)_{i=0}^N \mid \dim \mathcal{F}^i = i, \mathcal{F}^j \subset \mathcal{F}^{j+1}, 1 \leq j \leq N-1, \mathcal{F}^N = \mathbb{C}^N\}.$$

Let f_1, f_2 be consecutive faces sharing a point x in X . Then, the corresponding flags $\mathcal{F}^\bullet(f_1), \mathcal{F}^\bullet(f_2)$ satisfy

$$\mathcal{F}^i(f_1) = \mathcal{F}^i(f_2) \Leftrightarrow x \notin X_i. \quad (3.1)$$

The flags $\mathcal{F}_\lambda = \{\mathcal{F}_\lambda^\bullet(f_k)\}_{k \in K}$ in \mathbb{C}^N satisfying the conditions will be called simply by *flags on λ* . Let us denote the moduli space of such flags by $\tilde{\mathcal{M}}(\lambda)$; then, the general linear group $\mathrm{GL}_N(\mathbb{C})$ acts on all flags at once. The *flag moduli space* for Legendrian link λ is defined by the quotient space

$$\mathcal{M}(\lambda) := \tilde{\mathcal{M}}(\lambda) / \mathrm{GL}_N(\mathbb{C}).$$

It is well known that $\mathcal{M}(\lambda)$ is isomorphic to $\mathrm{Sh}_\lambda^1(\mathbb{R}^2)_0$ which is a Legendrian isotopy invariant; see [44, Theorem 1.1].

Remark 3.34. In general, we may consider moduli of flags $\{\mathcal{F}_\lambda^\bullet(f_k)\}_{k \in K}$ which possibly have non-trivial monodromy along the base \mathbb{S}^1 . In the current manuscript, however, we are only interested in flags which can be extended to \mathbb{D}^2 , which is adapted to the N -graphs. So, it is enough to consider the current setup $\{\mathcal{F}_\lambda^N(f_j) = \mathbb{C}^N\}_{k \in K}$ of trivial monodromy along \mathbb{S}^1 .

3.4.2. Flag moduli spaces for N -graphs. Let $\mathcal{G} = (\mathcal{G}_1, \dots, \mathcal{G}_{N-1})$ be an N -graph on \mathbb{D}^2 . Let $\{F_\ell\}_{\ell \in L}$ be a set of closures of connected components of $\mathbb{D}^2 \setminus \mathcal{G}$, call each closure a *face*. The *framed flag moduli space* $\tilde{\mathcal{M}}(\mathcal{G})$ is a collection of flags $\mathcal{F}_{\Lambda(\mathcal{G})} = \{\mathcal{F}^\bullet(F_\ell)\}_{\ell \in L}$ in \mathbb{C}^N satisfying the following: let F_1, F_2 be a pair of faces sharing an edge e in \mathcal{G} . Then, the corresponding flags $\mathcal{F}^\bullet(F_1), \mathcal{F}^\bullet(F_2)$ satisfy the condition

$$\mathcal{F}^i(F_1) = \mathcal{F}^i(F_2) \Leftrightarrow e \notin \mathcal{G}_i,$$

which is equivalent to the condition (3.1).

Then, *flag moduli space* for the N -graph \mathcal{G} is defined by

$$\mathcal{M}(\mathcal{G}) := \tilde{\mathcal{M}}(\mathcal{G}) / \mathrm{GL}_N(\mathbb{C}),$$

which is a stack in general.

Let $\text{Sh}(\mathbb{D}^2 \times \mathbb{R})$ be the category of *constructible sheaves* on $\mathbb{D}^2 \times \mathbb{R}$. Under the identification $J^1\mathbb{D}^2 \cong T^{\infty,-}(\mathbb{D}^2 \times \mathbb{R})$, an N -graph $\mathcal{G} \subset \mathbb{D}^2$ gives a Legendrian

$$\Lambda(\mathcal{G}) \subset J^1\mathbb{D}^2 \cong T^{\infty,-}(\mathbb{D}^2 \times \mathbb{R}) \subset T^\infty(\mathbb{D}^2 \times \mathbb{R}).$$

This can be used to define a Legendrian isotopy invariant $\text{Sh}_{\Lambda(\mathcal{G})}^1(\mathbb{D}^2 \times \mathbb{R})_0$ of $\text{Sh}(\mathbb{D}^2 \times \mathbb{R})$ consisting of constructible sheaves

- whose singular support at infinity lies in $\Lambda(\mathcal{G}) \subset T^\infty(\mathbb{D}^2 \times \mathbb{R})$,
- whose microlocal rank is one, and
- which are zero near $\mathbb{D}^2 \times \{-\infty\}$.

See [15, 32, 44] for more details.

Theorem 3.35 ([15, Theorem 5.3]). *The flag moduli space $\mathcal{M}(\mathcal{G})$ is isomorphic to $\text{Sh}_{\Lambda(\mathcal{G})}^1(\mathbb{D}^2 \times \mathbb{R})_0$. Hence, $\mathcal{M}(\mathcal{G})$ is a Legendrian isotopy invariant of $\Lambda(\mathcal{G})$.⁴*

We end this section by introducing a concept relating two moduli spaces $\mathcal{M}(\mathcal{G})$ and $\mathcal{M}(\partial\mathcal{G})$ as follows. For each \mathcal{G} on \mathbb{D}^2 , we have a canonical map

$$\mathcal{M}(\mathcal{G}) \rightarrow \mathcal{M}(\partial\mathcal{G})$$

induced by the restriction map, which does not have to be injective or surjective. However, since each internal edge in \mathcal{G} gives us an additional open condition, the image of $\mathcal{M}(\mathcal{G})$ is open in $\mathcal{M}(\partial\mathcal{G})$, and therefore, it is a birational equivalence if it is injective.

Definition 3.36 (Deterministic N -graphs). An N -graph \mathcal{G} on \mathbb{D}^2 is said to be *deterministic* if the induced map $\mathcal{M}(\mathcal{G}) \rightarrow \mathcal{M}(\partial\mathcal{G})$ between flag moduli spaces is a birational equivalence, or equivalently, the function field of $\mathcal{M}(\mathcal{G})$ is canonically isomorphic to $\mathcal{M}(\partial\mathcal{G})$, i.e.,

$$\mathbb{C}(\mathcal{M}(\mathcal{G})) \cong \mathbb{C}(\mathcal{M}(\partial\mathcal{G})).$$

Example 3.37. Let us compare $\mathcal{M}(\mathcal{G}(a, b, c))$ and $\mathcal{M}(\partial\mathcal{G}(a, b, c))$. Interior edges of $\mathcal{G}(a, b, c)$ produce additional open conditions on flags adapted to $\partial\mathcal{G}(a, b, c)$. Moreover, each flag on $(\mathbb{S}^1, \partial\mathcal{G}(a, b, c))$ can be extended uniquely on $(\mathbb{D}^2, \mathcal{G}(a, b, c))$ if possible. This implies that $\mathcal{M}(\mathcal{G}(a, b, c))$ can be seen as an open subset (indeed, an algebraic torus) of $\mathcal{M}(\partial\mathcal{G}(a, b, c))$. So, $\mathcal{M}(\mathcal{G}(a, b, c))$ and $\mathcal{M}(\partial\mathcal{G}(a, b, c))$ are birationally equivalent. A similar argument works for $\mathcal{G}(\tilde{\mathcal{D}}_n)$. We have $\mathcal{G}(a, b, c)$ and $\mathcal{G}(\tilde{\mathcal{D}}_n)$ are deterministic.

The following observations are obvious: let \mathcal{G} be an N -graph on \mathbb{D}^2 . (i) If \mathcal{G} consists of trees, then it is deterministic; (ii) if an N -graph $\mathcal{G} \subset \mathbb{D}^2$ is deterministic and $[\mathcal{G}] = [\mathcal{G}']$, then so is \mathcal{G}' .

⁴Indeed, the actual theorem is about a connected surface, not only for \mathbb{D}^2 .

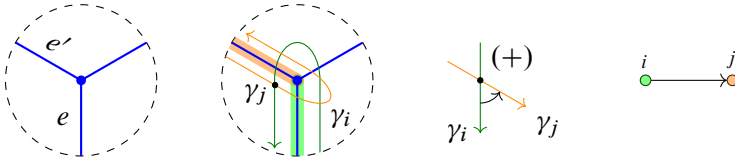


Figure 28. l-cycles with intersections.

3.5. Y-seeds and Legendrian mutations

Let $\mathcal{G} \subset \mathbb{D}^2$ be an N -graph, and let $\mathcal{B} = \{[\gamma_1], \dots, [\gamma_n]\}$ be a set of good (absolute) cycles in $H_1(\Lambda(\mathcal{G}))$. For two cycles $[\gamma_i]$ and $[\gamma_j]$, let $i([\gamma_i], [\gamma_j])$ be the algebraic intersection number. In particular, if γ_i is an l-cycle $\gamma(\ell(e))$ and γ_j is a T-cycle for some admissible subgraph \mathbb{T} , then

$$i([\gamma_i], [\gamma_j]) = \sum_{e' \in \mathbb{T}} i(e, e'),$$

where $i(e, e') \in \{0, 1, -1\}$ is defined as follows:

$$i(e, e') := \begin{cases} 0 & \text{if } e = e' \text{ or } e \cap e' = \emptyset; \\ 1 & \text{if } e' \text{ is lying on the left side of } e; \\ -1 & \text{if } e' \text{ is lying on the right side of } e. \end{cases}$$

Geometrically, two representatives of γ_i and γ_j look locally as depicted in Figure 28. Their intersection $i([\gamma_i], [\gamma_j])$ is defined to be +1 by using the counterclockwise rotation convention of two tangent directions of cycles γ_i and γ_j at the intersection point as depicted in the third picture in Figure 28. Note that our convention is opposite to the one in [15].

Definition 3.38. For each a pair $(\mathcal{G}, \mathcal{B})$ of an N -graph and a set of good cycles, we define a quiver $\mathcal{Q} = \mathcal{Q}(\mathcal{G}, \mathcal{B})$ as follows: let $n = \#(\mathcal{B})$.

- (1) The set of vertices is $[n]$.
- (2) The (i, j) -entry $b_{i,j}$ for $\mathcal{B}(\mathcal{Q}) = (b_{i,j})$ is the algebraic intersection number between $[\gamma_i]$ and $[\gamma_j]$:

$$b_{i,j} = i([\gamma_i], [\gamma_j]) \quad \text{for } 1 \leq i, j \leq n.$$

In order to assign a coefficient to each cycle, let us review the microlocal monodromy functor from [44]

$$\mu_{\text{mon}_\Lambda} : \text{Sh}_\Lambda^\bullet \rightarrow \mathcal{L}\text{oc}^\bullet(\Lambda).$$

In our case, this functor sends microlocal rank-one sheaves

$$\mathcal{F} \in \mathcal{M}(\mathcal{G}) \cong \mathrm{Sh}_{\Lambda(\mathcal{G})}^1(\mathbb{D}^2 \times \mathbb{R})_0,$$

or equivalently, flags $\{\mathcal{F}^\bullet(F_i)\}_{i \in I} \in \mathcal{M}(\mathcal{G})$, to rank-one local systems $\mu_{\mathrm{mon}_{\Lambda(\mathcal{G})}}(\mathcal{F})$ on the Legendrian surface $\Lambda(\mathcal{G})$. From now on, we regard flags \mathcal{F} as a formal parameter for the flag moduli space $\mathcal{M}(\mathcal{G})$. Then, the coefficients in the coefficient tuple \mathbf{y} for the pair $(\mathcal{G}, \mathcal{B})$ are defined by

$$\mathbf{y}(\mathcal{G}, \mathcal{B}) = (\mu_{\mathrm{mon}_{\Lambda(\mathcal{G})}}(-)([\gamma_1]), \dots, \mu_{\mathrm{mon}_{\Lambda(\mathcal{G})}}(-)([\gamma_n])),$$

where $\mu_{\mathrm{mon}_{\Lambda(\mathcal{G})}}(-)([\gamma_j]) : \mathcal{M}(\mathcal{G}) \rightarrow \mathbb{C}$. Let us denote the above assignment by

$$\Psi(\mathcal{G}, \mathcal{B}) = (\mathbf{y}(\mathcal{G}, \mathcal{B}), \mathcal{Q}(\mathcal{G}, \mathcal{B})).$$

By the Legendrian isotopy invariance of $\mathrm{Sh}_{\Lambda(\mathcal{G})}^1(\mathbb{D}^2 \times \mathbb{R})_0$ in [32], and the functorial property of the microlocal monodromy functor μ_{mon} [44], the assignment Ψ is well defined up to isotopy of $\Lambda(\mathcal{G})$. That is, if two pairs $(\Lambda(\mathcal{G}), \mathcal{B})$ and $(\Lambda(\mathcal{G}'), \mathcal{B}')$ are Legendrian isotopic, or $[\mathcal{G}, \mathcal{B}] = [\mathcal{G}', \mathcal{B}']$ in particular, then they give us the same seed via Ψ .

Theorem 3.39 ([15, Section 7.2.1]). *Let $\mathcal{G} \subset \mathbb{D}^2$ be a N -graph with a tuple of cycles \mathcal{B} in $H_1(\Lambda(\mathcal{G}))$. Then, the assignment Ψ to a Y -seed in a cluster structure*

$$\Psi([\mathcal{G}, \mathcal{B}]) = (\mathbf{y}(\mathcal{G}, \mathcal{B}), \mathcal{Q}(\mathcal{G}, \mathcal{B}))$$

is well defined.

When an N -graph \mathcal{G} is deterministic, the coefficient tuple \mathbf{y} originally defined on $\mathbb{C}[\mathcal{M}(\mathcal{G})]$ can be restricted to the coordinate ring $\mathbb{C}[\mathcal{M}(\lambda)]$ of the moduli spaces of flags on $\lambda = \partial\mathcal{G}$, which is actually a \mathcal{X} -cluster variety due to the result of Shen–Weng [42, Theorem 1.1].

The monodromy $\mu_{\mathrm{mon}_{\Lambda(\mathcal{G})}}(\mathcal{F})$ along a loop $[\gamma] \in H_1(\Lambda(\mathcal{G}))$ can be obtained by restricting the constructible sheaf \mathcal{F} to a tubular neighborhood of γ . Let us investigate how the monodromy can be computed explicitly in terms of flags $\{\mathcal{F}^\bullet(F_i)\}_{i \in I}$.

Let us consider an l -cycle $[\gamma]$ represented by a loop $\gamma(e)$ for some monochromatic edge e as in Figure 29a. Let us denote four flags corresponding to each region by F_1, F_2, F_3, F_4 , respectively. Suppose that $e \subset \mathcal{G}_i$; then, by the construction of flag moduli space $\mathcal{M}(\mathcal{G})$, a two-dimensional vector space $V := \mathcal{F}^{i+1}(F_*)/\mathcal{F}^{i-1}(F_*)$ is independent of $* = 1, 2, 3, 4$. Moreover, $\mathcal{F}^i(F_*)/\mathcal{F}^{i-1}(F_*)$ defines a one-dimensional subspace $v_* \subset V$ for $* = 1, 2, 3, 4$, satisfying

$$v_1 \neq v_2 \neq v_3 \neq v_4 \neq v_1.$$

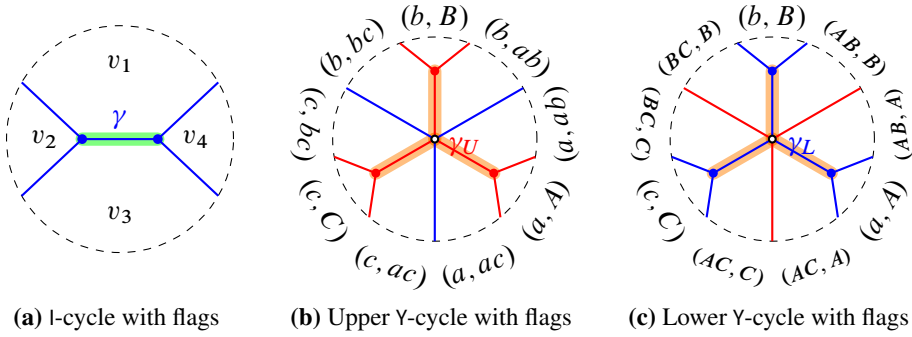


Figure 29. I- and Y-cycles with flags. Here, ab means the span of a and b , and AB means the intersection of A and B .

Then, $\mu_{\text{mon}_{\Lambda(\mathcal{G})}}(\mathcal{F})$ along the one-cycle $[\gamma(e)]$ is defined by the cross ratio

$$\mu_{\text{mon}_{\Lambda(\mathcal{G})}}(\mathcal{F})([\gamma]) := \langle v_1, v_2, v_3, v_4 \rangle = \frac{v_1 \wedge v_2}{v_2 \wedge v_3} \cdot \frac{v_3 \wedge v_4}{v_4 \wedge v_1}.$$

Suppose that local flags $\{F_j\}_{j \in J}$ near the upper Y-cycle $[\gamma_U]$ look like in Figure 29b. Let \mathcal{G}_i and \mathcal{G}_{i+1} be the N -subgraphs in red and blue, respectively. Then, the 3-dimensional vector space

$$V = \mathcal{F}^{i+2}(F_*) / \mathcal{F}^{i-1}(F_*)$$

is independent of $* \in J$. Now, regard a, b, c and A, B, C are subspaces of V of dimension one and two, respectively. Then, the microlocal monodromy along the Y-cycle $[\gamma_U]$ becomes

$$\mu_{\text{mon}_{\Lambda(\mathcal{G})}}(\mathcal{F})([\gamma_U]) := \frac{A(c)B(a)C(b)}{A(b)B(c)C(a)}.$$

Here, $B(a)$ can be seen as a pairing between a vector v_a with $\langle v_a \rangle = a$ and a covector w_B with $\langle w_B \rangle = B^\perp$.

Now, consider the lower Y-cycle $[\gamma_L]$ whose local flags given as in Figure 29c. We already have seen that the orientation convention of the loop in Figure 26 for the upper and lower Y-cycle is different. Then, microlocal monodromy along $[\gamma_L]$ follows the opposite orientation and becomes

$$\mu_{\text{mon}_{\Lambda(\mathcal{G})}}(\mathcal{F})([\gamma_L]) := \frac{A(b)B(c)C(a)}{A(c)B(a)C(b)}.$$

Let us define an operation called (*Legendrian*) *mutation* on N -graphs \mathcal{G} which corresponds to a geometric operation on the induced Legendrian surface $\Lambda(\mathcal{G})$ that

produces a smoothly isotopic but not necessarily Legendrian isotopic to $\Lambda(\mathcal{G})$; see [15, Definition 4.19]. Note that operation has an intimate relation with the wall-crossing phenomenon [3], Lagrangian surgery [40], and quiver (or Y -seed) mutations [25].

Definition 3.40 ([15]). Let \mathcal{G} be a (local) N -graph and $e \in \mathcal{G}_i \subset \mathcal{G}$ an edge between two trivalent vertices corresponding to an l-cycle $[\gamma] = [\gamma(e)]$. The mutation $\mu_\gamma(\mathcal{G})$ of \mathcal{G} along γ is obtained by applying the local change depicted in Figure 30a.

For the Y -cycle, the Legendrian mutation becomes as in the right of Figure 30b. Note that the mutation at Y -cycle can be decomposed into a sequence of Move (I) and Move (II) together with a mutation at l-cycle; see Example 3.31.

One can easily verify Legendrian (local) mutations on degenerate N -graph shown in Figures 30d and 30e via perturbation. For Figures 30f and 30g, see Appendix B.2.

Remark 3.41. Note that Figures 30e, 30f, and 30g depict the effect of the Legendrian mutation on a certain *part* of T -cycles. Since the boundaries of each side do not match, they seem not well-defined local operations at first glance. Indeed, they produce a well-defined operation when we apply each of the local operations to the (whole part of) T -cycle. By combining Figures 30c and 30f, for example, we obtain Figure 30h.

Let us recall our main purpose of finding exact embedded Lagrangian fillings for a Legendrian links. The following lemma guarantees that Legendrian mutation preserves the embedding property of Lagrangian fillings.

Proposition 3.42 ([15, Lemma 7.4]). *Let $\mathcal{G} \subset \mathbb{D}^2$ be a free N -graph. Then, mutation $\mu(\mathcal{G})$ at any l- or Y -cycle is again free N -graph.*

An important observation is the Legendrian mutation on $(\mathcal{G}, \mathcal{B})$ induces a Y -seed mutation on the induced seed $\Psi(\mathcal{G}, \mathcal{B})$.

Proposition 3.43 ([15, Section 7.2]). *Let $\mathcal{G} \subset \mathbb{D}^2$ be an N -graph and \mathcal{B} a set of good cycles in $H_1(\Lambda(\mathcal{G}))$. Let $\mu_{\gamma_i}(\mathcal{G}, \mathcal{B})$ be a Legendrian mutation of $(\mathcal{G}, \mathcal{B})$ along a one-cycle γ_i . Then,*

$$\Psi(\mu_{\gamma_i}(\mathcal{G}, \mathcal{B})) = \mu_i(\Psi(\mathcal{G}, \mathcal{B})).$$

Here, μ_i is the Y -seed mutation at the vertex i .

Remark 3.44. Let λ and λ' be two isotopic closures of positive N -braids. By fixing an isotopy between them, we have an annular N -graph $\mathcal{G}_{\lambda\lambda'}$ which induces a bijection between sets of N -graphs for λ and λ' by attaching $\mathcal{G}_{\lambda\lambda'}$. Then, indeed, this bijection is equivariant under the Legendrian mutation if it is defined, that is, for $[\gamma] \in H_1(\Lambda(\mathcal{G}))$,

$$\mu_\gamma(\mathcal{G}_{\lambda\lambda'} \cdot \mathcal{G}) = \mathcal{G}_{\lambda\lambda'} \cdot \mu_\gamma(\mathcal{G}).$$

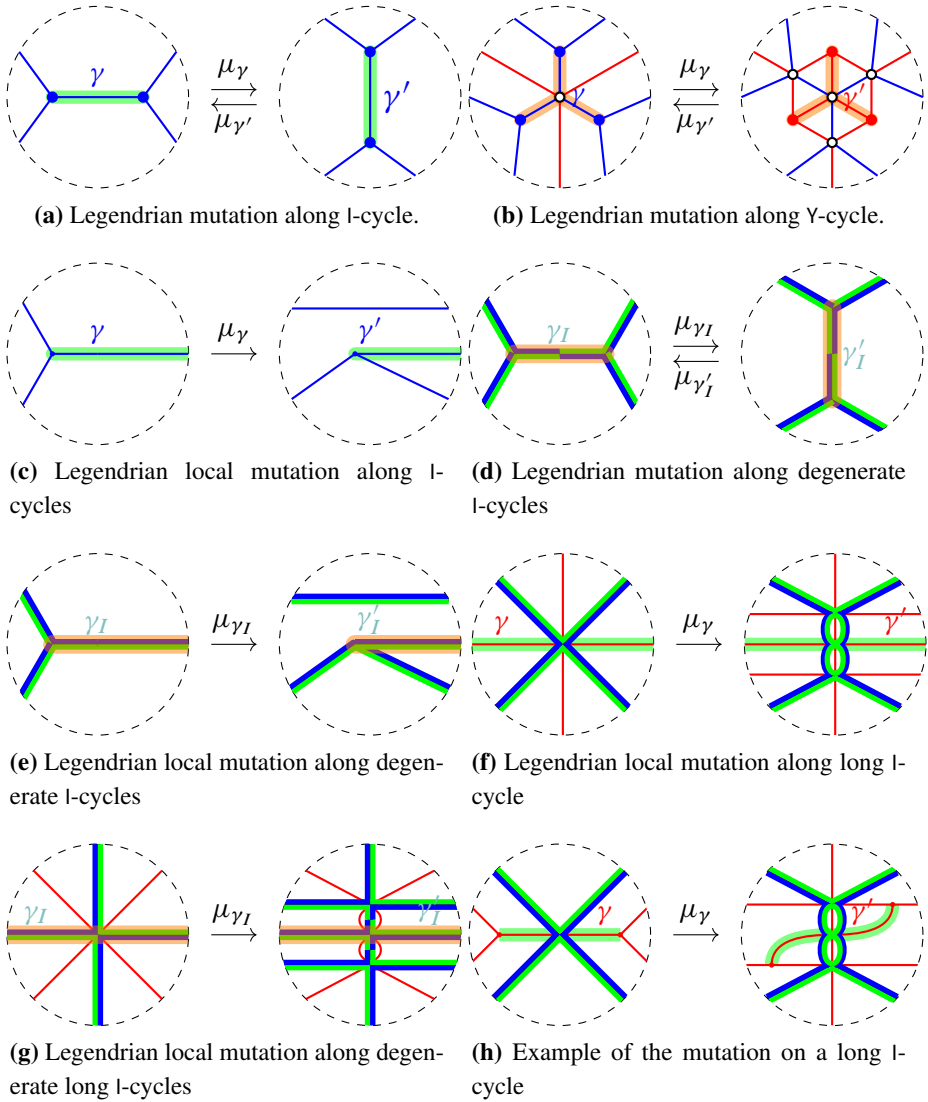


Figure 30. Legendrian (local) mutations at (degenerate, long) l- and Y-cycles.

In other words, two ∂ -Legendrian isotopic N -graphs will generate equivariantly bijective sets of N -graphs under Legendrian mutations.

Remark 3.45. Similarly, a stabilization $S(\mathcal{G})$ of \mathcal{G} will generate equivariantly bijective sets of N -graphs under Legendrian mutations as well since the stabilization part in $S(\mathcal{G})$ is away from the chosen cycles and does not affect the Legendrian mutability.

Proposition 3.46. *Let $\mathcal{G} \subset \mathbb{D}^2$ be a deterministic N -graph. Then, for any l - or Y -cycle γ , the mutation $\mu_\gamma(\mathcal{G})$ is again a deterministic N -graph.*

Proof. The proof is straightforward from the notion of the deterministic N -graph in Definition 3.36 and of the Legendrian mutation depicted in Figure 30a. Note that the Legendrian mutation $\mu_\gamma(\mathcal{G})$ at Y -cycle γ is also deterministic, since $\mu_\gamma(\mathcal{G})$ is a composition of Moves (I) and (II), and a mutation at l -cycle. ■

3.6. Relative cycles and a seed from a Y -seed

For a pair $(\mathcal{G}, \mathcal{B})$, we have constructed a Y -seed $\Psi(\mathcal{G}, \mathcal{B})$ in a Y -pattern. On the other hand, the pair corresponds to an exact Lagrangian filling $L = L(\mathcal{G})$ of $\lambda = \partial\mathcal{G}$ which gives a toric chart $Loc(L) \cong \mathcal{M}(\mathcal{G})$ in the corresponding \mathcal{X} -cluster variety $\mathcal{M}(\lambda)$ by considering local systems on L . Unfortunately, distinct seeds in a Y -pattern may share the same cluster chart in the \mathcal{X} -cluster variety, e.g., two Y -seeds in A_1 cluster pattern. In the \mathcal{A} -cluster structure, however, cluster charts in the \mathcal{A} -cluster variety can be distinguished by seeds in the cluster pattern. This is suitable for our purpose of distinguishing Lagrangian fillings via cluster charts for distinct seeds. Our strategy is to construct a seed in the cluster pattern (or \mathcal{A} -cluster structure) from a Y -seed by considering additional relative cycles. See also [14] for the role of relative cycles and microlocal merodromy in the study of Lagrangian fillings of Legendrian links and cluster structure.

Let \mathcal{G} be an N -graph on \mathbb{D}^2 and $\tilde{\mathcal{B}} = \{[\gamma_1], \dots, [\gamma_m]\}$ be a set of good (relative) cycles in $H_1(\Lambda(\mathcal{G}), \lambda(\partial\mathcal{G}))$. We define the *extended exchange matrix*

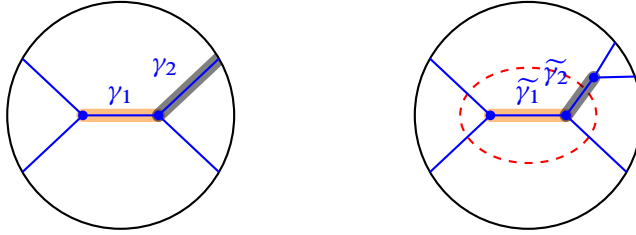
$$\tilde{\mathcal{B}} = \tilde{\mathcal{B}}(\mathcal{G}, \tilde{\mathcal{B}})$$

of size $m \times m$ by the algebraic intersection number among cycles in $\tilde{\mathcal{B}}$ as before.

Definition 3.47. We call $\tilde{\mathcal{B}}$ *admissible* if

- (1) $\tilde{\mathcal{B}}$ is the union of $\mathcal{B} = \{[\gamma_1], \dots, [\gamma_n]\}$ and $\mathcal{B}_{rel} = \{[\gamma_{n+1}], \dots, [\gamma_m]\}$ consisting of absolute and relative cycles, respectively,
- (2) \mathcal{B} forms a basis of $H_1(\Lambda(\mathcal{G}))$,
- (3) $\tilde{\mathcal{B}}$ forms a basis of $H_1(\Lambda(\mathcal{G}), \lambda(\partial\mathcal{G}))$, and
- (4) $\tilde{\mathcal{B}}$ has determinant ± 1 .

Now, let us introduce a new pair $(\tilde{\mathcal{G}}, \tilde{\mathcal{B}})$. Here, $\tilde{\mathcal{G}}$ is an N -graph on \mathbb{D}^2 which is obtained from \mathcal{G} by padding an annular N -graph containing (trivalent) vertices for each point in $\gamma \cap \partial\mathbb{D}^2$ for all $[\gamma] \in \mathcal{B}_{rel}$; see Figure 31. Note that the above annular N -graph gives a (fixed) Lagrangian cobordism from $\lambda = \lambda(\partial\mathcal{G})$ to $\tilde{\lambda} := \lambda(\partial\tilde{\mathcal{G}})$; let us denote it by $L_{\lambda\tilde{\lambda}}$.



(a) An N -graph \mathcal{G} with relative cycle γ_2 . (b) The extended N -graph $\tilde{\mathcal{G}}$ with corresponding cycles.

Figure 31. An example N -graph with relative cycle and the induced extended N -graph with cycle. The inner side of dotted red line of $\tilde{\mathcal{G}}$ can be identified with the N -graph \mathcal{G} .

Note that there is a natural inclusion $i : \mathcal{G} \rightarrow \tilde{\mathcal{G}}$. For a (good) cycle $[\gamma]$ in $H_1(\Lambda(\mathcal{G}))$, we have a corresponding (good) cycle $[\tilde{\gamma}] = [i(\gamma)]$ in $H_1(\Lambda(\tilde{\mathcal{G}}))$. When $[\gamma]$ is a good *relative* cycle in $H_1(\Lambda(\mathcal{G}), \lambda(\partial\mathcal{G}))$, we associate a good (absolute) cycle $[\tilde{\gamma}]$ in $H_1(\Lambda(\tilde{\mathcal{G}}))$ by using the trivalent vertex corresponding to γ in the annular N -graph; see Figure 31. By the same construction as in Section 3.5, we have the coefficient tuple $\tilde{\mathbf{y}} = (\tilde{y}_1, \dots, \tilde{y}_m)$ for the pair $(\tilde{\mathcal{G}}, \tilde{\mathcal{B}})$ which are defined by measuring microlocal monodromies along the cycles

$$\tilde{y}_i = \mu_{\text{mon}}_{\Lambda(\tilde{\mathcal{G}})}(-)([\tilde{\gamma}_i]) : \mathcal{M}(\Lambda(\tilde{\mathcal{G}})) \rightarrow \mathbb{C}, \quad i = 1, \dots, m.$$

In summary, we have constructed the pair $(\tilde{\mathbf{y}}, \tilde{\mathcal{B}})$ out of $(\tilde{\mathcal{G}}, \tilde{\mathcal{B}})$. Denote this assignment by $\tilde{\Psi}$.

Let us produce new pairs from $(\tilde{\mathcal{G}}, \tilde{\mathcal{B}})$ by applying Legendrian mutations *only* along the cycles in \mathcal{B} . We then obtain pairs $\{(\tilde{\mathbf{y}}_t, \tilde{\mathcal{B}}_t)\}_{t \in \mathbb{T}_n}$ which are obviously corresponding to the Y -seeds $\{(\mathbf{y}_t, \mathcal{B}_t)\}_{t \in \mathbb{T}_n}$ of the cluster pattern. Here, we have additional tuple $(\tilde{y}_{n+1}, \dots, \tilde{y}_m)$ and regard it as an analogy the frozen variables (or formal variables) in the Y -seed.

Now, we investigate the relation between flag moduli spaces $\mathcal{M}(\mathcal{G})$, $\mathcal{M}(\tilde{\mathcal{G}})$, $\mathcal{M}(\lambda)$, and $\mathcal{M}(\tilde{\lambda})$. Note that the Legendrian link $\tilde{\lambda}$ can be obtained from λ by adding $\#(\mathcal{B}_{rel})$ positive crossings in suitable positions. Again, by the work of Shen–Weng [42, Theorem 1.1], the moduli space $\mathcal{M}(\tilde{\lambda})$ becomes an \mathcal{X} -cluster variety.

Using the language of local system, see [35], we have the following embeddings:

$$i_{\mathcal{G}} : \mathcal{M}(\mathcal{G}) \rightarrow \mathcal{M}(\lambda), \quad i_{\tilde{\mathcal{G}}} : \mathcal{M}(\tilde{\mathcal{G}}) \rightarrow \mathcal{M}(\tilde{\lambda}).$$

On the other hand, we have a (natural) restriction

$$r_{\mathcal{G}} : \mathcal{M}(\tilde{\mathcal{G}}) \rightarrow \mathcal{M}(\mathcal{G}).$$

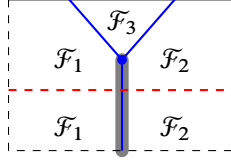


Figure 32. Local flag configuration near a relative cycle.

The variables $y_i \in \mathbb{C}[\mathcal{M}(\mathcal{G})]$ and $\tilde{y}_i \in \mathbb{C}[\mathcal{M}(\tilde{\mathcal{G}})]$ for $1 \leq i \leq n$ can be identified via the restriction $r_{\mathcal{G}}$.

Now, we collect N -graphs $\{\tilde{\mathcal{G}}_t\}_{t \in \mathbb{T}_n}$ which are obtained from $\tilde{\mathcal{G}}$ by a sequence of Legendrian mutations *only* along the cycles in \mathcal{B} . Then, consider an \mathcal{X} -cluster subvariety inside $\mathcal{M}(\tilde{\lambda})$ which consists of cluster charts $\{\mathcal{M}(\tilde{\mathcal{G}}_t)\}_{t \in \mathbb{T}_n}$. Let us denote the subvariety by $\mathcal{M}(\tilde{\lambda})'$. Note that the tuple $\tilde{\mathbf{y}}$ is originally in $\mathbb{C}[\mathcal{M}(\tilde{\mathcal{G}})]$ and can be seen as in $\mathbb{C}[\mathcal{M}(\tilde{\lambda})']$ the coordinate ring of the newly considered \mathcal{X} -cluster variety.

For each relative cycle $[\gamma]$ in \mathcal{B}_{rel} , we have the following local flag description in $\mathcal{M}(\tilde{\mathcal{G}})$.

As seen in Figure 32, the regions below the dotted red line are the ones in the original N -graph \mathcal{G} . Even though $\mathcal{F}_i, i = 1, 2, 3$ are flags in \mathbb{C}^N in general, we may assume that they are flags in \mathbb{C}^2 by modding out identical vector spaces in $\mathcal{F}_i, i = 1, 2, 3$. Every cluster charts $\{\mathcal{M}(\tilde{\mathcal{G}}_t)\}_{t \in \mathbb{T}_n}$ should satisfy $\mathcal{F}_1 \neq \mathcal{F}_2$ for each relative cycle. Since $\mathcal{M}(\tilde{\lambda})'$ is the gluing of such charts, the same holds for $\mathcal{M}(\tilde{\lambda})'$. This condition allows us to define a restriction

$$r_{\lambda} : \mathcal{M}(\tilde{\lambda})' \rightarrow \mathcal{M}(\lambda).$$

Note that there is no natural restriction from $\mathcal{M}(\tilde{\lambda})$ to $\mathcal{M}(\lambda)$. One can easily check that the following diagram commutes:

$$\begin{array}{ccc} \mathcal{M}(\mathcal{G}) & \xrightarrow{i_{\mathcal{G}}} & \mathcal{M}(\lambda) \\ \uparrow r_{\mathcal{G}} & & \uparrow r_{\lambda} \\ \mathcal{M}(\tilde{\mathcal{G}}) & \xrightarrow{i_{\tilde{\mathcal{G}}}} & \mathcal{M}(\tilde{\lambda})' \end{array}$$

Now, we are ready to prove that there are at least as many Lagrangian fillings for Legendrian link as seeds in the cluster structure.

Proposition 3.48. *Let $(\mathcal{G}, \mathcal{B})$ and $(\mathcal{G}', \mathcal{B}')$ be pairs of free and deterministic N -graphs on \mathbb{D}^2 and sets of good 1-cycles such that*

- (1) $\partial \mathcal{G} = \partial \mathcal{G}'$,
- (2) \mathcal{B} and \mathcal{B}' can be extended to admissible sets of good cycles, and
- (3) there exists a sequence of Legendrian mutations from $(\mathcal{G}, \mathcal{B})$ to $(\mathcal{G}', \mathcal{B}')$.

If $(\mathcal{G}, \mathcal{B})$ and $(\mathcal{G}', \mathcal{B}')$ define different Y -seeds via Ψ , then there is no exact Lagrangian isotopy between two Lagrangian fillings $L(\mathcal{G})$ and $L(\mathcal{G}')$ of a Legendrian link

$$\lambda(\partial\mathcal{G}) = \lambda(\partial\mathcal{G}').$$

Proof. We first notice that $\Psi(\mathcal{G}, \mathcal{B}) \neq \Psi(\mathcal{G}', \mathcal{B}')$ implies that

$$\tilde{\Psi}(\tilde{\mathcal{G}}, \tilde{\mathcal{B}}) \neq \tilde{\Psi}(\tilde{\mathcal{G}}', \tilde{\mathcal{B}}').$$

Since $\tilde{\mathcal{B}}$ is of full rank, by Proposition 2.9, the cluster charts $\mathcal{M}(\tilde{\mathcal{G}})$ and $\mathcal{M}(\tilde{\mathcal{G}}')$ are different in $\mathcal{M}(\tilde{\lambda})$, and so is in $\mathcal{M}(\tilde{\lambda})'$ by Corollary 2.10.

Assume on the contrary that there is an exact Lagrangian isotopy between $L(\mathcal{G})$ and $L(\mathcal{G}')$, then so is between $L(\tilde{\mathcal{G}})$ and $L(\tilde{\mathcal{G}}')$. Then, by [35], the toric charts

$$\mathcal{L}oc^1(L(\tilde{\mathcal{G}})) \cong \mathcal{M}(\tilde{\mathcal{G}})$$

and

$$\mathcal{L}oc^1(L(\tilde{\mathcal{G}}')) \cong \mathcal{M}(\tilde{\mathcal{G}}')$$

have the same images in $\mathcal{M}(\tilde{\lambda})$ under $i_{\tilde{\mathcal{G}}}$ and $i_{\tilde{\mathcal{G}}'}$, which yields a contradiction. ■

4. Lagrangian fillings for Legendrian links of finite or affine type

Let $\lambda \subset J^1\mathbb{S}^1$ be a Legendrian knot or link which is a closure of a positive braid and bounds a Legendrian surface $\Lambda(\mathcal{G})$ in $J^1\mathbb{D}^2$ for some free N -graph \mathcal{G} . We fix a set \mathcal{B} of good cycles in the sense of Definition 3.30. Then, by Theorem 3.39, we obtain a Y -seed $\Psi(\mathcal{G}, \mathcal{B})$ which is a pair of a coefficient tuple $\mathbf{y}(\Lambda(\mathcal{G}), \mathcal{B})$ and a quiver $\mathcal{Q}(\Lambda(\mathcal{G}), \mathcal{B})$.

We say that the pair $(\mathcal{G}, \mathcal{B})$ is of *finite type* or of *infinite type* if so is the cluster algebra defined by $\mathcal{Q}(\Lambda(\mathcal{G}), \mathcal{B})$. Similarly, it is said to be of *type Z* for some Dynkin diagram Z if so is the associated cluster algebra. In particular, it is said to be of *type ADE* or of *affine type* if the quiver is of type ADE or of affine type. See Definition 2.12.

4.1. N -graphs of finite or affine types

In [29], Gao, Shen, and Weng describe a procedure as follows. Starting from a (positive) braid word, they associate a so-called brick diagram, which includes the data of a quiver. The reader is encouraged to see their paper for more details. We will not define these notions here but will sketch their result for a number of examples which yield quivers of finite and affine type. We will prefer to use mutation-equivalent models for our purposes, as they are more amenable to performing the desired Legendrian

mutations, though we include the Gao–Shen–Weng procedure to indicate that finding models for a given Dynkin type Z is essentially algorithmic using their work.

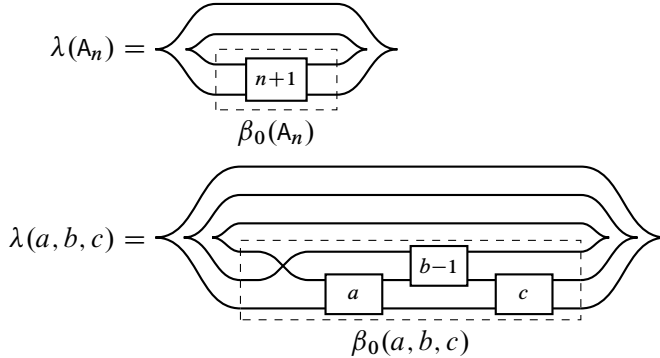
Remark 4.1. In this section, we will define braids β and $\tilde{\beta}$ of each type, where $\tilde{\beta}$ is obtained from β by doubling chosen generators so that the closure of $\tilde{\beta}$ has only one component. The chosen generator of β will be decorated by the box. For example, if $\beta = \sigma_1^n \boxed{\sigma_1}$, then $\beta = \sigma_1^{n+1}$ and $\tilde{\beta}$ is either σ_1^{n+1} or σ_1^{n+2} .

4.1.1. Linear and tripod N -graphs. For $n \geq 1$ and a triple (a, b, c) with $a, b, c \geq 1$, let us define positive braids $\beta_0(A_n)$, $\beta(A_n)$, $\beta_0(a, b, c)$, and $\beta(a, b, c)$ as follows:

$$\begin{aligned} \beta_0(A_n) &:= \sigma_1^n \boxed{\sigma_1}, & \beta_0(a, b, c) &:= \sigma_2 \boxed{\sigma_1} \sigma_1^{a-1} \sigma_2^{b-1} \sigma_1^{c-1} \boxed{\sigma_1}, \\ \beta(A_n) &:= \Delta_2 \beta_0(A_n) \Delta_2 \doteq \sigma_1^{n+1} \boxed{\sigma_1} \sigma_1, & \beta(a, b, c) &:= \Delta_3 \beta_0(a, b, c) \Delta_3. \end{aligned}$$

Then, the braids $\tilde{\beta}_0(A_n)$ and $\tilde{\beta}_0(a, b, c)$ are exactly the same as $\tilde{\beta}_0(A_n) := \beta_0(A_{n+\varepsilon})$ and $\tilde{\beta}_0(a, b, c) := \beta_0(a + \varepsilon_1, b, c + \varepsilon_2)$, where ε and ε_i are either 0 or 1 such that $n + \varepsilon$ is odd, and exactly two of $a + \varepsilon_1, b$, and $c + \varepsilon_2$ are odd.

We define $\lambda(A_n)$, $\tilde{\lambda}(A_n)$, $\lambda(a, b, c)$, and $\tilde{\lambda}(a, b, c)$ as the rainbow closures of $\beta_0(A_n)$, $\tilde{\beta}_0(A_n)$, $\beta_0(a, b, c)$, and $\tilde{\beta}_0(a, b, c)$, or equivalently, the (-1) -closures of $\beta(A_n)$ and $\beta(a, b, c)$, respectively,



where \boxed{r} is equivalent to $\underbrace{\sigma_1 \dots \sigma_1}_r$.

One can easily check that the quivers $\mathcal{Q}^{\text{brick}}(A_n)$ and $\mathcal{Q}^{\text{brick}}(a, b, c)$ from brick diagrams of $\beta_0(A_n)$ and $\beta_0(a, b, c)$ described in [29] look as follows:

$$\begin{aligned} &\mathcal{Q}^{\text{brick}}(A_n) \\ = & \begin{array}{c} \begin{array}{|c|c|c|c|c|} \hline \circ & \circ & \cdots & \circ & \circ \\ \hline \sigma_1 & \sigma_1 & \sigma_1 & \sigma_1 & \sigma_1 \\ \hline \end{array} \\ \underbrace{\hspace{10em}}_{n+1} \end{array} \end{aligned}$$

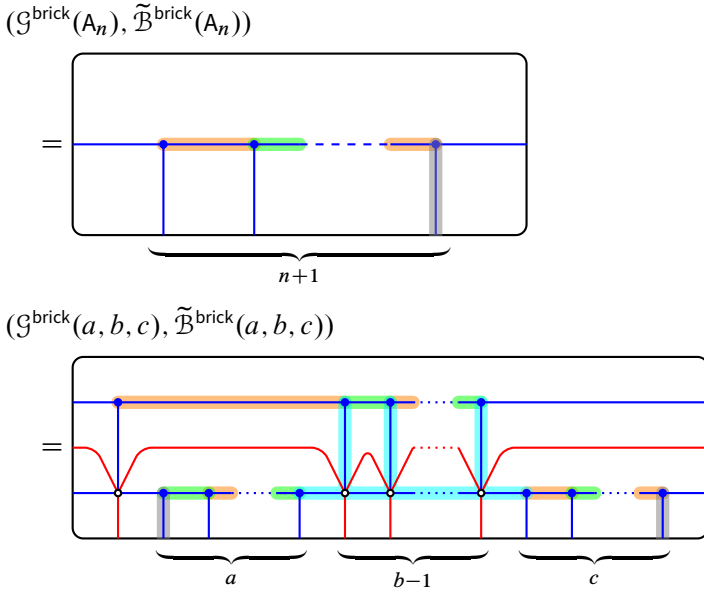
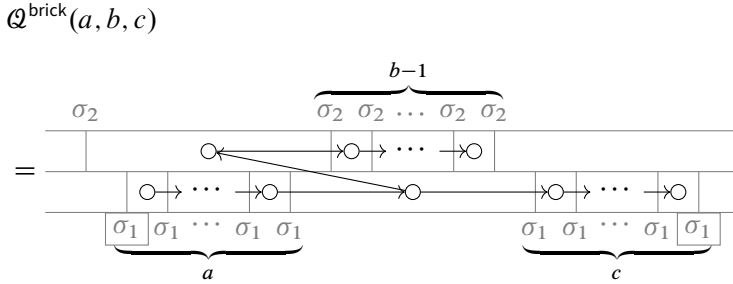


Figure 33. Brick linear and tripod N -graphs with (relative) cycles.



Then, there are canonical N -graphs $(\mathcal{G}^{\text{brick}}(A_n), \tilde{\mathcal{B}}^{\text{brick}}(A_n))$ and $(\mathcal{G}^{\text{brick}}(a, b, c), \tilde{\mathcal{B}}^{\text{brick}}(a, b, c))$ on \mathbb{D}^2 with (relative) cycles as shown in Figure 33 such that

$$\begin{aligned} \mathcal{Q}^{\text{brick}}(A_n) &= \mathcal{Q}(\mathcal{G}^{\text{brick}}(A_n), \tilde{\mathcal{B}}^{\text{brick}}(A_n)), \\ \mathcal{Q}^{\text{brick}}(a, b, c) &= \mathcal{Q}(\mathcal{G}^{\text{brick}}(a, b, c), \tilde{\mathcal{B}}^{\text{brick}}(a, b, c)). \end{aligned}$$

The colors on cycles in Figure 33 are nothing to do with the bipartite coloring, but we define N -graphs with bipartite coloring, which is equivalent to the original brick N -graphs and will play the roles of the initial seeds. Throughout this section, relative cycles are indicated in gray.

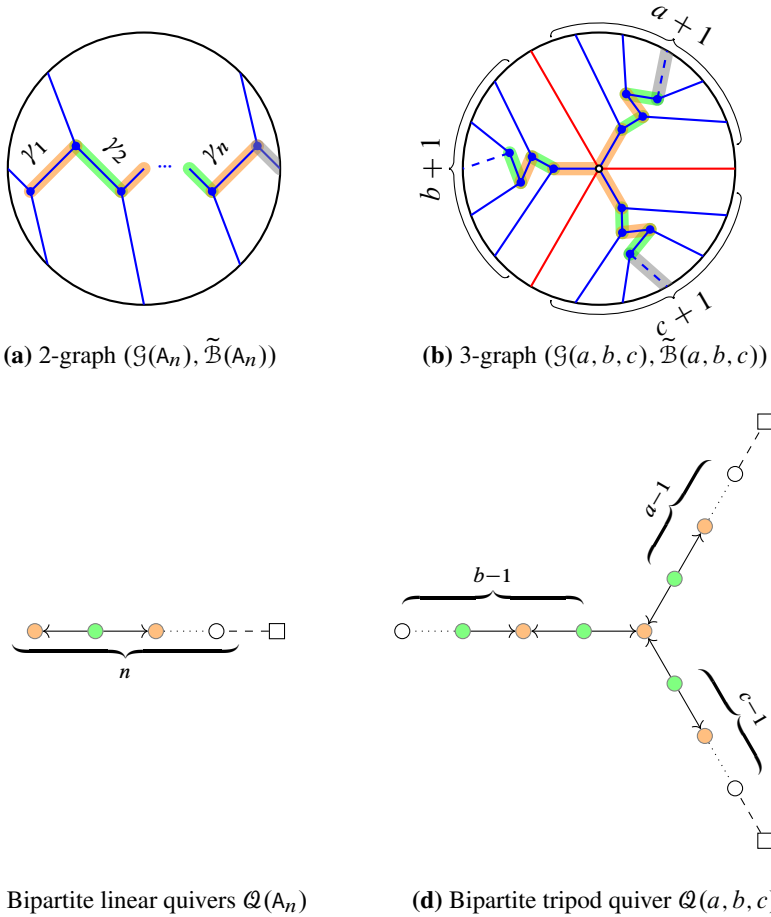


Figure 34. Bipartite linear and tripod N -graphs with chosen cycles and their quivers.

Definition 4.2 (Linear and tripod N -graphs). For each $n \geq 1$, the *linear N -graph* $(\mathcal{G}(A_n), \tilde{\mathcal{B}}(A_n))$ is the 2-graph on \mathbb{D}^2 depicted in Figure 34a.

For $a, b, c \geq 1$, the *tripod N -graph* $(\mathcal{G}(a, b, c), \tilde{\mathcal{B}}(a, b, c))$ is a free 3-graph on \mathbb{D}^2 depicted in Figure 34b.

Lemma 4.3. For each $n \geq 1$ and each triple (a, b, c) with $a, b, c \geq 1$, both N -graphs $(\mathcal{G}^{\text{brick}}(A_n), \tilde{\mathcal{B}}^{\text{brick}}(A_n))$ and $(\mathcal{G}^{\text{brick}}(a, b, c), \tilde{\mathcal{B}}^{\text{brick}}(a, b, c))$ are free, deterministic, and equivalent to $(\mathcal{G}(A_n), \tilde{\mathcal{B}}(A_n))$ and $(\mathcal{G}(a, b, c), \tilde{\mathcal{B}}(a, b, c))$ up to ∂ -Legendrian isotopy and mutations, respectively, and their quivers are the same as shown in Figures 34c and 34d:

$$\mathcal{Q}(A_n) = \mathcal{Q}(\mathcal{G}(A_n), \tilde{\mathcal{B}}(A_n)), \quad \mathcal{Q}(a, b, c) = \mathcal{Q}(\mathcal{G}(a, b, c), \tilde{\mathcal{B}}(a, b, c)).$$

Proof. For A_n , this is trivial.

For a triple (a, b, c) , the freeness and deterministicity of $\mathcal{G}(a, b, c)$ follow from Lemma 3.9. Since $\lambda(a, b, c)$ is the (-1) -closure of $\beta(a, b, c)$, we need to check that $\lambda(a, b, c)$ and $\partial\mathcal{G}(a, b, c)$ are equivalent in $J^1\mathbb{S}^1$. Indeed,

$$\beta(a, b, c) \doteq \sigma_2 \boxed{\sigma_1} \sigma_1^{a-1} \Delta_3 \sigma_1^{b-1} \Delta_3 \sigma_1^{c-1} \boxed{\sigma_1},$$

whose the (-1) -closure is the same as $\partial\mathcal{G}(a, b, c)$. Here, Δ_N is the half-twist braid of N -strands.

The N -graph equivalence for $\mathcal{G}(a, b, c)$ will be given in Appendix B.4 and it is easy to check that the quiver $\mathcal{Q}^{\text{brick}}(a, b, c)$ is mutation equivalent to $\mathcal{Q}(a, b, c)$. ■

Note that the linear and tripod N -graphs have certain symmetries as follows.

Lemma 4.4 (Rotational symmetries). *By ignoring relative cycles,*

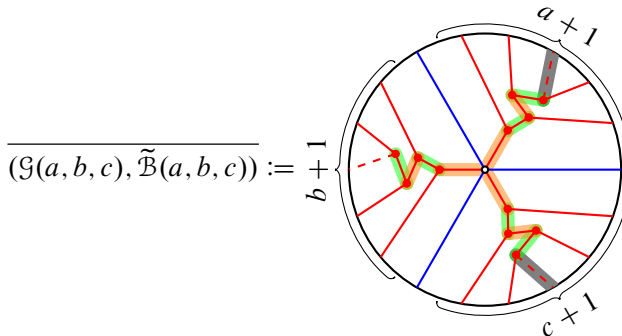
- (1) *the N -graph $(\mathcal{G}(A_n), \mathcal{B}(A_n))$ with cycles is invariant under π -rotation for odd $n \geq 1$, and*
- (2) *the N -graph $(\mathcal{G}(a, a, a), \mathcal{B}(a, a, a))$ with cycles is invariant under $2\pi/3$ -rotation for each $a \geq 1$.*

Lemma 4.5 (Conjugation symmetries). *The N -graph $(\mathcal{G}(A_n), \tilde{\mathcal{B}}(A_n))$ with cycles is invariant under the conjugation.*

For any triple (a, b, c) , the N -graph $\mathcal{G}(a, b, c)$ is never invariant under conjugation, which acts on the Legendrian $\lambda(a, b, c)$ as interchanging σ_1 and σ_2 so that $\overline{\lambda(a, b, c)}$ is the rainbow closure of

$$\overline{\beta_0(a, b, c)} = \sigma_1 \sigma_2^a \sigma_1^{b-1} \sigma_2^c.$$

The N -graph $(\mathcal{G}(a, b, c), \tilde{\mathcal{B}}(a, b, c))$ corresponding to $\overline{\lambda(a, b, c)}$ is depicted below.



On the other hand, if one of a, b, c is 1, then the quiver $\mathcal{Q}(a, b, c)$ is of type A_n . As seen in Example 3.15, the Legendrian link $\lambda(1, b, c)$ is a stabilization of $\lambda(A_n)$ for

$$n = b + c - 1.$$

Z	A_n	D_n	E_6	E_7
(a, b, c)	$(1, b, c)$	$(2, 2, n - 2)$	$(2, 3, 3)$	$(2, 3, 4)$
Z	E_8	\tilde{E}_6	\tilde{E}_7	\tilde{E}_8
(a, b, c)	$(2, 3, 5)$	$(3, 3, 3)$	$(2, 4, 4)$	$(2, 3, 6)$

Table 8. Triples (a, b, c) of types ADE and \tilde{E} .

Indeed, the N -graph $\mathcal{G}(1, b, c)$ is a stabilization of $\mathcal{G}(A_n)$. See Appendix B.3 for the proof.

Lemma 4.6. *The N -graph $\mathcal{G}(1, b, c)$ is a stabilization of $\mathcal{G}(A_n)$ for $n = b + c - 1$.*

One consequence of this lemma is that two N -graphs $\mathcal{G}(A_n)$ and $\mathcal{G}(1, b, c)$ with $n = b + c - 1$ will generate bijective sets of N -graphs under mutations as seen in Remarks 3.44 and 3.45, where the bijection preserves the mutation.

Notice that the quivers $\mathcal{Q}(a, b, c)$ together with $\mathcal{Q}(A_n)$ cover all quivers of finite type and some quivers of affine type. Indeed, for $1 \leq a \leq b \leq c$ and $n = a + b + c - 2$, the quivers $\mathcal{Q}(1, b, c)$ and $\mathcal{Q}(A_n)$ are of type A_n , and the quivers $\mathcal{Q}(2, 2, n - 2)$ and $\mathcal{Q}(2, 3, m - 3)$ are of types D_n and E_m . Moreover, $\mathcal{Q}(3, 3, 3)$, $\mathcal{Q}(2, 4, 4)$, and $\mathcal{Q}(2, 3, 6)$ are of types \tilde{E}_6 , \tilde{E}_7 , and \tilde{E}_8 , respectively. Hence, we denote Legendrians, quivers, N -graphs, and so on by using Z for $Z = D_n, E_n$, or \tilde{E}_n instead of the triple (a, b, c) corresponding to Z as seen in Table 8.

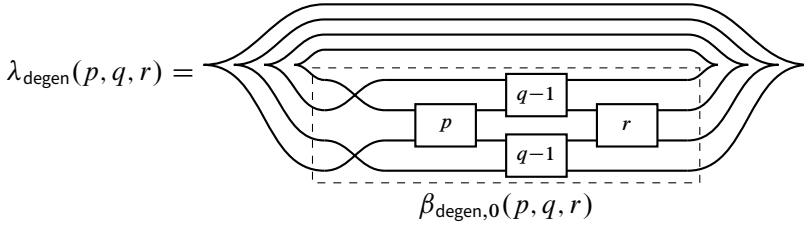
4.1.2. Degenerate N -graphs. For each triple (p, q, r) with $p, q, r \geq 1$, we define the positive 4-braids $\beta_{\text{degen},0}(p, q, r)$ and $\beta_{\text{degen}}(p, q, r)$ as

$$\begin{aligned} \beta_{\text{degen},0}(p, q, r) &:= \sigma_{1,3} \sigma_2^p \sigma_{1,3}^{q-2} \boxed{\sigma_{1,3}} \sigma_2^{r-1} \boxed{\sigma_2}, \\ \beta_{\text{degen}}(p, q, r) &:= \Delta_4 \beta_{\text{degen},0}(p, q, r) \Delta_4. \end{aligned}$$

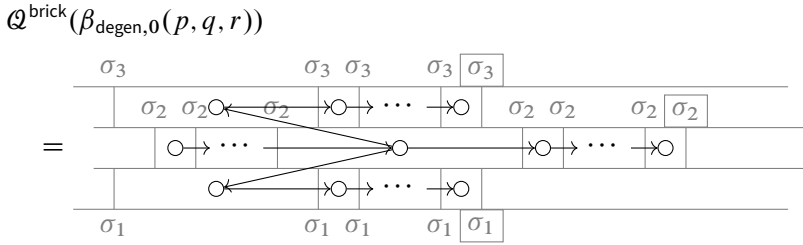
Then, $\tilde{\beta}_{\text{degen},0}(p, q, r)$ is the positive braid $\beta_{\text{degen},0}(p, q', r')$ for some $q \leq q' \leq q + 1$ and $r \leq r' \leq r + 1$ such that both q' and $p + r'$ are odd.

Let $\lambda_{\text{degen}}(p, q, r)$ be the rainbow closures of $\beta_{\text{degen},0}(p, q, r)$, or equivalently, the (-1) -closure of $\beta_{\text{degen}}(p, q, r)$. Then, we denote its brick quiver and canonical N -graph with cycles by $\mathcal{Q}^{\text{brick}}(\beta_{\text{degen},0}(p, q, r))$ and $(\mathcal{G}_{\text{degen}}^{\text{brick}}(p, q, r), \tilde{\mathcal{B}}_{\text{degen}}^{\text{brick}}(p, q, r))$ as before. See Figure 35.

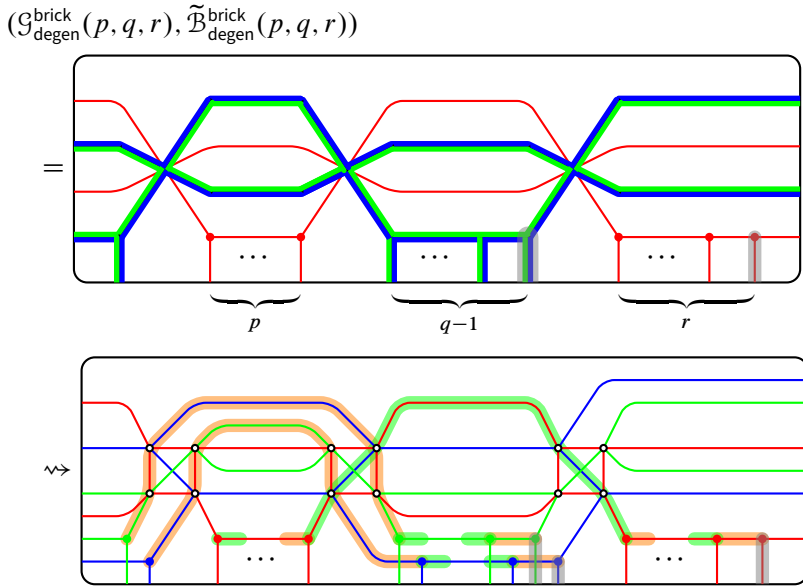
Definition 4.7 (Degenerate 4-graph for $\lambda_{\text{degen}}(p, q, r)$). We define a degenerate 4-graph $\mathcal{G}_{\text{degen}}(p, q, r)$ for $\lambda_{\text{degen}}(p, q, r)$ as depicted in the left of Figure 36.



(a) Legendrian link $\lambda_{\text{degen}}(p, q, r)$



(b) Brick quiver for $\beta_{\text{degen},0}(p, q, r)$



(c) Brick N -graph and its perturbation

Figure 35. Brick quiver and N -graph with cycles and its perturbation for the Legendrian link $\lambda_{\text{degen}}(p, q, r)$.

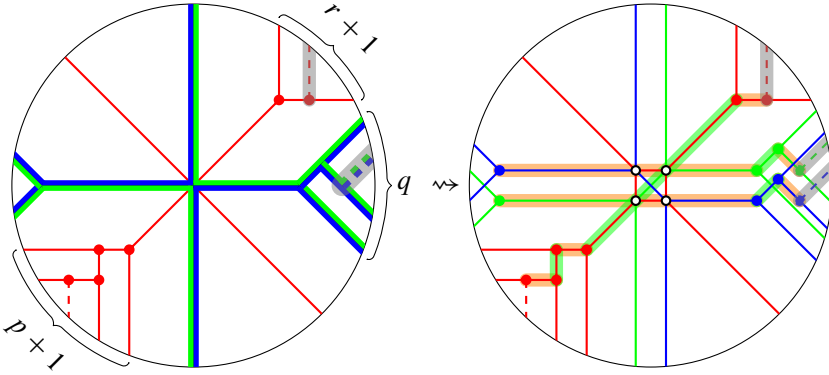


Figure 36. Degenerate 4-graphs $(\mathcal{G}_{\text{degen}}(p, q, r), \tilde{\mathcal{B}}_{\text{degen}}(p, q, r))$ and cycles in the perturbation.

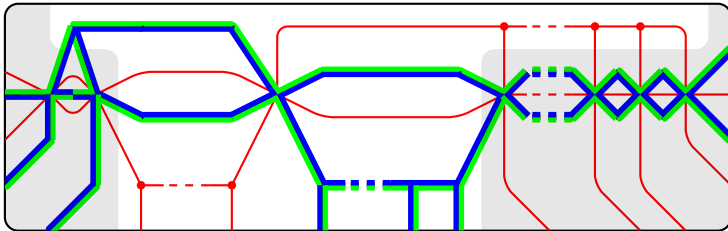
Lemma 4.8. *The N -graphs with cycles $(\mathcal{G}_{\text{degen}}(p, q, r), \tilde{\mathcal{B}}_{\text{degen}}(p, q, r))$ and $(\mathcal{G}_{\text{degen}}^{\text{brick}}(p, q, r), \tilde{\mathcal{B}}_{\text{degen}}^{\text{brick}}(p, q, r))$ are equivalent up to ∂ -Legendrian isotopy and Legendrian mutations.*

Proof. We first show that $\lambda_{\text{degen}}(p, q, r)$ is the same as $\partial\mathcal{G}_{\text{degen}}(p, q, r)$ as follows:

$$\begin{aligned} \beta_{\text{degen}}(p, q, r) &\doteq \sigma_2^p (\sigma_2 \sigma_{1,3} \sigma_2 \sigma_{1,3}) \sigma_{1,3}^{q-1} \sigma_2^r (\sigma_2 \sigma_{1,3} \sigma_2 \sigma_{1,3}) \sigma_{1,3} \\ &= \sigma_2^{p+1} \sigma_{1,3} \sigma_2 \sigma_{1,3}^q \sigma_2^{r+1} \sigma_{1,3} \sigma_2 \sigma_{1,3}^2, \end{aligned}$$

whose (-1) -closure is the same as $\partial\mathcal{G}_{\text{degen}}(p, q, r)$.

It is straightforward to check that we obtain the following degenerate N -graph from $\mathcal{G}_{\text{degen}}^{\text{brick}}(p, q, r)$ by applying a sequence of Move (DI) to the left part of the figure and Move (DII) to the right part.



Let us ignore the shaded regions whose union is tame under perturbation, see Section 3.2.3; then, it is obvious that the resulting N -graph together with a set of one-cycles become $(\mathcal{G}_{\text{degen}}(p, q, r), \tilde{\mathcal{B}}_{\text{degen}}(p, q, r))$ in Figure 36 after a sequence of Legendrian mutations. ■

The following observation is obvious since all of $\beta_{\text{degen}}(p, q, r)$ and $\lambda_{\text{degen}}(p, q, r)$ are invariant under conjugation, so is the pair $(\mathcal{G}_{\text{degen}}(p, q, r), \tilde{\mathcal{B}}_{\text{degen}}(p, q, r))$.

Lemma 4.9. *The degenerate N -graph $(\mathcal{G}_{\text{degen}}(p, q, r), \tilde{\mathcal{B}}_{\text{degen}}(p, q, r))$ with cycles is invariant under conjugation.*

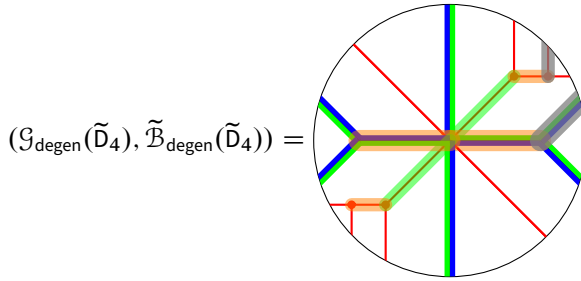
Note that the 4-graph $\mathcal{G}_{\text{degen}}(p, q, 1)$ is indeed a stabilization of the tripod 3-graph $\mathcal{G}(p, q, q)$ up to ∂ -Legendrian isotopy and Legendrian mutations. In particular, when $(p, q, r) = (n - 2, 2, 1), (2, 3, 1), (3, 3, 1),$ and $(2, 4, 1)$, we denote the braid, their closures, and N -graphs by $\beta_{\text{degen}}(Z), \lambda_{\text{degen}}(Z),$ and $\mathcal{G}_{\text{degen}}(Z)$ for $Z = D_n, E_6, \tilde{E}_6,$ and $\tilde{E}_7,$ respectively. The degenerate N -graphs and the perturbed N -graphs with cycles listed above are depicted in Table 9.

Remark 4.10. As observed in Lemma 4.6, one can think of $\mathcal{Q}(1, n, n)$ and $\mathcal{G}(1, n, n)$ for A_{2n-1} instead of $\mathcal{Q}(A_{2n-1})$ and $\mathcal{G}(A_{2n-1})$. Therefore, we may obtain a degenerate N -graph $\mathcal{G}_{\text{degen}}(A_{2n-1}) = \mathcal{G}_{\text{degen}}(1, n, 1)$, which is obviously invariant under the conjugation.

We also consider the degenerate 4-graph

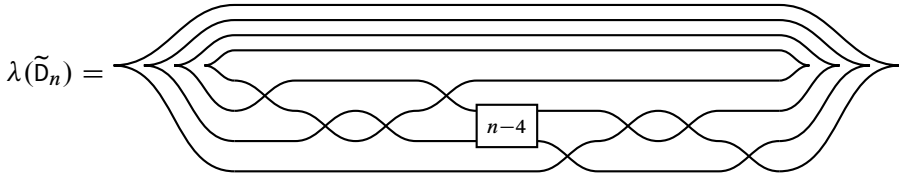
$$(\mathcal{G}_{\text{degen}}(\tilde{D}_4), \tilde{\mathcal{B}}_{\text{degen}}(\tilde{D}_4)) = (\mathcal{G}_{\text{degen}}(2, 2, 2), \tilde{\mathcal{B}}_{\text{degen}}(2, 2, 2))$$

with cycles of type \tilde{D}_4 as follows:



which defines a bipartite quiver of type \tilde{D}_4 .

4.1.3. N -graphs of type \tilde{D}_n . Let us start by defining the Legendrian link $\lambda(\tilde{D}_n)$ of type \tilde{D}_n



Then, $\lambda(\tilde{D}_n)$ is the rainbow closure of the positive braid $\beta_0(\tilde{D}_n)$

$$\beta_0(\tilde{D}_n) = \sigma_3 \boxed{\sigma_2} \sigma_2 \sigma_3 \boxed{\sigma_2} \sigma_2^{n-5} \sigma_1 \boxed{\sigma_2} \sigma_2 \sigma_1,$$

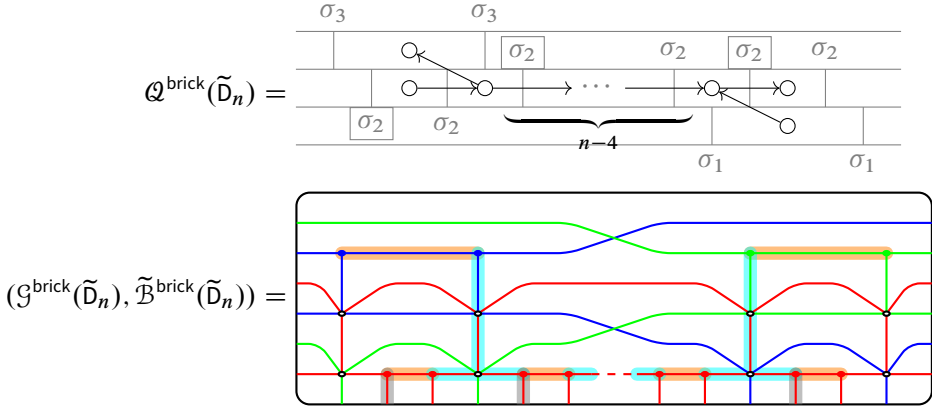
Z	D_n	E_6
$\beta_{\text{degen}}(Z)$	$\beta_{\text{degen}}(n - 2, 2, 1)$	$\beta_{\text{degen}}(2, 3, 1)$
$\lambda_{\text{degen}}(Z)$	$\lambda_{\text{degen}}(n - 2, 2, 1)$	$\lambda_{\text{degen}}(2, 3, 1)$
$\mathcal{G}_{\text{degen}}(Z)$		
Perturb.		
Z	\tilde{E}_6	\tilde{E}_7
$\beta_{\text{degen}}(Z)$	$\beta_{\text{degen}}(3, 3, 1)$	$\beta_{\text{degen}}(2, 4, 1)$
$\lambda_{\text{degen}}(Z)$	$\lambda_{\text{degen}}(3, 3, 1)$	$\lambda_{\text{degen}}(2, 4, 1)$
$\mathcal{G}_{\text{degen}}(Z)$		
Perturb.		

Table 9. Degenerate 4-graphs $\mathcal{G}_{\text{degen}}(Z)$ and cycles in the perturbations for $Z = D_n, E_6, \tilde{E}_6,$ and \tilde{E}_7 .

or the (-1) -closure of $\beta(\tilde{D}_n) = \Delta_4 \beta_0(\tilde{D}_n) \Delta_4$. Since $\lambda(\tilde{D}_n)$ has three or four components, we have

$$\tilde{\beta}_0(\tilde{D}_n) = \begin{cases} \sigma_3 \sigma_2^3 \sigma_3 \sigma_2^{n-4} \sigma_1 \sigma_2^3 \sigma_1 & n \text{ is odd,} \\ \sigma_3 \sigma_2^3 \sigma_3 \sigma_2^{n-3} \sigma_1 \sigma_2^3 \sigma_1 & n \text{ is even.} \end{cases}$$

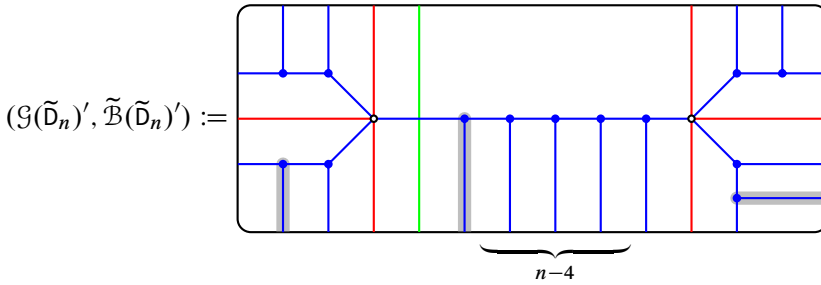
The Legendrian link $\lambda(\tilde{D}_n)$ admits the brick quiver diagram $\mathcal{Q}^{\text{brick}}(\tilde{D}_n)$:



Definition 4.11 (N -graph of type \tilde{D}_n). We define a free 4-graph $\mathcal{G}(\tilde{D}_n)$ for $\lambda(\tilde{D}_n)$ as depicted in Figure 37.

Lemma 4.12. *The pairs $(\mathcal{G}(\tilde{D}_n), \mathcal{B}(\tilde{D}_n))$ and $(\mathcal{G}^{\text{brick}}(\tilde{D}_n), \mathcal{B}^{\text{brick}}(\tilde{D}_n))$ are equivalent up to ∂ -Legendrian isotopy and Legendrian mutations.*

Proof. We first introduce an auxiliary N -graph $(\mathcal{G}(\tilde{D}_n)', \tilde{\mathcal{B}}(\tilde{D}_n)')$:



Then, $\partial \mathcal{G}(\tilde{D}_n)' = \sigma_2 \sigma_1^3 \sigma_2 \sigma_1 \boxed{\sigma_1} \sigma_1 \sigma_2 \sigma_3 \boxed{\sigma_1} \sigma_1^{n-5} \sigma_2 \sigma_1^3 \sigma_2 \sigma_1 \boxed{\sigma_1} \sigma_1 \sigma_2 \sigma_3$ is equivalent to $\lambda(\tilde{D}_n)$ as follows:

$$\begin{aligned} \beta(\tilde{D}_n) &= \Delta_4 \sigma_3 \boxed{\sigma_2} \sigma_2 \sigma_3 \boxed{\sigma_2} \sigma_2^{n-5} \sigma_1 \boxed{\sigma_2} \sigma_2 \sigma_1 \Delta_4 \\ &\doteq \sigma_2 \sigma_1^2 \sigma_2 \sigma_1 \sigma_2 \sigma_3 \sigma_2 \sigma_1 \boxed{\sigma_2} \sigma_2 \sigma_3 \boxed{\sigma_2} \sigma_2^{n-4} \sigma_1 \sigma_2 \sigma_1 \sigma_2 \boxed{\sigma_1} \sigma_1 \sigma_2 \sigma_3 \\ &= \partial \mathcal{G}(\tilde{D}_n)'. \end{aligned}$$

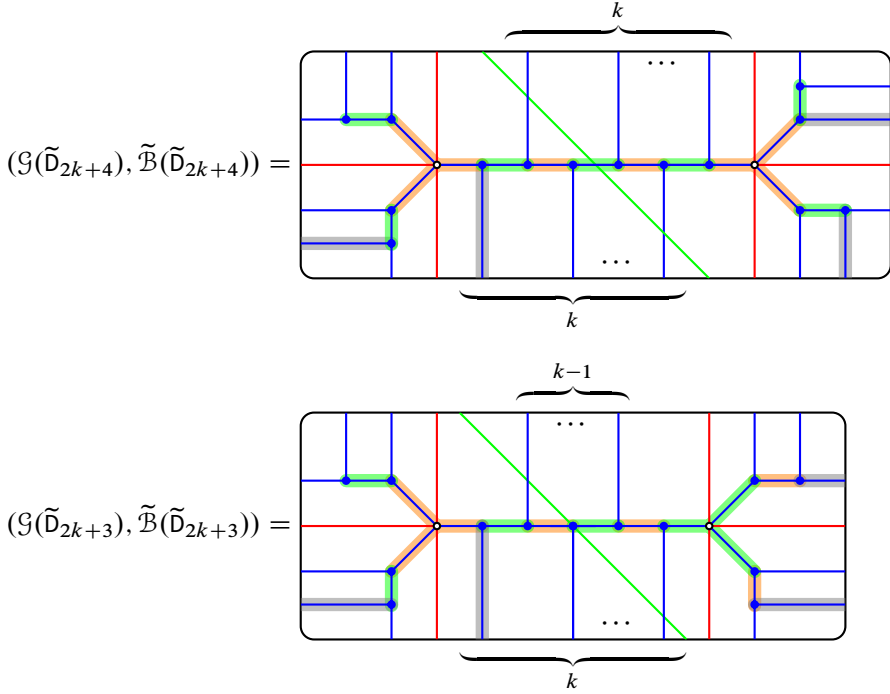


Figure 37. N -graphs of type \tilde{D}_{2k+3} and \tilde{D}_{2k+4} for $k \geq 0$.

Moreover, as seen in Appendix B.5, $(\mathcal{G}^{\text{brick}}(\tilde{D}_n), \mathcal{B}^{\text{brick}}(\tilde{D}_n))$ is equivalent to $(\mathcal{G}(\tilde{D}_n)', \tilde{\mathcal{B}}(\tilde{D}_n)')$, which is equivalent to $(\mathcal{G}(\tilde{D}_n)', \tilde{\mathcal{B}}(\tilde{D}_n)')$ up to ∂ -Legendrian isotopy and Legendrian mutations. ■

Similar to before, the freeness is obvious since $\mathcal{G}(\tilde{D}_n)$ consists of trees. Moreover, $\mathcal{G}(\tilde{D}_{2k+4})$ has a π -rotation symmetry. That is, we obtain the following lemma.

Lemma 4.13. *The pair $\mathcal{G}(\tilde{D}_{2k+4})$ is invariant under π -rotation.*

Finally, two canonical N -graphs $\mathcal{G}(\tilde{D}_4)$ and $\mathcal{G}_{\text{degen}}(\tilde{D}_4)$ for \tilde{D}_4 , which are indeed equivalent.

Lemma 4.14. *The N -graph with cycles $(\mathcal{G}(\tilde{D}_4), \tilde{\mathcal{B}}(\tilde{D}_4))$ is equivalent to the pair $(\mathcal{G}_{\text{degen}}(\tilde{D}_4), \tilde{\mathcal{B}}_{\text{degen}}(\tilde{D}_4))$ up to ∂ -Legendrian isotopy and Legendrian mutations.*

See Appendix B.6 for the proof.

4.1.4. Exchange matrices and graphs. Notice that the N -graphs $\mathcal{G}(Z)$ and $\mathcal{G}^{\text{brick}}(Z)$ are deterministic for $Z = A, D, E, \tilde{D}, \tilde{E}$. Therefore, the coefficients in $\mathbf{y}(\mathcal{G}(Z), \mathcal{B}(Z))$ are

defined on $\mathbb{C}[\mathcal{M}(\lambda(Z))]$. Here, $\mathcal{M}(\lambda)$ is the moduli spaces of flags on λ and is turned out to be a cluster Poisson variety as mentioned earlier.

In addition, one can show that the variables $\{X_a\}_{a \in I_\lambda}$, Shen–Weng constructed in [42, Section 3.2], coincide with $\mathbf{y}(\mathcal{G}^{\text{brick}}(A_n), \mathcal{B}^{\text{brick}}(A_n))$, $\mathbf{y}(\mathcal{G}^{\text{brick}}(a, b, c), \mathcal{B}^{\text{brick}}(a, b, c))$, $\mathbf{y}(\mathcal{G}_{\text{degen}}^{\text{brick}}(p, q, r), \mathcal{B}_{\text{degen}}^{\text{brick}}(p, q, r))$, or $\mathbf{y}(\mathcal{G}^{\text{brick}}(\tilde{D}_n), \mathcal{B}^{\text{brick}}(\tilde{D}_n))$. Moreover, coefficients are algebraically independent. In summary, we have the following corollary, which is a direct consequence of the above discussion, Proposition 2.29, and (2.4).

Corollary 4.15. *Let $(\mathcal{G}_{t_0}, \mathcal{B}_{t_0})$ be either $(\mathcal{G}(a, b, c), \mathcal{B}(a, b, c))$ or $(\mathcal{G}(n), \mathcal{B}(n))$ of type Z , and let $(\mathbf{y}_{t_0}, \mathcal{B}_{t_0}) = \Psi(\mathcal{G}_{t_0}, \mathcal{B}_{t_0})$ and $\mathcal{B}_{t_0} = \mathcal{B}(\mathcal{Q}(\mathcal{G}_{t_0}, \mathcal{B}_{t_0}))$. Then, the exchange graph of the Y -pattern given by the initial Y -seed $(\mathbf{y}_{t_0}, \mathcal{B}_{t_0})$ is the same as the exchange graph $\text{Ex}(\Phi)$ of the root system Φ of type Z .*

For each $n \geq 1$ and triples (a, b, c) and (p, q, r) , let β_0 be either $\beta_0(A_n)$, $\beta_0(a, b, c)$, $\beta_0(p, q, r)$, or $\beta_0(\tilde{D}_n)$, and let $\tilde{\beta}_0$ be the braid obtained by doubling chosen generators of β_0 if necessary so that the closure of $\tilde{\beta}_0$ has only one component as before. Notice that the N -graph $\mathcal{G}^{\text{brick}}(\tilde{\beta}_0)$ is equivalent to the N -graph $\widetilde{\mathcal{G}^{\text{brick}}(\beta_0)}$ under the mutation on the cycle corresponding to each relative cycle in $\mathcal{G}^{\text{brick}}(\beta_0)$.

Lemma 4.16. *Let λ and $\tilde{\lambda}$ be the rainbow closures of β_0 and $\tilde{\beta}_0$, respectively.*

- (1) *Both $\mathcal{M}(\lambda)$ and $\mathcal{M}(\tilde{\lambda})$ admit the \mathcal{X} -cluster structure.*
- (2) *There is a cluster subvariety $\mathcal{M}(\tilde{\lambda})'$ in $\mathcal{M}(\tilde{\lambda})$, whose cluster structure coincides with that of $\mathcal{M}(\lambda)$.*
- (3) *For each N -graph $(\mathcal{G}, \tilde{\mathcal{B}})$ for λ , the canonical extension $(\tilde{\mathcal{G}}, \tilde{\tilde{\mathcal{B}}})$ yields the restriction map*

$$\mathcal{M}(\tilde{\mathcal{G}}) \rightarrow \mathcal{M}(\mathcal{G})$$

between toric charts in $\mathcal{M}(\tilde{\lambda})'$ and $\mathcal{M}(\lambda)$.

- (4) *For N -graphs $(\mathcal{G}(A_n), \tilde{\mathcal{B}}(A_n))$, $(\mathcal{G}(a, b, c), \tilde{\mathcal{B}}(a, b, c))$, $(\mathcal{G}(\tilde{D}_n), \tilde{\mathcal{B}}(\tilde{D}_n))$, and $(\mathcal{G}_{\text{degen}}(p, q, r), \tilde{\mathcal{B}}_{\text{degen}}(p, q, r))$, their exchange matrices are admissible in the sense of Definition 3.47.*

Proof. (1) This follows from [42].

(2) and (3) These are observed in Section 3.6.

(4) This follows easily from the direct computation. ■

4.2. Legendrian Coxeter mutations

For a bipartite quiver \mathcal{Q} , we have two sets of vertices I_+ and I_- so that all edges are oriented from I_+ to I_- . Let μ_+ and μ_- be sequences of mutations defined by compositions of mutations corresponding to each and every vertex in I_+ and I_- ,

respectively. A Coxeter mutation $\mu_{\mathcal{Q}}$ and its inverse $\mu_{\mathcal{Q}}^{-1}$ are the compositions

$$\mu_{\mathcal{Q}} = \prod_{i \in I_+} \mu_i \cdot \prod_{i \in I_-} \mu_i, \quad \mu_{\mathcal{Q}}^{-1} = \prod_{i \in I_-} \mu_i \cdot \prod_{i \in I_+} \mu_i.$$

Note that $\prod_{i \in I_+} \mu_i$ does not depend on the order of composition of mutations μ_i among $i \in I_+$, and the same holds for I_- .

Remark 4.17. For any sequence μ of mutations, we will use the right-to-left convention. Namely, the rightmost mutation will be applied first on the quiver \mathcal{Q} .

Let us say that a pair $(\mathcal{G}, \mathcal{B})$ is *bipartite* if so is $\mathcal{Q} = \mathcal{Q}(\mathcal{G}, \mathcal{B})$. In this case, we decompose \mathcal{B} into \mathcal{B}_+ and \mathcal{B}_- corresponding to sets I_+ and I_- of vertices in \mathcal{Q} .

Then, similarly, we define the Legendrian Coxeter mutation, which will be denoted by $\mu_{\mathcal{G}}$, on a bipartite N -graph \mathcal{G} as follows.

Definition 4.18 (Legendrian Coxeter mutation). For a bipartite N -graph \mathcal{G} with decomposed sets of cycles $\mathcal{B} = \mathcal{B}_+ \cup \mathcal{B}_-$, we define the *Legendrian Coxeter mutation* $\mu_{\mathcal{G}}$ and its inverse $\mu_{\mathcal{G}}^{-1}$ as the compositions of Legendrian mutations

$$\mu_{\mathcal{G}} = \prod_{\gamma \in \mathcal{B}_+} \mu_{\gamma} \cdot \prod_{\gamma \in \mathcal{B}_-} \mu_{\gamma}, \quad \mu_{\mathcal{G}}^{-1} = \prod_{\gamma \in \mathcal{B}_-} \mu_{\gamma} \cdot \prod_{\gamma \in \mathcal{B}_+} \mu_{\gamma}.$$

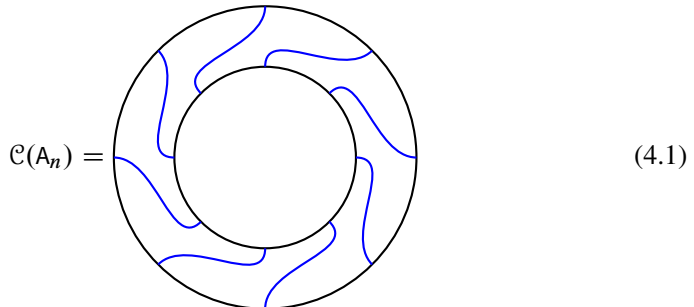
It is worth mentioning that the Legendrian Coxeter mutations make sense only when each Legendrian mutation μ_{γ} exists. Also, note that each $\mu_{\mathcal{G}}^{\pm 1}$ does not depend on the order of mutations if cycles in each of \mathcal{B}_{\pm} are disjoint. This directly implies that $\mu_{\mathcal{G}}^{-1}$ is indeed the inverse of $\mu_{\mathcal{G}}$. Note that all cycles in each of $\mathcal{B}_{\pm}(Z)$ for $Z = A, D, E, \tilde{D}, \tilde{E}$ are disjoint as seen in Figures 34a, 34b, and 37.

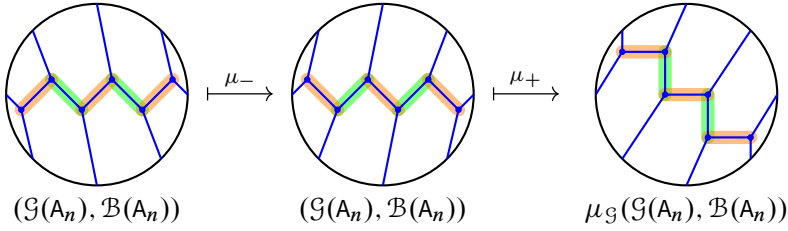
4.2.1. Legendrian Coxeter mutation for linear N -graphs.

Lemma 4.19. *The effect of the Legendrian Coxeter mutation on $(\mathcal{G}(A_n), \mathcal{B}(A_n))$ is the clockwise $\frac{2\pi}{n+3}$ -rotation and therefore*

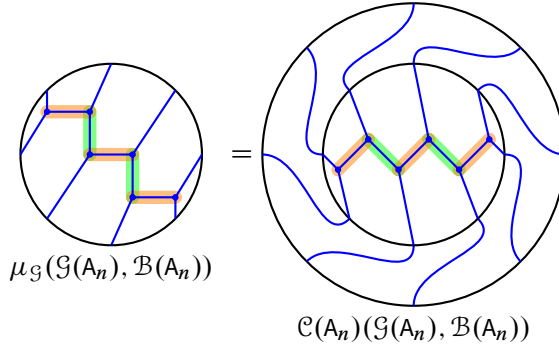
$$\mu_{\mathcal{G}}(\mathcal{G}(A_n), \mathcal{B}(A_n)) = \mathcal{C}(A_n)(\mathcal{G}(A_n), \mathcal{B}(A_n)),$$

where $\mathcal{C}(A_n)$ is an annular N -graph called the Coxeter padding of type A_n as follows:





(a) Legendrian Coxeter mutation for $\mathcal{G}(A_n)$



(b) Coxeter padding $\mathcal{C}(A_n)$ of type A_n

Figure 38. Legendrian Coxeter mutation $\mu_{\mathcal{G}}$ on $(\mathcal{G}(A_n), \mathcal{B}(A_n))$.

Proof. We may assume that the Coxeter element $\mu_{\mathcal{G}}$ can be represented by the sequence

$$\mu_{\mathcal{G}} = \mu_+ \mu_- = (\mu_{\gamma_2} \mu_{\gamma_4} \mu_{\gamma_6} \cdots) (\mu_{\gamma_1} \mu_{\gamma_3} \mu_{\gamma_5} \cdots).$$

Then, the action of $\mu_{\mathcal{G}}$ on $\mathcal{G}(A_n)$ is as depicted in Figure 38a, which is nothing but the clockwise $\frac{2\pi}{n+3}$ -rotation of the original N -graph $(\mathcal{G}(A_n), \mathcal{B}(A_n))$, as claimed.

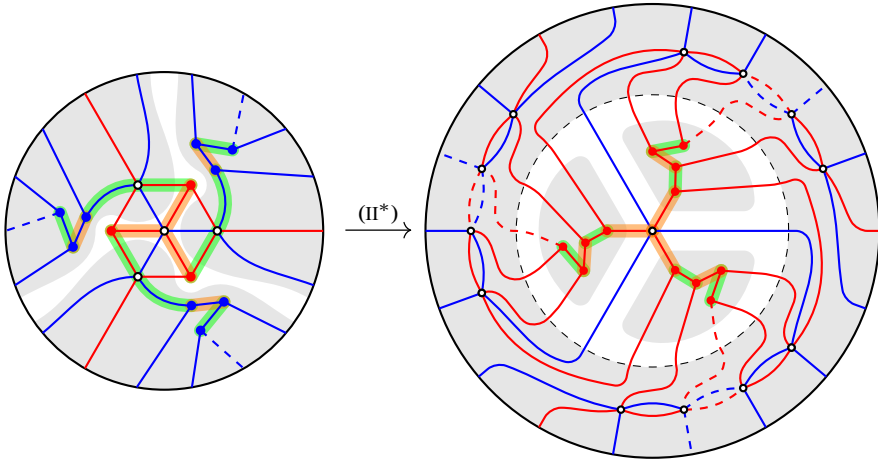
The last statement is obvious as seen in Figure 38b. ■

Remark 4.20. The order of the Coxeter mutation is either $(n + 3)/2$ if n is odd or $n + 3$ otherwise. Since the Coxeter number

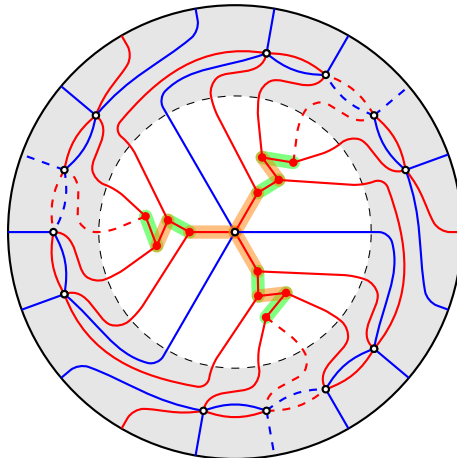
$$h = n + 1$$

for A_n , this verifies Lemma 2.36 in this case.

4.2.2. Legendrian Coxeter mutation for tripod N -graphs. Let us consider the Legendrian Coxeter mutation for tripod N -graphs. By the mutation convention mentioned in Remark 4.17, for each tripod $\mathcal{G}(a, b, c)$, we always take a mutation at the



(a) After the mutation at the central vertex



(b) After Legendrian Coxeter mutation

Figure 39. Legendrian Coxeter mutation for $(\mathcal{G}(a, b, c), \mathcal{B}(a, b, c))$.

central Y-cycle γ first. After the Legendrian mutation on $(\mathcal{G}(a, b, c), \mathcal{B}(a, b, c))$ at γ , we have the N -graph on the left in Figure 39a. Then, there are three shaded regions that we can apply the generalized push-through moves to, see Appendix B.3, so that we obtain the N -graph on the right in Figure 39a.

Notice that, in each triangular shaded region, the N -subgraph looks like the N -graph of type A_{a-1} , A_{b-1} , or A_{c-1} . Moreover, the mutations corresponding to the rest sequence are just a composition of Legendrian Coxeter mutations of types A_{a-1} , A_{b-1} , and A_{c-1} , which are essentially the same as the clockwise rotations by Lemma 4.19.

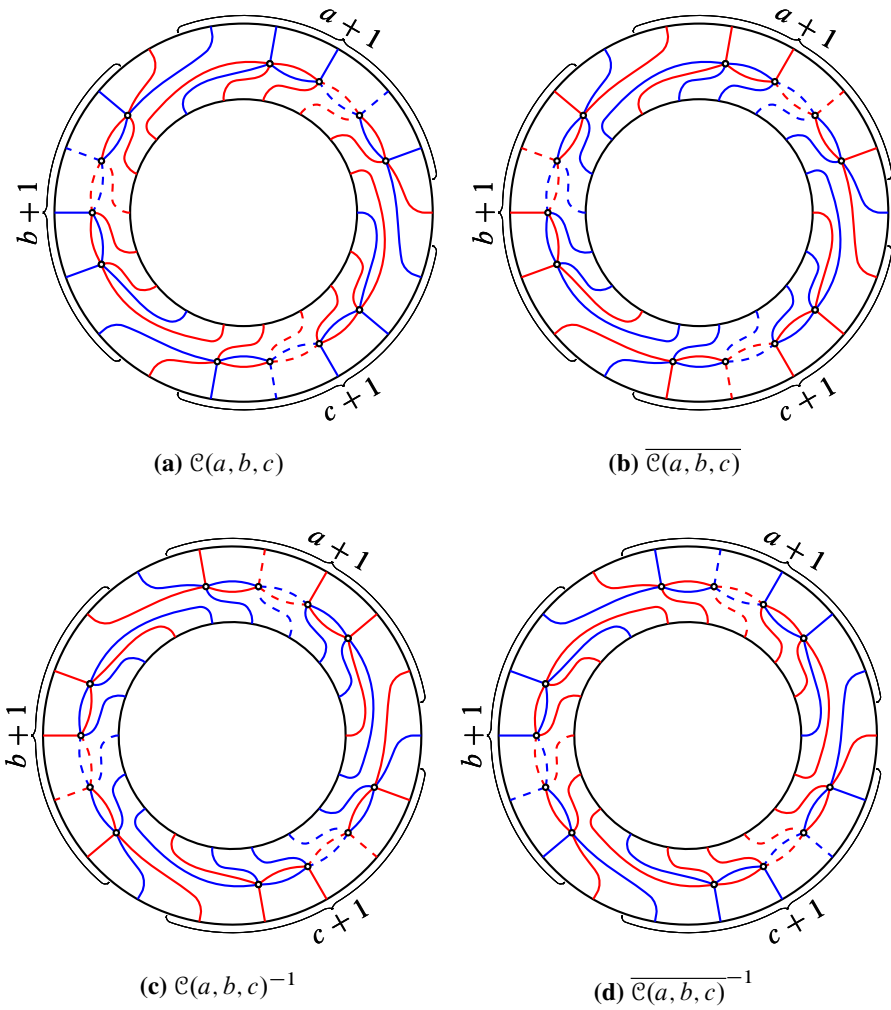


Figure 40. Coxeter paddings $\mathcal{C}(a, b, c)$, $\overline{\mathcal{C}(a, b, c)}$ and their inverses.

Therefore, the result of the Legendrian Coxeter mutation will be given as depicted in Figure 39b.

Then, the resulting N -graph is essentially the same as the original N -graph $\mathcal{G}(a, b, c)$. Indeed, the inside is identical to $\mathcal{G}(a, b, c)$ but the colors are switched, which is the conjugation $\overline{\mathcal{G}(a, b, c)}$ by definition. The complement of $\overline{\mathcal{G}(a, b, c)}$ in $\mu_{\mathcal{Q}}(\mathcal{G}(a, b, c), \mathcal{B}(a, b, c))$ is an annular N -graph.

Definition 4.21 (Coxeter padding of type (a, b, c)). For each triple a, b, c , the annular N -graph depicted in Figure 40 is denoted by $\mathcal{C}(a, b, c)$ and called the *Coxeter*

padding of type (a, b, c) . We also denote the Coxeter padding with color switched by $\overline{\mathcal{C}(a, b, c)}$, which is the conjugation of $\mathcal{C}(a, b, c)$.

Notice that two Coxeter paddings $\mathcal{C}(a, b, c)$ and $\overline{\mathcal{C}(a, b, c)}$ can be glued without any ambiguity, and so, we can also pile up Coxeter paddings $\mathcal{C}(a, b, c)$ and $\overline{\mathcal{C}(a, b, c)}$ alternatively as many times as we want.

We also define the concatenation of the Coxeter padding $\overline{\mathcal{C}(a, b, c)}$ on the pair $(\mathcal{G}(a, b, c), \mathcal{B}(a, b, c))$ as the pair $(\mathcal{G}', \mathcal{B}')$ such that

- (1) the N -graph \mathcal{G}' is obtained by gluing $\overline{\mathcal{C}(a, b, c)}$ on $\mathcal{G}(a, b, c)$, and
- (2) the set \mathcal{B}' of cycles is the set of I - and Y -cycles identified with $\mathcal{B}(a, b, c)$ in a canonical way.

Proposition 4.22. *Let*

$$(\mathcal{G}, \mathcal{B}) = (\mathcal{G}(a, b, c), \mathcal{B}(a, b, c)).$$

The Legendrian Coxeter mutation on $(\mathcal{G}, \mathcal{B})$ or $\overline{(\mathcal{G}, \mathcal{B})}$ is given as the concatenation

$$\begin{aligned} \mu_{\mathcal{G}}(\mathcal{G}, \mathcal{B}) &= \overline{\mathcal{C}(\mathcal{G}, \mathcal{B})}, & \mu_{\mathcal{G}}^{-1}(\mathcal{G}, \mathcal{B}) &= \overline{\mathcal{C}^{-1}(\mathcal{G}, \mathcal{B})}, \\ \mu_{\mathcal{G}}\overline{(\mathcal{G}, \mathcal{B})} &= \overline{\mathcal{C}(\mathcal{G}, \mathcal{B})}, & \mu_{\mathcal{G}}^{-1}\overline{(\mathcal{G}, \mathcal{B})} &= \mathcal{C}^{-1}(\mathcal{G}, \mathcal{B}), \end{aligned}$$

where $\mathcal{C} = \mathcal{C}(a, b, c)$, $\overline{\mathcal{C}} = \overline{\mathcal{C}(a, b, c)}$.

In general, for $r \geq 0$, we have

$$\begin{aligned} \mu_{\mathcal{G}}^r(\mathcal{G}, \mathcal{B}) &= \begin{cases} \overline{\mathcal{C}\overline{\mathcal{C}}\dots\overline{\mathcal{C}}(\mathcal{G}, \mathcal{B})} & \text{if } r \text{ is even,} \\ \overline{\mathcal{C}\overline{\mathcal{C}}\dots\mathcal{C}(\mathcal{G}, \mathcal{B})} & \text{if } r \text{ is odd,} \end{cases} \\ \mu_{\mathcal{G}}^{-r}(\mathcal{G}, \mathcal{B}) &= \begin{cases} \overline{\mathcal{C}^{-1}\mathcal{C}^{-1}\dots\mathcal{C}^{-1}(\mathcal{G}, \mathcal{B})} & \text{if } r \text{ is even,} \\ \overline{\mathcal{C}^{-1}\mathcal{C}^{-1}\dots\overline{\mathcal{C}^{-1}}(\mathcal{G}, \mathcal{B})} & \text{if } r \text{ is odd.} \end{cases} \end{aligned}$$

Proof. This follows directly from the above observation. ■

It is important that this proposition holds only when we take the Legendrian Coxeter mutation on the very standard N -graph $\mathcal{G}(a, b, c)$ with the cycles $\mathcal{B}(a, b, c)$. Otherwise, the Legendrian Coxeter mutation will not be expressed as simple as above.

Let $(\mathcal{G}, \mathcal{B})$ be a pair of a deterministic N -graph, a set of good cycles. Suppose that the quiver $\mathcal{Q}(\mathcal{G}, \mathcal{B})$ is bipartite and the Legendrian Coxeter mutation $\mu_{\mathcal{G}}(\mathcal{G}, \mathcal{B})$ is realizable. Then, by Proposition 3.43, we have

$$\Psi(\mu_{\mathcal{G}}(\mathcal{G}, \mathcal{B})) = \mu_{\mathcal{Q}}(\Psi(\mathcal{G}, \mathcal{B})).$$

In particular, for quivers of type A_n or tripods, we have the following corollary.

Corollary 4.23. *For each $n \geq 1$ and $a, b, c \geq 1$, the Legendrian Coxeter mutation $\mu_{\mathcal{G}}$ on $(\mathcal{G}(A_n), \mathcal{B}(A_n))$ or $(\mathcal{G}(a, b, c), \mathcal{B}(a, b, c))$ corresponds to the Coxeter mutation $\mu_{\mathcal{Q}}$ on $\mathcal{Q}(A_n)$ or $\mathcal{Q}(a, b, c)$, respectively. In other words,*

$$\begin{aligned}\Psi(\mu_{\mathcal{G}}(\mathcal{G}(A_n), \mathcal{B}(A_n))) &= \mu_{\mathcal{Q}}(\Psi(\mathcal{G}(A_n), \mathcal{B}(A_n))), \\ \Psi(\mu_{\mathcal{G}}(\mathcal{G}(a, b, c), \mathcal{B}(a, b, c))) &= \mu_{\mathcal{Q}}(\Psi(\mathcal{G}(a, b, c), \mathcal{B}(a, b, c))).\end{aligned}$$

Theorem 4.24. *For $a, b, c \geq 1$ with $\frac{1}{a} + \frac{1}{b} + \frac{1}{c} \leq 1$, the Legendrian knot or link $\lambda(a, b, c)$ in $J^1\mathbb{S}^1$ admits infinitely many distinct exact embedded Lagrangian fillings.*

Proof. By Proposition 4.22, the effect of the Legendrian Coxeter mutation $\mu_{\mathcal{G}}$ on $(\mathcal{G}(a, b, c), \mathcal{B}(a, b, c))$ is just to attach the Coxeter padding on $(\bar{\mathcal{G}}(a, b, c), \bar{\mathcal{B}}(a, b, c))$. In particular, as mentioned earlier, the iterated Legendrian Coxeter mutation

$$\mu_{\mathcal{G}}^r(\mathcal{G}(a, b, c), \mathcal{B}(a, b, c))$$

is well defined for each $r \in \mathbb{Z}$. Each of these N -graphs defines a Legendrian weave $\Lambda(\mu_{\mathcal{G}}^r(\mathcal{G}(a, b, c), \mathcal{B}(a, b, c)))$, whose Lagrangian projection is a Lagrangian filling

$$L_r(a, b, c) := (\pi \circ \iota)(\Lambda(\mu_{\mathcal{G}}^r(\mathcal{G}(a, b, c), \mathcal{B}(a, b, c))))),$$

as desired. Therefore, it suffices to prove that Lagrangians $L_r(a, b, c)$ for $r \geq 0$ are pairwise distinct up to exact Lagrangian isotopy when $\frac{1}{a} + \frac{1}{b} + \frac{1}{c} \leq 1$.

Now, suppose that $\frac{1}{a} + \frac{1}{b} + \frac{1}{c} \leq 1$, or equivalently, $\mathcal{Q}(a, b, c)$ is of infinite type; that is, it is not of finite Dynkin type (cf. Definition 2.12 (1)). Then, the order of the Coxeter mutation is infinite by Lemma 2.36, and so is the order of the Legendrian Coxeter mutation by Corollary 4.23. In particular, the set

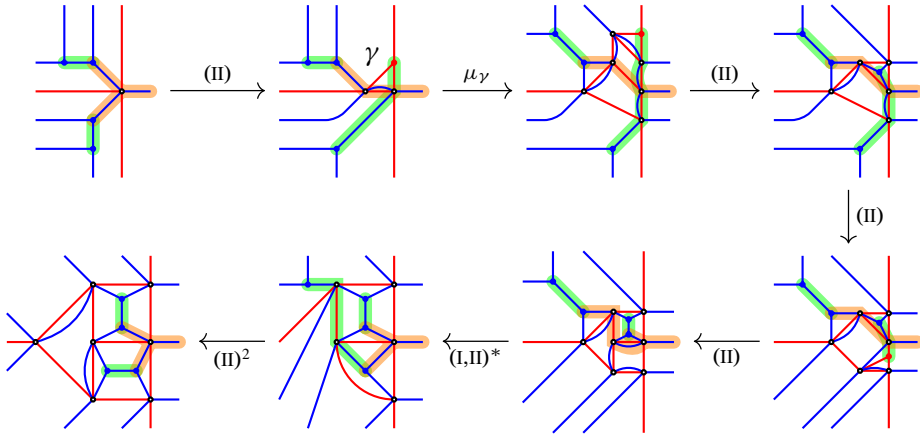
$$\{\Psi(\mu_{\mathcal{G}}^r(\mathcal{G}(a, b, c), \mathcal{B}(a, b, c))) \mid r \in \mathbb{Z}\}$$

is a set of infinitely many pairwise distinct Y -seeds in the Y -pattern for $\mathcal{Q}(a, b, c)$. Hence, by Lemma 4.16 and Proposition 3.48, we have pairwise distinct Lagrangian fillings $L_r(a, b, c)$. ■

Remark 4.25. For Legendrian links of non-ADE-type, there are lots of examples having infinitely many distinct Lagrangian fillings given by a number of different researchers and groups. A non-exhaustive list includes [12, 13, 15, 29].

4.2.3. Legendrian Coxeter mutations for N -graphs of type $\tilde{\mathcal{D}}_n$. We will perform the Legendrian Coxeter mutation $\mu_{\mathcal{G}}$ on $(\mathcal{G}(\tilde{\mathcal{D}}_n), \mathcal{B}(\tilde{\mathcal{D}}_n))$ in order to provide the pictorial proof of Proposition 4.27.

Before we take mutations, we first introduce a useful operation on N -graphs described below, called the *move* (Z).



Remark 4.26. The reader should not confuse that even though we call this operation the *move*, it does not induce any equivalence on N -graphs since it involves a mutation μ_γ .

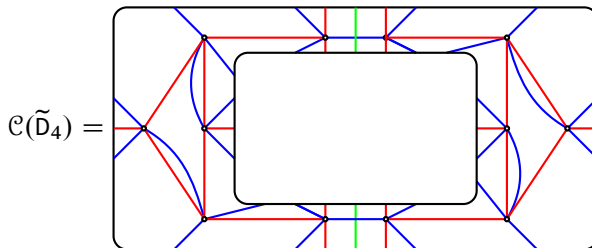
One important observation is that one can take the move (Z) instead of the Legendrian mutation μ_γ on the Y -like cycle⁵ γ , and after the move, the Y -like cycle becomes the Y -like cycle and l -cycles become l -cycles again.

For example, let us consider $(\mathcal{G}(\tilde{D}_4), \mathcal{B}(\tilde{D}_4))$. Then, the Legendrian Coxeter mutation $\mu_{\mathcal{G}}(\mathcal{G}(\tilde{D}_4), \mathcal{B}(\tilde{D}_4))$ is obtained by the composition $(\mu_{\gamma_2}\mu_{\gamma_3}\mu_{\gamma_4}\mu_{\gamma_5})$ followed by the mutation μ_{γ_1} . See Figure 41.

Therefore, $\mu_{\mathcal{G}}(\mathcal{G}(\tilde{D}_4), \mathcal{B}(\tilde{D}_4))$ is the same as the concatenation

$$\mu_{\mathcal{G}}(\mathcal{G}(\tilde{D}_4), \mathcal{B}(\tilde{D}_4)) = \mathcal{C}(\tilde{D}_4)(\mathcal{G}(\tilde{D}_4), \mathcal{B}(\tilde{D}_4)),$$

where the annular N -graph $\mathcal{C}(\tilde{D}_4)$ looks as follows:



⁵We use an ambiguous terminology ‘ Y -like cycle’ since the global shape of γ is unknown. However, the meaning is obvious and we omit the details.

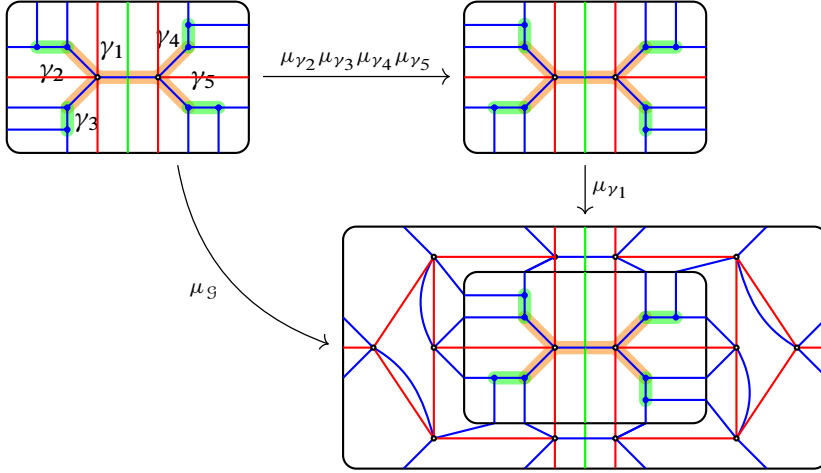


Figure 41. Legendrian Coxeter mutation for $\mathcal{G}(\tilde{D}_4)$.

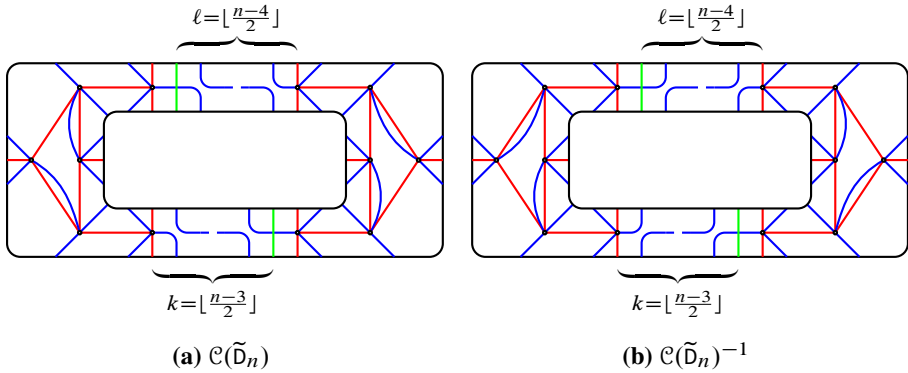


Figure 42. Coxeter paddings $\mathcal{C}(\tilde{D}_n)^{\pm 1}$.

In general, for the N -graph $(\mathcal{G}(\tilde{D}_n), \mathcal{B}(\tilde{D}_n))$, the Legendrian Coxeter mutation is the same as the concatenation of the Coxeter padding of type $\mathcal{C}^{\pm 1}(\tilde{D}_n)$, which is an annular N -graph depicted in Figure 42.

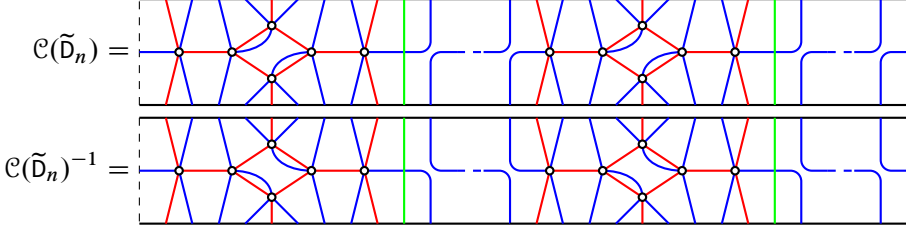
Proposition 4.27. *For any $r \in \mathbb{Z}$, the Legendrian Coxeter mutation $\mu_{\mathcal{G}}^r$ on the pair $(\mathcal{G}(\tilde{D}_n), \mathcal{B}(\tilde{D}_n))$ is given by piling the Coxeter paddings $\mathcal{C}(\tilde{D}_n)^{\pm 1}$. That is,*

$$\mu_{\mathcal{G}}^r(\mathcal{G}(\tilde{D}_n), \mathcal{B}(\tilde{D}_n)) = \begin{cases} \mathcal{C}(\tilde{D}_n)\mathcal{C}(\tilde{D}_n)\cdots\mathcal{C}(\tilde{D}_n)(\mathcal{G}(\tilde{D}_n), \mathcal{B}(\tilde{D}_n)) & r \geq 0, \\ \mathcal{C}(\tilde{D}_n)^{-1}\mathcal{C}(\tilde{D}_n)^{-1}\cdots\mathcal{C}(\tilde{D}_n)^{-1}(\mathcal{G}(\tilde{D}_n), \mathcal{B}(\tilde{D}_n)) & r < 0. \end{cases}$$

Corollary 4.28. *For any $r \in \mathbb{Z}$, the Legendrian Coxeter mutation $\mu_{\mathcal{G}}^r(\mathcal{G}(\tilde{\mathcal{D}}_n), \mathcal{B}(\tilde{\mathcal{D}}_n))$ is realizable by N -graphs and set of good cycles.*

For the notational clarity, it is worth mentioning that $\mathcal{C}(\tilde{\mathcal{D}}_n)$ and $\mathcal{C}(\tilde{\mathcal{D}}_n)^{-1}$ are the inverse to each other with respect to the concatenation introduced in Section 3.2.3.

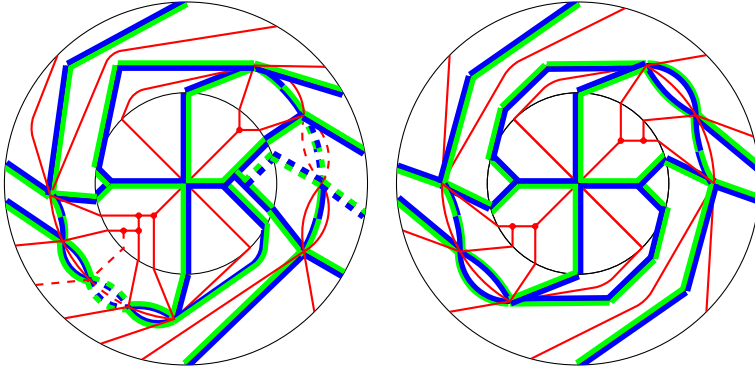
For example, one can present the Coxeter padding $\mathcal{C}(\tilde{\mathcal{D}}_n)^{\pm 1}$ as follows:



Then, it is direct to check that the concatenations $\mathcal{C}(\tilde{\mathcal{D}}_n)\mathcal{C}(\tilde{\mathcal{D}}_n)^{-1}$ and $\mathcal{C}(\tilde{\mathcal{D}}_n)^{-1}\mathcal{C}(\tilde{\mathcal{D}}_n)$ become trivial annulus N -graphs after a sequence of Move (I) for all $n \geq 4$.

4.2.4. Legendrian Coxeter mutations for degenerate N -graphs. For degenerate N -graphs $\mathcal{G}_{\text{degen}}(p, q, 1)$ and $\mathcal{G}_{\text{degen}}(\tilde{\mathcal{D}}_4) = \mathcal{G}_{\text{degen}}(2, 2, 2)$, the Legendrian Coxeter mutations are as depicted in Figure 43.

Then, by using (DI) and (DII) several times, one can show easily that the Legendrian Coxeter mutations are equivalent to N -graphs depicted below:



Therefore, one can conclude that the effect of the Legendrian Coxeter mutation on each degenerate N -graph $\mathcal{G}_{\text{degen}}(p, q, 1)$ or $\mathcal{G}_{\text{degen}}(\tilde{\mathcal{D}}_4)$ is equivalent to attaching an annular N -graph which defines the Coxeter padding $\mathcal{C}_{\text{degen}}(p, q, 1)$ or $\mathcal{C}_{\text{degen}}(\tilde{\mathcal{D}}_4)$.

Proposition 4.29. *Let $(\mathcal{G}_{\text{degen}}, \mathcal{B}_{\text{degen}})$ be either $(\mathcal{G}_{\text{degen}}(p, q, 1), \mathcal{B}_{\text{degen}}(p, q, 1))$ or $(\mathcal{G}_{\text{degen}}(\tilde{\mathcal{D}}_4), \mathcal{B}_{\text{degen}}(\tilde{\mathcal{D}}_4))$. Then, for each $r \in \mathbb{Z}$, the Legendrian Coxeter mutation $\mu_{\mathcal{G}}^r$ on the pair $(\mathcal{G}_{\text{degen}}, \mathcal{B}_{\text{degen}})$ is given as*

$$\mu_{\mathcal{G}}^r(\mathcal{G}_{\text{degen}}, \mathcal{B}_{\text{degen}}) = \begin{cases} \mathcal{C}_{\text{degen}} \mathcal{C}_{\text{degen}} \cdots \mathcal{C}_{\text{degen}}(\mathcal{G}_{\text{degen}}, \mathcal{B}_{\text{degen}}) & r \geq 0, \\ \mathcal{C}_{\text{degen}}^{-1} \mathcal{C}_{\text{degen}}^{-1} \cdots \mathcal{C}_{\text{degen}}^{-1}(\mathcal{G}_{\text{degen}}, \mathcal{B}_{\text{degen}}) & r < 0, \end{cases}$$

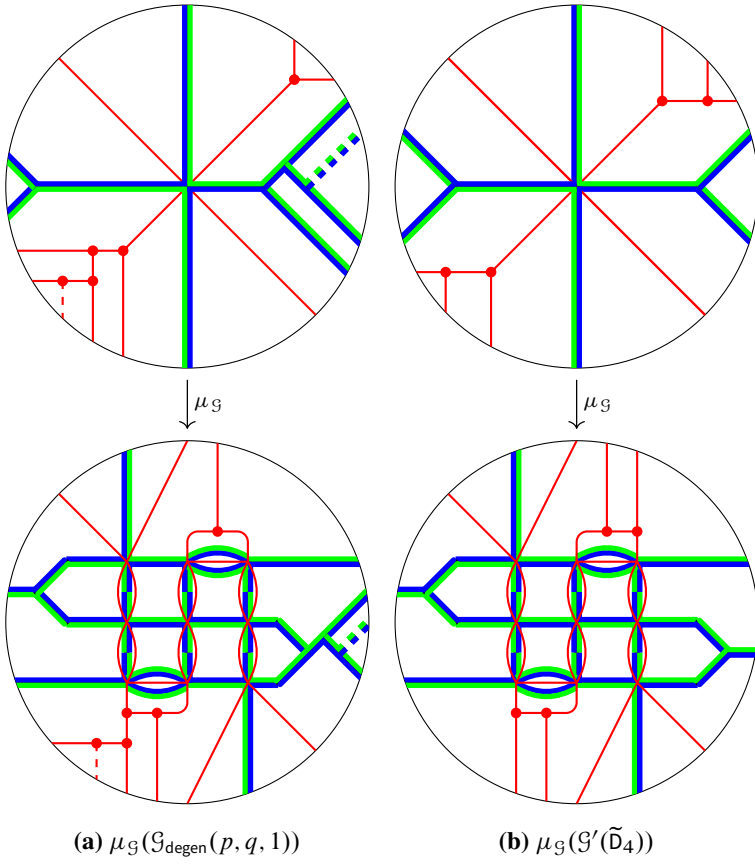
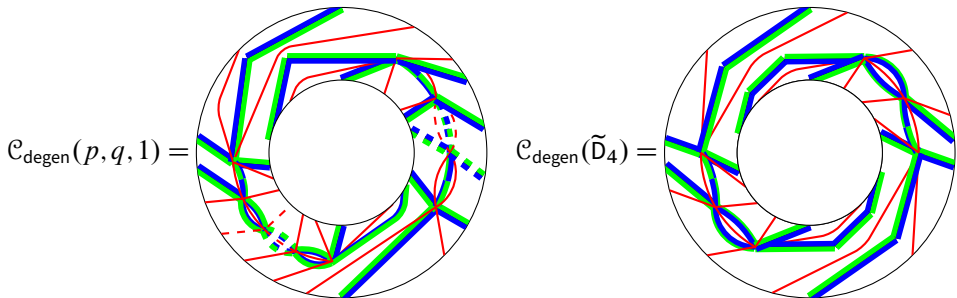


Figure 43. Legendrian Coxeter mutations for degenerate N -graphs.

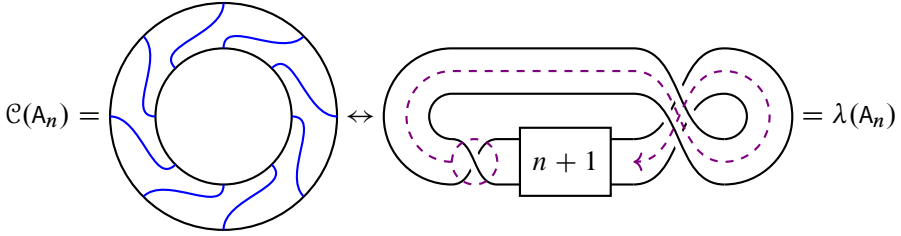
where $\mathcal{C}_{\text{degen}}$ is either $\mathcal{C}_{\text{degen}}(p, q, 1)$ or $\mathcal{C}_{\text{degen}}(\tilde{D}_n)$, which are degenerate annular N -graphs defined as follows:



4.3. Legendrian loops

Recall Legendrian loops defined in Definition 3.22. The goal of this section is to interpret the Legendrian Coxeter paddings with tame Legendrian loops.

Obviously, the Legendrian Coxeter paddings for A_n depicted in (4.1) are tame. Moreover, they correspond to the tame ∂ -Legendrian isotopy which moves the very first generator σ_1 to the rightmost position along the closure part of $\lambda(A_n)$ as follows:



Lemma 4.30. Legendrian Coxeter paddings of types (a, b, c) and \tilde{D} are tame.

Proof. We provide decompositions of the Coxeter paddings $\mathcal{C}(a, b, c)$ and $\mathcal{C}(\tilde{D}_4)$ into sequences of elementary annular N -graphs in Figures 44a and 44b, respectively. We omit other cases. ■

Then, we may translate the sequence of Reidemeister moves corresponding to $\bar{\mathcal{C}}(a, b, c)\mathcal{C}(a, b, c)$ into the Legendrian loop $\vartheta(a, b, c)$ depicted as in Figure 45. Note that the path of Legendrians from the bottom left to the top right Legendrian corresponds to $\mathcal{C}(a, b, c)$ while the path from the top right to the bottom left one corresponds to $\bar{\mathcal{C}}(a, b, c)$.

In order to see the effect of Legendrian Coxeter mutation of type \tilde{D}_n efficiently, let us present it by a sequence of braid moves together with keep tracking braid words shaded by violet color as follows:

$$\begin{aligned}
 & \beta(\tilde{D}_n) \\
 &= \sigma_2 \sigma_1 \sigma_1 \sigma_1 \sigma_2 \sigma_1 \sigma_1 \sigma_1 \sigma_2 \sigma_1 \sigma_1^{k-1} \sigma_3 \sigma_2 \sigma_1 \sigma_1 \sigma_1 \sigma_2 \sigma_1 \sigma_1 \sigma_1 \sigma_2 \sigma_1 \sigma_1^{\ell-1} \sigma_3 \\
 &= \sigma_2 \sigma_1 \sigma_1 \sigma_2 \sigma_1 \sigma_2 \sigma_1 \sigma_1 \sigma_2 \sigma_1 \sigma_1^{k-1} \sigma_3 \sigma_2 \sigma_1 \sigma_1 \sigma_2 \sigma_1 \sigma_2 \sigma_1 \sigma_1 \sigma_2 \sigma_1 \sigma_1^{\ell-1} \sigma_3 \\
 &= \sigma_2 \sigma_1 \sigma_2 \sigma_1 \sigma_2 \sigma_2 \sigma_1 \sigma_2 \sigma_1 \sigma_2 \sigma_1^{k-1} \sigma_3 \sigma_2 \sigma_1 \sigma_2 \sigma_1 \sigma_2 \sigma_2 \sigma_1 \sigma_2 \sigma_1 \sigma_2 \sigma_1^{\ell-1} \sigma_3 \\
 &= \sigma_1 \sigma_2 \sigma_1 \sigma_1 \sigma_2 \sigma_1 \sigma_2 \sigma_1 \sigma_1 \sigma_2 \sigma_1^{k-1} \sigma_3 \sigma_1 \sigma_2 \sigma_1 \sigma_1 \sigma_2 \sigma_1 \sigma_2 \sigma_1 \sigma_1 \sigma_2 \sigma_1^{\ell-1} \sigma_3 \\
 &\doteq \sigma_2 \sigma_1 \sigma_1 \sigma_2 \sigma_1 \sigma_2 \sigma_1 \sigma_1 \sigma_2 \sigma_1^{k-1} \sigma_3 \sigma_1 \sigma_2 \sigma_1 \sigma_1 \sigma_2 \sigma_1 \sigma_2 \sigma_1 \sigma_1 \sigma_2 \sigma_1^{\ell-1} \sigma_3 \sigma_1 \\
 &= \sigma_2 \sigma_1 \sigma_1 \sigma_2 \sigma_1 \sigma_2 \sigma_1 \sigma_1 \sigma_2 \sigma_1^{k-1} \sigma_1 \sigma_3 \sigma_2 \sigma_1 \sigma_1 \sigma_2 \sigma_1 \sigma_2 \sigma_1 \sigma_1 \sigma_2 \sigma_1^{\ell-1} \sigma_1 \sigma_3 \\
 &= \sigma_2 \sigma_1 \sigma_1 \sigma_1 \sigma_2 \sigma_1 \sigma_1 \sigma_1 \sigma_2 \sigma_1^{k-1} \sigma_1 \sigma_3 \sigma_2 \sigma_1 \sigma_1 \sigma_1 \sigma_2 \sigma_1 \sigma_1 \sigma_2 \sigma_1^{\ell-1} \sigma_1 \sigma_3 \\
 &= \beta(\tilde{D}_n)
 \end{aligned}$$

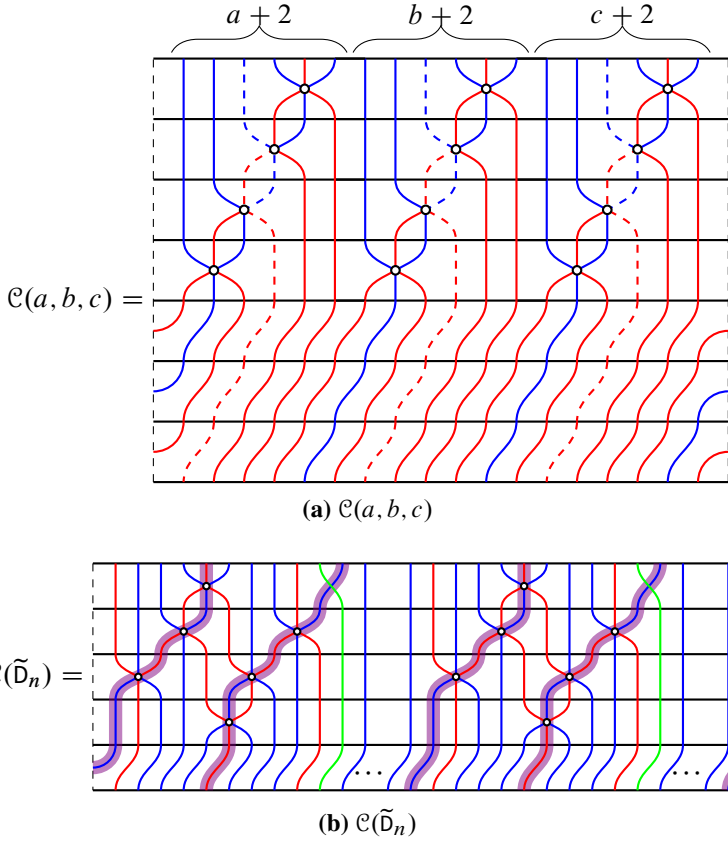


Figure 44. A sequence of elementary annulus N -graphs for Legendrian Coxeter paddings.

The corresponding annular N -graph is depicted in Figure 44b. Finally, the effect of Coxeter padding $\mathcal{C}(\tilde{\mathcal{D}}_n)$ onto $\beta(\tilde{\mathcal{D}}_n)$ can be presented as a Legendrian loop $\vartheta(\tilde{\mathcal{D}}_n)$, which is a composition

$$\vartheta(\tilde{\mathcal{D}}_n) = \varphi \vartheta_0(\tilde{\mathcal{D}}_n) \varphi^{-1}$$

as depicted in Figure 46, where φ is a Legendrian Reidemeister move (III).

Theorem 4.31. *The Legendrian Coxeter mutation $\mu_{\mathfrak{S}}^2$ on $(\mathfrak{S}(a, b, c), \mathcal{B}(a, b, c))$ and the Legendrian Coxeter mutation $\mu_{\mathfrak{S}}$ on $(\mathfrak{S}(\tilde{\mathcal{D}}), \mathcal{B}(\tilde{\mathcal{D}}))$ induce tame Legendrian loops $\vartheta(a, b, c)$ and $\vartheta(\tilde{\mathcal{D}})$ in Figures 45 and 46, respectively.*

4.4. Lagrangian fillings

In this section, we will prove one of our main theorem on ‘as many exact embedded Lagrangian fillings as seeds’ as follows.

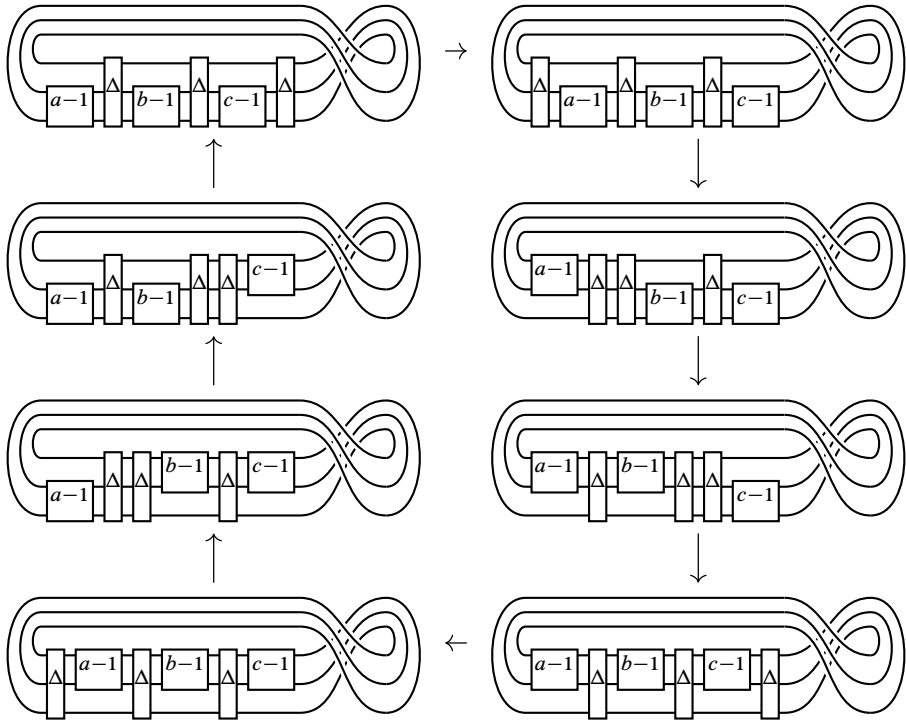


Figure 45. A Legendrian loop $\vartheta(a, b, c)$ induced from Legendrian Coxeter mutation $\mu_{\mathcal{G}}^2$ on $(\mathcal{G}(a, b, c), \mathcal{B}(a, b, c))$.

Theorem 4.32. *Let λ be a Legendrian knot or link of type ADE or type \widetilde{DE} . Then, it admits at least as many distinct exact embedded Lagrangian fillings up to exact Lagrangian isotopy (rel boundary) as the number of seeds in the seed pattern of the same type.*

Indeed, this theorem follows from considering the following general question.

Question 4.33. For a given N -graph \mathcal{G} with a chosen set \mathcal{B} of cycles, can we take a Legendrian mutation as many times as we want? Or equivalently, after applying a mutation μ_k on $(\mathcal{G}, \mathcal{B})$, is the set $\mu_k(\mathcal{B})$ still good in $\mu_k(\mathcal{G})$?

This question has been raised previously in [15, Remark 7.13]. One of the main reasons making the question non-trivial is the potential difference of geometric and algebraic intersections between two cycles.

Instead of attacking Question 4.33 directly, we will prove the following.

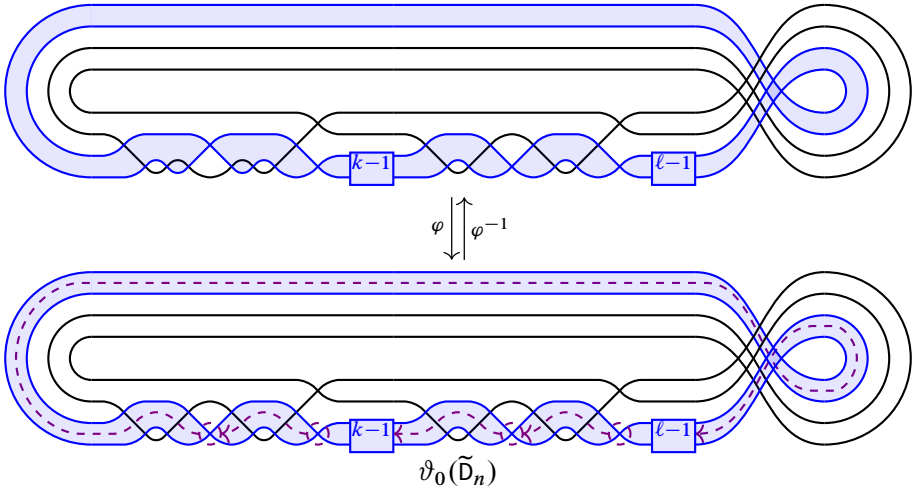


Figure 46. A Legendrian loop $\vartheta(\tilde{D}) = \varphi\vartheta_0(\tilde{D}_n)\varphi^{-1}$ induced from Legendrian Coxeter mutation $\mu_{\mathcal{G}}$ on $(\mathcal{G}(\tilde{D}_n), \mathcal{B}(\tilde{D}_n))$.

Proposition 4.34. For $Z = A, D, E, \tilde{D}, \tilde{E}$, let $(\mathcal{G}_{t_0}, \mathcal{B}_{t_0}) = (\mathcal{G}(Z), \mathcal{B}(Z))$, as depicted in Figures 34a, 34b, and 37. Suppose that $(\mathbf{y}, \mathcal{B})$ is a Y -seed in the Y -pattern given by the initial Y -seed $(\mathbf{y}_{t_0}, \mathcal{B}_{t_0}) = \Psi(\mathcal{G}_{t_0}, \mathcal{B}_{t_0})$. Then, $\lambda(Z)$ admits an N -graph $(\mathcal{G}, \mathcal{B})$ on \mathbb{D}^2 with $\partial\mathcal{G} = \lambda(Z)$ such that

$$\Psi(\mathcal{G}, \mathcal{B}) = (\mathbf{y}, \mathcal{B}).$$

Under the aid of this proposition, one can prove Theorem 4.32.

Proof of Theorem 4.32. Let λ be given as above. Then, by Proposition 4.34, we have the set of pairs of N -graphs and set of good cycles which has a one-to-one correspondence via Ψ with the set of Y -seeds in the Y -pattern of type Z . Hence, any pair of the Lagrangian fillings coming from these N -graphs is never exact Lagrangian isotopic by Lemma 4.16 and Proposition 3.48. Finally, by Corollary 4.15, there is a one-to-one correspondence between the set of Y -seeds and that of seeds, which completes the proof. ■

4.4.1. Proof of Proposition 4.34. We use an induction argument on the rank n of the root system $\Phi(Z)$. The initial step is either

$$(\mathcal{G}_{t_0}, \mathcal{B}_{t_0}) = (\mathcal{G}(1, 1, 1), \mathcal{B}(1, 1, 1)) \quad \text{or} \quad (\mathcal{G}_{t_0}, \mathcal{B}_{t_0}) = (\mathcal{G}(A_1), \mathcal{B}(A_1)).$$

Since there are no obstructions for mutations on these N -graphs, we are done for the initial step of the induction.

Now, suppose that $n \geq 2$. By the induction hypothesis, we assume that the assertion holds for each type $Z' = A, D, E, \tilde{D}, \tilde{E}$ having rank strictly small than n .

Let $(\mathbf{y}, \mathcal{B})$ be an Y -seed of type Z . By Lemma 2.32, there exist $r \in \mathbb{Z}$ and a sequence $\mu_{j_1}, \dots, \mu_{j_L}$ of mutations such that

$$(\mathbf{y}, \mathcal{B}) = \mu'((\mu_{\mathcal{Q}})^r(\mathbf{y}_{t_0}, \mathcal{B}_{t_0})), \quad \mu' = \mu_{j_L} \cdots \mu_{j_1},$$

where indices j_1, \dots, j_L miss at least one index i . It suffices to prove that the N -graph

$$(\mathcal{G}, \mathcal{B}) = \mu'((\mu_{\mathcal{G}})^r(\mathcal{G}_{t_0}, \mathcal{B}_{t_0}))$$

is well defined.

Notice that by Lemma 4.19 and Propositions 4.22 and 4.27, the Legendrian Coxeter mutation $\mu_{\mathcal{G}}^r(\mathcal{G}_{t_0}, \mathcal{B}_{t_0})$ is realizable so that

$$\Psi(\mu_{\mathcal{G}}^r(\mathcal{G}_{t_0}, \mathcal{B}_{t_0})) = (\mu_{\mathcal{Q}})^r(\mathbf{y}_{t_0}, \mathcal{B}_{t_0}).$$

Since $\mu_{\mathcal{G}}^r(\mathcal{G}_{t_0}, \mathcal{B}_{t_0})$ is the concatenation of Coxeter paddings on the initial N -graph $(\mathcal{G}_{t_0}, \mathcal{B}_{t_0})$, it suffices to prove that the Legendrian mutation $\mu'(\mu_{\mathcal{G}}^r(\mathcal{G}_{t_0}, \mathcal{B}_{t_0}))$ is realizable, which is equivalent to the realizability of $\mu'(\mathcal{G}_{t_0}, \mathcal{B}_{t_0})$.

By assumption, the indices j_1, \dots, j_L miss the index i and therefore the sequence of mutations $\mu_{j_1}, \dots, \mu_{j_L}$ can be performed inside the subgraph of the exchange graph $\text{Ex}(\Phi(Z))$, which is isomorphic to $\text{Ex}(\Phi(Z \setminus \{i\}))$. Here, with abuse of notation, we denote by Z the Dynkin diagram of type Z . Moreover, we denote by $\Phi(Z \setminus \{i\})$ the root system corresponding to the Dynkin diagram $Z \setminus \{i\}$. Then, the root system $\Phi(Z \setminus \{i\})$ is not necessarily irreducible and may be decomposed into $\Phi(Z^{(1)}), \dots, \Phi(Z^{(\ell)})$ for $Z \setminus \{i\} = Z^{(1)} \cup \dots \cup Z^{(\ell)}$ so that

$$\begin{aligned} \Phi(Z \setminus \{i\}) &\cong \Phi(Z^{(1)}) \times \dots \times \Phi(Z^{(\ell)}), \\ \text{Ex}(Z \setminus \{i\}) &\cong \text{Ex}(Z^{(1)}) \times \dots \times \text{Ex}(Z^{(\ell)}), \\ \mathcal{Q}_{t_0} \setminus \{i\} &\cong \mathcal{Q}^{(1)} \amalg \dots \amalg \mathcal{Q}^{(\ell)}, \end{aligned}$$

where the subquiver $\mathcal{Q}^{(k)}$ is of type $Z^{(k)}$. Moreover, the composition μ' of mutations can be decomposed into sequences $\mu^{(1)}, \dots, \mu^{(\ell)}$ of mutations on $\mathcal{Q}^{(1)}, \dots, \mathcal{Q}^{(\ell)}$.

Similarly, we may decompose the N -graph $(\mathcal{G}_{t_0}, \mathcal{B}_{t_0})$ into N -subgraphs

$$(\mathcal{G}^{(1)}, \mathcal{B}^{(1)}), \dots, (\mathcal{G}^{(\ell)}, \mathcal{B}^{(\ell)})$$

along $\gamma_i \in \mathcal{B}_{t_0}$, which are the restrictions of $(\mathcal{G}_{t_0}, \mathcal{B}_{t_0})$ onto $\mathbb{D}^{(i)} \subset \mathbb{D}^2$ as follows.

(1) For $\lambda = \lambda(A_n)$, we have the following two cases (Figure 47):

- (a) If γ_i corresponds to a univalent vertex, that is, a *leaf*, then we have the 2-subgraph $(\mathcal{G}(A_{n-1}), \mathcal{B}(A_{n-1}))$.

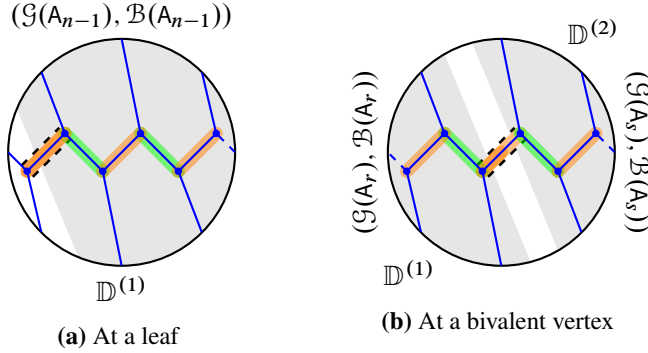


Figure 47. Decompositions of $\mathcal{G}(A_n)$.

- (b) If γ_i corresponds to a bivalent vertex, then, for some $1 \leq r, s$ with $r + s + 1 = n$, we have two 2-subgraphs $(\mathcal{G}(A_r), \mathcal{B}(A_r))$ and $(\mathcal{G}(A_s), \mathcal{B}(A_s))$.
- (2) For $\lambda = \lambda(a, b, c)$, we have the following three cases (Figure 48).
 - (a) If γ_i corresponds to the central vertex, then we have three 3-subgraphs $(\mathcal{G}_{(3)}(A_{a-1}), \mathcal{B}_{(3)}(A_{a-1}))$, $(\mathcal{G}_{(3)}(A_{b-1}), \mathcal{B}_{(3)}(A_{b-1}))$, and $(\mathcal{G}_{(3)}(A_{c-1}), \mathcal{B}_{(3)}(A_{c-1}))$.
 - (b) If γ_i corresponds to a bivalent vertex, then, for some $1 \leq r, s$ with $r + s + 1 = a$, up to permuting indices a, b, c , we have two 3-subgraphs $(\mathcal{G}_{(3)}(A_s), \mathcal{B}_{(3)}(A_s))$ and $(\mathcal{G}(r, b, c), \mathcal{B}(r, b, c))$.
 - (c) Otherwise, if γ_i corresponds to a leaf, then up to permuting indices a, b, c , we have the 3-subgraph $(\mathcal{G}(a - 1, b, c), \mathcal{B}(a - 1, b, c))$.
- (3) For $\lambda = \lambda(\tilde{D}_n)$, we have the following four cases (Figure 49).
 - (a) If $n = 4$ and γ_i corresponds to the central vertex, then we have four 4-graphs of type A_1 .
 - (b) If $n \geq 5$ and γ_i corresponds to a trivalent vertex, then we have three 4-graphs of types A_1, A_1 , and $(2, 2, n - 4)$.
 - (c) If $n \geq 6$, γ_i corresponds to a bivalent vertex, then, for some $r + s = n - 3$, we have two 4-graphs of type $(2, 2, r)$ and $(2, 2, s)$.
 - (d) If γ_i corresponds to a leaf, then we have the 4-graph $(\mathcal{G}'(D_n), \mathcal{B}'(D_n))$.

Here, $\mathcal{G}_{(3)}(A_{n'})$, $\mathcal{G}_{(4)}(A_{n'})$, and $\mathcal{G}_{(4)}(a', b', c')$ are the 3- and 4-graphs obtained from $\mathcal{G}(A_{n'})$ and $\mathcal{G}(a', b', c')$ by adding trivial planes at the top. Hence, the realizabilities of Legendrian mutations on $\mathcal{G}_{(3)}(A_{n'})$, $\mathcal{G}_{(4)}(A_{n'})$, and $\mathcal{G}_{(4)}(a', b', c')$ are the same as those on $\mathcal{G}(A_{n'})$ and $\mathcal{G}(a', b', c')$.

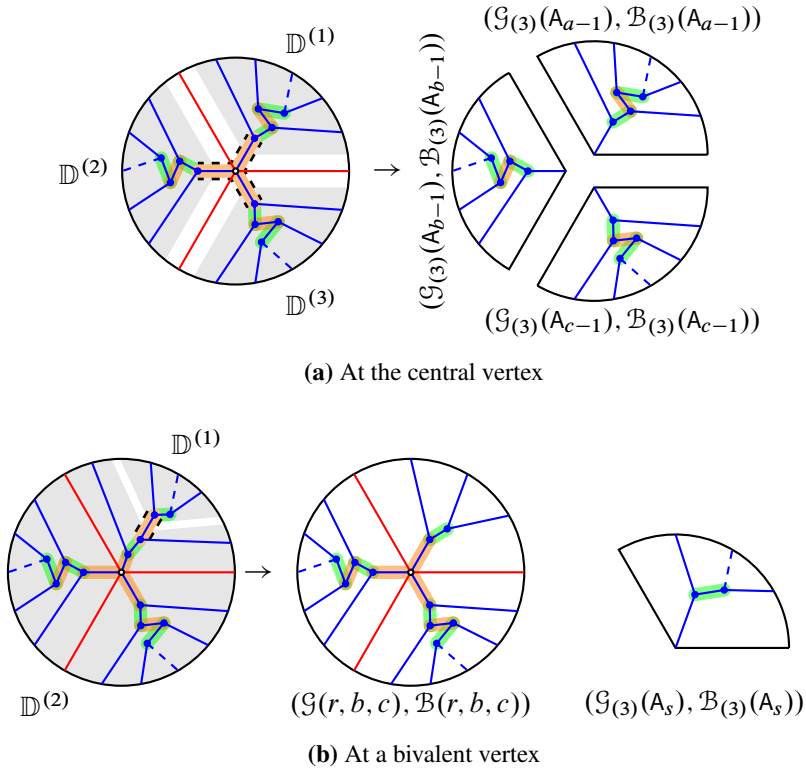
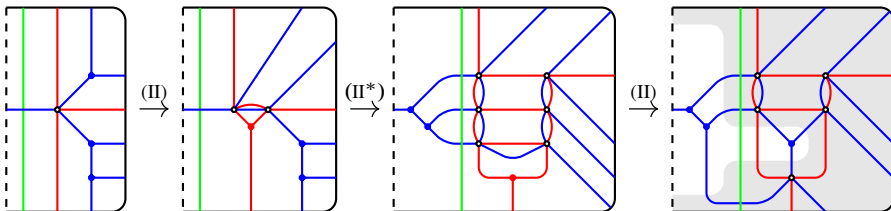


Figure 48. Decomposition of $\mathcal{G}(a, b, c)$.

Except for the very last case (3d), all the other cases are reduced to either linear and tripod N -graphs with strictly lower rank. Hence, by the induction hypothesis, any composition $\mu^{(k)}$ of mutations on $\mathcal{Q}^{(k)}$ for $1 \leq k \leq \ell$ can be realized as a composition of Legendrian mutations on $(\mathcal{G}^{(k)}, \mathcal{B}^{(k)})$. This guarantees the realizability of $\mu'(\mathcal{G}_{t_0}, \mathcal{B}_{t_0})$.

For the case (3d), one can apply a sequence of Move (II) on $(\mathcal{G}'(D_n), \mathcal{B}'(D_n))$ as follows:



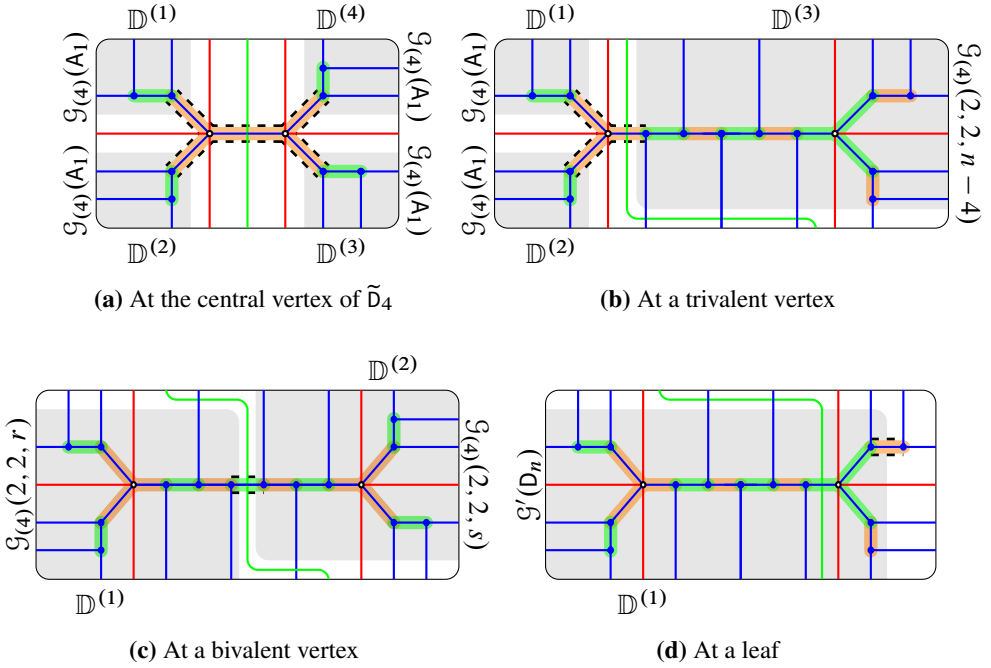
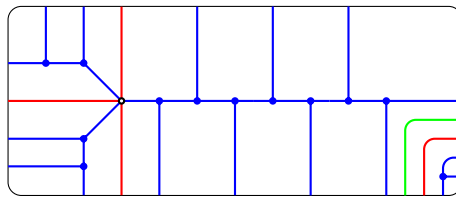


Figure 49. Decompositions of $\mathcal{G}(\tilde{D}_n)$.

Then, in the last picture, the shaded part corresponds to a tame annular N -graph, and so, the N -graph $(\mathcal{G}'(D_n), \mathcal{B}'(D_n))$ is ∂ -Legendrian isotopic to the following N -graph:



which is a stabilization of

$$(\mathcal{G}(D_n), \mathcal{B}(D_n)) = (\mathcal{G}(2, 2, n - 2), \mathcal{G}(2, 2, n - 2)).$$

Therefore, the induction hypothesis completes the proof.

Remark 4.35. It is not claimed above that two mutations μ' and $\mu_{\mathcal{G}}$ commute. Indeed, if we first mutate $(\mathcal{G}_{t_0}, \mathcal{B}_{t_0})$ via μ' , then the result may not look like either $(\mathcal{G}_{t_0}, \mathcal{B}_{t_0})$ or $\overline{(\mathcal{G}_{t_0}, \mathcal{B}_{t_0})}$, and hence, $\mu_{\mathcal{G}}$ will not work as expected. Besides it is not even clear whether $\mu_{\mathcal{G}}\mu'(\mathcal{G}_{t_0}, \mathcal{B}_{t_0})$ is realizable.

Rotation	$(A_{2n-1}, \mathbb{Z}/2\mathbb{Z}, B_n)$	$(D_4, \mathbb{Z}/3\mathbb{Z}, G_2)$	$(\tilde{E}_6, \mathbb{Z}/3\mathbb{Z}, \tilde{G}_2)$
	$(\tilde{D}_{2n \geq 6}, \mathbb{Z}/2\mathbb{Z}, \tilde{B}_n)$	$(\tilde{D}_4, \mathbb{Z}/2\mathbb{Z}, \tilde{C}_2)$	
Conjugation	$(D_{n+1}, \mathbb{Z}/2\mathbb{Z}, C_n)$	$(E_6, \mathbb{Z}/2\mathbb{Z}, F_4)$	
	$(\tilde{E}_6, \mathbb{Z}/2\mathbb{Z}, E_6^{(2)})$	$(\tilde{E}_7, \mathbb{Z}/2\mathbb{Z}, \tilde{F}_4)$	$(\tilde{D}_4, \mathbb{Z}/2\mathbb{Z}, A_5^{(2)})$

Table 10. Folding by rotation and conjugation.

5. Foldings

In this section, we will consider cluster structures of type BCFG and all standard affine type on N -graphs with certain symmetry.

Recall that if a quiver of type Z is globally foldable with respect to the G -action, then the folded cluster pattern is of type Z^G . We consider the triples (Z, G, Z^G) shown in Table 10.

5.1. Group actions on N -graphs

For each triple (Z, G, Z^G) , we first consider the G -action on each N -graph of type Z .

5.1.1. Rotation action. Let (Z, G, Z^G) be one of five cases in the first row of Table 10. We will denote the generator of $G = \mathbb{Z}/2\mathbb{Z}$ or $\mathbb{Z}/3\mathbb{Z}$ by τ , which acts on N -graphs \mathcal{G} by π -rotation or $2\pi/3$ -rotation, respectively.

Notice that, for each $Z = A_{2n-1}, D_4, \tilde{E}_6, \tilde{D}_{2n \geq 6}$, or \tilde{D}_4 , we may assume that the Legendrian $\lambda(Z)$ in $J^1\mathbb{S}^1$ is invariant under the π -rotation or $2\pi/3$ -rotation since the braid $\beta(Z)$ representing $\lambda(Z)$ has the rotation symmetry as follows:

$$\begin{aligned} \beta(A_{2n-1}) &= (\sigma_1^{n+1})^2, & \beta(D_4) &= (\sigma_2\sigma_1^3)^3, \\ \beta(\tilde{E}_6) &= (\sigma_2\sigma_1^4)^3, & \beta(\tilde{D}_{2n}) &= (\sigma_2\sigma_1^3\sigma_2\sigma_1^3\sigma_2\sigma_3\sigma_1^{n-2})^2, \quad n \geq 3, \\ \beta(\tilde{D}_4) &= (\sigma_2\sigma_1^3\sigma_2\sigma_1^3\sigma_2\sigma_3)^2. \end{aligned}$$

Now, the generator τ acts on the set $\mathcal{N}\text{graphs}(\lambda(Z))$ of equivalent classes of N -graphs with cycles whose boundary is precisely $\lambda(Z)$. Indeed, for each $(\mathcal{G}, \mathcal{B})$ in $\mathcal{N}\text{graphs}(\lambda(Z))$, we have

$$\tau \cdot (\mathcal{G}, \mathcal{B}) = \begin{cases} R_\pi(\mathcal{G}, \mathcal{B}) & \text{if } \tau \in \mathbb{Z}/2\mathbb{Z}, \\ R_{2\pi/3}(\mathcal{G}, \mathcal{B}) & \text{if } \tau \in \mathbb{Z}/3\mathbb{Z}, \end{cases}$$

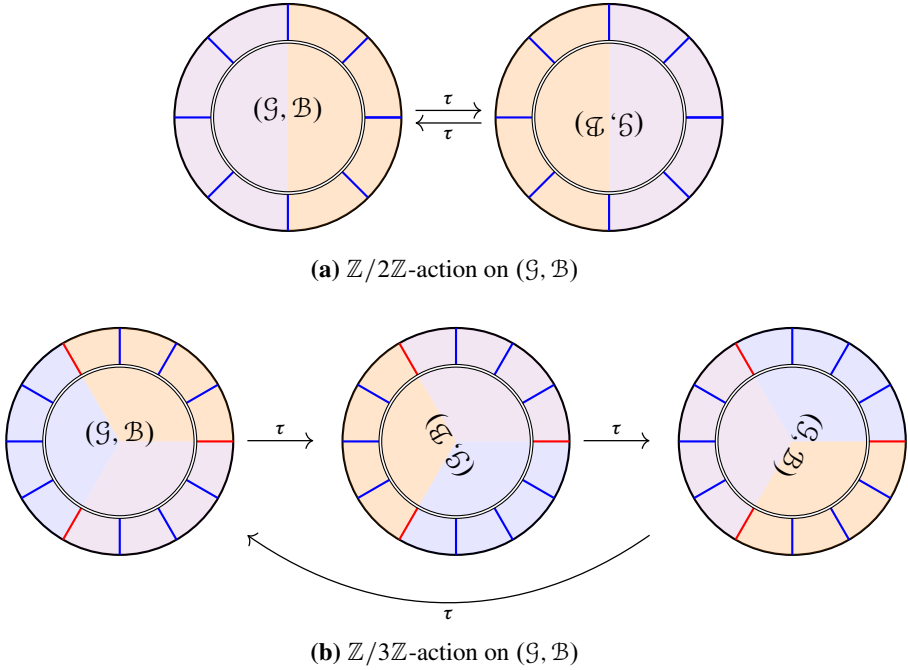


Figure 50. Rotation actions on N -graphs.

where R_θ is the induced action on N -graphs with cycles from the θ -rotation on \mathbb{D}^2 . See Figure 50a.

5.1.2. Conjugation action. Assume that (Z, G, Z^G) is one of five cases in the second row of Table 10. We denote the generator for $G = \mathbb{Z}/2\mathbb{Z}$ by η . Then, as before, the Legendrian $\tilde{\lambda}(Z)$ is represented by the braid $\tilde{\beta}(Z)$ which is invariant under the conjugation as follows:

$$\begin{aligned} \tilde{\beta}(\mathbb{D}_{n+1}) &= \sigma_2^n \sigma_{1,3} \sigma_2 \sigma_{1,3}^3 \sigma_2 \sigma_{1,3} \sigma_2^2 \sigma_{1,3}, & \tilde{\beta}(E_6) &= \sigma_2^3 \sigma_{1,3} \sigma_2 \sigma_{1,3}^4 \sigma_2 \sigma_{1,3} \sigma_2^2 \sigma_{1,3}, \\ \tilde{\beta}(\tilde{E}_6) &= \sigma_2^4 \sigma_{1,3} \sigma_2 \sigma_{1,3}^4 \sigma_2 \sigma_{1,3} \sigma_2^2 \sigma_{1,3}, & \tilde{\beta}(\tilde{E}_7) &= \sigma_2^3 \sigma_{1,3} \sigma_2 \sigma_{1,3}^5 \sigma_2 \sigma_{1,3} \sigma_2^2 \sigma_{1,3}, \\ \tilde{\beta}(\tilde{D}_4) &= (\sigma_2 \sigma_{1,3} \sigma_2 \sigma_{1,3}^2)^2. \end{aligned}$$

Therefore, the generator η acts on the set $\text{Ngraphs}(\tilde{\lambda}(Z))$ by conjugation. That is, for each $(\mathcal{G}, \mathcal{B}) \in \text{Ngraphs}(\tilde{\lambda}(Z))$, we have

$$\eta \cdot (\mathcal{G}, \mathcal{B}) = \overline{(\mathcal{G}, \mathcal{B})}.$$

Remark 5.1. One may also consider the conjugation invariant degenerate N -graph $\tilde{\mathcal{G}}(A_{2n-1})$ instead of the rotation invariant N -graph $\mathcal{G}(A_{2n-1})$ as seen earlier in Remark 4.10. Then, it can be checked that these two actions are identical.

Remark 5.2. The denegerated N -graph $\tilde{\mathcal{G}}(\tilde{D}_4)$ admits the π -rotation action as well, which is essentially equivalent to the conjugation action on $\tilde{\mathcal{G}}(\tilde{D}_4)$. We omit the details.

5.2. Invariant N -graphs and Lagrangian fillings

Throughout this section, we assume that (Z, G, Z^G) is one of the triples in Table 10. For an N -graph \mathcal{G} in $\mathcal{N}\text{graphs}(\lambda(Z))$ or $\mathcal{N}\text{graphs}(\tilde{\lambda}(Z))$, we say that $(\mathcal{G}, \mathcal{B})$ is G -invariant if, for each $g \in G$,

$$g \cdot (\mathcal{G}, \mathcal{B}) = (\mathcal{G}, \mathcal{B}).$$

Namely,

- (1) the N -graph \mathcal{G} is invariant under the action of g ;
- (2) the sets of cycles \mathcal{B} and $g(\mathcal{B})$ are identical up to relabeling $\gamma \leftrightarrow g(\gamma)$ for $\gamma \in \mathcal{B}$.

The following statements are obvious but important observations.

Lemma 5.3. *For a free N -graph \mathcal{G} , let*

$$L(\mathcal{G}) := (\pi \circ \iota)(\Lambda(\mathcal{G}))$$

be the Lagrangian surface defined by \mathcal{G} in \mathbb{C}^2 .

- (1) *If \mathcal{G} is invariant under the θ -rotation, then $L(\mathcal{G})$ is invariant under the θ -rotation in \mathbb{C}^2*

$$(z_1, z_2) \mapsto (z_1 \cos(\theta) + z_2 \sin(\theta), -z_1 \sin(\theta) + z_2 \cos(\theta)).$$

- (2) *If \mathcal{G} is invariant under the conjugation, then $L(\mathcal{G})$ is invariant under the anti-symplectic involution in \mathbb{C}^2*

$$(z_1, z_2) \mapsto (\bar{z}_1, \bar{z}_2).$$

Lemma 5.4. *The N -graphs with cycles $(\mathcal{G}(Z), \mathcal{B}(Z))$ for $Z = A_{2n-1}, D_4, \tilde{E}_6, \tilde{D}_{2n \geq 6}, \tilde{D}_4$ and the degenerate N -graphs with cycles $(\tilde{\mathcal{G}}(Z), \mathcal{B}(Z))$ for $Z = D_{n+1}, E_6, \tilde{E}_6, \tilde{E}_7, \tilde{D}_4$ are all invariant under the G -action.*

Lemma 5.5. *Suppose that $g \in G$ acts on $(\mathcal{G}, \mathcal{B})$. If the Legendrian mutation $\mu_\gamma(\mathcal{G}, \mathcal{B})$ is realizable, then*

$$\mu_{g(\gamma)}(g \cdot (\mathcal{G}, \mathcal{B})) = g \cdot (\mu_\gamma(\mathcal{G}, \mathcal{B})).$$

In particular, for a G -orbit, $I \subset \mathcal{B}$ consists of pairwise disjoint cycles; if $(\mathcal{G}, \mathcal{B})$ is G -invariant and the Legendrian orbit mutation $\mu_I(\mathcal{G}, \mathcal{B})$ is realizable, then $\mu_I(\mathcal{G}, \mathcal{B})$ is G -invariant as well.

On the other hand, if we have a G -invariant N -graph $(\mathcal{G}, \mathcal{B})$ with cycles, it gives us a G -admissible quiver $\mathcal{Q}(\mathcal{G}, \mathcal{B})$.

Lemma 5.6. *Let $(\mathcal{G}, \mathcal{B})$ be a G -invariant N -graph with cycles. Then, the quiver $\mathcal{Q}(\mathcal{G}, \mathcal{B})$ is globally foldable.*

Proof. By definition of G -invariance of $(\mathcal{G}, \mathcal{B})$, it is obvious that the quiver $\mathcal{Q} = \mathcal{Q}(\mathcal{G}, \mathcal{B})$ is G -invariant. On the other hand, since Z is either a finite or an affine Dynkin diagram, the G -invariance of the quiver \mathcal{Q} implies the globally foldability of \mathcal{Q} by Corollary 2.24. Hence, the result follows. ■

Proposition 5.7. *For each Y -seed $(\mathbf{y}', \mathcal{B}')$ of type Z^G , there exists a G -invariant N -graph with cycles $(\mathcal{G}, \mathcal{B})$ of type Z such that*

$$\Psi(\mathcal{G}, \mathcal{B})^G = (\mathbf{y}', \mathcal{B}').$$

Proof. We use a similar argument as in the proof of Proposition 4.34. For each Z , let $(\mathcal{G}_{t_0}, \mathcal{B}_{t_0})$ be the N -graph with cycles defined as follows:

$$(\mathcal{G}_{t_0}, \mathcal{B}_{t_0}) := \begin{cases} (\mathcal{G}(Z), \mathcal{B}(Z)) & \text{if } Z = A_{2n-1}, D_4, \tilde{E}_6, \tilde{D}_{2n \geq 6}, \tilde{D}_4, G \text{ acts as rotation,} \\ (\tilde{\mathcal{G}}(Z), \mathcal{B}(Z)) & \text{if } Z = D_{n+1}, E_6, \tilde{E}_6, \tilde{E}_7, \tilde{D}_4, G \text{ acts as conjugation.} \end{cases}$$

We regard the Y -seed defined by $(\mathcal{G}_{t_0}, \mathcal{B}_{t_0})$ as the initial seed $(\mathbf{y}_{t_0}, \mathcal{B}_{t_0})$

$$(\mathbf{y}_{t_0}, \mathcal{B}_{t_0}) = \Psi(\mathcal{G}_{t_0}, \mathcal{B}_{t_0}).$$

As seen in Lemma 5.4, the tuple $(\mathcal{G}_{t_0}, \mathcal{B}_{t_0})$ of the N -graph with cycles is G -invariant. Therefore, the quiver $\mathcal{Q}(\mathcal{G}_{t_0}, \mathcal{B}_{t_0})$ is globally foldable by Lemma 5.6. Therefore, we have the folded seed $(\mathbf{y}_{t_0}, \mathcal{B}_{t_0})^G$ which plays the role of the initial seed of the Y -pattern of type Z^G .

Let $(\mathbf{y}', \mathcal{B}')$ be an Y -seed of the Y -pattern of type Z^G . By Lemma 2.32, there exist $r \in \mathbb{Z}$ and a sequence of mutations $\mu_{j_1}^{Z^G}, \dots, \mu_{j_L}^{Z^G}$ such that

$$(\mathbf{y}', \mathcal{B}') = (\mu_{j_L}^{Z^G} \cdots \mu_{j_1}^{Z^G})((\mu_{\mathcal{Q}}^{Z^G})^r((\mathbf{y}_{t_0}, \mathcal{B}_{t_0})^G)).$$

Moreover, the indices j_1, \dots, j_L miss at least one index, say i .

Then, Theorem 2.25 implies the existence of the G -admissible Y -seed $(\mathbf{y}, \mathcal{B})$ of type Z such that $(\mathbf{y}, \mathcal{B})^G = (\mathbf{y}', \mathcal{B}')$ and

$$(\mathbf{y}, \mathcal{B}) = (\mu_{I_L}^Z \cdots \mu_{I_1}^Z)((\mu_{\mathcal{Q}}^Z)^r(\mathbf{y}_{t_0}, \mathcal{B}_{t_0})),$$

where I_k is G -orbit corresponding to j_k for each $1 \leq k \leq L$. It suffices to prove that the N -graph

$$(\mathcal{G}, \mathcal{B}) = (\mu_{I_L} \cdots \mu_{I_1})((\mu_{\mathcal{G}})^r(\mathcal{G}_{t_0}, \mathcal{B}_{t_0}))$$

is well defined and G -invariant so that

$$(\mathbf{y}, \mathcal{B}) = \Psi(\mathcal{G}, \mathcal{B})$$

is G -admissible by Proposition 3.43, as desired.

By Lemma 4.19 and Propositions 4.22, 4.27, and 4.29, the Legendrian Coxeter mutation $\mu_{\mathcal{G}}^r(\mathcal{G}_{t_0}, \mathcal{B}_{t_0})$ is realizable so that

$$\Psi(\mu_{\mathcal{G}}^r(\mathcal{G}_{t_0}, \mathcal{B}_{t_0})) = (\mu_{\mathcal{Q}})^r(\mathbf{y}_{t_0}, \mathcal{B}_{t_0}).$$

Since $\mu_{\mathcal{G}}^r(\mathcal{G}_{t_0}, \mathcal{B}_{t_0})$ is the concatenation of Coxeter paddings on the initial N -graph $(\mathcal{G}_{t_0}, \mathcal{B}_{t_0})$, the realizability of $(\mu_{I_L} \cdots \mu_{I_1})(\mathcal{G}_{t_0}, \mathcal{B}_{t_0})$ by Legendrian mutations implies that our desired mutation $(\mu_{I_L} \cdots \mu_{I_1})(\mu_{\mathcal{G}}^r(\mathcal{G}_{t_0}, \mathcal{B}_{t_0}))$ is also realizable by Legendrian mutations because the corresponding mutations of the former do not interact with the Coxeter padding.

On the other hand, since the indices j_1, \dots, j_L miss the index i , the orbits I_1, \dots, I_L miss one orbit I corresponding to i . In other words, the sequence of mutations $\mu_{I_1}, \dots, \mu_{I_L}$ can be performed inside the subgraph of the exchange graph $\text{Ex}(\Phi(Z))$, which is isomorphic to $\text{Ex}(\Phi(Z \setminus I))$. Then, the root system $\Phi(Z \setminus I)$ is decomposed into $\Phi(Z^{(1)}), \dots, \Phi(Z^{(\ell)})$, where $Z \setminus I = Z^{(1)} \cup \dots \cup Z^{(\ell)}$. Moreover, the sequence of mutations $\mu_{I_1}, \dots, \mu_{I_L}$ can be decomposed into sequences $\mu^{(1)}, \dots, \mu^{(\ell)}$ of mutations on $Z^{(1)}, \dots, Z^{(\ell)}$.

Similarly, we may decompose the N -graph $(\mathcal{G}_{t_0}, \mathcal{B}_{t_0})$ into N -subgraphs

$$(\mathcal{G}^{(1)}, \mathcal{B}^{(1)}), \dots, (\mathcal{G}^{(\ell)}, \mathcal{B}^{(\ell)})$$

along cycles in $I \subset \mathcal{B}_{t_0}$ as done in the previous section. Then, the Legendrian mutation $(\mu_{I_L} \cdots \mu_{I_1})(\mathcal{G}_{t_0}, \mathcal{B}_{t_0})$ is realizable if and only if so is $\mu^{(j)}(\mathcal{G}^{(j)}, \mathcal{B}^{(j)})$ for each $1 \leq j \leq \ell$. This can be done by induction on rank of the root system, and so, the N -graph $(\mathcal{G}, \mathcal{B})$ with $\Psi(\mathcal{G}, \mathcal{B}) = (\mathbf{y}, \mathcal{B})$ is well defined.

Finally, the G -invariance of $(\mathcal{G}, \mathcal{B})$ follows from Lemma 5.5. ■

Theorem 5.8 (Folding of N -graphs). *The following holds.*

- (1) *The Legendrian $\lambda(A_{2n-1})$ has at least $\binom{2n}{n}$ distinct Lagrangian fillings up to exact Lagrangian isotopy (rel boundary) which are invariant under the π -rotation and admit the Y -pattern of type B_n .*
- (2) *The Legendrian $\lambda(D_4)$ has at least 8 distinct Lagrangian fillings up to exact Lagrangian isotopy (rel boundary) which are invariant under the $2\pi/3$ -rotation and admit the Y -pattern of type G_2 .*
- (3) *The Legendrian $\lambda(\tilde{E}_6)$ has infinitely many distinct Lagrangian fillings up to exact Lagrangian isotopy (rel boundary) which are invariant under the $2\pi/3$ -rotation and admit the Y -pattern of type \tilde{G}_2 .*

- (4) *The Legendrian $\lambda(\tilde{D}_{2n})$ with $n \geq 3$ has infinitely many distinct Lagrangian fillings up to exact Lagrangian isotopy (rel boundary) which are invariant under the π -rotation and admit the Y -pattern of type \tilde{B}_n .*
- (5) *The Legendrian $\lambda(\tilde{D}_4)$ has infinitely many distinct Lagrangian fillings up to exact Lagrangian isotopy (rel boundary) which are invariant under the π -rotation and admit the Y -pattern of type \tilde{C}_2 .*
- (6) *The Legendrian $\tilde{\lambda}(E_6)$ has at least 105 distinct Lagrangian fillings up to exact Lagrangian isotopy (rel boundary) which are invariant under the antisymplectic involution and admit the Y -pattern of type F_4 .*
- (7) *The Legendrian $\tilde{\lambda}(D_{n+1})$ has at least $\binom{2n}{n}$ Lagrangian fillings up to exact Lagrangian isotopy (rel boundary) which are invariant under the antisymplectic involution and admit the Y -pattern of type C_n .*
- (8) *The Legendrian $\tilde{\lambda}(\tilde{E}_6)$ has infinitely many distinct Lagrangian fillings up to exact Lagrangian isotopy (rel boundary) which are invariant under the anti-symplectic involution and admit the Y -pattern of type $E_6^{(2)}$.*
- (9) *The Legendrian $\tilde{\lambda}(\tilde{E}_7)$ has infinitely many distinct Lagrangian fillings up to exact Lagrangian isotopy (rel boundary) which are invariant under the anti-symplectic involution and admit the Y -pattern of type \tilde{F}_4 .*
- (10) *The Legendrian $\tilde{\lambda}(\tilde{D}_4)$ has infinitely many distinct Lagrangian fillings up to exact Lagrangian isotopy (rel boundary) which are invariant under the antisymplectic involution and admit the Y -pattern of type $A_5^{(2)}$.*

Proof. Let (Z, G, Z^G) be one of the triples in Table 10. By Proposition 5.7, each Y -seed of the Y -pattern of type Z^G is realizable by a G -invariant N -graph, which gives us a Lagrangian filling with a certain symmetry by Lemma 5.3. This completes the proof. ■

A. G -invariance and G -admissibility of finite type

In this section, we will provide a proof of Theorem 2.23. Recall from Definition 2.12 that, for a finite or affine Dynkin type Z , a quiver \mathcal{Q} is of type Z if it is mutation equivalent to an acyclic quiver whose underlying graph is isomorphic to the Dynkin diagram of type Z .

Lemma A.1. *Let \mathcal{Q} be a quiver of type A_{2n-1} . Suppose that \mathcal{Q} is invariant under an action of $G = \mathbb{Z}/2\mathbb{Z}$. Let $\tau \in \mathbb{Z}/2\mathbb{Z}$ be the generator of G . Then, there is no oriented cycle of the form*

$$j \rightarrow i \rightarrow \tau(j) \rightarrow \tau(i) \rightarrow j$$

for any vertices i and j of \mathcal{Q} which are not invariant under τ . Here, we are allowing any labeling of the vertices of \mathcal{Q} .

Proof. It is well known that a quiver \mathcal{Q} of type A corresponds to a triangulation of a polygon, where diagonals and triangles define mutable vertices and arrows (cf. [23, Definition 2.2.1]). More precisely, for a triangulation T of an $(n + 2)$ -gon, the quiver $\mathcal{Q}(T)$ is defined as follows. The frozen vertices of $\mathcal{Q}(T)$ are labeled by the sides of the $(n + 2)$ -gon, and the mutable vertices of $\mathcal{Q}(T)$ are labeled by the diagonals of T . If two diagonals, or a diagonal and a boundary segment, belong to the same triangle, we connect the corresponding vertices in $\mathcal{Q}(T)$ by an arrow whose orientation is determined by the clockwise orientation of the boundary of the triangle. Therefore, any minimal cycle in \mathcal{Q} if exists is of length 3, which is also proved in [8, Section 2]. Hence, if an oriented cycle $j \rightarrow i \rightarrow \tau(j) \rightarrow \tau(i) \rightarrow j$ of length 4 exists, then there must be an edge connecting i and $\tau(i)$, or an edge connecting j and $\tau(j)$ in \mathcal{Q} . Hence, $b_{i,\tau(i)} \neq 0$ or $b_{j,\tau(j)} \neq 0$ for $\mathcal{B} = (b_{k,\ell}) = \mathcal{B}(\mathcal{Q})$.

This is impossible because \mathcal{Q} is $\mathbb{Z}/2\mathbb{Z}$ -invariant, and so,

$$b_{i,\tau(i)} = b_{\tau(i),\tau(\tau(i))} = b_{\tau(i),i} = -b_{i,\tau(i)} \Rightarrow b_{i,\tau(i)} = 0. \quad (\text{A.1})$$

Therefore, we are done. ■

Proposition A.2. *Let \mathcal{Q} be a quiver of type A_{2n-1} , which is $\mathbb{Z}/2\mathbb{Z}$ -invariant as above. Then, \mathcal{Q} is $\mathbb{Z}/2\mathbb{Z}$ -admissible.*

Proof. We will check the conditions (2a), (2b), and (2c) for the admissibility according to Definition 2.17. Let τ be the generator of $\mathbb{Z}/2\mathbb{Z}$ and $\mathcal{B} = (b_{i,j}) = \mathcal{B}(\mathcal{Q})$.

(2a) Since all vertices in \mathcal{Q} are mutable, the condition (2a) is obviously satisfied.

(2b) The $\mathbb{Z}/2\mathbb{Z}$ -invariance of \mathcal{Q} implies $b_{i,\tau(i)} = 0$ by (A.1).

(2c) Finally, we need to prove that, for each i, j ,

$$b_{i,j}b_{\tau(i),j} \geq 0.$$

If j is invariant under the action of τ , i.e., $\tau(j) = j$, then we have

$$b_{i,j}b_{\tau(i),j} = b_{i,j}b_{\tau(i),\tau(j)} = b_{i,j}b_{i,j} \geq 0.$$

Similarly, if i is invariant under the action of τ , i.e., $\tau(i) = i$, then we have

$$b_{i,j}b_{\tau(i),j} = b_{i,j}b_{i,j} \geq 0.$$

Suppose that for some i, j , which are not invariant under τ , we have

$$b_{i,j}b_{\tau(i),j} < 0.$$

By changing the roles of i and $\tau(i)$ if necessary, we may assume that $b_{i,j} < 0 < b_{\tau(i),j}$. Then, we also have

$$b_{\tau(i),\tau(j)} < 0 < b_{i,\tau(j)},$$

which implies that there is an oriented cycle in \mathcal{Q}

$$j \rightarrow i \rightarrow \tau(j) \rightarrow \tau(i) \rightarrow j.$$

However, this contradicts Lemma A.1, and therefore, \mathcal{Q} satisfies all conditions in Definition 2.17. ■

Proposition A.3. *Let \mathcal{Q} be a quiver of type D_4 , which is invariant under the $\mathbb{Z}/3\mathbb{Z}$ -action given by*

$$1 \xleftrightarrow{\tau} 1, \quad 2 \xrightarrow{\tau} 3 \xrightarrow{\tau} 4 \xrightarrow{\tau} 2.$$

Here, we denote by τ the generator of $\mathbb{Z}/3\mathbb{Z}$, and we are allowing any labeling of the vertices of \mathcal{Q} . Then, the quiver \mathcal{Q} is $\mathbb{Z}/3\mathbb{Z}$ -admissible.

Proof. (2a) This is obvious as before.

(2b) Let $\mathcal{B} = (b_{i,j}) = \mathcal{B}(\mathcal{Q})$. Suppose that $b_{2,3} \neq 0$. Since the quiver is $\mathbb{Z}/3\mathbb{Z}$ -invariant, then

$$b_{2,3} = b_{3,4} = b_{4,2} \neq 0,$$

and so, \mathcal{Q} has a directed cycle either

$$2 \rightarrow 3 \rightarrow 4 \rightarrow 2 \quad \text{or} \quad 2 \rightarrow 4 \rightarrow 3 \rightarrow 2.$$

Then, according to the value $b_{1,2}$, the underlying graph of the quiver \mathcal{Q} is either the complete graph K_4 or a disconnected graph. However, both are impossible as shown in [7, Figure 1]. Therefore, we obtain

$$b_{2,3} = b_{3,4} = b_{4,2} = 0.$$

(2c) The only entries we need to check are $b_{1,j}$'s, which are all equal by the $\mathbb{Z}/3\mathbb{Z}$ -invariance of \mathcal{Q} . Therefore,

$$b_{1,j}b_{1,j'} \geq 0.$$

This completes the proof. ■

Lemma A.4. *Let \mathcal{Q} be a quiver on [6] of type E_6 , which is invariant under the $\mathbb{Z}/2\mathbb{Z}$ -action defined by*

$$i \xleftrightarrow{\eta} i, i \leq 2, \quad 3 \xleftrightarrow{\eta} 5, \quad 4 \xleftrightarrow{\eta} 6.$$

Here, we denote by η the generator of $\mathbb{Z}/2\mathbb{Z}$ and we are allowing any labeling of the vertices of \mathcal{Q} . Then, there is no oriented cycle, which is either

$$3 \rightarrow 4 \rightarrow 5 \rightarrow 6 \rightarrow 3 \quad \text{or} \quad 3 \rightarrow 6 \rightarrow 5 \rightarrow 4 \rightarrow 3. \tag{A.2}$$

Proof. We first recall from [26, Theorem 1.8] that

$$|b_{i,j}| \leq 1 \quad \text{for all } i, j \in [6]. \tag{A.3}$$

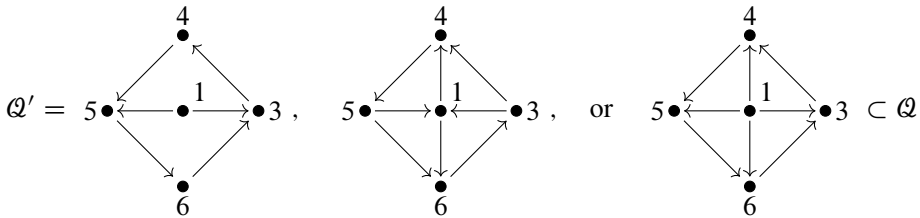
Otherwise, \mathcal{Q} produces a cluster pattern of infinite type. Hence, \mathcal{Q} is a simple directed graph.

Suppose that \mathcal{Q} contains an oriented cycle in (A.2). By relabeling if necessary, we may assume that the \mathcal{Q} contains an oriented cycle

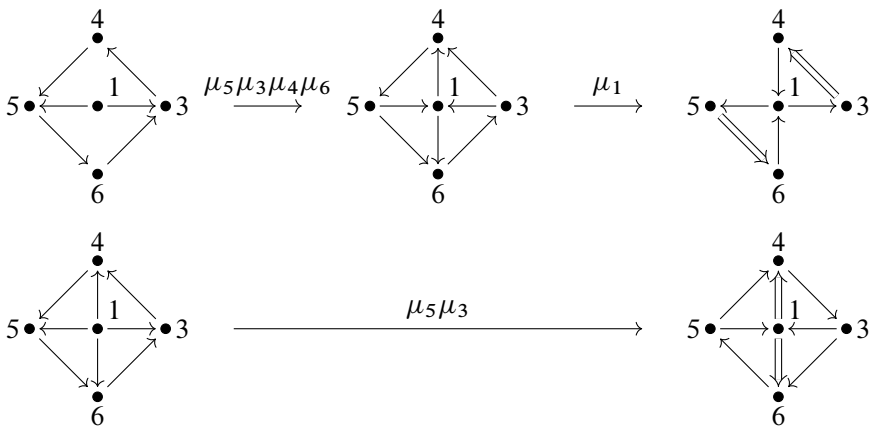
$$3 \rightarrow 4 \rightarrow 5 \rightarrow 6 \rightarrow 3.$$

Then, since \mathcal{Q} is connected, at least one of vertices 1 and 2 is joined with one of vertices 3, 4, 5, and 6 by an edge. Without loss of generality, we may assume that such a vertex is 1.

Let \mathcal{Q}' be the quiver on $\{1, 3, 4, 5, 6\}$ obtained by forgetting the vertex 2 in \mathcal{Q} . Then, by the invariance of \mathcal{Q} under $\mathbb{Z}/2\mathbb{Z}$ -action,



up to relabeling and the mutation μ_1 . Then, via further mutations, each of these quivers can be transformed to a quiver producing a cluster pattern of infinite type because of the condition (A.3) as follows:



Here, the label $\mu_5\mu_3\mu_4\mu_6$ means that we are applying the mutation μ_6 first, then μ_4 , and so on. Since any subquiver of a quiver mutation equivalent to \mathcal{Q} is of finite type, we get a contradiction which completes the proof. ■

Remark A.5. Since there are only finitely many quivers of type E_6 , the above lemma can be verified by a computer, but we gave here a combinatorial proof.

Proposition A.6. *Let \mathcal{Q} be a quiver of type $Z = D_{n+1}$ or E_6 , which is invariant under $\mathbb{Z}/2\mathbb{Z}$ -action defined by*

$$i \overset{\eta}{\leftrightarrow} i, i < n, \quad n \overset{\eta}{\leftrightarrow} n + 1$$

for $Z = D_{n+1}$, or

$$i \overset{\eta}{\leftrightarrow} i, i \leq 2, \quad 3 \overset{\eta}{\leftrightarrow} 5, \quad 4 \overset{\eta}{\leftrightarrow} 6$$

for $Z = E_6$. Here, η is the generator of $\mathbb{Z}/2\mathbb{Z}$ and we are allowing any labeling of the vertices of \mathcal{Q} . Then, the quiver \mathcal{Q} is $\mathbb{Z}/2\mathbb{Z}$ -admissible.

Proof. (2a) This is obvious as before.

(2b) Let $\mathcal{B} = (b_{i,j}) = \mathcal{B}(\mathcal{Q})$. Then, by the $\mathbb{Z}/2\mathbb{Z}$ -invariance of \mathcal{Q} ,

$$b_{i,\eta(i)} = b_{\eta(i),\eta(\eta(i))} = b_{\eta(i),i} = -b_{i,\eta(i)} \Rightarrow b_{i,\eta(i)} = 0.$$

(2c) If $Z = D_{n+1}$, then we only need to show that

$$b_{i,n}b_{i,n+1} \geq 0$$

for $i < n$. This is obvious since

$$b_{i,n+1} = b_{\eta(i),\eta(n+1)} = b_{i,n}.$$

If $Z = E_6$, then all we need to show that inequalities

$$b_{i,j}b_{i,j+2} \geq 0, \quad b_{3,4}b_{3,6} \geq 0$$

hold for $i = 1, 2$ and $j = 3, 4$.

The first inequality is obvious since

$$b_{i,j+2} = b_{\eta(i),\eta(j+2)} = b_{i,j}.$$

Suppose that $b_{3,4}b_{3,6} < 0$. Then, since $b_{3,4} = b_{5,6}$ and $b_{3,6} = b_{5,4}$, the \mathcal{Q} has a loop either

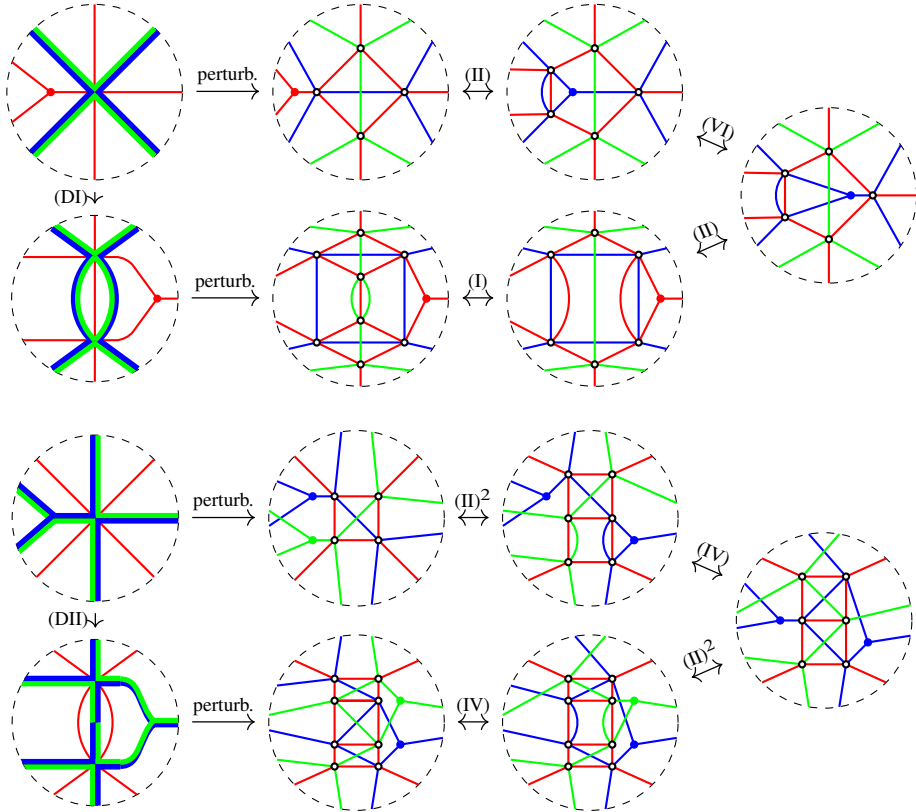
$$3 \rightarrow 4 \rightarrow 5 \rightarrow 6 \rightarrow 3 \quad \text{or} \quad 3 \rightarrow 6 \rightarrow 5 \rightarrow 4 \rightarrow 3,$$

which yields a contradiction by Lemma A.4. This completes the proof. ■

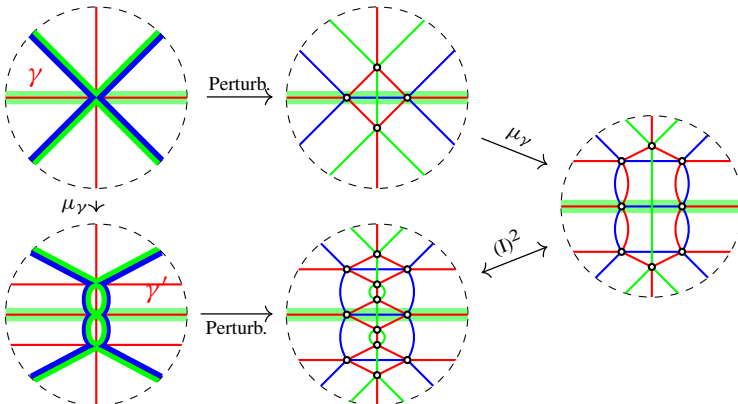
Proof of Theorem 2.23. Let \mathcal{Q} be a G -invariant quiver. Then, it is G -admissible because of Propositions A.2, A.3, and A.6. ■

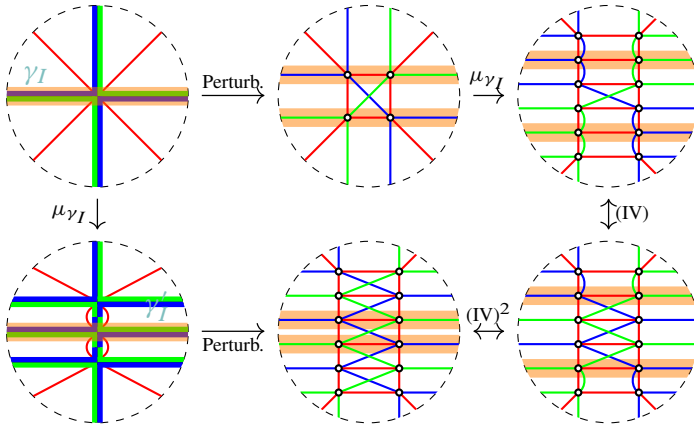
B. Supplementary pictorial proofs

B.1. Justification of moves (DI) and (DII) for degenerate N -graphs



B.2. Justification of Legendrian local mutations in degenerate N -graphs

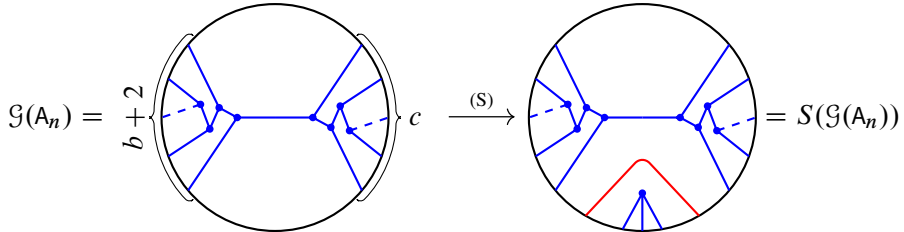




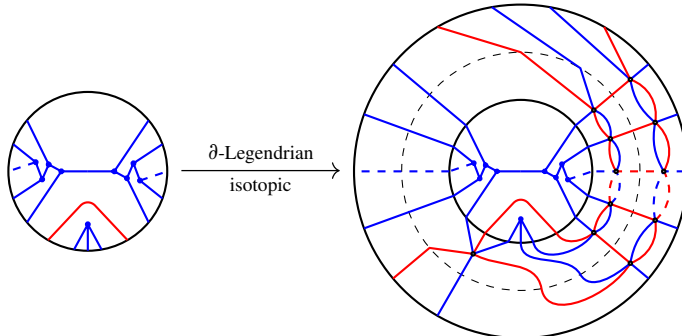
See Remark 3.41 for the incoherency of the boundaries of the initial N -graphs and the terminal ones.

B.3. Equivalence between $\mathcal{G}(1, b, c)$ and a stabilization of $\mathcal{G}(A_n)$

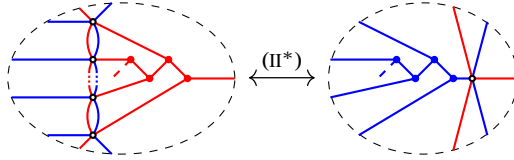
A stabilization of $\mathcal{G}(A_n)$ is a 3-graph which is ∂ -Legendrian isotopic to a 3-graph $S(\mathcal{G}(A_n))$ given as follows:



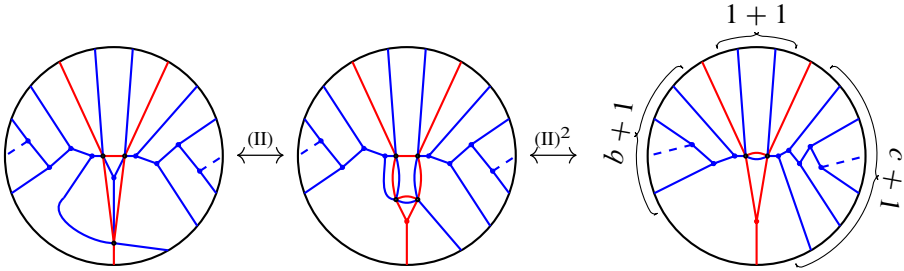
Now, we attach the annular 3-graph corresponding to Legendrian isotopy from $S(\beta(A_n))$ to $\beta(1, b, c)$ given above. Then, we have the following 3-graph which is ∂ -Legendrian isotopic to $S(\mathcal{G}(A_n))$.



By applying the following generalized push-through move twice, once for each attached annulus region,

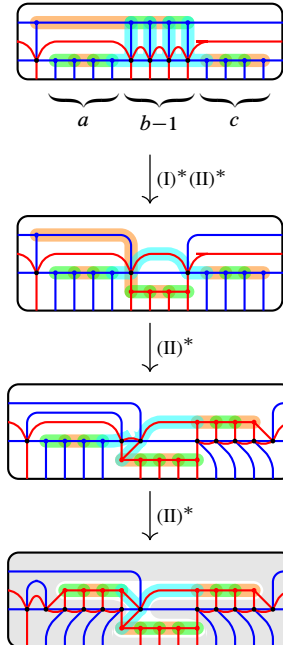


we obtain the 3-graph in the left of the following three equivalent 3-graphs:



where the right one is equivalent to the 3-graph $\mathcal{G}(1, b, c)$ via the Move (II), as claimed.

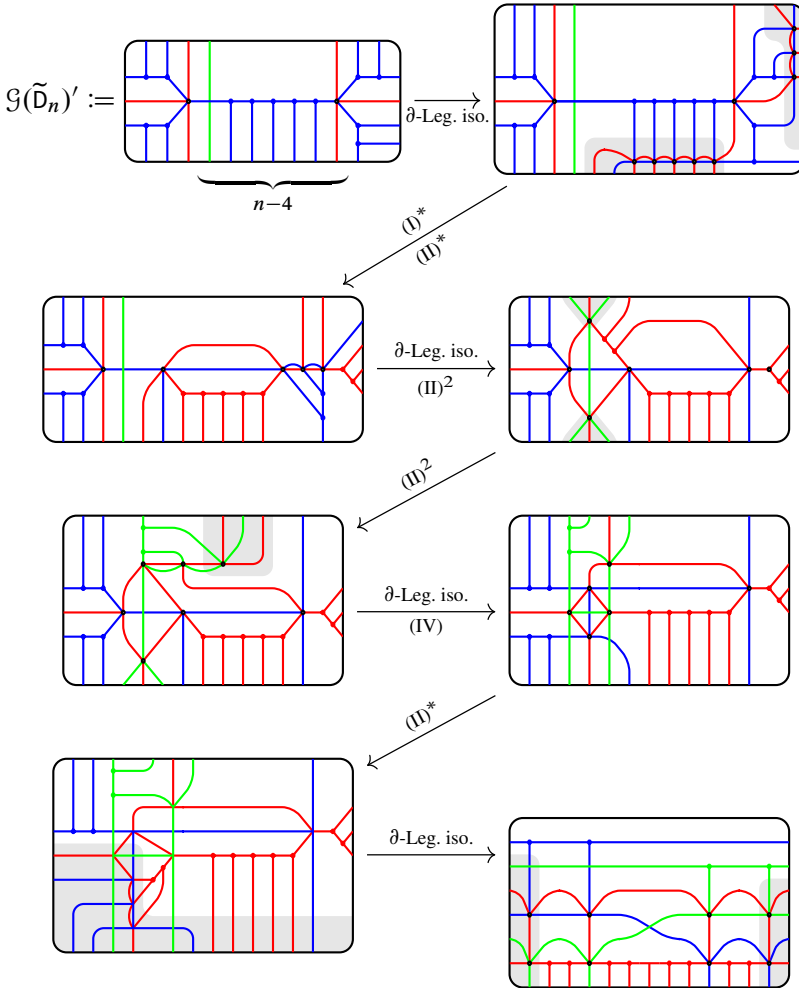
B.4. Proof of Lemma 4.3: Equivalence between $(\mathcal{G}^{\text{brick}}(a, b, c), \mathcal{B}^{\text{brick}}(a, b, c))$ and $(\mathcal{G}(a, b, c), \mathcal{B}(a, b, c))$



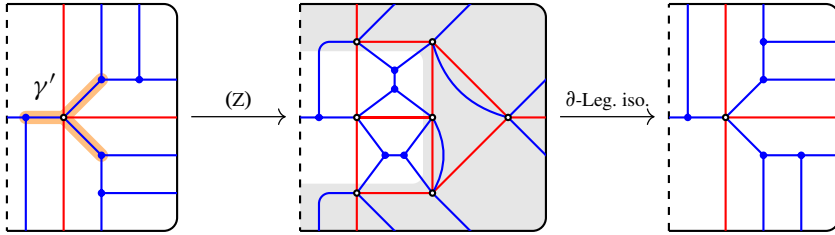
The innermost N -graph is the same as $\overline{\mathcal{G}(a, b, c)}$ up to Legendrian mutations, which is ∂ -Legendrian isotopic to the Legendrian Coxeter mutation of $\mathcal{G}(a, b, c)$ by Proposition 4.22.

B.5. The proof of Lemma 4.12: Equivalence between $(\mathcal{G}^{\text{brick}}(\tilde{\mathcal{D}}_n), \mathcal{B}^{\text{brick}}(\tilde{\mathcal{D}}_n))$ and $(\mathcal{G}(\tilde{\mathcal{D}}_n), \mathcal{B}(\tilde{\mathcal{D}}_n))$

We first show that $\mathcal{G}^{\text{brick}}(\tilde{\mathcal{D}}_n)$ is Legendrian mutation equivalent to the following N -graph up to ∂ -Legendrian isotopy. Even though we omit the data of cycles for the pictorial simplicity, one can keep track of $\mathcal{B}(\tilde{\mathcal{D}}_n)$ through the following (∂ -)Legendrian isotopies:



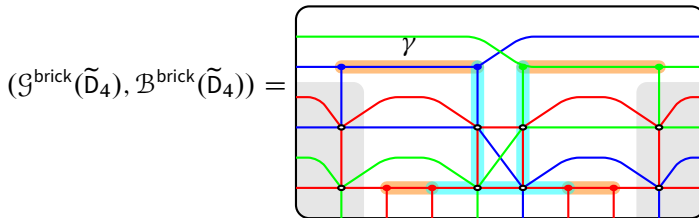
On the other hand, we have the following move (Z) from Section 4.2.3:



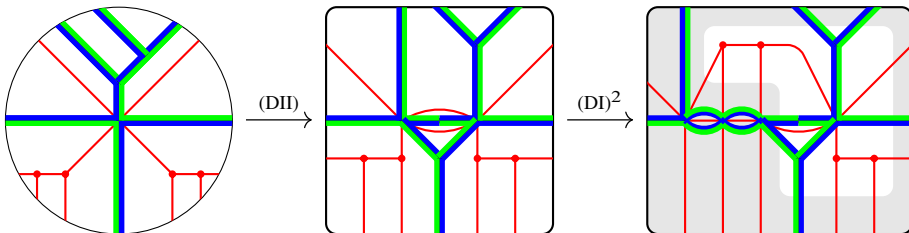
which flips up the downward leg. Finally, the downward and upward legs can be interchanged via Legendrian mutations, and therefore, the N -graph $\mathcal{G}(\tilde{\mathcal{D}}_n)'$ is Legendrian mutation equivalent to $\mathcal{G}(\tilde{\mathcal{D}}_n)$ up to ∂ -Legendrian isotopy.

B.6. A proof of Lemma 4.14: Equivalence between $(\tilde{\mathcal{G}}(\tilde{\mathcal{D}}_4), \tilde{\mathcal{B}}(\tilde{\mathcal{D}}_4))$ and $(\mathcal{G}(\tilde{\mathcal{D}}_4), \mathcal{B}(\tilde{\mathcal{D}}_4))$

It is enough to show the equivalence between two N -graphs with cycles $(\tilde{\mathcal{G}}(\tilde{\mathcal{D}}_4), \tilde{\mathcal{B}}(\tilde{\mathcal{D}}_4))$ and $(\mathcal{G}^{\text{brick}}(\tilde{\mathcal{D}}_4), \mathcal{B}^{\text{brick}}(\tilde{\mathcal{D}}_4))$ by Lemma 4.12.



By cutting out the shaded region and taking a Legendrian mutation on γ , the 1-cycle between the two blue vertices, we have a degenerate N -graph below (here, we omit cycle data,) which is $\tilde{\mathcal{G}}(\tilde{\mathcal{D}}_4)$ up to ∂ -Legendrian isotopy and Legendrian mutations.



Acknowledgments. The authors thank the anonymous referees for their careful reading and detailed comments on the previous manuscripts, and thank Salvatore Stella for valuable conversations on the combinatorics of cluster algebras on affine types. They

also heartily thank the IBS Center for Geometry and Physics for their warm hospitality during the project.

Funding. B. H. An was supported by the National Research Foundation of Korea (NRF) grants funded by the Korea government (MSIT) (RS-2023-00208405 and No. 2020R1A2C1A0100320). Y. Bae was supported by the National Research Foundation of Korea (NRF) grants funded by the Korea government (MSIT) (RS-2022-NR071798). E. Lee was supported by the Institute for Basic Science (IBS-R003-D1), the National Research Foundation of Korea (NRF) grant funded by the Korea government (MSIT) (Nos. RS-2022-00165641 and RS-2023-00239947), and POSCO Science Fellowship of POSCO TJ Park Foundation.

References

- [1] B. H. An and E. Lee, [On folded cluster patterns of affine type](#). *Pacific J. Math.* **318** (2022), no. 2, 401–431 Zbl 1498.13061 MR 4474368
- [2] V. I. Arnol'd, *Singularities of caustics and wave fronts*. Math. Appl. (Soviet Ser.) 62, Kluwer Academic Publishers, Dordrecht, 1990 Zbl 0734.53001 MR 1151185
- [3] D. Auroux, [Mirror symmetry and \$T\$ -duality in the complement of an anticanonical divisor](#). *J. Gökova Geom. Topol. GGT* **1** (2007), 51–91 Zbl 1181.53076 MR 2386535
- [4] A. Berenstein, S. Fomin, and A. Zelevinsky, [Cluster algebras. III. Upper bounds and double Bruhat cells](#). *Duke Math. J.* **126** (2005), no. 1, 1–52 Zbl 1135.16013 MR 2110627
- [5] L. Bossinger, X. Fang, G. Fourier, M. Hering, and M. Lanini, [Toric degenerations of \$\text{Gr}\(2, n\)\$ and \$\text{Gr}\(3, 6\)\$ via plabic graphs](#). *Ann. Comb.* **22** (2018), no. 3, 491–512 Zbl 1454.14119 MR 3845745
- [6] N. Bourbaki, *Lie groups and Lie algebras. Chapters 4–6*. Elements of Mathematics (Berlin), Springer, Berlin, 2002; Translated from the 1968 French original by Andrew Pressley MR 1890629
- [7] A. B. Buan and H. A. Torkildsen, [The number of elements in the mutation class of a quiver of type \$D_n\$](#) . *Electron. J. Combin.* **16** (2009), no. 1, article no. 49 Zbl 1175.16009 MR 2505091
- [8] A. B. Buan and D. F. Vatne, [Derived equivalence classification for cluster-tilted algebras of type \$A_n\$](#) . *J. Algebra* **319** (2008), no. 7, 2723–2738 Zbl 1155.16010 MR 2397404
- [9] P. Caldero and B. Keller, [From triangulated categories to cluster algebras. II](#). *Ann. Sci. École Norm. Sup. (4)* **39** (2006), no. 6, 983–1009 Zbl 1115.18301 MR 2316979
- [10] P. Cao, M. Huang, and F. Li, [A conjecture on \$C\$ -matrices of cluster algebras](#). *Nagoya Math. J.* **238** (2020), 37–46 Zbl 1442.13060 MR 4092846
- [11] R. Casals, [Lagrangian skeleta and plane curve singularities](#). *J. Fixed Point Theory Appl.* **24** (2022), no. 2, article no. 34 Zbl 1501.53088 MR 4405603
- [12] R. Casals and H. Gao, [Infinitely many Lagrangian fillings](#). *Ann. of Math. (2)* **195** (2022), no. 1, 207–249 Zbl 1494.53090 MR 4358415

- [13] R. Casals and L. Ng, [Braid loops with infinite monodromy on the Legendrian contact DGA](#). *J. Topol.* **15** (2022), no. 4, 1927–2016 Zbl [1527.53080](#) MR [4584583](#)
- [14] R. Casals and D. Weng, [Microlocal theory of Legendrian links and cluster algebras](#). *Geom. Topol.* **28** (2024), no. 2, 901–1000 Zbl [1547.13030](#) MR [4718130](#)
- [15] R. Casals and E. Zaslow, [Legendrian weaves: \$N\$ -graph calculus, flag moduli and applications](#). *Geom. Topol.* **26** (2022), no. 8, 3589–3745 Zbl [1521.53061](#) MR [4562568](#)
- [16] G. Cerulli Irelli, B. Keller, D. Labardini-Fragoso, and P.-G. Plamondon, [Linear independence of cluster monomials for skew-symmetric cluster algebras](#). *Compos. Math.* **149** (2013), no. 10, 1753–1764 Zbl [1288.18011](#) MR [3123308](#)
- [17] Y. Chekanov, [Differential algebra of Legendrian links](#). *Invent. Math.* **150** (2002), no. 3, 441–483 Zbl [1029.57011](#) MR [1946550](#)
- [18] G. Dupont, [An approach to non-simply laced cluster algebras](#). *J. Algebra* **320** (2008), no. 4, 1626–1661 Zbl [1155.16011](#) MR [2431998](#)
- [19] T. Ekholm, K. Honda, and T. Kálmán, [Legendrian knots and exact Lagrangian cobordisms](#). *J. Eur. Math. Soc. (JEMS)* **18** (2016), no. 11, 2627–2689 Zbl [1357.57044](#) MR [3562353](#)
- [20] Y. Eliashberg, A. Givental, and H. Hofer, [Introduction to symplectic field theory](#). *Geom. Funct. Anal.* (2000), no. Special Volume, Part II, 560–673; GAFA 2000 (Tel Aviv, 1999) Zbl [0989.81114](#) MR [1826267](#)
- [21] A. Felikson, M. Shapiro, and P. Tumarkin, [Cluster algebras of finite mutation type via unfoldings](#). *Int. Math. Res. Not. IMRN* **2012** (2012), no. 8, 1768–1804 Zbl [1283.13020](#) MR [2920830](#)
- [22] S. Fomin, M. Shapiro, and D. Thurston, [Cluster algebras and triangulated surfaces. I. Cluster complexes](#). *Acta Math.* **201** (2008), no. 1, 83–146 Zbl [1263.13023](#) MR [2448067](#)
- [23] S. Fomin, L. Williams, and A. Zelevinsky, [Introduction to cluster algebras. Chapters 1–3](#). 2021, arXiv:[1608.05735v4](#)
- [24] S. Fomin, L. Williams, and A. Zelevinsky, [Introduction to cluster algebras. Chapters 4–5](#). 2021, arXiv:[1707.07190v3](#)
- [25] S. Fomin and A. Zelevinsky, [Cluster algebras. I. Foundations](#). *J. Amer. Math. Soc.* **15** (2002), no. 2, 497–529 Zbl [1021.16017](#) MR [1887642](#)
- [26] S. Fomin and A. Zelevinsky, [Cluster algebras. II. Finite type classification](#). *Invent. Math.* **154** (2003), no. 1, 63–121 Zbl [1054.17024](#) MR [2004457](#)
- [27] S. Fomin and A. Zelevinsky, [\$Y\$ -systems and generalized associahedra](#). *Ann. of Math. (2)* **158** (2003), no. 3, 977–1018 Zbl [1057.52003](#) MR [2031858](#)
- [28] S. Fomin and A. Zelevinsky, [Cluster algebras. IV. Coefficients](#). *Compos. Math.* **143** (2007), no. 1, 112–164 Zbl [1127.16023](#) MR [2295199](#)
- [29] H. Gao, L. Shen, and D. Weng, [Positive braid links with infinitely many fillings](#). 2020, arXiv:[2009.00499v1](#)
- [30] H. Gao, L. Shen, and D. Weng, [Augmentations, fillings, and clusters](#). *Geom. Funct. Anal.* **34** (2024), no. 3, 798–867 Zbl [07862380](#) MR [4743511](#)
- [31] H. Geiges, [An introduction to contact topology](#). Cambridge Stud. Adv. Math. 109, Cambridge University Press, Cambridge, 2008 Zbl [1153.53002](#) MR [2397738](#)
- [32] S. Guillermou, M. Kashiwara, and P. Schapira, [Sheaf quantization of Hamiltonian isotopies and applications to nondisplaceability problems](#). *Duke Math. J.* **161** (2012), no. 2, 201–245 Zbl [1242.53108](#) MR [2876930](#)

- [33] J. Hughes, [Weave-realizability for \$D\$ -type](#). *Algebr. Geom. Topol.* **23** (2023), no. 6, 2735–2776 Zbl [1542.53082](#) MR [4640139](#)
- [34] J. E. Humphreys, *Introduction to Lie algebras and representation theory*. Grad. Texts in Math. 9, Springer, New York, 1978; Second printing, revised Zbl [0447.17001](#) MR [0499562](#)
- [35] X. Jin and D. Treumann, [Brane structures in microlocal sheaf theory](#). *J. Topol.* **17** (2024), no. 1, article no. e12325 Zbl [1547.53094](#) MR [4821225](#)
- [36] V. G. Kac, *Infinite-dimensional Lie algebras. An introduction*. Progr. Math. 44, Birkhäuser, Boston, MA, 1983 Zbl [0537.17001](#) MR [0739850](#)
- [37] T. Kálmán, [Braid-positive Legendrian links](#). *Int. Math. Res. Not.* (2006), article no. ID Zbl [1128.57006](#) MR [2272097](#)
- [38] L. Ng, D. Rutherford, V. Shende, S. Sivek, and E. Zaslow, [Augmentations are sheaves](#). *Geom. Topol.* **24** (2020), no. 5, 2149–2286 Zbl [1457.53064](#) MR [4194293](#)
- [39] Y. Pan, [Exact Lagrangian fillings of Legendrian \$\(2, n\)\$ torus links](#). *Pacific J. Math.* **289** (2017), no. 2, 417–441 Zbl [1432.53127](#) MR [3667178](#)
- [40] L. Polterovich, [The surgery of Lagrange submanifolds](#). *Geom. Funct. Anal.* **1** (1991), no. 2, 198–210 Zbl [0754.57027](#) MR [1097259](#)
- [41] N. Reading and S. Stella, [An affine almost positive roots model](#). *J. Comb. Algebra* **4** (2020), no. 1, 1–59 Zbl [1454.13038](#) MR [4073889](#)
- [42] L. Shen and D. Weng, [Cluster structures on double Bott–Samelson cells](#). *Forum Math. Sigma* **9** (2021), article no. e66 Zbl [1479.13028](#) MR [4321011](#)
- [43] V. Shende, D. Treumann, H. Williams, and E. Zaslow, [Cluster varieties from Legendrian knots](#). *Duke Math. J.* **168** (2019), no. 15, 2801–2871 Zbl [1475.53094](#) MR [4017516](#)
- [44] V. Shende, D. Treumann, and E. Zaslow, [Legendrian knots and constructible sheaves](#). *Invent. Math.* **207** (2017), no. 3, 1031–1133 Zbl [1369.57016](#) MR [3608288](#)
- [45] D. Treumann and E. Zaslow, [Cubic planar graphs and Legendrian surface theory](#). *Adv. Theor. Math. Phys.* **22** (2018), no. 5, 1289–1345 Zbl [07430949](#) MR [3952351](#)
- [46] D. F. Vatne, [The mutation class of \$D_n\$ quivers](#). *Comm. Algebra* **38** (2010), no. 3, 1137–1146 Zbl [1196.16011](#) MR [2650396](#)

Received 26 February 2021.

Byung Hee An

Department of Mathematics Education, Kyungpook National University, 80 Daehak-ro, 41566 Daegu, South Korea; anbyhee@knu.ac.kr

Youngjin Bae

Department of Mathematics, Incheon National University, 119 Academy-ro, 22012 Incheon, South Korea; yjbae@inu.ac.kr

Eunjeong Lee

Center for Geometry and Physics, Institute for Basic Science, 79 Jigok-ro 127beon-gil, 37673 Pohang; current address: Department of Mathematics, Chungbuk National University, 1 Chungdae-ro, 28644 Cheongju, South Korea; eunjeong.lee@chungbuk.ac.kr